Investigating GAP45 Localisation and Phosphorylation During *Plasmodium falciparum* Schizont Development

Mohd Ridzuan Bin Mohd Abd Razak

June 2012

Division of Parasitology
MRC National Institute for Medical Research
The Ridgeway
Mill Hill, London
NW7 1AA

Department of Structural and Molecular Biology
University College London

This thesis is submitted to University College London for the degree of

Doctor of Philosophy

Declaration

I, Mohd Ridzuan Bin Mohd Abd Razak, confirm that the work presented in this thesis is my own. Where information has been derived from other sources, I confirm that this has been indicated in the thesis.

(Mohd Ridzuan Bin Mohd Abd Razak)

June 2012

Abstract

The invasion of erythrocytes by merozoites is driven by an actomyosin motor assembled below the parasite's plasma membrane, with the myosin anchored on the inner membrane complex (IMC). The myosin (MyoA) is within a protein complex that is comprised of several proteins including myosin tail domain interacting protein (MTIP) and glideosome associated proteins (GAP) 45 and 50. A ternary complex of MyoA, MTIP and GAP45 is formed and later associates with GAP50. GAP45 is acylated by both myristoyl- and palmitoyl-fatty acids and is phosphorylated. This study has highlighted the GAP45 phosphorylation by calcium dependent protein kinase 1 (CDPK1) *in vitro* and its possible roles in schizogony. By site directed mutagenesis, substitution of S31, S89, S103 and S156 to alanine decreased the level of GAP45 phosphorylation, with S103A exhibiting a major decrease in ^{32}P incorporation. Phosphorylation on S89 and S103 was studied further in parasites as both residues were among the phospho-sites in phosphopeptides identified *in vivo*. This study also showed that full length GAP45 labelled internally with GFP (FL-GAP45) is assembled into the motor complex, phosphorylated and transported to the developing IMC in early schizogony, where it accumulates during intracellular development until merozoite release. The C-terminal truncated GFP-GAP45 (N-GAP45; residues 1-29) localised at the plasma membrane instead of the IMC and was not assembled into the motor complex. The N-terminal truncated GFP-GAP45 (C-GAP45; residues 30-205) behaved like FL-GAP45. Modifying serine residues, S89 and S103, in GAP45 with alanine or aspartate had no apparent effect on its assembly into the protein complex or its intracellular location during schizont development and merozoite maturation. A second highly phosphorylated component of the complex (GAP40) was also identified. The early assembly of the motor complex suggests that it has functions in addition to its role in erythrocyte invasion.

Acknowledgement

With the achievement of this project, I would like to thank my supervisor Dr. Anthony A. Holder for providing me the opportunity to work in his lab and for his continuous guidance and support throughout my project. I would also like to thank Dr. Judith L. Green for her generous help and advice overall on my project. I also would like to thank Dr. Ellen Knuepfer and Dr. Robert W. Moon for their supportive and constructive opinions which have ensured the smoothness of my project. This acknowledgement is extended to my thesis committee panel, Dr. Steve Smerdon and Dr. Roger Buxton and my co-supervisor, Dr. Delmiro Fernandez-Reyes for their time and helpful advice. I would like to acknowledge the Director of Institute for Medical Research, Ministry of Health, and Ministry of Science, Technology and Innovation, Malaysia for granting me a full time study leave and scholarship to run this project. I would like to thank to Dr. Steven Howell and Dr. Steve Martin for their help and advice in mass spectrometry and circular dichroism analysis respectively. I would also like to thank Munira Grainger for her help and training in *Plasmodium falciparum* culture techniques. Thanks to Dr. Yan Gu and Kate Sullivan for consultation and providing the facilities for high resolution fluorescence Deltavision microscopy. Thanks go to all the members of the Tony and Delmiro labs for the help, advice and interesting discussions on my project particularly during the lab meeting sessions. A special thanks to Dr. Liz McMinn and Alana Price for their hard work in maintaining the lab administration, safety and comfort which led to the achievement of this study. I would like particularly to thank Sola Ogun, Dr. Madhusudan Kadekoppala, Azian Yusuf, Suraya Diaz, Oniz Suleyman and Claire Hastings for their support throughout.

I would like to dedicate this thesis to my parents, Mohd Abd Razak and Maziah Che Hassan, and also to my sister, Mazni Mohd Abd Razak for their encouragement and support in everything I have done. Last but not least, I would also like to dedicate this thesis to my wife Malissa Kamal for her love and support throughout my study and for always being there for me.

Table of contents

		Pages
Title Page		1
Declaration		2
Abstract		3
Acknowledgement		4
Table of contents		5
List of figures		10
List of tables		15
Abbreviations		16
References		188
Appendixes		223
Chapter 1 - Introduction		21
1.1	Malaria: History, global distribution and control	21
	1.1.1 The symptoms and clinical features of malaria	23
	1.1.2 The human *Plasmodium* parasites	24
1.2	The life-cycle of *Plasmodium*	26
	1.2.1 Liver stage	26
	1.2.2 Blood stage	27
	1.2.3 Mosquito stage	29
1.3	Invasion of red blood cell by merozoites	30
	1.3.1 Attachment to red blood cell surface	31
	1.3.2 Tight or moving junction formation	32
1.4	Biogenesis of the inner membrane complex and actin-myosin motor complex assembly in apicomplexan parasites	35
1.5	Actin-myosin motor complex of *P. falciparum*	37
	1.5.1 Inter-relationship between myosin A and actin	37

1.5.2 Myosin tail domain-interacting protein 39
1.5.3 Glideosome-associated proteins (GAPs) 40
1.6 Protein phosphorylation in human health and disease 41
1.7 The importance of protein phosphorylation in *Plasmodium* life cycle 44
1.8 Calcium-dependant protein kinases 46
1.9 The relevance of GAP45 phosphorylation by CDPK1 49
1.10 Aims and hypothesis 50

Chapter 2 – Materials and methods 65
2.1 General DNA manipulation and transformation 65
2.1.1 Buffer and reagents 65
2.1.2 Methods 65
2.1.2.1 DNA concentration determination 65
2.1.2.2 Agarose gel electrophoresis 66
2.1.2.3 Polymerase Chain Reaction (PCR) 66
2.1.2.4 Restriction endonuclease digestion 66
2.1.2.5 Ligation of DNA fragments 66
2.1.2.6 Purification of DNA 67
2.1.2.7 The propagation and transformation of plasmid DNA by *E. coli* 67
2.1.2.8 Isolation of plasmid DNA 67
2.1.2.9 Sequencing of DNA 67
2.1.2.10 Bacterial cell storage 68
2.1.2.11 Oligonucleotides 68
2.2 Expression and purification of recombinant GAP45 protein 68
2.2.1 Buffers and reagents 68
2.2.2 Methods 69
2.3 Site-directed mutagenesis of GAP45 gene 70
2.3.1 Buffers and reagents 70
2.3.2 Methods 70

2.4 CDPK1 kinase assay and analysis 71
2.4.1 Buffers and reagents 71
2.4.2 Methods 71
2.4.2.1 Autoradiography 71
2.4.2.2 Scintillation counting 72
2.4.2.3 Electrospray mass spectrometry analysis (ES-MS) 72
2.5 Far UV circular dichroism (CD) spectroscopy 72
2.6 Parasite culture and synchronisation 73
2.6.1 Buffers and reagents 73
2.6.2 Methods 73
2.7 The parasite DNA manipulation and transfection 74
2.7.1 Buffers and reagents 74
2.7.2 Methods 75
2.7.2.1 Transfection vector contruct 75
2.7.2.2 DNA precipitation 76
2.7.2.3 Transfection processes 77
2.7.2.4 Freezing and thawing of *P. falciparum* 77
2.8 Parasites protein subcellular fractionation 78
2.8.1 Buffers and reagents 78
2.8.2 Methods 78
2.9 SDS-PAGE and western blotting technique 79
2.9.1 Buffers and reagents 79
2.9.2 Methods 79
2.10 Live and indirect-immunofluorescene microscopy assay (IFA) 80
2.10.1 Buffers and reagents 80
2.10.2 Methods 80
2.11 Co-immunoprecipitation or pull-down assay 81
2.11.1 Buffers and reagents 81
2.11.2 Methods 81
2.12 Protein phosphatase treatment 83
2.12.1 Buffers and reagents 83
2.12.2 Methods 83

2.13 ^{32}P-phosphate metabolic labelling of *P. falciparum* schizont 84
2.13.1 Buffers and reagents 84
2.13.2 Methods 84
2.14 Parasite protein identification by liquid chromatography- mass spectrometry (LC-MS/MS) 84
2.14.1 Buffers and reagents 84
2.14.2 Methods 85

Chapter 3 - *In vitro* phosphorylation of GAP45 protein by CDPK1 90
3.1 Introduction 90
3.2 Extraction and purification of recombinant GAP45 protein 91
3.3 *In vitro* CDPK1 kinase assay 92
3.4 Other possible CDPK1 phosphorylation sites on GAP45 93
3.5 Electrospray mass spectrometry analysis on unphosphorylated and phosphorylated recombinant GAP45 protein 95
3.6 Secondary structure of phosphorylated GAP45 97
3.7 Discussion 98

Chapter 4 - Characterization of *P. falciparum* GFP-tagged GAP45 116
4.1 Introduction 116
4.2 Expression and localisation of GFP tagged GAP45 protein in *P. falciparum* schizonts 118
4.3 IMC localisation pattern of GFP-tagged GAP45 protein 120
4.4 Tetrameric motor complex of GFP-tagged GAP45 in *P. falciparum* 124
4.5 Discussion 125

Chapter 5 - Phosphorylation of GFP-tagged GAP45 in parasite 146
5.1 Introduction 146
5.2 The effect of phosphatase treatment on GFP-tagged GAP45 protein 147
5.3 ^{32}P-phosphate incorporation on GFP-tagged GAP45 protein in

parasites 148
5.4 GAP40 is part of the motor complex protein 150
5.5 The effect of S89 and S103 phosphorylation on the localisation of GFP-tagged GAP45 151
5.6 The effect of S89 and S103 mutation on the GAP45 tetrameric actin-myosin motor complex 152
5.7 Discussion 153

Chapter 6 – Research summary 176
6.1 CDPK1phosphorylates multiple residues on GAP45 protein 176
6.2 GFP-tagged GAP45 forms the actin myosin motor complex protein at the inner membrane complex: a possible interaction with IMC and parasite membrane via its C-terminal and N-terminal region respectively 177
6.3 Localisation and motor complex assembly of GAP45 is not affected by phosphorylation on S89 and S103 in parasites 180
6.4 Future studies 181

List of figures

Figures	Title	Pages
Figure 1.1	Morphology and conserved organelles of the *P. falciparum* merozoite, ookinete, sporozoite and *T. gondii* tachyzoite	52
Figure 1.2	Life cycle of *P. falciparum* in the human host and the *Anopheles* mosquito vector	53
Figure 1.3	Developmental stages of the *P. falciparum* gametocyte in red blood cell	55
Figure 1.4	The steps of red blood cell invasion by *P. falciparum* merozoites	56
Figure 1.5	The endodyogeny and schizogony of *Toxoplasma* and *Plasmodium* respectively	57
Figure 1.6	Actin-myosin motor complex components of motile apicomplexan parasites	59
Figure 1.7	The GAP45 protein sequence alignment from different species of apicomplexan parasite: *Plasmodium falciparum*, *Plasmodium yoelii*, *Toxoplasma gondii*, *Babesia bovis*, *Theileria parva* and *Cryptosporidium parvum*	61

Figure 1.8 The distinct activation mechanism for CDPKs and CaMKs 62

Figure 1.9 The role of CDPKs and other cyclic nucleotide dependent kinases in the *Plasmodium* life cycle 63

Figure 1.10 *Plasmodium* GAP45 protein alignment 64

Figure 3.1 Recombinant PfGAP45 protein extraction 103

Figure 3.2 Purification of recombinant *Plasmodium falciparum* GAP45 104

Figure 3.3 *In vitro* CDPK1 phosphorylation of recombinant PfGAP45 at 30^{o}C, 10 minutes using 100 nM CDPK1 105

Figure 3.4 CDPK1-dependent phosphorylation of recombinant GAP45 proteins *in vitro* by incorporation of ^{32}P at 30^{o}C, using 100 nM CDPK1 and 0.1 mM [^{32}P]ATP and detection by scintillation counting 106

Figure 3.5 *In vitro* CDPK1 phosphorylation of recombinant PfGAP45 at 30^{o}C, 10 minutes using 100 nM CDPK1 107

Figure 3.6 CDPK1-dependent phosphorylation of recombinant GAP45 proteins *in vitro* by incorporation of ^{32}P at 30^{o}C, using 100 nM CDPK1 and 0.1 mM [^{32}P]ATP and detection by scintillation counting 108

Figure 3.7 Electrospray-mass spectrometry analysis of unphosphorylated and phosphorylated recombinant WT GAP45, phosphorylated S89A, S103A, S89A/S103A,

S142A and S149A mutant GAP45 109

Figure 3.8 Far UV circular dichroism (CD) spectra of WT GAP45 and its variants 112

Figure 3.9 Far UV circular dichroism (CD) spectra of unphosphorylated and phosphorylated WT and S142A GAP45 113

Figure 4.1 The design of GFP-tagged GAP45 episomal transfection constructs 129

Figure 4.2 The subcellular fractionation of WT or full length (FL-GAP45), N-terminal truncated (C-GAP45) and C-terminal truncated (N-GAP45) GFP-tagged GAP45 proteins 131

Figure 4.3 The time course live microscopy analysis on full length GFP-tagged GAP45 (FL-GAP45), C-terminal truncated GFP-tagged GAP45 (N-GAP45) and N-terminal truncated GFP-tagged GAP45 (C-GAP45) expressing *P. falciparum* 132

Figure 4.4 The indirect immunofluorescent assay (IFA) microscopy analysis on FL-GAP45, C-terminal truncated (N-GAP45) and N-terminal truncated (C-GAP45) GFP-tagged GAP45 expressing parasites 135

Figure 4.5 The localisation of GFP-tagged GAP45 variants at early schizont stage after high resolution immunofluorescent imaging analysis with Z-stack and deconvolution processing 139

Figure 4.6 The location of GFP-tagged wild type GAP45 (FL-GAP45) and GFP-tagged C-terminal truncated GAP45 (N-GAP45) during schizont development (30-42 hours post invasion) 141

Figure 4.7 N-GAP45 is associated with the residual body whereas FL-GAP45 is not 143

Figure 4.8 The FL-GAP45 and C-GAP45 proteins assemble into the motor protein complex, whereas N-GAP45 does not 145

Figure 5.1 Far UV circular dichroism (CD) spectra WT, S89D, S103D and S89D/S103D GAP45 recombinant proteins 159

Figure 5.2 The GFP-GAP45 protein is phosphorylated in the parasite 160

Figure 5.3 The S89A/S103A GFP-GAP45 protein is also phosphorylated in the parasite 161

Figure 5.4 The S89A/S103A GFP-GAP45 is phosphorylated and similar level as WT GFP-GAP45 (FL) 162

Figure 5.5 The identification of GAP40 as a phosphorylated motor complex protein 163

Figure 5.6 The subcellular fractionation of S89 and S103 variants of GFP-tagged GAP45 proteins 164

Figure 5.7 The location of GFP-tagged GAP45 and a number of variants determined in early and late schizonts, by live fluorescence microscopy 165

Figure 5.8 Localisation of GFP-tagged GAP45 variants in mature schizonts 166

Figure 5.9 Localisation of GFP-tagged GAP45 variants in young schizonts 171

Figure 5.10 WT/FL-GAP45 proteins and its variants were assembled into the motor protein complex, whereas N-GAP45 does not 174

Figure 6.1 The development and location of the IMC interacting protein GFP-tagged GAP45 during schizogony 184

Figure 6.2 GAP45 was highly phosphorylated in merozoite blood stage 186

List of tables

Tables	Title	Pages
Table 2.1	The primers used for substitution of GAP45 serine or threonine to alanine in mutagenesis experiment	87
Table 2.2	The list of antibodies used in this experiment	89
Table 3.1	*In vitro* CDPK1 phosphorylation of recombinant PfGAP45 and its variants at 30^{o}C, 10 minutes using 100 nM CDPK1	114
Table 3.2	Sequence motifs (± residues) flanking the phosphorylation sites identified in PfGAP45	115

Abbreviations

ABRA	acid basic repeat antigen
AMA-1	apical membrane antigen-1
AMP	adenosine monophosphate
ATP	adenosine triphosphate
BC	before christ
CamK	calcium/calmodulin-dependent protein kinase
CaM-LD	calmodulin like domain
cAMP	cyclic adenosine monophosphate
CBD_{1-15}	calmodulin binding domain 1-15
CD	circular dichroism
CDK	cyclin-dependent kinase
CDPK	calcium dependent protein kinase
C-GAP45	N-$terminal_{1-29}$ truncated green fluorescent protein tagged GAP45
cGMP	cyclic guanosine monophosphate
CHAPS	3-([3-Cholamidopropyl]dimethylammonium)-1-propanesulfonate
CK1	casein kinase 1
CLK	CDK-like kinase
CML	chronic myelogenous leukemia

CSP	circumsporozoite protein
DAPI	4',6-diamidino-2-phenylindole
DBL	duffy binding-like protein
DNA	deoxyribonucleic acid
dNTP	deoxyribonucleotide triphosphate
DTT	dithiothreitol
EBA	erythrocyte binding antigen
EDTA	ethylenediaminetetraacetic acid
EGTA	ethylene glycol bis(2-aminoethyl ether)-*N*,*N*,*N*'*N*'-tetraacetic acid
EPEC	enteropathogenic *Escherichia coli*
ER	endoplasmic reticulum
ES-MS	electrospray-mass spectrometry
FL-GAP45	full length green fluorescent protein tagged GAP45
GAP 40/45/50	gliding/glideosome associated protein 40/45/50
GAPM 1/2	glideosome associated protein with multiple membrane spans 1/2
GFP	green fluorescene protein
GFP-GAP45	green fluorescent protein tagged GAP45
GPI	glycosylphosphatidylinositol
GSK3	glycogen synthase kinase 3
HCL	hydrochloric acid
HRP	horse radish peroxidase

HSPGs	highly sulphated heparin sulphate proteoglycans
ID	inactivation domain
IgG	immunoglobulin
IMC	inner membrane complex
IPTG	isopropyl-β-D-thiogalactopyranoside
ISP	inner membrane complex sub-compartment proteins
J domain	junction domain
LB	Luria-Bertani
LC-MS/MS	liquid chromatography-tandem mass spectrometry
MESA	mature-parasite-infected erythrocyte surface antigen
MLC	myosin light chain
MOPS	Nu-PAGE® 3-(N-morpholino)-propanesulphonic acid buffer
MS-MALDI TOF	matrix-assisted laser desorption/ionization time of flight mass spectrometer
MSP	merozoite surface protein
MTIP	myosin A tail interacting protein
MTRAP	merozoite thrombospondin-related anonymous protein
MudPIT	Multi-dimensional liquid chromatography Protein Identification Technology
MyoA	myosin A
N-GAP45	C-terminal$_{30-204}$ truncated green fluorescent protein tagged GAP45
Ni-NTA	nickel-nitrilotriacetic acid

NMR	nuclear magnetic resonance
NP-40	nonidet P-40
OPK	other protein kinase
PbAC*α*	*P. berghei* adenylyl cyclase
PBS	phosphate buffered saline
PBST	phosphate buffered saline with tween 20
PFA	paraformaldehyde
PfEMP1	*P. falciparum* erythrocyte membrane protein 1
PfMap2	*P. falciparum* atypical mitogen activated protein kinase
PfRh	*P. falciparum* reticulocyte binding protein
PH	plekstrin homology domain
PK2	protein kinase 2
PKA	protein kinase A
PKB	protein kinase B
PKC	protein kinase C
PKG	protein kinase G
PLC	phospholipase C
PMSF	phenylmethanesulfonylfluoride
PP2B	protein phosphatase 2B
PV	parasitophorous vacuole
PVM	parasitophorous vacuole membrane
RBC	red blood cell

RON	rhoptry neck protein
RON10	rhoptry neck protein 10
RPMI	Roswell Park Memorial Institute 1640
SDS	sodium dodecyle sulphate
SDS-PAGE	sodium dodecyle sulphate-polyacrylamide gel electrophoresis
SERA5	serine repeat antigen 5
SILAC	Stable Isotope of Amino Acids in Culture
SPECT	sporozoite microneme protein essential traversal
SPN	subpellicular network
TgALD1	*T. gondii* aldolase 1
TKL	tyrosine kinase-like
TRAP	thrombospondin-related anonymous protein
TRAP	thrombospondin-related anonymous protein
TSR	thrombospondin repeat domain
Tyr K	tyrosine kinase
UPLC-ESI-MS/MS	nano-ultra performance liquid chromatography-electrospray ionization-tandem mass spectrometry
UV	ultra violet
WT	wild type

Chapter 1

Introduction

1.1 Malaria: History, global distribution and control

Malaria is an ancient disease; its existence is recorded in Chinese documents (~2700 BC), clay tablets from Mesopotamia (2000 BC), Egyptian papyri (1570 BC) and Hindu text from the sixth century BC. It was also well known in Greece around 850 BC where it was recognised by the characteristics of poor health, malarial fevers and enlarged spleens seen in people living in swampy areas. At that time, they believed that this disease was caused by miasmas rising from swamps hence contributing to the name of the disease, mal'aria meaning bad air in Italian (Cox, 2010). Now, malaria is recognised as a disease caused by apicomplexan parasites of the genus *Plasmodium*. The mammalian *Plasmodium* parasites are primarily transmitted by the female *Anopheles* mosquito but infections also occasionally occur through exposure to infected blood products (transfusion malaria) and by congenital transmission (Trampuz et al., 2003). The disease is best known for its intermittent fevers and chills, whose periodicity reflects the nature of the asexual blood stage infection, described in detail in section 1.2.

By the 1940s, malaria had spread to almost two thirds of the world including temperate and tropical zones. However, in the middle of the 20th century, malaria cases were concentrated in tropical areas due to successful disease control and eradication in temperate zones (Sachs and Malaney, 2002). There are several factors that contribute to the malaria transmission pattern. One of them is seasonality and temperature which can affect the reproduction and the growth cycle of malaria parasites. When the temperature falls below 16 to 18^{o}C, the life cycle of the malaria parasite will be disrupted because of the impairment of biting activity for most

mosquito vectors. These conditions have helped control and eradication of malaria disease programmes to be more successful in temperate countries (Sachs and Malaney, 2002). On the other hand, tropical regions offer ideal conditions that favour the mosquito and parasite development. Other climatic features that favour malaria distribution are rainfall and humidity (Sachs and Malaney, 2002).

Globally, it was estimated that 3.3 billion people were at risk of malaria. Out of 216 million cases, about 655 000 persons died of malaria in 2010. 86 % of the victims were children under 5 years old and 91 % of malaria deaths occurred in African region (WHO, 2011). In contrast, a different study by Murray et al. (2012) has estimated twice the number of malaria mortality cases in 2010 as reported by WHO (2011). The fluctuation of malaria mortality cases has also been addressed by Murray et al. (2012). Briefly, starting in 1980, malaria mortality cases increased from 995,000 to 1,817,000 in 2004 and decreased to 1,238,000 in 2010. The majority of malaria mortality cases were reported in Africa, where figures increased from 493,000 in 1980 to 1,613,000 in 2004 and decreased to 1,133,000 cases in 2010. Outside Africa, malaria mortality cases steadily decreased from 502,000 in 1980 to 104,000 in 2010 (Murray et al., 2012). The decrease in mortality cases starting from 2004 to 2010 was the result of a scale up of control activities supported by international donors (Murray et al., 2012; WHO, 2011).

Malaria vector control programmes focus on the anopheline mosquito vector, through removal of breeding sites, use of insecticides, and prevention of contact with humans by the use of screens or bed nets impregnated with insecticides (Phillips, 2001). Since an effective vaccine is still unavailable, the treatment of clinical cases relies on the use of antimalarial drugs. All of the first line antimalarial drugs, particularly chloroquine, mefloquine, pyrimethamine and atovaquone are no longer effective due to the emergence of drug resistant malaria parasites (Carter and Mendis, 2002; Phillips, 2001). Even the most effective antimalarial drug to date, artemisinin, has been reported to have reduced efficacy in parasite clearance in some areas, including the existence of artemisinin resistant *P. falciparum* on the Thailand-Myanmar border (Phyo et al., 2012). The emergence of drug resistant parasites is caused by the increased selection pressures on *P. falciparum* in particular, due to

indiscriminate and incomplete drug use for self-treatment especially using the long half-life drugs such as chloroquine and pyrimethamine. The only cost effective and potent treatment remaining is by combination treatment with both long and short half-life antimalarial drugs. For example, treatment with artemisinins (short half-life but potent) will help to reduce the parasite load, allowing other long half-life drugs such as mefloquine to fully clear the parasite. These conditions reduce the chances that drug-resistant mutants will be selected (Phillips, 2001). However, resistance to existing anti-malarials, and the heavy reliance on just a single drug such as artemisinin and its derivatives to treat malaria means new drugs are desperately needed. Unravelling the biology of malaria parasites such as the invasion mechanism and signalling pathways involving kinases may elucidate new drug targets.

1.1.1 The symptoms and clinical features of malaria

The signs and symptoms of malaria infection in humans are caused by the asexual blood stage of the parasite, specifically when the parasites mature and rupture their host red blood cell (Trampuz et al., 2003). Most of the symptoms start to appear at an average of 12 days after the inoculation of sporozoites from the mosquito saliva into the bloodstream. Malaria infections are broadly divided into mild and severe cases (Weatherall et al., 2002). Mild malaria symptoms often include headache, myalgia, malaise, coughing, shaking, chills, fever, and intermittent sweating. These may also be accompanied with nausea, vomiting, diarrhoea, and abdominal pain. Other obvious signs are the enlargement of the spleen and liver and mild jaundice (Trampuz et al., 2003; Weatherall et al., 2002).

In severe malaria, patients may exhibit a number of serious syndromes such as coma caused by cerebral malaria, respiratory distress, anemia, and hypoglycemia (Weatherall et al., 2002). Cerebral malaria results in reduced consciousness and coma. It is caused by the sequestration of parasitized red blood cells in cerebral capillaries. (Weatherall et al., 2002). Anemia may be caused by the cyclical invasion and destruction of blood cells by the parasite. Infected red blood cells may also be phagocytosed by macrophages following opsonisation by immunoglobulin and/or

complement components. Not only that, the non-infected red blood cells may also be phagocytosed due to an increase in signal for recognition of uninfected red blood cells by macrophages (Weatherall et al., 2002). In addition, the survival of non-infected red blood cells may also be shortened due to dyserythropoiesis, the abnormal development of erythroid precursors in bone marrow. There is no clear evidence of what causes the dyserythropoiesis in severe malaria, although the inhibitory effect of parasite hemozoin (haemoglobin digestion product) to erythropoiesis has been reported (Casals-Pascual et al., 2006; Giribaldi et al., 2004; Lamikanra et al., 2009; Skorokhod et al., 2010). Respiratory distress is a common symptom in severe malaria. It is defined by tachypnea (rapid breathing), gasping breathing and usually represents metabolic acidosis. Acidosis is caused by the excessive lactate (Weatherall et al., 2002) due to tissue hypoxia secondary to microvascular obstruction (Clark and Cowden, 2003). Hypoglycaemia is most common in children with severe malaria. It happens because of hepatic gluconeogenesis failure and increased consumption of glucose in peripheral tissues and by parasites (Dekker et al., 1997).

1.1.2 The human *Plasmodium* parasites

There are 5 species of malaria parasites infecting humans. These parasites are *Plasmodium falciparum*, *Plasmodium vivax*, *Plasmodium malariae*, *Plasmodium ovale* and *Plasmodium knowlesi* (Antinori et al., 2012). The parasites have been characterized from ancient times by the periodicity of their reproduction in the blood. For example, ‘tertian’ and ‘quartian’ refers to their characteristic feature of an acute febrile episode, or paroxysm, that returns respectively every third and fourth day (Carter and Mendis, 2002; Garnham, 1966). The latest recognised human malaria parasites species, *P. knowlesi* (quotidian or daily cycle) was originally known to be a simian malaria parasite particularly in the long tailed and pig tailed macaques, *Macaca fascicularis* and *Macaca nemestrina* respectively. It has been defined as the fifth human malaria species following the discovery of human *P. knowlesi* infection cases in Malaysia Borneo (Cox-Singh et al., 2008; Singh and Daneshvar, 2010) and other Asian countries such as Thailand (Jongwutiwes et al., 2011; Jongwutiwes et al.,

2004), Philipines (Luchavez et al., 2008), Singapore (Ng et al., 2008) and Vietnam (Van den Eede et al., 2009).

P. falciparum is highly pathogenic and the most deadly parasite causing malaria in human as it often leads to severe malaria. In 2010, 91% of the estimated malaria cases were due to *P. falciparum* infection (WHO, 2011). It has 48 hours of asexual blood stage (tertian) and invades both reticulocyte and mature red blood cells. The liver stage (exoerythrocytic schizogony) of this parasite takes 5-6 days to mature without hypnozoites, a dormant form causing relapse of the infection (Antinori et al., 2012).

Similar to *P. falciparum*, *P. vivax* has 48 hours of asexual blood stage (tertian) and often lead to severe malaria cases. However, it only invades young red blood cell (reticulocytes). The liver stage of this parasite takes 6-8 days to mature and it can also form hypnozoites. Another malaria parasite that has similar characteristics of infection is *P. ovale* which only develops in young red blood cells for 48 hours. It takes 9 days to develop in liver cells and has the ability to form hypnozoites. In contrast, *P. ovale* infection will not lead to severe malaria (Antinori et al., 2012).

P. malariae is responsible of the quartan malaria. It has a slow development in human (15 to 16 days in the liver, 72 hours in the blood). It only invades mature red blood cells. Different to *P. vivax* and *P. ovale*, it will not form hypnozoite. The malaria patients infected with this parasite will not develop severe malaria (Antinori et al., 2012).

P. knowlesi has 24 hours of asexual blood stage (quotidian) and it is not restricted to young or mature red blood cells. It takes 9 to 12 days to develop within the liver cells. It does have the ability to form hypnozoites. This parasite is often mistakenly diagnosed as *P. malariae* because of the similarity of the red blood cell forms between these parasites (Antinori et al., 2012). The patients infected with *P. knowlesi* have been reported to develop severe malaria resembling that of *P. falciparum* (Cox-Singh et al., 2008; William et al., 2011).

1.2 The life-cycle of *Plasmodium*

The life cycle of *Plasmodium* is completed by its motile forms which are specialized to invade different types of cell in different stages of the life cycle. The motile forms are known as sporozoite, ookinete and merozoite. Sporozoites and merozoites invade and develop in the liver cell (liver stage), and red blood cell (blood stage) respectively, and ookinetes cross the mosquito midgut (mosquito stage) (Figure 1.1). These parasite forms possess apical organelles such as micronemes, rhoptries, dense granules and exonemes (Figure 1.1). These apical organelles are secretory organelles and function in secreting the proteins involved during and after host cell invasion. The different composition of organelles in each zoite relates to their specialized behaviour. For example, the merozoites with fewer micronemes and large rhoptries do not traverse but rapidly invade red blood cell once; ookinetes do not need rhoptries as they only traverse the mosquito midgut epithelium; and sporozoites have abundant of micronemes and rhoptries as they have to traverse, glide and infect cells (Baum et al., 2008a).

1.2.1 Liver stage

The infection begins when a *Plasmodium*-infected mosquito bites the vertebrate host for a blood meal, releasing saliva containing sporozoites into the skin and the blood stream (Figure 1.2). The sporozoites move in the skin by a form of motility known as 'gliding' in order to reach a blood vessel where they breach the endothelial barrier to enter blood circulation (Garnham, 1966). During gliding motility, the contents of the micronemes are externalised onto the sporozoite surface by mechanisms that are poorly understood. These proteins are thrombospondin-related anonymous protein (TRAP), a micronemal protein that mediates gliding motility and invasion both in mosquito vector salivary gland and in mammalian host (Sultan, 1999; Sultan et al., 1997), and sporozoite microneme protein essential traversal 1 and 2 (SPECT1 and SPECT2) that are needed to traverse through host cells by membrane disruption, allowing for parasite movement in and out of skin, blood endothelium and liver cells (Amino et al., 2008; Ishino et al., 2005; Ishino et al., 2004; Vaughan et al., 2008).

Sporozoites are carried to the liver where they glide along the sinusoidal epithelium and invade Kupffer cells, the resident macrophage, traverse them, and cross into the space of Disse, the location in the liver between the sinusoid and hepatocytes (Frevert et al., 2005). The sporozoite then traverses through several liver cells before invading a hepatocyte and at the same time forming a parasitophorous vacuole (PV) in which it will finally reside (Frevert et al., 2005). The ability of sporozoites to switch from traversal state to invasive state is dependant on interaction between the sporozoite surface protein, circumsporozoite protein (CSP) and host heparin sulphate proteoglycan (HSPG) surface protein (Frevert et al., 1993). After the formation of the PV, the sporozoite differentiates into a liver trophozoite, a feeding stage. The liver trophozoite then continues to grow by harvesting all the nutrients from the host cell and then undergoes DNA replication and a form of cytokinesis termed schizogony, developing into the liver schizont stage (Frevert, 2004). Upon merozoite release, parasites induce the death and detachment of their host cells followed by the budding of merozoite-filled vesicles (extrusome/merosomes) into the sinuisoidal lumen (Sturm et al., 2006). It has also been reported that the merosome packaging protects hepatic merozoites from phagocytic attack by sinusoidal Kupffer cells. The extrusome/merosome containing 100 to 200 merozoites is released into the blood stream and resides in the capillary organs such as lungs prior to being released into the blood circulation (Baer et al., 2007; Sturm et al., 2006).

1.2.2 Blood stage

After the liver stage development, the merozoites invade red blood cells (RBCs) to begin the asexual blood-stage cycle (Garnham, 1966) (Figure 1.2). The invasion of a red blood cell requires the attachment of parasite to red cell receptors accompanied by the release of several parasite proteins and activation of the actin-myosin motor complex as described in detail in section 1.3. In the red blood cell, the parasite develops through ring, trophozoite and schizont stages within the membranous sac of the parasitophorous vacuole produced during invasion (Lingelbach and Joiner, 1998; Preiser et al., 2000). The ring stage parasites form a biconcave disc and begin to feed

on the haemoglobin through a cytostome or cell mouth (part of the cell specialized to phagocytose food). The ring grows to a more rounded or irregular trophozoite (Bannister and Mitchell, 2003; Bannister et al., 2000a).

The trophozoites also form a single large food vacuole in which the degradation products of haemoglobin (haemozoin) accumulate (Figure 1.2). At this stage, the parasite is actively feeding, growing and inducing host red blood cell modification through the export of parasite proteins to the surface of the host cell. These modifications involve the formation of Maurer's clefts - flat membranous sacs seen in the red blood cell cytoplasm (Aikawa et al., 1986; Atkinson and Aikawa, 1990) and the formation of knobs on the red blood cell surface that contain proteins such as *P. falciparum* erythrocyte membrane protein 1 (PfEMP1) (Crabb et al., 1997). The presence of knobs is correlated with binding of infected red blood cells to endothelium of blood vessels, thereby preventing the parasite's clearance in the spleen (Cooke et al., 2000). In addition, the export of proteins by the trophozoite results in an increase of infected red blood cell permeability to essential nutrients such as sugars, amino acids, vitamins, choline and calcium (Kirk, 2001). At this stage, the toxic product of haemoglobin digestion by parasite proteases, haem, is coverted to haemozoin, a dark pigment accumulated in the food vacuole (Bannister and Mitchell, 2003; Francis et al., 1997). To form individual merozoites DNA replication occurs (which generates about 16 to 20 nuclei), the assembly of merozoite components must also occur, beginning with the formation of apical organelles such as rhoptries, micronemes and dense granules followed by the formation of cytoskeletal components such as microtubules and polar rings present beneath the merozoite surface. The cleavage furrow forms on each nascent merozoite, the first stage of cytokinesis (Bannister et al., 2000a). Once cytokinesis is complete at the end of the schizont stage, the red blood cell membrane and PVM lyse by a protease-dependent process, releasing free merozoites into the blood circulation. The merozoites then invade further red blood cells and begin another asexual blood stage cycle (Bannister and Mitchell, 2003) (Figure 1.2).

Some parasites will develop into male or female gametocytes in the bloodstream, which are the initial sexual stages of the parasite (Figure 1.2).

Nevertheless, it is still unclear how, when, and why the parasites decide to form into this sexual stage. It may be triggered by a number of environmental and genetic factors, including host immunity, drug treatment and population density (Dixon et al., 2008). There are five morphologically recognisable stages (I-V) in gametocyte development which takes about 9-23 days post invasion (Figure 1.3A). Stage I and II gametocytes are difficult to distinguish from young trophozoites. However, as a result of developing sub-pellicular membrane and microtubules, they appear roundish with a pointed end (Sinden, 1982) and show a distinctive pigment pattern in Giemsa staining (Dixon et al., 2008) (Figure 1.3B). The expansion of the sub-pellicular membrane and microtubules produces a stage III gametocyte with a 'D' shape. In stage IV, they form an elongated crescent shape (due to complete formation of sub-pellicular membrane and microtubules) and sexual dimorphism is most apparent (Sinden, 1982). The female gametocyte (macrogametocyte) has a small nucleus with a nucleolus and a concentrated pigment pattern. In contrast, the male gametocyte (microgametocyte) has a bigger nucleus without nucleolus (Sinden, 1982) (Figure 1.3A). The mature gametocyte (stage V), which is the most distinguishable stage and the only form found in the circulation, has rounded ends due to the breakdown of sub-pellicular microtubules forming sausage or crescent-shaped structures (Sinden, 1982) (Figure 1.3A and B). Due to a higher density of ribosomes in female gametocytes, they can be easily identified by their blue appearance on a Giemsa stained blood film; by contrast male gametocytes are pink in Giemsa stain (Sinden, 1982) (Figure 1.3B). In addition, the female gametocytes can also be characterized by the centralized condensed hemozoin pigment, while the hemozoin pigment of the male gametocyte is dispersed throughout the infected red blood cell (Dixon et al., 2008) (Figure 1.3B).

1.2.3 Mosquito stage

Gametocyte stage parasites are taken up by a mosquito during feeding. Gametogenesis is induced in the mosquito gut resulting in gamete formation (Garnham, 1966) (Figure 1.2). Briefly, the male gametocytes undergo mitosis involving three rounds of DNA replication followed by cytokinesis forming eight

slender, flagellar-shaped and highly motile male gametes (Garnham, 1966; Kooij and Matuschewski, 2007). This process is triggered by a sudden drop in temperature from the warm-blooded mammalian environment to the ambient temperature in the mosquito midgut (approximately 5^{o}C cooler), a change in pH (from 7.2 to about 8), and mosquito factors for example xanthurenic acid, a by-product of eye pigment synthesis (Billker et al., 1998; Billker et al., 1997).

The male and female gametes undergo fertilization to form a diploid zygote (Figure 1.2). Within 24 hours, the zygote develops into a motile form called an ookinete. The ookinete grows in size and male and female nuclei fuse (Garnham, 1966). The motile ookinete traverses the basal lamina of the mosquito midgut (Garnham et al., 1962) and transforms into an oocyst (Garnham et al., 1969). Here it secretes a thin cyst wall and grows in a sphere. The cyst projects outwards into the haemocoelumina cavity from which it is separated by the remnants of the intestinal coat. The diploid nucleus undergoes a meiotic division followed by mitotic divisions producing a multinucleated oocyst (Garnham et al., 1969). The multinucleated oocyst then matures and differentiates by invagination of the parasite membrane to form sporozoites (Garnham, 1966; Sinden and Strong, 1978). The mature oocyst bursts and thousands of haploid sporozoites are released into the haemocoel, which then migrate to the salivary glands ready for the next infection of a human host (Garnham, 1966) (Figure 1.2).

1.3 Invasion of red blood cell by merozoites

The merozoite is a unicellular, egg shaped cell approximately 1.5 μm in length. This makes it the smallest invasive stage of *Plasmodium*; smaller than the ookinete (10-13 μm), sporozoite (12-15 μm) and the *Toxoplasma* invasive form, the tachyzoite (around 7.5 μm) (Baum et al., 2008a) (Figure 1.1). The narrow pointed end of the merozoite contains the apical complex formed by secretory organelles as mentioned earlier (Section 1.2) (Figure 1.1). It also contains the apical polar ring which acts as a microtubule organising centre (Morrissette and Sibley, 2002). Behind the apical complex towards the posterior end, lie the nucleus, apicoplast and a mitochondrion.

Beneath the plasma membrane of the merozoite there is a continuous double membrane structure called the inner membrane complex (IMC) (Bannister et al., 2000a). The parasite cytoskeleton consists of two or three microtubules situated on the inner surface of the IMC (Figure 1.1) (Morrissette and Sibley, 2002). The merozoite invades the red blood cell in a number of steps including attachment, reorientation and penetration (Figure 1.4) (Cowman and Crabb, 2006). These processes involve receptor recognition and protein secretion from secretory organelles accompanied by shedding of the parasite's surface coat digested by intramembrane proteases called rhomboid proteases which are located at the posterior surface of the parasites (Baker et al., 2006). A study in *Toxoplasma* has demonstrated that the cleavage activity on adhesins occurs within their transmembrane domains in tachyzoites (Brossier et al., 2005; Dowse et al., 2005; Opitz et al., 2002). In addition, the second protease that might be involved in parallel with rhomboids is PfSUB2, an integral membrane subtilisin-like protease (Harris et al., 2005). PfSUB2 is a micronemal protein released onto the parasite surface and localised at the parasite's posterior pole before invasion (Harris et al., 2005). Invasion is completed within seconds, with the junction moving at 1-10 μm/s to the posterior pole of the parasite (Dvorak et al., 1975; Holder and Veigel, 2009).

1.3.1 Attachment to red blood cell surface

The initial attachment of the merozoite involves specific molecular interactions (Gaur et al., 2004). Host cell receptor recognition is thought to depend largely on merozoite surface proteins containing a glycosylphosphatidylinositol (GPI) anchor. The GPI anchored proteins are the most abundant proteins that coat the surface of the merozoite via attachment of the C-terminus to the plasma membrane. These proteins are the merozoite surface protein family (MSP-1, 2, 4, 5, 8 and 10) (Black et al., 2003; Black et al., 2001; Gerold et al., 1996; Marshall et al., 1997; Marshall et al., 1998), and Pf12, Pf38 and Pf92 (Sanders et al., 2005). In addition, all of the GPI anchored merozoite surface proteins (except MSP-2) possess an epidermal growth factor (EGF)-like domain or a six-cysteine domain at their C terminus, which might have a role in protein-protein interactions including receptor-binding functions (Gaur

et al., 2004; Sanders et al., 2005). Other merozoite surface proteins such as MSP-3, MSP-6, MSP-7 and MSP-9 (acidic basic repeat antigen, ABRA) are peripheral membrane proteins, associated with the merozoite surface by virtue of an interaction with directly anchored membrane proteins (McColl and Anders, 1997; Pachebat et al., 2001; Stahl et al., 1986; Trucco et al., 2001; Weber et al., 1988).

The most extensively studied protein in this group that may mediate initial binding to the red blood cell is MSP-1 (Holder et al., 1985). Studies in *P. falciparum* have shown that MSP-1 undergoes extensive proteolytic processing (Blackman et al., 1996; Blackman et al., 1991; Holder et al., 1987) by SUB1 (Koussis et al., 2009) and SUB2 (Harris et al., 2005) during late schizogony and after merozoite release. In *P. falciparum*, MSP-1 is cleaved into 4 fragments with masses: 83 kDa (N-terminus), 30 and 38 kDa (central regions), and 42 kDa (C terminus) (Holder et al., 1987). The 42 kDa C-terminal fragment which is attached to the parasite's plasma membrane (Gerold et al., 1996) is further cleaved into a 33 kDa fragment that is shed during invasion and a 19 kDa membrane bound fragment that remains attached to the merozoite surface after invasion (Blackman et al., 1996; Blackman et al., 1991). Antibodies directed to MSP-1_{42} (Singh et al., 2003) and MSP-1_{19} (Daly and Long, 1993; Kumar et al., 1995; Ling et al., 1994) have been shown to protect against parasite challenge. These findings highlighted the crucial role of MSP-1 in red blood cell invasion. In addition, the full length MSP-1 was found to bind erythrocytes in a sialic acid-dependent manner, while the processed MSP-1_{42} together with MSP-9 (ABRA) form a co-ligand complex that binds to band 3, the anion transport glycoprotein present on the red blood cell surface (Goel et al., 2003; Kariuki et al., 2005; Li et al., 2004).

1.3.2 Tight or moving junction formation

From electron microscopy analysis, during invasion the moving junction between the parasite and host cell travels from the anterior to the posterior end of the merozoite (Aikawa et al., 1978). This movement is driven by the actin-myosin motor complex that lies between the plasma membrane and inner membrane complex of the

merozoite (Figure 1.6). Invasion is activated by direct binding of ligands at the apical end of the parasite with red blood cell surface receptors (Gaur and Chitnis, 2011). Duffy binding-like (DBL) proteins such as EBA-175, EBA-140, EBA-181 and EBL1 are thought to mediate the interaction with red blood cell receptors. EBA-175 and EBA-140 bind to glycophorin A and C, respectively (Lobo et al., 2003; Maier et al., 2003; Sim et al., 1994). Another parasite ligand EBL1 has been shown to bind red blood cell receptor, glycophorin B (Mayer et al., 2009). The *P. falciparum* reticulocyte binding proteins (PfRh1, PfRh2a, PfRh2b, PfRh4 and PfRh5) also play their part in red blood cell binding at this stage (Baum et al., 2009; Triglia et al., 2011; Triglia et al., 2009). PfRh4 and PfRh5 have been demonstrated to bind red blood cell receptors known as complement receptor 1 (CR1) (Tham et al., 2010) and Basigin (Crosnier et al., 2011), respectively. The differential expression of PfRh proteins has been implicated in multiple pathways of invasion (Baum et al., 2005). For example, some strains of *P. falciparum* were able to switch their red blood cell receptor preference by expression of PfRh4 (Stubbs et al., 2005). The possible involvement of DBL and PfRh proteins in mediating the tight junction formation could not be excluded because these proteins are located at the tight junction during merozoite invasion (Baum et al., 2009; Triglia et al., 2011; Triglia et al., 2009) and most of them can be cleaved by *P. falciparum* rhomboids (Baker et al., 2006). However, any direct association of DBL or PfRh with the actin myosin motor remains to be established.

There are two proteins that are proposed to mediate the interaction between the red blood cell surface receptors and the parasite actin myosin motor complex. One of them is merozoite thrombospondin-related anonymous protein (MTRAP) (Baum et al., 2006b). This protein plays a similar role to sporozoite TRAP in liver cell infection (Kappe et al., 1999; Sultan et al., 1997). Both proteins are type I membrane proteins, with a single membrane spanning helix, a large external domain and a relatively short cytoplasmic region (Morahan et al., 2009). Both proteins can bind to aldolase through an interaction involving a crucial tryptophan residue in their C terminal cytoplasmic tails (Baum et al., 2006b; Bosch et al., 2007a; Buscaglia et al., 2003; Jewett and Sibley, 2003). Aldolase is a glycolytic enzyme that is associated with actin in the actin-myosin motor complex of apicomplexan parasites (Buscaglia

et al., 2003; Jewett and Sibley, 2003) (Figure 1.6). MTRAP has been reported to bind the red blood cell through its thrombospondin repeat domain (TSR) (Uchime et al., 2012). Another merozoite protein that has been shown to interact with aldolase is apical membrane antigen-1 (AMA-1) (Srinivasan et al., 2011). Similar to PfRh proteins, MTRAP is cleaved by *P. falciparum* rhomboids (Baker et al., 2006) and AMA-1 is cleaved by both rhomboids (Baker et al., 2006) and SUB2 (Harris et al., 2005).

AMA-1 is translocated from the micronemes to the merozoite surface and concentrated at the apical pole before the invasion. Antibodies specific to AMA-1 blocked the reorientation of the merozoite (Mitchell et al., 2004) and hence abolished apical attachment. AMA-1 is also a type I integral membrane protein that is expressed in the late schizont stage of the asexual life cycle of the parasite (Hodder et al., 1996). The *P. falciparum* AMA-1 molecule is expressed as an 83 kDa precursor from which an N terminal prodomain (Narum and Thomas, 1994) is cleaved resulting in a mature 66 kDa form that is located in the micronemes (Bannister et al., 2003; Healer et al., 2002). AMA-1 is further proteolytically processed during its translocation to the merozoite surface resulting in a 44-48 kDa fragment (Dutta et al., 2003; Howell et al., 2001). Expression of the rodent-restricted *P. chabaudi* AMA-1 in *P. falciparum* led to an increase in the parasite's ability to invade mouse red blood cells (Triglia et al., 2000). These results indicate an important role for AMA-1 in the invasion of red blood cells, specifically in initial apical attachment of the merozoites to specific (as yet unidentified) red blood cell proteins. The AMA-1 binding partners, rhoptry neck protein 2 and 4 (RON 2 and RON 4) are secreted prior to junction formation (Riglar et al., 2011; Srinivasan et al., 2011). RON 2 and RON 4 have been localised to the outer and inner red blood cell surface respectively, before forming a complex with AMA-1 that acts as a "molecular seal" of the tight junction (Riglar et al., 2011) . Other RONs such as RON 5 and RON 8 (restricted to the coccidia) have also been proposed to participate in this complex formation and were found to be localised to the moving junction (Richard et al., 2010; Straub et al., 2009).

1.4 Biogenesis of the inner membrane complex and actin-myosin motor complex assembly in apicomplexan parasites

The assembly of motor complex protein components starts during cytokinesis in the parasite. In general, cytokinesis occurs as a final step during cell division right after DNA replication. In animal cells, this process relies on the formation of an actin/myosin based contractile ring that forms in the middle of the anaphase spindle which serves as a plane for the cell to divide (D'Avino et al., 2006; D'Avino et al., 2005). The situation is different for apicomplexan parasites, where the production of daughter cells or new parasite cells involves the internal budding from inside the mother cell. In *Toxoplasma*, the plasma membrane of the mother cell invaginates around the daughter cells to form the pellicle of the mature daughter cell in a process termed endodyogeny (Figure 1.5). In the case of *Plasmodium*, the nuclei move to the periphery of the mother cell prior to daughter cell formation through the appearance of IMC adjacent to the mother cell plasma membrane. This process is termed schizogony, where the daughter cell growth is associated with budding from the surface of the mother cell that generates the daughters with an intact pellicle (Figure 1.5) (Striepen et al., 2007).

The appearance of IMC may serve as a scaffold for the assembly of the daughter parasites. During maturation of daughter cells, the complete set of organelles is transported or organized by de novo synthesis (micronemes, rhoptries) or replication (ER, Golgi, mitochondria and apicoplast) (Hu, 2008; Nishi et al., 2008). Once the daughter cell has completed its maturation process, the parasites will initiate a budding processes or egress, leaving the unwanted material behind in a residual body (Nishi et al., 2008). The apicomplexan IMC is generated by fusion of Golgi-IMC transport vesicles mediated by the specific GTPase Rab11B. The overexpression of a dominant-negative Rab11B caused the ablation of IMC formation hence affecting *T. gondii* daughter cell formation and polarity (Agop-Nersesian et al., 2010). Several proteins residing within the IMC have been identified. IMC1 is a member of the alveolin family, which provide mechanical stability and gliding motility for *T. gondii* (Mann and Beckers, 2001) and *P. berghei* ookinetes and sporozoites (Khater et al., 2004; Tremp and Dessens, 2011; Tremp et

al., 2008). The other new IMC proteins such as glideosome associated proteins with multiple membrane spans (GAPMs) and IMC sub-compartment proteins (ISP1, 2 and 3) have been well characterized in *P. falciparum* (Bullen et al., 2009) and *T. gondii* tachyzoite (Beck et al., 2010) respectively. The latter proteins were also found in the *P. falciparum* genome (Beck et al., 2010).

Another group of proteins that is known to be associated with the outer face of the IMC is the glideosome, the motor complex required for gliding motility and invasion. The actin-myosin motor complex proteins consist of glideosome associated proteins GAP50, GAP45 and myosin tail domain-interacting protein (MTIP) anchoring the myosin A (MyoA) (Baum et al., 2006b; Gaskins et al., 2004; Jones et al., 2006) (Figure 1.6). It has been proposed that the parasite receptor is linked to the actin-myosin motor via aldolase which directly binds to filamentous actin (F actin). When the moving junction is established, MyoA will pull the complex of actin-aldolase-parasite-host receptor rearward and thereby moving the parasite forward into the red blood cell (Figure 1.6) (Baum et al., 2008a).

Glideosome assembly has been studied extensively in *T. gondii*, and has been shown to occur in two stages. The integral membrane protein, GAP50, localises to the IMC first and acts as an anchor for assembly of the remaining motor complex proteins (MyoA, MTIP/MLC and GAP45) (Gaskins et al., 2004). The tetrameric protein complex is only associated with the IMC of the daughter cells at the final stage of parasite replication when the mother cell plasma membrane envelops the two daughter tachyzoites (Agop-Nersesian et al., 2009).

Rab11A has a role in transporting certain plasma membrane receptors via recycling endosomes in eukaryotes (Saraste and Goud, 2007). It has been shown to deliver plasma membrane to the cleavage furrow in animal cells (Fielding et al., 2005; Wilson et al., 2005) and has been localised to the division plane of plant cells (Chow et al., 2008). The apicomplexan Rab11A was first described in *P. falciparum* and is highly expressed in asexual blood stage parasites (Langsley and Chakrabarti, 1996; Quevillon et al., 2003). Further studies of Rab11A have been conducted using *Toxoplasma* where it was found to be associated with rhoptries (Bradley et al., 2005) and the dominant negative version of Rab11A expression reduced parasite growth

(Herm-Gotz et al., 2007). Agop-Nersesian et al. (2009) demonstrated that TgRab11A interacts with MLC and transports vesicles derived from the secretary pathway from Golgi to the plasma membrane of the daughter cells. The authors suggest that the Rab11A-motor complex is disassembled when the vesicle fuses to the daughter plasma membrane, upon which the trimeric glideosome motor complex associates with GAP50 at the IMC (Agop-Nersesian et al., 2009).

1.5 Actin-myosin motor complex of *P. falciparum*

The actin-myosin motor complex, an essential component for the invasion machinery is conserved across apicomplexan zoites such as *Plasmodium* ookinetes, sporozoites, merozoites and *Toxoplasma* tachyzoites (Baum et al., 2006b; Bergman et al., 2003; Buscaglia et al., 2003; Gaskins et al., 2004; Herm-Gotz et al., 2002; Jewett and Sibley, 2003; Johnson et al., 2007; Jones et al., 2006; Keeley and Soldati, 2004; Meissner et al., 2002; Pinder et al., 2000; Pinder et al., 1998).

1.5.1 Inter-relationship between myosin A and actin

Myosin is a motor protein that binds to actin filaments. As a functional protein, myosin "walks" along the actin filaments towards the barbed end using energy derived from the actin-activated hydrolysis of myosin-bound ATP. Myosin is made of three structural regions: the head, the neck, which are conserved, and the tail which confers the specific function of different myosin classes (Pinder et al., 2000). To date, myosin has been grouped into 24 classes based on comparisons and phylogenetic analysis of the conserved motor domain. The conventional myosins, which are involved in the contraction and relaxation of skeletal and smooth muscle belong to class II (Foth et al., 2006). In *P. falciparum*, myosin proteins were grouped into class XIV (MyoA, MyoB and MyoE), XXII (MyoF, previously known as MyoC) and VI (MyoJ and MyoK, previously known as MyoD and MyoF respectively) (Foth et al., 2006). The type XIV myosins are very small in size (~90 kDa), without a recognizable neck region, single headed and have a very short C-

terminal tail (Farrow et al., 2011). So far, there are 4 different myosin reported to be expressed in *P. falciparum* blood stages, MyoA, MyoB, MyoF (previously known as MyoC) (Pinder et al., 2000) and MyoJ (previously known as MyoD) (Chaparro-Olaya et al., 2005).

Plasmodium myosin A is essential for gliding motility in ookinetes (Siden-Kiamos et al., 2011; Siden-Kiamos et al., 2006b), sporozoites (Bergman et al., 2003; Matuschewski et al., 2001) and red blood cell invasion by merozoites (Pinder et al., 1998). It was found to be localised between the parasite inner membrane complex (IMC) and parasite membrane, predominantly towards the apex (Pinder et al., 2000; Pinder et al., 1998). PfMyoA binds to actin to generate force and movement into the red blood cell, supported by the moving junction complex. By *in vitro* motility assay, PfMyoA moves actin filaments at speeds of 3.51 μm/s, a speed similar to TgMyoA and actin skeletal muscle myosin II (Green et al., 2006). Based on mechanical studies as demonstrated using single molecule optical tweezers, PfMyoA produces a short-lived working stroke of 5 nm (again similar to TgMyoA and skeletal muscle myosin II) (Farrow et al., 2011) suggesting several molecules must be coupled together in order to keep hold of an individual actin filament.

Pfactin is known to form short filaments *in vitro* (~100 nm) (Schmitz et al., 2005). Pfactin polymerisation is tightly regulated by depolymerizing binding partners such as profilin, cofilin and CAP. Given the short actin filament produced, it might be localised around or close to the moving junction, rather than running the length of the parasite (Holder and Veigel, 2009). This was further supported by a recent 3D immunofluorescent microscopy study (3D SIM) conducted using the antibody with high preferential binding to the apicomplexan polymerized actin (anti-$Act_{239-253}$) (Angrisano et al., 2012). This experiment has demonstrated the localisation of *Plasmodium* filamentous actin at the tight junction (the ring like formation) during merozoite invasion. The breakdown of the ring like formation pattern of polymerized actin upon treatment with a high concentration of the marine sponge cyclodepsipeptide Jasplakinolide (JAS) (agent that binds and stabilizes the actin filament) suggests that the actin polymerisation is dependent on filament turnover (Angrisano et al., 2012). In *Plasmodium*, the major proteins responsible for

nucleation of actin polymerization, such as the ARP2/3 complex, are absent (Gordon and Sibley, 2005). Instead, this process is controlled by polymerizing factor called PfFormin-1(Baum et al., 2008b). Formin-1 localises beneath the cell membrane with a concentration at the apical region of the merozoites prior to invasion (Baum et al., 2008b). Apicomplexan formin, together with capping protein, directs actin polymerization at the barbed end. The filamentous actin (Factin) will form the templates for moving junction formation especially by bridging the aldolase, an abundant glycolytic enzyme and MyoA which indirectly interacts with the parasite-host cell receptor (Baum et al., 2006a).

1.5.2 Myosin tail domain-interacting protein

P. falciparum myosin tail domain-interacting protein (MTIP) was first found to be expressed and interact with PfMyoA in the sporozoite stage (Bergman et al., 2003). It was also found to be located at the merozoite's periphery (Green et al., 2006; Green et al., 2008). The linkage between the PfMyoA and MTIP has been proposed to provide a stable anchor for myosin and also to contribute to the so-called lever arm of the motor (Green et al., 2006). An orthologue of MTIP, myosin light chain (MLC) was found in *T. gondii* together with other motor complex proteins, TgMyoA, TgGAP45 and TgGAP50 forming a protein complex (Gaskins et al., 2004). MTIP has been shown to interact with PfMyoA tail via its C-terminal region (Bosch et al., 2006; Bosch et al., 2007b; Green et al., 2006; Thomas et al., 2010) and form a complex with glideosome associated proteins (GAP45 and GAP50) (Jones et al., 2006) to anchor and immobilize the MyoA at the IMC. The N-terminus of the MTIP homologue, TgMLC1, has been shown to be involved in GAP45 interaction (Frenal et al., 2010).

1.5.3 Glideosome-associated proteins (GAPs)

GAP45 was firstly identified as a 45 kDa protein in *T. gondii* where it was detected at the parasite periphery specifically between the parasite plasma membrane and inner membrane complex, and was shown to be part of the glideosome (MyoA and MLC1 [equivalent to MTIP in *Plasmodium*]) complex (Gaskins et al., 2004). This protein is conserved throughout apicomplexan parasites including *P. falciparum* (Figure 1.7). In addition, it is associated with GAP50, a 50 kDa integral membrane protein that anchors and immobilizes the motor complex or glideosome in the IMC (Johnson et al., 2007). It was demonstrated that GAP45 and GAP50 assemble into the motor complex at different stages. By pulse chase experiment, the complex of MyoA, MLC1, and GAP45 is formed first in a soluble form which associates later with GAP50 at the IMC. These results showed that TgGAP45, TgMLC1, and TgMyoA are synthesized on cytoplasmic ribosomes and associate co-translationally. On the other hand, GAP50 is targeted for the secretory pathway by insertion into the parasite endoplasmic reticulum and is transported to the IMC (Gaskins et al., 2004).

In *Plasmodium*, GAP45 was also found to be in a similar location as in *Toxoplasma*, localized to the IMC (Baum et al., 2006b). PfGAP45 also forms a complex with MyoA, MTIP, and PfGAP50 and is highly expressed at late schizont stage (Jones et al., 2006). PfGAP45 was suspected to undergo post translational modification as it appeared as multiple bands on SDS-PAGE (Jones et al., 2006). Studies by Rees-Channer and co-workers showed that PfGAP45 can be myristoylated *in vitro* and *in vivo*. In addition palmitoylation of PfGAP45 in parasite cultures was coincident with the binding of the protein to GAP50. The dual acylation of PfGAP45 may be needed for a strong binding to GAP50 and also to the membrane compartment of the IMC (Rees-Channer et al., 2006). GAP45 was also found to be a phosphorylated protein in both *P. falciparum* and *T. gondii* (Gilk et al., 2009; Green et al., 2008; Solyakov et al., 2011; Treeck et al., 2011). The amount of PfGAP45 in a phosphorylated form was increased from early to late schizont stages of *P. falciparum*, which paralleled the increase in the level of calcium dependent protein kinase 1 (CDPK1) and protein kinase B (PKB) expression. Both CDPK1 and PKB

are enzymes implicated in GAP45 phosphorylation (Green et al., 2008; Thomas et al., 2012; Vaid et al., 2008).

In addition, there is another relatively recently identified GAP protein in *T.gondii*, GAP40, which is also found to be expressed in *P. falciparum* (Frenal et al., 2010). This protein was demonstrated to co-precipitate with other motor complex proteins in *T. gondii*. However, the function of this protein remains to be elucidated.

1.6 Protein phosphorylation in human health and disease

Protein phosphorylation and dephosphorylation is a biochemical process catalysed by protein kinases and protein phosphatases through respectively adding or removing a phosphate group to a serine, threonine or tyrosine using ATP as a phosphoryl donor. Protein phosphorylation was firstly found to be important in eukaryotic cells in the 1950s. It started with the discovery of metabolic enzyme phosphorylase which is responsible for the conversion of glycogen to glucose-1-phosphate (Krebs and Fischer, 1955). Phosphorylase is activated by phosphorylase kinase, the protein kinase that catalyses the attachment of phosphate to phosphorylase (Fischer and Krebs, 1955), which itself is sequentially activated by protein kinase A (PKA), a cyclic AMP-dependent protein kinase (Hayes and Mayer, 1981). Since then protein phosphorylation has been implicated in most physiological processes such as the cardiovascular system, gastrointestinal action, neurologic mechanism and behaviour, immune response regulation, endocrine action and musculoskeletal regulation (Tarrant and Cole, 2009). Protein phosphorylation is important in controlling protein function such as by modulating its biological activity, by affecting the protein's stability, by regulating movement between subcellular compartments, or by initiating or disrupting protein-protein interactions (Cohen, 2002).

Here are a few examples showing the importance of protein phosphorylation which demonstrates the above functions. The phosphorylation of retinoblastoma (Rb) is important in regulating the progression of the cell cycle. Retinoblastoma which is one of the tumour suppressor proteins, functions to arrest the cell cycle at early G1

phase by associating with the transcription factor complex, E2F, inhibiting gene expression required for the transition from the G1 into the S phase. Once the cell is ready for the next cell cycle progression, Rb will be phosphorylated by cyclin dependent kinase/cyclin complexes hence dissociating the Rb from E2F and activating the cell cycle progression into S phase and G2/M (Knudsen and Knudsen, 2006).

The kinase enzyme can be activated by phosphorylation by another kinase. This has been shown by the cascade activation of mitogen-activated protein kinase (MAPK) which is important in regulating cell proliferation and differentiation. The cascade activation is started by the extracellular signal that mediates the activation of Raf kinase. Raf kinase then phosphorylates MAP kinase kinase (MAPKK). Activated MAPKK then phosphorylates MAPK. This will lead to the activation of MAPK which then phosphorylates a number of substrates that are important in regulation of gene expression for cell proliferation (Avruch et al., 2001; Seger and Krebs, 1995).

Protein phosphorylation is important in targeting the phosphorylated protein for proteasome degradation. One good example is the Wnt signalling mechanism. This pathway is important in embryogenesis and adults' cell proliferation. It is regulated by the protein called β-catenin. In the absence of Wnt signal, β-catenin is bound to the destruction complex that contains adenomatous polyposis coli protein (APC)-axin-glycogen synthase kinase-3 (GSK3). This will lead to the phosphorylation of β-catenin by GSK-3. The phosphorylated β-catenin is targeted for degradation by ubiquitin mediated proteolytic destruction. In the presence of Wnt, destruction complex is destroyed hence allowing the β-catenin to accumulate and localise to the nucleus (Peifer and Polakis, 2000).

About 30% of human proteins are phosphorylated. There are 500 protein kinases and a third of that number of protein phosphatases encoded by the human genome (Cohen, 2001, 2002). Abnormal phosphorylation has been implicated in major human diseases such as cancer and diabetes resulting from the mutation of particular protein kinases and phosphatases. A good example for this is a chronic myelogenous leukemia (CML). It is a blood cancer caused by Philadelphia chromosome, a chromosomal abnormality causing the fusion of Abelson (Abl)

tyrosine kinase gene and break point cluster region (Bcr), to produce the constitutively active Bcr-Abl tyrosine kinase (Faderl et al., 1999). One of the effects of the constitutively active Bcr-Abl tyrosine kinase is the down regulation of the tumour suppressor gene (CCN3) (McCallum et al., 2006) which will lead to the rapid growth of abnormal white blood cells in bone marrow. The tyrosine phosphorylation is needed in insulin signalling pathway to store the excessive glucose in glycogen form (Chang et al., 2004). Deletion of the tyrosine kinase domain of the insulin receptor is one of the causes of insulin resistance in diabetes Mellitus type 2 patients (Taira et al., 1989).

Thus several kinase and phosphatase inhibitors have been developed to be used in the treatment of the affected diseases. The first therapeutic protein kinase and phosphatase inhibitors were developed in the 1990s. They were first used as immunosuppressive drugs. Cyclosporine and FK506, indirectly cause a reduction in activity of the protein phosphatase calcineurin, and rapamycin inhibits the protein kinase mTOR (mammalian target of rapamycin), hence affecting interleukin-2-dependent T cell proliferation (Liu et al., 1991). These drugs have been widely used in organ transplantation. In addition, another drug, the Abl tyrosine kinase inhibitor imatinib (Gleevec), was developed for treatment of patients with chronic myelogenous leukemia (CML) (Capdeville et al., 2002).

Naturally occurring toxins and pathogens can also exert their effects by altering the phosphorylation states of proteins. The natural occurring toxin okadaic acid, a potent inhibitor of Type 1 and 2A protein phosphatases (serine/threonine protein phosphatases) is produced by shellfish and can cause diarrhetic seafood poisoning (Cohen, 2001; Cohen et al., 1990). Another Type 1and 2A protein phosphatase inhibitor is cyclic heptapeptide microcyctin, a powerful hepatoxin and neurotoxin that is produced by blue-green algae (MacKintosh et al., 1990). At much lower concentrations microcyctin can cause liver cancer which has been reported in certain parts of China due to microcyctin water pollution (Carmichael, 1994; Cohen, 2001).

In *Yersinia pestis* bacterial infections (the pathogen that causes bubonic plague), host cell protein signal transduction mechanisms are broken down by the

activity of a bacterial phosphatase. This affects many cell types, and results in serious disease (Guan and Dixon, 1990). Other than that, common diseases such as diarrhoea caused by enteropathogenic *Escherichia coli* (EPEC) infection involve the dysregulation of host cell kinases. During EPEC infection, an attachment/effacement (A/E) lesion on the intestinal surface is created. The EPEC protein, Tir was secreted by the bacteria into the host cell plasma membrane to act as a receptor for an EPEC outer membrane protein, intimin. Delivery of Tir into the host cell results in its phosphorylation by the host tyrosine kinase and protein kinase A, followed by Tir–intimin binding. This will initiate actin nucleation at the binding site hence induce lesion formation. The lesion formation results in a loss of absorption surface of the intestine causing diarrhoea (Goosney et al., 2000; Reis and Horn, 2010).

1.7 The importance of protein phosphorylation in the *Plasmodium* life cycle

The human genome encodes more than 500 protein kinases (Kostich et al., 2002; Manning et al., 2002). Most protein kinases show conserved amino acid sequence elements and a common structural fold of their catalytic domain consisting of amino-terminal (for ATP-binding) and carboxy-terminal (for peptide binding and phosphotransfer) lobes connected with the hinge region (Hanks, 2003). The eukaryotic protein kinases are distributed in seven major groups : CK1 (casein kinase 1), CMGC (CDK [cyclin-dependent protein kinase], GSK3 [glycogen synthase kinase 3] and CLK [CDK-like kinase]), TKL (tyrosine kinase-like), AGC (PKA [cyclic adenosine monophosphate dependent protein kinase], PKG [protein kinase G], PKC [protein kinase C] and related proteins), CamK (calcium/calmodulin-dependent protein kinase), STE (protein kinases acting as regulators of MAPKs), Tyr K (tyrosine kinase) and OPK (other protein kinase) (Doerig et al., 2008; Hanks, 2003).

Smaller eukaryotes such as *Plasmodium falciparum* also share a similar phylogenetic tree of metazoan protein kinases, with some divergences. With 86 to 99 eukaryotic protein kinase related enzymes (depending on the stringency applied to

include borderline sequences) some of the kinases show quite distinct behaviour in terms of kinase regulation, in addition the absence of certain kinases emphasises the existence of novel pathways that could be manipulated for drug targeted intervention. The differences are the apparent lack of Tyr K and STE families, the presence of a family of calcium-dependent protein kinases (CDPKs) that carry a kinase domain fused to a calmodulin-like domain, and the presence of protein kinases with a lack of clear mammalian eukaryotic protein kinase orthologues (Doerig et al., 2008). The identification of many protein kinases and also protein phosphatases (27 phosphatase genes have been identified in the *P. falciparum* genome) shows the importance of protein phosphorylation in the *Plasmodium* life cycle including cell cycle, cell proliferation and differentiation, parasite egress, invasion and host-parasite interaction (Chung et al., 2009). This is clear, with the identification of over 5000 protein phosphorylation sites, including tyrosine residues, on *P. falciparum* proteins made in recent studies (Solyakov et al., 2011; Treeck et al., 2011).

Studies involving genetic manipulation of *Plasmodium* parasites have demonstrated the importance of kinases throughout the *Plasmodium* life cycle in processes such as gamete formation, ookinete gliding, sporozoite behaviour and schizogony (Figure 1.9). In gamete formation, PbCDPK4 was identified to be essential for male gamete maturation (Billker et al., 2004) (Figure 1.9). Another kinase that is responsible for male gamete formation is PfMap2 (atypical mitogen activated protein kinase) which can be activated by PfCDPK4 phosphorylation *in vitro* (Tewari et al., 2005) (Figure 1.9). Other than calcium dependent signalling, the role of cGMP (cyclic GMP) in mediating gamete formation has been highlighted suggesting the involvement of PKG (protein kinase G) upstream of this process, particularly in inducing the differentiation of gametocytes to become spherical ("rounding up") (McRobert et al., 2008). The "rounding up" of gametocytes is a part of the process of gamete formation that happens upon entering the mosquito midgut.

CDPK3 (Ishino et al., 2006; Siden-Kiamos et al., 2006a) and PKG (Moon et al., 2009) have also been found to be essential in ookinete motility (Figure 1.9). Both *P. berghei* CDPK6 (Coppi et al., 2007) and PKG (Falae et al., 2010) have also been reported to be involved in sporozoite infectivity and merosome release at the liver

stage respectively. In addition, deletion of a membrane bound adenylyl cyclase, (PbACα) perturbs sporozoite motility (Ono et al., 2008) (Figure 1.9) suggesting the involvement of a cAMP (cyclic AMP) dependent pathway which may involve PKA in switching to the cell invasion mode of the sporozoite.

In asexual blood stage parasite development, PfPKA (Leykauf et al., 2010), PfCDPK1 (Green et al., 2008) and PKB (protein kinase B) (Vaid et al., 2008) have been shown to likely be involved in merozoite invasion, as these kinases are able to phosphorylate AMA1 (by PKA) and motor complex protein (MTIP and GAP45 by CDPK1; GAP45 by PKB). Further development of blood stages or schizogony was interrupted by the inhibition or degradation of PfPKG (Taylor et al., 2010) and PfCDPK5 (Dvorin et al., 2010) respectively. Other kinases such as *P. falciparum* protein kinase 2 (PfPK2), a human homolog of calcium calmodulin dependent protein kinase, has been reported to be expressed in merozoites. The invasion of merozoites was inhibited by the PfPK2 inhibitor, a calmodulin antagonist called W-7 (Kato et al., 2008a).

Of all the *Plasmodium* protein kinases, CDPKs as well as PKG have been well studied to date. The CDPKs are promising drug target candidates as there is no mammalian homologue. The studies on CDPKs are also influenced by their regulator, calcium, which is known to play an important role in several stages of the apicomplexan life cycle such as gamete maturation, secretion of adhesins from the micronemes, gliding motility, cell invasion and egress (Moreno and Docampo, 2003).

1.8 Calcium-dependent protein kinases

Calcium is a molecule that acts as a messenger in signal transduction processes in both animal and plant cells. These processes often lead to activation or inactivation of certain protein functions, especially kinases such as the calcium-dependent protein kinase family (CDPKs), which control many aspects of living organisms. CDPKs form an unusual protein kinase family that so far has only been found in plants and alveolates including the apicomplexan parasites such as *Plasmodium* and

Toxoplasma (Billker et al., 2009; Harper and Harmon, 2005). Generally, CDPK is an enzyme that consists of an N-terminal kinase domain that is fused with a calmodulin like domain (CaM-LD). The CaM-LD contains 4 EF hands that bind calcium ions (Harper et al., 1991). A study by Wernimont and colleagues on TgCDPK1 has demonstrated that CaM-LD was integrated with an autoinhibitory region containing pseudosubstrate sequence known as a CDPK-activating domain (CAD) (Figure 1.8) (Wernimont et al., 2010). In the absence of calcium, CAD interacts with the kinase domain preventing the access of substrate to the active site. Upon calcium-CAD binding, the CAD domain moves to a different position on the kinase domain, opposite the catalytic pocket (ATP binding site), hence exposing the kinase active site for substrate binding (Figure 1.8) (Wernimont et al., 2010).

In plants, CDPK is an abundant protein kinase family that has been estimated to have 27 and 34 isoforms in *Oryza sativa* and *Arabidopsis,* respectively (Harper and Harmon, 2005). It was found to be a multifunctional enzyme family as members phosphorylate more than one substrate for different cellular processes. It plays an important function in carbon, nitrogen and sulphur metabolism, secondary metabolism and defence responses, ethylene synthesis, phospholipid metabolism, ion and water transport, cytoskeleton regulation, transcription, proteosome regulation and fertilization regulation (Harper and Harmon, 2005).

There are five major classes of apicomplexan CDPK, based on their different domain structures (Billker et al., 2009). The first group of CDPK is similar to the plant CDPKs and consists of an N-terminal kinase domain and 4 EF hands. The short N terminal region of some members of this group has been reported to be acylated, as shown for PfCDPK1 (Moskes et al., 2004) and PfCDPK4 (Ranjan et al., 2009). There are other apicomplexan CDPKs, including orthologues in *T. gondii* and *C. parvum:* TgCDPK1 and TgCDPK3, and CpCDPK1 and CpCDPK3, respectively (Billker et al., 2009). The second group of CDPKs have a long N-terminal extension (PfCDPK3 and PfCDPK5 together with their orthologues from *C. parvum* and *T. gondii*) (Billker et al., 2009). A third group of these kinases are only found in *T. gondii* and *C. parvum* where the kinases, TgCDPK4A, TgCDPK4, TGCDPK8 and CpCDPK4 only contain three C-terminal EF hands. The fourth group contains two or

three EF hands but they are situated at the N-terminal end and connected to the kinase domain via a plekstrin homology domain (PH), referred as CDPK7 which only exist in *T. gondii* and *P. falciparum*. Finally, there is also a CDPK group that has one or more EF hands at their N- and C-termini, such as PfCDPK6 (Billker et al., 2009).

The function of CDPKs has been highlighted in regulating the growth of apicomplexan parasites such as *Plasmodium* and *Toxoplasma*. As in plants, these CDPKs seem to phosphorylate quite a number of substrates *in vitro* (Green et al., 2008; Kato et al., 2008b; Kugelstadt et al., 2007). In *Plasmodium*, CDPKs have been reported to play an important role in merozoite invasion (CDPK1) (Green et al., 2008) and egress (CDPK5) (Dvorin et al., 2010) in the blood stage, male gametogenesis (CDPK4) (Billker et al., 2004), and ookinete (CDPK3) (Ishino et al., 2006; Siden-Kiamos et al., 2006a) differentiation in the mosquito stage, and sporozoite infectivity in the liver stage (CDPK6) (Coppi et al., 2007) (Figure 1.9). In *Toxoplasma*, there are only two CDPKs that are well studied. The TgCDPK1, an orthologue of PfCDPK4, was found to be important in *Toxoplasma* tachyzoite motility. Treatment with KT5926, a general CDPK inhibitor (although the selectivity of this inhibitor towards TgCDPK1 is uncertain), inhibited TgCDPK1 activity and blocked parasite attachment to host cells (Kieschnick et al., 2001). Further study on TgCDPK1 by conditional knockout and analysis of gatekeeper mutants revealed the essentiality of this enzyme in regulating exocytosis through microneme secretion (Lourido et al., 2010). TgCDPK3, the orthologue of PfCDPK1, was found to be localised at the apical end of tachyzoites. It was shown to phosphorylate *T. gondii* aldolase 1 (TgALD1) *in vitro* and was found to be in a complex with TgALD1 by a co-immunoprecipitation assay, suggesting the involvement of TgCDPK3 in the motility of *T. gondii* through the phosphorylation of the glideosome complex (Sugi et al., 2009).

1.9 The relevance of GAP45 phosphorylation by CDPK1

The mechanism of motor complex regulation is still not clearly defined. A previous study found that GAP45 was phosphorylated *in vivo* (Green et al., 2008). GAP45 has also been reported to be a substrate for calcium-dependent protein kinase 1 (CDPK1) and protein kinase B (PKB) *in vitro* thus highlighting the potential importance of phosphorylation in regulating the parasite motor complex machinery (Green et al., 2008; Vaid et al., 2008). These observations are further supported by the involvement of calcium regulation during *Plasmodium* growth and invasion (Billker et al., 2009) as both of the kinases, CDPK1 and PKB, are dependent on calcium for their activity. The importance of GAP45 phosphorylation was further supported by studies on its orthologue in the *T. gondii* tachyzoite. Expression of a form of TgGAP45 with phosphomimetic residues affected MyoA-MLC1-GAP45 association with GAP50 without perturbing parasite growth and invasion, or the localisation of GAP45 protein (Gilk et al., 2009). The expression of CDPK1 peaks at the late schizont stage when the merozoite is ready to be released and reinvade red blood cells. Co-localisation of CDPK1 with MTIP, the IMC marker (Green et al., 2008), is consistent with the potential of CDPK1 as a kinase that closely localizes with and phosphorylates parasite motor complex proteins, such as GAP45.

Furthermore, invasion of red blood cells by the merozoite was inhibited by a known CDPK1 inhibitor, Bisindolocarbazole K252a (Green et al., 2008). This compound is related to the KT926 inhibitor that reduced the TgCDPK1 activity *in vitro* (Kieschnick et al., 2001). However, the selectivity and specificity of K252a inhibitor towards PfCDPK1 is doubtful. The *P. falciparum* GAP45 phosphopeptides (peptide 81-96 [DYATQENKSFEEKHLE], 97-112 [DLERSNSDIYSESQKF] and 141-155 [LSEPAHEESIYFTYR]) were detected by MALDI-TOF MS analysis, and are conserved across the *Plasmodium* genus (Figure 1.10). The phosphopeptides contain either one threonine and one to four serine residues than could potentially be phosphorylated. Threonine is probably not to be phosphorylated as the phosphorylated GAP45 did not react with a phosphothreonine specific antibody (Green, J. unpublished). Moreover, the GAP45 peptide 81-96, which is phosphorylated by CDPK1 *in vitro* was also detected in extracts of cultured parasites

(Green et al., 2008). It is likely that S89 in GAP45 peptide 81-96 (DYATQENKSFEEKHLE) is the target site for CDPK1 as it is the only phosphorylatable residue excluding the threonine. The inability to identify the specific phosphorylated residues by mass spectrometry, due to the multiple serine residues in peptides 97-112 and 141-155 of GAP45 has led this study to concentrate on modified recombinant proteins in order to identify specific target residues of CDPK1 in GAP45.

1.10 Aims and hypothesis

GAP45 has been shown to be a substrate for CDPK1 *in vitro* while it was also found to be phosphorylated *in vivo*. These findings suggest the importance of GAP45 phosphorylation, although this is yet to be demonstrated. As it is crucial to demonstrate this event *in vivo*, this study will investigate the role of GAP45 phosphorylation in *P. falciparum* starting from determination of the CDPK1 phosphorylation site(s) leading on to the consequences of its phosphorylation in the parasite.

What is the role of GAP45 phosphorylation in the parasite? There are several possible consequences of GAP45 phosphorylation. It may increase or decrease the affinity of this protein in binding to other motor complex proteins. TgGAP45 phosphorylation was demonstrated to prevent binding of the trimeric motor complex protein, GAP45-MTIP-MyoA, to GAP50 (Gilk et al., 2009). Whether or not the same phenomenon could be happening in *P. falciparum* will be discussed further in this study. Phosphorylation-dephosphorylation of GAP45 might be important in GAP45 localisation to the IMC. As the phosphorylation of this protein begins at early schizont stage, it is possible that phosphorylation might promote the specific localisation of GAP45 protein to the IMC together with other post-translational modifications mentioned earlier such as palmitoylation and myristoylation. Further effects of GAP45 phosphorylation on parasite growth or merozoite invasion will also be monitored.

In order to determine the actual role of GAP45 phosphorylation specifically by CDPK1, it is proposed to carry out experiments that will give a clear picture of GAP45 function. The specific objectives of this study are:

i. To identify the CDPK1 phosphorylation sites on GAP45. *These in vitro experiments can be done by performing site-directed mutagenesis by substituting the serine or threonine residues with alanine. The mutants produced will be further analysed by a CDPK1 kinase assay to determine which mutants exhibit any change in GAP45 phosphorylation. The results will also be further analysed to obtain useful information for further studies.*

ii. To study the role of GAP45 phosphorylation in regulating the actin-myosin motor complex during merozoite invasion and other potential roles in parasite development. *The in vivo experiments will be carried out using P. falciparum 3D7 culture. GAP45 protein and its variants (identified from the first objective) will be tagged with GFP and transfected into P. falciparum, with expression of the protein from an episomal plasmid. The GFP-tagged GAP45 expressing P. falciparum parasites will be isolated and maintained in the culture. The localisation of GFP-tagged GAP45 will be observed and characterized. This will also include a protein-protein interaction study between the motor complex proteins and GFP-tagged GAP45.*

(Baum et al., 2008a)

Figure 1.1: Morphology and conserved organelles of the *P. falciparum* merozoite, ookinete, sporozoite (a) and *T. gondii* tachyzoite (b). Organelles such as rhoptries, exonemes, micronemes and dense granules are important in motility and invasion. Rhoptries secrete proteins involved in host-cell invasion and parasitophorous vacuole formation. Micronemes releases proteins onto the parasite and host surface during parasite invasion. Dense granules released their contents after parasite invasion to establish the parasitophorous vacuole (PV) within the infected host cells. Exonemes contain proteases that are released into the parasitophorous vacuole prior to microneme release, responsible for parasite egress from the host cell. Other structures are nucleus (NUC), sub-pellicular microtubules (MT), inner membrane complex (IMC) and tubulin-rich apical polar rings (APR) with collar (ookinete only) or conoid (tachyzoite only) (Baum et al., 2008a).

(Bannister and Mitchell, 2003)

Figure 1.2: Life cycle of *P. falciparum* in the human host and the *Anopheles* mosquito vector. The infection begins when the *Plasmodium*-infected mosquito bites the host for a blood meal releasing saliva containing sporozoites into the blood stream. Sporozoites are carried to the liver where they invade hepatocytes and multiply into liver merozoites. These merozoites are released into the bloodstream and invade red blood cells to begin the asexual blood-stage of the life cycle. In the

red blood cell, the parasite develops through ring, trophozoite and schizont stages. At the end of the schizont stage, daughter merozoites egress from the red cell. These free merozoites then invade new red blood cells and perpetuate the asexual-blood life cycle. Some parasites will develop into male or female gametocytes in the bloodstream, which are the initial sexual stages of the parasite. These parasites are taken up by a mosquito during feeding and gametogenesis in the mosquito gut results in gamete formation followed by fertilization to form zygotes. Zygotes develop into a motile form called an ookinete, which crosses the midgut wall and transforms into an oocyst. Mature oocysts release sporozoites which then migrate to salivary glands ready for the next infection of a human host.

(Dixon et al., 2008)

Figure 1.3: **Developmental stages of the *P. falciparum* gametocyte in red blood cell.** (A) The morphology of stage I and II is indistinguishable from ring stage asexual parasites. The differences between the gametocyte and the asexual parasite start to become obvious in stage II and III where the gametocyte appears more elongated as a result of subpellicular microtubule network formation. The change in morphology will progress to late stage III and IV when it appears as a crescent shape gametocyte. When it reached stage V (mature stage), the *P. falciparum* gametocyte crescent shape will form a sausage shape as it loses the characteristic of pointed ends due to the depletion of the microtubule network. After the mosquito bloodmeal, the male and female gametocytes will differentiate into micro- and macrogametocytes respectively. (B) The *P. falciparum* gametocyte morphology changes from stage I to V (mature stage) shown in thin blood film stained with Giemsa. The differences between male and female gametocytes can be distinguished at mature stage by the intensity of the stains. The female gametocytes can be identified by the blue appearance in Giemsa stained blood film; by contrast male gametocytes are pink in Giemsa stain. The hemozoin pigment of the female gametocyte is more centralized within the gametocyte, while the hemozoin pigment of the male gametocyte is dispersed throughout the infected red blood cell.

(Cowman and Crabb, 2006)

Figure 1.4: The steps of red blood cell invasion by *P. falciparum* merozoites. A merozoite invades the red blood cell by recognition of surface receptors (A), reorientation and formation of an apical end tight junction contact (B), movement of the tight junction from the apical to posterior pole driven by the actin-myosin motor complex (C and D). During invasion, the surface coat is removed by proteases (E). In the red blood cell, the parasite resides in a special compartment called the parasitophorous vacuole formed during the invasion process (Cowman and Crabb, 2006).

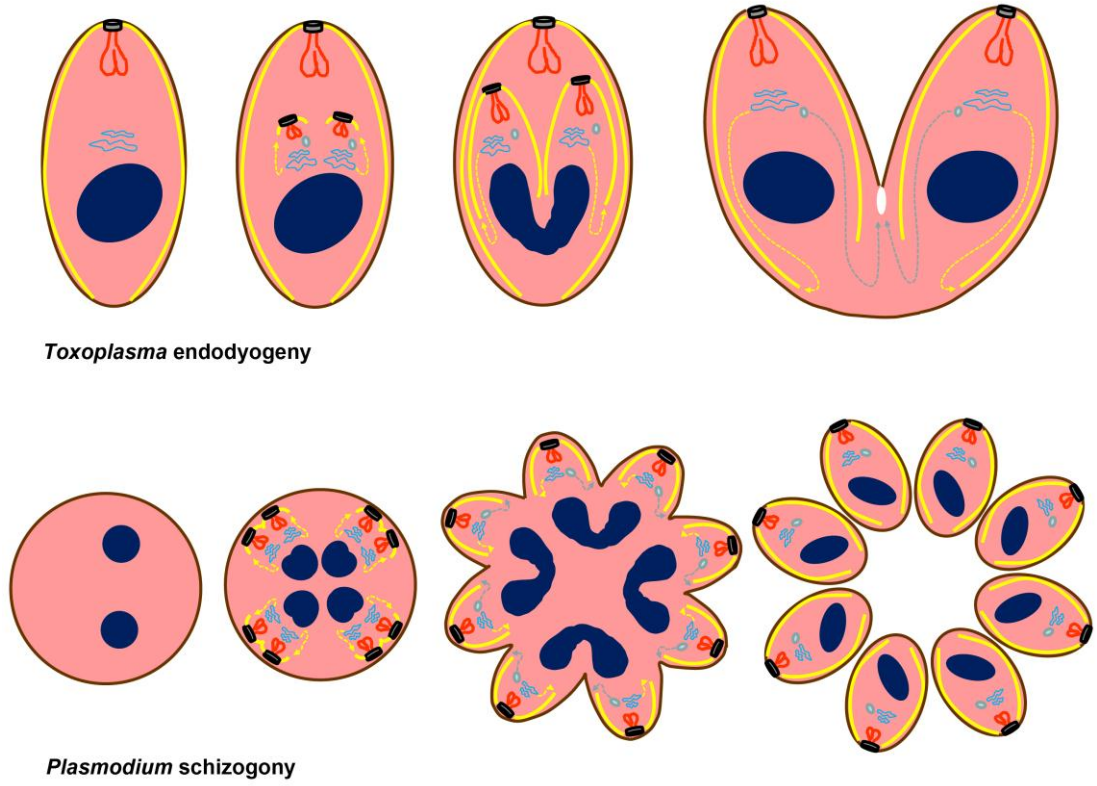

Figure 1.5: The endodyogeny and schizogony of *Toxoplasma* and *Plasmodium* respectively. *Toxoplasma* parasite completes its lifecyle after each round of DNA replication producing 2 daughter cells, the tachyzoites. In contrast *Plasmodium* replicates its DNA (blue) for multiple times (~4 times) to produce 8 to 16 daughter cells, the merozoites. In *Toxoplasma*, the daughter cells are produced within the parasite cytoplasm (pink). The DNA replication proceeds together with the IMC development surrounding daughter cells. The invagination of plasma membrane (brown) from the mother cell occurs later probably with the help or fusion of newly synthesized plasma membrane of daughter cells. In *Plasmodium*, the nuclei move to the periphery of the parasite. The IMC development in the daughter cell of *Plasmodium* occurs together with the plasma membrane invagination. As suggested by Agop-Nersesian et al. for *Toxoplasma*, both plasma membrane generation (grey arrow) and IMC biogenesis (yellow arrow) require components transported by

vesicle and mediated by the proteins, Rab11A and Rab11B respectively. Both vesicle mediated proteins have their orthologues in *Plasmodium* which suggests a similar kind of IMC and plasma membrane generation could happen in this parasite (Agop-Nersesian et al., 2010; Agop-Nersesian et al., 2009; Striepen et al., 2007). Other organelles in this diagram are apical tips (black), golgi apparatus (cyan), rhoptries (red) and endosome-like compartment (grey circle).

(Baum et al., 2008a)

Figure 1.6: Actin-myosin motor complex components of motile apicomplexan parasites. (1) The tetrameric complex of MyoA-MTIP-GAP45-GAP50 was hypothesised to be immobilized in the IMC which could be mediated by proteins such as GAPM (Bullen et al., 2009). (2) The MyoA heavy chain is supported by the association of its light chain (MTIP) and two other glideosome associated proteins (GAP45 and GAP50). The initiation of invasion or motility involves several steps upon tight junction formation which lead to intracellular signalling activation through messenger molecules such as calcium: (3) It starts with the polymerization

of actin governed by formin 1 and profilin. (4) The polymerized actin serves as a binding platform for MyoA creating a directed force bringing the polymerized actin rearward through myosin movement, powered by ATP hydrolysis. (5) As the complex of host cell receptor-TRAP like adhesin indirectly binds to polymerized actin through aldolase, the force generated by MyoA propels this protein complex rearward hence moving the parasite forward into the host. (6) The adhesin complex is dissociated by intramembrane proteases of the rhomboid family. (7-8) This machinery also includes the depolymerisation and recycling of actin governed by cofilin and cyclase-associated protein (CAP) (Baum et al., 2008a).

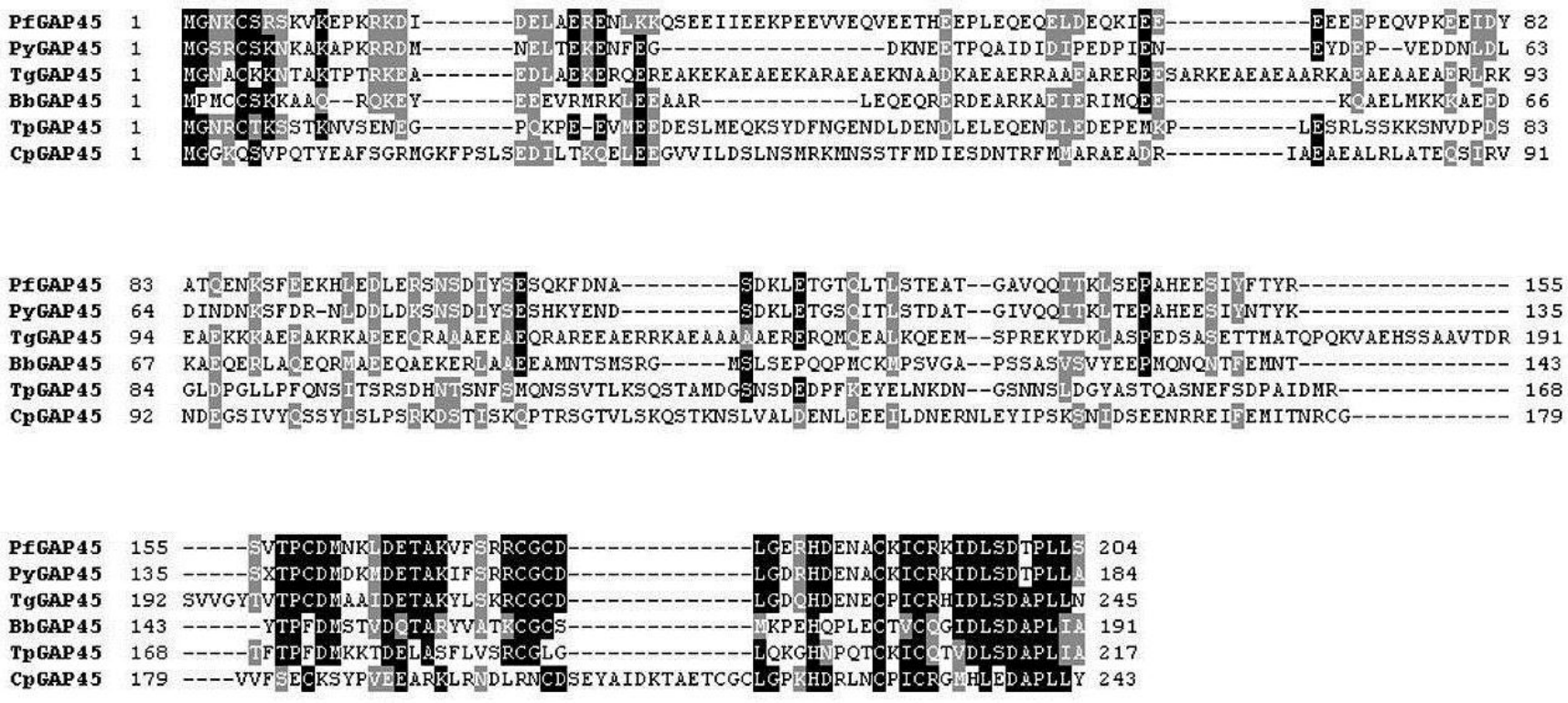

Figure 1.7: GAP45 protein sequence alignment from different species of apicomplexan parasite: *Plasmodium falciparum*, *Plasmodium yoelii*, *Toxoplasma gondii*, *Babesia bovis*, *Theileria parva* and *Cryptosporidium parvum* sequences are shown. Amino acid residues identical in at least four of the six sequences are highlighted in black; similar residues in gray.

(Doerig and Billker, 2010)

Figure 1.8: The distinct activation mechanism for CDPKs and CaMKs. The CDPK is structurally different from CaMK as CDPKs have the CaM-like domain covalently bound to the enzyme. The autoinhibitory region containing pseudosubstrate motif of mammalian CaMKs is located adjacent to the kinase domain. The autoinhibitory region of CDPKs is integrated with the CaM-like domain which all together form a new domain called CDPK-activating domain (CAD) blocking the enzyme active site. In CaMKs, calcium-calmodulin (CaM) interacts directly with the autoinhibitory domain and activates the kinase by exposing the substrate binding site. The mechanism of activation in CDPKs is quite complex as it involves a different set of comformational changes that reflect with the different domain composition. The calcium-bound CAD remains bound to the kinase domain but translocates to a new position (about 135^{o} clockwise away from its inactivated position) hence allowing substrates access to the active site. The green line represents the CH1 helix of the autoinhibitory region (Doerig and Billker, 2010; Wernimont et al., 2010).

(Billker et al., 2009)

Figure 1.9: The role of CDPKs and other cyclic nucleotide dependent kinases in the *Plasmodium* life cycle. The studies on these kinases or their messenger molecules are summarized from both human (*P. falciparum* infected red blood cell *in vitro* culture) and a mouse model (*P. berghei*). The findings are discussed further in the text. Abbreviations: CDPK, calcium dependent protein kinase; PKB, protein kinase B; PKG, protein kinase G; PfPDEδ, *P. falciparum* phosphodiesterase delta; PbGCβ, *P. berghei* guanylyl cyclase β; PbMap2, *P. berghei* mitogen activated protein kinase 2; PbACα, *P. berghei* adenylyl cyclase α (Billker et al., 2009).

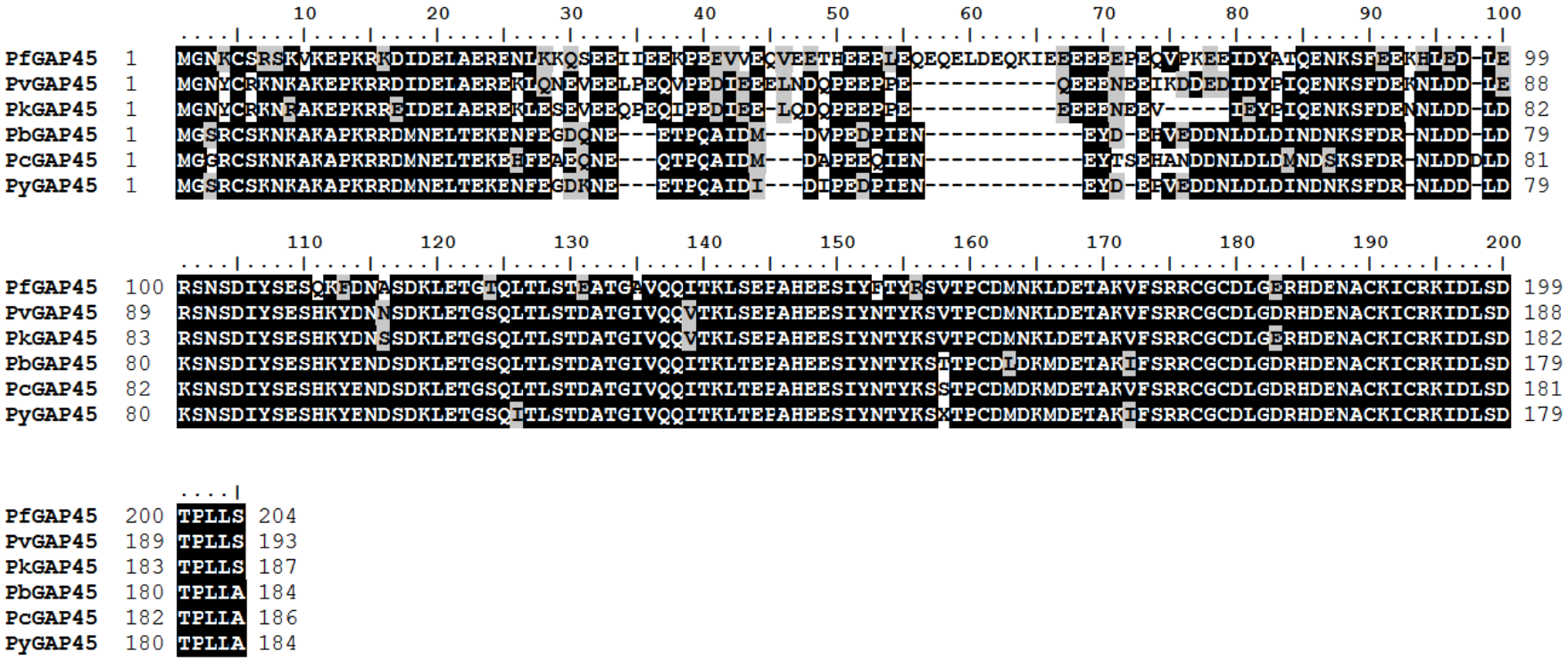

Figure 1.10: ***Plasmodium*** **GAP45 protein alignment.** The GAP45 protein is conserved across the genus. The identical amino acid residues are highlighted in black; similar residues in gray.

Chapter 2

Materials and methods

2.1 General DNA manipulation and transformation

2.1.1 Buffer and reagents

Solutions for used were 1 X TAE (45 mM Tris-acetate pH 8.0, 1 mM ethylenediaminetetraacetic acid [EDTA]), Luria-Bertani (LB) broth (1% (w/v) Bacto-tryptone, 0.5% (w/v) Bacto-yeast extract, 1% (w/v) NaCl in distilled water pH 7.0), LB agar (LB broth supplemented with 1.5% (w/v) Bacto- agar), SOC (2% (w/v) Bacto-tryptone, 0.5% (w/v) Bacto-yeast extract, 0.5% (w/v) NaCl in distilled water, pH 7.5). Reagents used were ethidium bromide, AccuPrime™ *Pfx* DNA polymerase kit (Invitrogen), restriction endonuclease enzyme, T4 DNA ligase (Promega), oligonucleotides, gel extraction kit (Qiagen), PCR purification kit (Qiagen), ampicillin, QIAprep Spin Miniprep, QIAGEN Plasmid Maxi kits (Qiagen) and glycerol. The chemical competent cells used were *E. coli* Novablue Gigasingles (Novagen), BL21-CodonPlus-RIL (Stratagene) and XL1-Blue (Stratagene).

2.1.2 Methods

2.1.2.1 DNA concentration determination

DNA was quantified using UV absorbance spectrometry. Appropriate dilutions were made and absorbance at 260 nm recorded using a UNICAM UV1 spectrophotometer. An absorbance of 1 corresponds to approximately 50 μg/ml dsDNA.

2.1.2.2 Agarose gel electrophoresis

Gels were prepared by melting agarose (Roche) in 1 X TAE to a final concentration of 0.8-1% (w/v) depending on the resolution required. For UV detection of DNA, 0.5 μg ml^{-1} ethidium bromide was added to melted agarose prior to casting gels in horizontal plates (Anachem Ltd, Luton, UK). Once cooled, gels were immersed in 1 X TAE and DNA samples were supplemented with 1 X DNA loading dye (Qiagen) before loading into wells. Separation was conducted at 110V using an EPS 500/400 DC Power Supply (Pharmacia).

2.1.2.3 Polymerase Chain Reaction (PCR)

DNA was amplified from plasmid DNA using high fidelity AccuPrime™ *Pfx* DNA polymerase (Invitrogen). Reactions contained 10 pg-200 ng template DNA, 0.3 μM each oligonucleotide and 1-2.5 U enzyme in supplied reaction buffer. Reaction buffer (10X) contained 10 mM $MgSO_4$, 3 mM dNTPs and thermostable proteins that enhance template-primer hybridization.

2.1.2.4 Restriction endonuclease digestion

For a typical reaction, 1 μg DNA was digested for 2 h at 37°C, in reaction buffer supplied with the specific enzyme being used. All enzymes were purchased from New England Biolabs, 1 Unit being defined as the amount of enzyme required to digest 1 μg DNA in 1 h at 37°C, in a 50 μl reaction. Where more than one enzyme was used in any given reaction, buffers were chosen in order to retain optimal activity of both enzymes.

2.1.2.5 Ligation of DNA fragments

Where restriction digestion was used in cloning, the resulting cohesive ends were ligated using T4 DNA ligase (Promega). Reactions contained 200 U enzyme, 50 ng vector DNA and a 3:1 molar excess of insert to vector DNA. Samples were incubated at 16°C overnight, in the supplied buffer.

2.1.2.6 Purification of DNA

Digested plasmid DNA and PCR amplicants were separated by agarose gel electrophoresis and the resulting bands were excised from gels. The DNA was subsequently purified from gel pieces using a gel extraction kit (Qiagen). The PCR product was also directly purified using PCR purification kit (Qiagen). DNA was eluted from the spin columns using 30 μl of the provided elution buffer and quantified.

2.1.2.7 The propagation and transformation of plasmid DNA by E. coli

Chemical competent *E. coli* strains were thawed on ice prior to the addition of 50 ng purified plasmid DNA or 2 μl ligation reaction. The cells were then heated at 42°C in a water bath for 30 seconds and immediately incubated on ice for 5 minutes. Pre-warmed SOC was then added to the cells and incubated for 1 hr at 37°C with agitation at 250 rpm. Transformed cells were then plated onto agar plates containing antibiotic for selection (100 μg/ml ampicillin) and incubated at 37°C overnight prior to positive colony picking. The colony was picked and grown in LB culture containing 100 μg/ml ampicillin at 37°C with agitation at 250 rpm.

2.1.2.8 Isolation of plasmid DNA

Plasmid DNA was isolated from *E. coli* overnight cultures using either the QIAprep Spin Miniprep or QIAGEN Plasmid Maxi kits (Qiagen) following the protocols provided in the QIAGEN plasmid purification handbook. If the resulting DNA was to be used for transformation or sequencing, 2-5 ml culture was sufficient and DNA was extracted using the Miniprep kit. For electroporation of *P. falciparum*, larger quantites of DNA were required and thus 250 ml cultures were grown and DNA extracted using the QIAGEN-tip 500 from the Maxiprep kit. All DNA was eluted and stored in elution buffer EB (10 mM Tris HCL, pH 8.5).

2.1.2.9 Sequencing of DNA

All DNA for sequencing was sent to the **Source BioScience LifeSciences UK Limited**, Cambridge. The samples sent comprised of 100 ng/μl plasmid DNA

extracted and purified by miniprep kit and 3.2 pmol/µl of each oligonucleotide in 10 µl de-ionised distilled water. ABI chromatogram files were viewed and manipulated using BioEdit sequence alignment editor.

2.1.2.10 Bacterial cell storage

Glycerol stocks of bacterial and yeast strains were made for long term storage of cells. Overnight cultures were grown and 800 µl cells added to 200 µl 100% glycerol in cryogenic vials (Nalgene). The mixture was mixed by vortex and stored at -80°C. To grow the bacterial glycerol stock, frozen bacteria were scraped using a 100 µl tip and mixed with 5 ml LB media containing 100 µg/ml ampicillin prior to overnight incubation at 37^{o}C with agitation at 250 rpm.

2.1.2.11 Oligonucleotides

Oligonucleotides were purchased from Sigma-Aldrich Company Ltd and used for plasmid construction and site-directed mutagenesis (Sections 2.3 and 2.6.2.1).

2.2 Expression and purification of recombinant GAP45 protein

2.2.1 Buffers and reagents

Solutions used for this experiment were LB media, LB agar, SOC as stated in 2.1.1 and Laemmli sample buffer (100 mM Tris HCl pH 6.8, 200 mM dithiothreitol (DTT), 4% sodium dodecyl sulphate (SDS), 20% glycerol, 0.2% bromophenol blue). The reagents used were ampicillin, bugbuster protein extraction reagent (Novagen), benzonase nuclease (Novagen), isopropyl-β-D-thiogalactopyranoside (IPTG), protease inhibitor cocktail without EDTA (Roche), rabbit anti-His tag antibody (Santa Cruz Biotechnology) and anti-rabbit IgG-HRP conjugate (Biorad). The chemical competent cell used was *E. coli* BL21-CodonPlus-RIL (Stratagene).

2.2.2 Methods

The GAP45 gene was inserted into pET 46 Ek/LIC expression vector (Novagen) which created a hexa-His tag at the protein N-terminus (provided by Dr. Judith L. Green, National Institute for Medical Research), and transformed into Codon Plus BL21 (DE3) RIL competent cells (Stratagene) as mentioned (Section 2.1.2.7). For expression, the competent cells were grown overnight in 10 ml LB medium containing 100 µg/ml of ampicillin at 37^{o}C, with shaking at 250 rpm. Then the overnight cultures were grown in 100 ml LB medium containing 100 µg/ml of ampicillin at 37^{o}C, with shaking at 250 rpm till the OD at 280 nm was 0.6-0.8. The expression of His-tagged GAP45 was induced with 0.1 mM or 1 mM of IPTG for 3 hours at 27^{o}C or 37^{o}C, with shaking at 250 rpm. The culture was centrifuged and the supernatant was discarded. The bacterial cell pellet was kept at -20^{o}C or processed as follows. The pellet was lysed and extracted with 10 ml Bugbuster (Novagen) solution containing 1x protease inhibitor cocktail without EDTA (Roche) and 25 U/ml benzonase (Novagen) for 20 minutes at room temperature with shaking. The lysate was centrifuged and both pellet and supernatant were subjected to SDS-PAGE and western blotting analysis. For solubility test, the protein from both pellet and supernatant were mixed 1:1 with 2X Laemmli sample buffer and separated with 12% NuPAGE gel (Invitrogen). The separated proteins were transferred onto nitrocellulose membrane (Whatman) by western blotting. The primary rabbit anti-His tag antibody (1:5000) was used for detection of expressed recombinant His-tagged GAP45 protein. The secondary antibody, anti-rabbit IgG-HRP conjugate (1:5000) was used for the ECL detection process.

Following protein extraction, the lysate supernatant was collected and added to 4 ml 50% Nickel-Nitrilotriacetic acid (Ni-NTA) agarose (Qiagen). The mixture of Ni-NTA agarose and supernatant was mixed for 30 minutes at room temperature to initiate His tagged protein-Ni-NTA agarose binding. The mixture was loaded into a column and the supernatant flow-through was collected. The resin was washed with 50 ml of washing buffer (250 mM NaCl, 20 mM $NaPO_4$, 10 mM Imidazole pH 6.5), then the bound GAP45 protein was eluted with 6 ml elution buffer (250 mM NaCl, 20 mM $NaPO_4$, 250 mM Imidazole pH 6.5). 5 µl of the purified GAP45 was loaded

onto SDS-PAGE and stained with coomassie brilliant blue solution. The eluted recombinant GAP45 was concentrated by using Vivaspin concentrator 10K MWCO (Sartorius), and buffer exchanged into PBS using a PD-10 column containing Sephadex G-25 (GE Healthcare). The protein concentration was determined by Bradford assay (Biorad).

2.3 Site-directed mutagenesis of GAP45 gene

2.3.1 Buffers and reagents

The site-directed mutagenesis was carried out using the QuikChange® II Site-Directed Mutagenesis kit by Stratagene. The kit contained PfuUltra® High-Fidelity DNA Polymerase (2.5U/ul), 10X reaction buffer, *Dpn* I restriction enzyme (10U/ul), dNTP mix and XL1-Blue supercompetent cells. Primers used for mutagenesis are listed in Table 2.1. The underlined sequences indicate the codon substitution from serine/threonine to alanine. The bold nucleotide is the one that has been substituted for coding alanine.

2.3.2 Methods

Mutations resulting in the substitution of serine/threonine by alanine in GAP45 were performed using QuikChange II Site-Directed Mutagenesis kit according to the manufacturer's instructions (Stratagene). Two complementary oligonucleotides containing S/T to alanine codons were synthesized by Sigma company and provided at HPLC purified grade. The 50 µl sample reactions contained 1X reaction buffer, 10 ng of plasmid DNA containing the GAP45 gene, 125 ng of each primer, 1 ul dNTP mix and 2.5U of PfuUltra HF DNA polymerase. The mutagenesis process was started using a thermal cycler with recommended cycling parameters. *Dpn* I (10U) was added directly to each amplification reaction to digest the parental DNA and incubated at 37^{o}C for 1 hour.

Dpn I-treated DNA was transformed into the XL1-Blue supercompetent cells and grown overnight on agar plate at 37^{o}C. The positive colonies were picked and

grew overnight in 10 ml LB medium containing 100 ug/ml of ampicillin prior to plasmid DNA extraction using a miniprep kit (Qiagen). The purified plasmid DNA was then transformed into expression host, BL21 (DE3) RIL competent cells (Stratagene) prior to expression induction and protein purification as mentioned in section 2.1.2.7 and 2.2.

2.4 CDPK1 kinase assay and analysis

2.4.1 Buffers and reagent

Recombinant CDPK1 was provided by Dr. Judith Green (National Institute for Medical Research). The radiolabelled agent used was adenosine 5`-triphosphate, [γ-^{32}P]-, 250 µCi (9.25 MBq), specific activity: 30Ci (1.11 TBq)/mMole, 10 mM Tricine (pH 7.6) (Perkin Elmer). The CDPK1 kinase assay reaction was performed in a solution containing final concentrations of 20 mM Tris HCl pH 8, 20 mM $MgCl_2$, 1 mM $CaCl_2$, 0.1 mM ATP, 658 nM or 100 nM CDPK1 and 8 µM GAP45 at 30^{o}C for 10 minutes or otherwise stated. All steps involving the [γ^{32}P] ATP was conducted in a radioactivity restricted area and shielded with Perspex glass.

2.4.2 Methods

2.4.2.1 Autoradiography

The assay conditions were as described above (Section 2.4.1). The ATP was spiked with 0.1 MBq of [γ^{32}P] ATP (Perkin Elmer) and this mixture was used to start the kinase reaction. The kinase assay was stopped by adding 1:1 (v/v) Laemmli sample buffer and incubation at 90^{o}C for 5 minutes. The sample was subjected to SDS-PAGE, and the gel was fixed with fixing solution (30% methanol, 5% glycerol) for 30 minutes at room temperature with some agitation. The fixed gel was dried and exposed to Kodak Biomax MR film to visualize the radiolabelled protein band. The intensity of the band was measured and analysed by ImageJ software (www.rsbweb.nih.gov/ij/).

2.4.2.2 Scintillation counting

The assay conditions were as described above (Section 2.4.1) and the reactions were started at 5 to 10 minutes intervals to ensure that incubation times were identical. The sample was spotted onto a P81 phosphocellulose disc (Whatman) and immersed into 75 mM phosphoric acid for 5 minutes with stirring. The paper was rinsed with acetone and dried at room temperature. The dried discs were transferred into scintillation vials and the radioactivity was measured by Cherenkov counting using a scintillation counter (Hastie et al., 2006).

2.4.2.3 Electrospray mass spectrometry analysis (ES-MS)

For ES-MS, the assay conditions were as described above (Section 2.4.1) with some modifications. To ensure a high amount of GAP45 phosphorylation, three times more GAP45 (24 µM), 658 nM CDPK1 and 1 mM ATP were used. The reaction was incubated for 90 minutes at 30^{o}C. The phosphorylated GAP45 was subjected to ES-MS by Dr. Steven Howell, National Institute for Medical Research. A total of 200 pmol phosphorylated GAP45 or non-phosphorylated GAP45 (incubated in the reaction buffer without Ca^{2+}) was subjected to ES-MS using a microTOFQ electrospray mass spectrometer (Bruker Daltonics, Coventry, UK) to determine the molecular mass. Protein was desalted using a 2 mm x 10 mm guard column (Upchurch Scientific, Oak Harbor WA) packed with Poros R2 resin (Perseptive Biosystems, Framingham), injected onto the column in 10% acetonitrile, 0.10% acetic acid, washed with the same solvent and eluted in 60% acetonitrile, 0.1% acetic acid. Desalted protein was then infused into the mass spectrometer at 3 µl/min using an electrospray voltage of 4.5 kV. Mass spectra were deconvoluted using maximum entropy software (Bruker Daltonics, Coventry, UK). The spectrum was selected on the desired range and presented in deconvoluted form.

2.5 Far UV circular dichroism (CD) spectroscopy

The WT and variant GAP45 proteins were phosphorylated under similar conditions as the ES-MS preparation (Section 2.4.2.3). The negative control was done with the

reaction buffer without Ca^{2+}. The sample (0.15 mg/ml in 250 µl PBS) was subjected to CD analysis by Dr. Steve Martin (National Institute for Medical Research). Briefly, CD measurements were made using a Jasco J-715 spectropolarimeter equipped with a PTC-348WI Peltier temperature control system. CD spectra were recorded at 20°C in PBS, using 1 mm QS cuvettes (Hellma GmbH & Co. KG). The secondary structure of recombinant proteins was determined by monitoring CD in the far-UV region (190-260 nm). Multiple scans were averaged and the appropriate buffer baseline was subtracted. Far UV CD intensities are presented on a mean residue weight ($\Delta\varepsilon_{MRW}$) basis. Secondary structure contents were estimated from far-UV CD spectra using the methods described by Sreerama and Woody (Sreerama and Woody, 2000).

2.6 Parasite culture and synchronisation

2.6.1 Buffers and reagents

The media used was Roswell Park Memorial Institute 1640 (RPMI) supplemented with 25 mM HEPES, 27 mM $NaHCO_3$, 2 mM L-glutamine, 25 µg/ml gentamycin, 50 µg/ml hypoxanthine and 2 mg/ml glucose and with or without 0.5% (w/v) AlbuMAX II. Other reagents used were 70% Percoll (70% isotonic Percoll [90% percoll, 10% 10X phosphate buffered saline], 30% RPMI 1640 without albumax) and 5% sorbitol.

2.6.2 Methods

The parasites were grown in RPMI medium containing AlbuMAX II pH 7.5 at 3% haematocrit. Cultures were gassed with a mixture of 5% O_2, 7% CO_2, 88% N_2 and incubated at 37°C. To examine cultures, thin blood smears were made on glass slides and cells stained using 1:1 Giemsa's stain:distilled water for 10 min. Slides were then viewed using a light microscope. At 10% parasitemia, the parasite-infected red blood cells were pelleted by centrifugation and washed with the RPMI medium without AlbuMAX II. The pellet was layered on top of 70% Percoll and centrifuged at 1,000 x g for 11 minutes at room temperature. The concentrated schizont layer was

harvested and washed with RPMI medium prior to reinvasion. For reinvasion, purified schizonts were added to the new culture containing fresh non infected red blood cell and incubated with agitation at 37^{o}C for 3 hours. The newly ring-infected red blood cells were collected by sorbitol treatment to eliminate the schizonts (Lambros and Vanderberg, 1979). The synchronized parasites were grown till they reached 10% parasitemia and harvested at schizont stage by using 70% Percoll as mentioned. The schizont pellets were washed with RPMI without AlbuMAX II and kept in -80^{o}C prior to use.

2.7 The parasite DNA manipulation and transfection

2.7.1 Buffers and reagents

For this experiment, solutions such as cytomix (120 mM potassium chloride (KCl), 0.15 mM calcium chloride ($CaCl_2$), 2 mM ethylene glycol bis(2-aminoethyl ether)-*N*,*N*,*N*'*N*'-tetraacetic acid (EGTA), 5 mM magnesium chloride (MgCl), 10 mM potassium phosphate (K_2HPO_4/KH_2PO_4), 25 mM 4-(2-hydroxyethyl)-1-piperazineethanesulfonic acid HEPES, pH 7.6), freezing solution (0.324g NaCl, 1.512g D-sorbitol, 14 ml glycerol in 50 ml volume) and thawing solution (3.5% NaCl) were used. The parasite used was *Plasmodium falciparum* 3D7 line. The transfection vector, phh3bsdGFPnG45, was provided by Dr. Ellen Knuepfer, National Institute for Medical Research, London. The vector contains the MSP3 promoter, the codon for the N terminal part of GAP45 and the GFP sequence at the C terminus (phh3bsdGFPnG45). For drug selection, the vector also contains the blastocidin resistant gene. Reagents that were used include plasmid DNA extraction maxiprep kit (Qiagen), Blastocidin (Merck), 70% Percoll (Amersham) and 5% sorbitol (Section 2.6.1). The medium used for parasite culture was RPMI 1640 with AlbuMAX II (Section 2.6.1).

2.7.2 Methods

The transfection vector (phh3bsdGFPnG45) was reconstructed by inserting the C terminal part of GAP45 which places the GFP tag in the middle of the GAP45 non-homologous region. The complete transfection vector was then cloned in *E. coli*. The plasmid DNA was extracted and purified by maxiprep kits prior to transfection.

2.7.2.1 Tranfection vector construct

The plasmid phh3bsdGFPnG45 was designed to episomally express the N-terminal 29 residues of GAP45 fused to GFP. DNA sequence coding for the N-terminal 29 amino acids of GAP45 was fused in front of sequence coding for GFP as follows: Two overlapping primer pairs (Gap45for [TTCACCTAGGATGGGAAATAAGTGTAGTAGGTCAAAGGTAAAAGAACC AAAGAGAAAAGATATTGACGAGTTAGCAGAAAGGGAG] /Gap45rev [GACAACTCCAGTGAAAAGTTCTTCTCCTTTACTTTTCTTCAAGTTCTCCCT TTCTGCTAACTCGTCAATATC]) were fused to generate a long forward primer encoding the N-terminal 29 amino acids of GAP45. Following this the long fusion-primer was used in combination with GFPrev primer (ATTTCTCCGCGGTTATTTGTATAGTTCATCCATGAAATGTGTAATCCC) to produce the GAP45-GFP fusion gene which was subsequently inserted via *Avr*II/*Sac*II restriction enzyme cleavage (sites underlined above) between the MSP3 promoter and the hrp2 3'UTR sequences in the pHH3 vector and cloned (Knuepfer and Holder, unpublished).

A second plasmid (phh3bsdGFPGAP45) was constructed to add an internal GFP tag to the GAP45 sequence, located between residues 29 and 30. The sequence encoding the N-terminal part of GAP45 fused with GFP was amplified by PCR eliminating the terminal stop codon using primers 5' GCGCGCCCTAGGATGGGAAATAAATGTTCAAG 3' and 5' GCGCGCCCGCGGTTTGTATAGTTCATCCATGC 3'. The PCR product was reinserted into the pHH3 vector via *Avr*II/*Sac*II restriction enzyme cleavage (sites underlined above) after the MSP3 promoter. The sequence encoding the C-terminal portion of GAP45 from residue 30 to the stop codon was amplified by PCR using

primers 5’ GCGCGCCCGCGGCAATCTGAAGAAATAATTGAAG 3’ and 5’GCGCGCCCGCGGTTAGCTCAATAAAGGTGTATCG 3’ and inserted into the transfection vector via SacII restriction enzyme cleavage (sites underlined above) after the GFP tag sequence. A series of additional constructs to express the full length GAP45 tagged with GFP and with amino acid substitutions were also made as mentioned in section 2.3. The same procedure also applies to the rest of the GAP45 variants (S89A, S103A, S89A/S103A, S89D, S103D, S89D/S103D).

A third plasmid (phh3bsdGFPcG45) to express the N-terminal truncated GFP-tagged GAP45 (C-GAP45) was also constructed by a similar approach by reconstructing the second plasmid phh3bsdGFPGAP45. The DNA coding the N-terminal 29 amino acids of GAP45 fused to GFP sequence in plasmid phh3bsdGFPGAP45 was cut out and replaced with the GFP sequence only (without stop codon) via *Avr*II/*Sac*II restriction enzyme cleavage after the MSP3 promoter. The sequence encoding the C-terminal portion of GAP45 from residue 30 to the stop codon was inserted via SacII restriction enzyme cleavage after the GFP tag sequence. This plasmid will express the GFP-tagged GAP45 that only contains residues 30-204 (lacking the first 29 amino acid N-terminus residues) (C-GAP45). The expression component of this plasmid, the MSP3 promoter and the GFP-tagged GAP45 gene were reconfirmed by plasmid digestion using double digestion enzymes, *EcoR*I/*Avr*II and *Avr*II/*Sac*II respectively.

The sequence and alignment of the insert was confirmed by DNA sequencing. The confirmed vector was cloned in Novablue Gigasingles *E. coli* cells (Novagen) and grown overnight at 37^{o}C prior to plasmid DNA extraction using maxiprep kits (Qiagen).

2.7.2.2 DNA precipitation

The plasmid DNA (100 μg) was purified by ethanol precipitation and mixed with TE buffer (10 mM Tris HCL, 1 mM EDTA, pH 8.0) and kept at –30^{o}C. Briefly, 1/10 volume of 3 M sodium acetate was added to the DNA sample, followed by 2 volumes of 100% ethanol. DNA was left to precipitate overnight at -20°C and

pelleted by centrifugation (20000 x g, 20 min). The pellet was washed in 70% (v/v) ethanol and spun again prior to air-drying and re-suspension in 30 µl of TE buffer.

2.7.2.3 Transfection processes

Prior to transfection, *P. falciparum* 3D7 was synchronised by Percoll separation and sorbitol treatment to get 10% red blood cell infected with ring stage parasite (Section 2.6). The plasmid DNA in TE buffer was mixed with 385 µl cytomix solution by pipeting up and down till the DNA dissolved (Fidock and Wellems, 1997; Wu et al., 1995). The mixture was then mixed with 150 µl of 10% ring-infected blood culture by using a Pasteur pipet and immediately transferred into the Gene Pulser cuvette. The elecroporations were done one at a time at 0.310 kV/950 uF with Ohms set to infinity. The electroporated samples were transferred into petri dishes containing 10 ml culture volume of 3% hematocrit of non-infected red blood cells. The petri dish was gassed with a mixture of 5% O_2, 7% CO_2, 88% N_2 and placed in an incubator at 37^{o}C. The RPMI medium (2.6.1) was replaced and maintained with new RPMI medium containing 2.5 µg/ml Blastocidin.

2.7.2.4 Freezing and thawing of P. falciparum

The parasites were kept in liquid nitrogen by using a freezing solution. The ring infected red blood cells (5% parasitemia) were pelleted at 1000 x g for 5 minutes. The supernatants were discarded. Warm freezing solution was added drop wise to the pellets (7:3 v/v). The mixtures were transferred to cryopreservation vials and stored in liquid nitrogen prior to use.

The parasites were thawed using 3.5% NaCl thawing solution. The cryopreserved samples were thawed in a 37^{o}C water bath and transferred to a 15 ml conical tube. The original volume of thawing solution was added drop wise and centrifuged at 250 x g for 5 minutes. This step was repeated twice prior to culture preparation. The pellet was mixed with warm RPMI plus albumax medium and the culture was incubated at 37^{o}C prior to use.

2.8 Parasite protein subcellular fractionation

2.8.1 Buffers and reagents

The buffers or solutions used were hypotonic lysis buffer (10 mM Tris HCl pH 8.0, 5 mM ethylenediaminetetraacetic acid (EDTA), 1X protease inhibitor cocktail), high salt buffer (50 mM Tris HCl pH 8.0, 5 mM EDTA, 500 mM NaCl, 1X protease inhibitor cocktail) and carbonate buffer (0.1 M sodium carbonate, pH 11.0). Other buffers used include 2X Laemmli sample buffer (Section 2.2.1).

2.8.2 Methods

The parasite was synchronized and harvested as mentioned (Section 2.6). For crude protein extraction, the frozen parasites were thawed and lysed with hypotonic lysis solution (1:10 v/v) for 1 hour at 4^{o}C. The mixture was centrifuged at 20,000 x g for 10 minutes at 4^{o}C. The pellet was mixed with 2X Laemmli sample buffer and kept at -20^{o}C prior to use.

For subcellular fractionation, the schizont pellet was lysed with hypotonic lysis buffer (1:10 v/v) for 1 hour at 4^{o}C with mixing up and down using syringes every 10 minutes. The mixture was centrifuged at 100,000 x g using an ultracentrifuge for 10 minutes at 4^{o}C. The supernatant was kept (Hypotonic lysis soluble) and the pellet was washed once with the hypotonic lysis buffer with mixing up and down using syringes at 4^{o}C. Then the insoluble materials were pelleted down at 100,000 x g using the ultracentrifuge for 10 minutes at 4^{o}C. The pellet was mixed with high salt buffer (1:10 v/v) and incubated for 1 hour at 4^{o}C with mixing up and down using syringes at 10 minutes interval. The supernatant was kept (High salt soluble) and the pellet was washed once with the high salt buffer again by mixing up and down using syringes at 4^{o}C. The similar process was done sequentially as above for the carbonate buffer. All the fractions were collected and mixed with 2X Laemmli buffer at 1:1 and heated at 95^{o}C for 10 minutes. The sample was kept at -20^{o}C prior to use or analysis by the western blotting technique where the appropriate primary antibodies used include anti GFP (Roche), anti GAP45 (1:5000), anti MTIP (1:5000), anti SERA5 (1:20000) and anti MSP7 (1:10000).

2.9 SDS-PAGE and western blotting technique

2.9.1 Buffers and reagents

The reagents used were Precision Plus Protein standards (Bio-Rad), Enhanced chemiluminescence substrate, ECL (Amersham), primary antibody (anti GFP [1:1000], anti GAP45 [1:5000], anti MTIP [1:5000], anti MSP7 [1:10000], anti CDPK1 [1:5000] and anti SERA5 [1:20000]) and secondary antibody (goat anti rabbit IgG or goat anti mouse IgG conjugated with horse radish peroxidase [1:5000]) (Biorad). Solutions used in this experiment were Coomassie blue stain (0.1% [w/v] Coomassie Brilliant Blue R-250, 45% [v/v] methanol, 10% [v/v] acetic acid), Nu-PAGE® 3-(N-morpholino)-propanesulphonic acid (MOPS) buffer, destaining solution (45% [v/v] methanol, 10% [v/v] acetic acid), phosphate buffered saline containing 0.2% Tween 20 (PBST) and blocking buffer (1% bovine serum albumin in PBST).

2.9.2 Methods

All protein samples were separated using 12% Nu-PAGE® pre-cast Bis-Tris gels and Xcell II™ Mini Cell gel cassette (Invitrogen). The Precision Plus Protein™ standards (Bio-Rad) were used as protein markers. The MOPS buffer was used as a running buffer by applying a constant 200 Volts (V) using an EPS 500/400 DC Power Supply (Pharmacia). The separated proteins were visualised by staining gels with coomassie blue stains, gels were immersed in coomassie blue stain for 2 hours, destaining solution was used to remove the staining background.

In western blotting, the separated proteins from the gel were transfered onto nitrocellulose membrane overnight at 12 V or 3 hours at 30V at room temperature. The nitrocellulose membranes were incubated in blocking solution for 1 hour at room temperature or overnight at 4^{o}C. Then, the membranes were incubated in the appropriate primary antibody (Table 2.2) for 1 hour and washed with PBST 3 times at 10 minutes intervals. The membranes were again incubated with appropriate secondary antibody prior to the washing step as mentioned. The membranes were immersed in enhanced chemiluminescene substrate solution (ECL, GE Healthcare)

for 1 minute and the protein band signal was detected by exposing the blot to Biomax MR film (Kodak) for between 10 sec and 1 minute and developed using a FujiFilm FPM-3800 AD developer.

2.10 Live and indirect-immunofluorescence microscopy assay (IFA)

2.10.1 Buffers and reagents

The chemicals used were PBS, 4% paraformaldehyde (PFA) in PBS, permeabilisation solution (0.2% Triton X-100 in PBS), GFP-Booster (1:200) (a specific GFP-binding protein coupled to the fluorescent dye ATTO 488) (Chromotek), Hoechst 33342 DNA stain reagent (Invitrogen) and Prolong® Gold antifade reagent with DAPI (Invitrogen). The primary antibodies used were anti GAP45 (1:1000), anti MTIP (1:1000), anti GAP50 (1:200), anti RON10 (1:2000) and anti MSP1 (1:1000). The secondary antibodies used were IgG-specific second antibody coupled with Alexafluor 594/488 (1:5000) (Sigma).

2.10.2 Methods

The parasites were synchronized and purified as mentioned (Section 2.6) and then diluted 1:10 with the RPMI 1640 containing albumax. DNA staining was done by adding 0.1 µg/ml Hoechst reagent (Invitrogen) and incubated for 30 minutes at room temperature. About 2 µl of the stained schizont-infected red blood cells were dropped onto the slide and overlaid with a Vaseline-rimmed coverslip.

For IFA, smears of purified schizonts were made. The slides were fixed with 4% PFA for 10 minutes at room temperature. The fixed slides were washed 3 times with PBS and permeabilised with PBS containing 0.5% Triton X-100 for 5 minutes at room temperature. Then the slides were washed 2 times with PBS and blocked overnight with 4% BSA in PBS at 4^{o}C. After blocking, the slides were incubated with GFP-Booster (Chromotek) (Table 2.2) for 1 hour at room temperature. The GFP-Booster is a specific GFP-binding protein (derived from *Camelidae* heavy chain antibodies) coupled to the fluorescent dye ATTO 488 to reactivate, boost and

stabilize the GFP signal. The slides were washed 3 times with PBS prior to an incubation step with protein marker antibodies (GAP45, MTIP, GAP50, MSP1 and RON10 antibodies) (Table 2.2). The slides were then incubated with IgG-specific second antibody coupled with Alexafluor 594/488 (Sigma) (Table 2.2) for 1 hr at room temperature and washed 3 times with PBS. The slides were mounted with Prolong® Gold antifade reagent with DAPI (Invitrogen) overnight. Then the slides were sealed with a coverslip and nail polish prior to imaging by epifluorescence microscopy on an Axio Imager M1 microscope (Zeiss). For Z-stack analysis, the images were acquired on a DeltaVision Core system (Applied Precision Inc., USA) based on an Olympus IX71 inverted microscope, using an Olympus 100X objective lens and images captured using a QuantEM 512SC EMCCD (Cascade 512x512) camera (Photometrics Ltd) using a Xenon light source. Images were deconvoluted using DeltaVision SoftWorx software suite 5.0 and edited using Adobe Photoshop.

2.11 Co-immunoprecipitation or pull-down assay

2.11.1 Buffers and reagents

The buffers used were lysis buffer (10 mM Tris HCl pH 7.5, 150 mM NaCl, 0.5 mM EDTA, 1% NP40, 1 mM PMSF and 1X protease inhibitor cocktail) (Roche), dilution buffer (10 mM Tris HCl pH 7.5, 150 mM NaCl, 0.5 mM EDTA, 1 mM PMSF and 1X protease inhibitor cocktail) (Roche), washing buffer (10 mM Tris HCl pH 7.5, 300 mM NaCl, 0.5 mM EDTA, 1 mM PMSF and 1X protease inhibitor cocktail) (Roche) and 2X Laemmli sample buffer. The reagent used was GFP-Trap® beads (Chromotek).

2.11.2 Methods

The purified schizonts were resuspended in 200 µl lysis buffer (1:10 v/v). The mixture was placed on ice for 30 minutes with extensively pipetting every 10 minutes. The cell lysates were spun at 20,000 x g for 10 minutes at 4^{o}C. The supernatant was transferred to a precooled tube and the volume was adjusted to 1000

µl with dilution buffer. The GFP-Trap® beads (Chromotek) were washed with dilution buffer by resuspending 30 µl beads slurry (Table 2.2) in 500 ul ice cold dilution buffer and spun down at 2700 x g for 2 minutes at 4^{o}C. The supernatant was discarded and the washing step was repeated for another 2 times. The cell lysate was incubated with non-coated agarose beads (bab-20, Chromotek) for 30 minutes at 4^{o}C with gentle mixing using rotator, to preclear the unspecific protein binding. The mixture was spun down at 2000 x g for 2 minutes at 4^{o}C. The supernatant (cell lysate) was added to the GFP-Trap® beads and incubated with gentle mixing for 1 to 2 hours at 4^{o}C. The mixture was spun down at 2000 x g for 2 minutes at 4^{o}C. The supernatant (non-bound materials) was kept for western blotting analysis. The remaining supernatant was discarded and the pellet was washed 2 times with dilution buffer and washing buffer respectively. The GFP-Trap® beads were resuspended in 100 µl of 2X Laemmli sample buffer. The resuspended beads were heated for 10 minutes at 95^{o}C to dissociate the immunocomplexes from the beads. The beads were collected by centrifugation at 2700 x g for 2 minutes at 4^{o}C and SDS-PAGE was performed with the supernatant (referred to as bound materials).

Protein samples were fractionated by SDS-PAGE as mentioned in section 2.9, using Precision Plus Protein™ standards (Bio-Rad) as markers. Following protein transfer to nitrocellulose membrane, the membrane was incubated in blocking solution and then incubated in primary antibody specific for GFP (1:1000) (Roche), GAP45 (1:5000), MTIP (1:5000), SERA5 (1:20000) and MSP7 (1:10000) (Table 2.2). Then, the membranes were incubated with appropriate secondary antibody (goat anti rabbit IgG or goat anti mouse IgG conjugated with HRP) and the immunoreactive protein bands were detected by enhanced chemiluminescence reagent (ECL, GE Healthcare) and exposure to Biomax MR film (Kodak) as mentioned (Section 2.9).

2.12 Protein phosphatase treatment

2.12.1 Buffers and reagents

The solutions used were hypotonic lysis buffer (10 mM Tris HCL pH 8.0 and 1X protease inhibitor), extraction buffer (7 M urea, 2 M thiourea, 4% CHAPS and 1% DTT) and phosphatase reaction buffer (5 mM, Tris HCL pH 8.0, 10 mM NaCl, 1 mM $MgCl_2$, 0.1 mM DTT and 1X protease inhibitor). The reagents used were bovine intestinal alkaline phosphatase (Sigma), phosphatase inhibitor cocktail (Sigma) and protease inhibitor cocktail EDTA-free (Roche).

2.12.2 Methods

Purified schizonts were lysed in hypotonic lysis buffer for 30 minutes on ice by pipetting up and down every 10 minutes and centrifuged at 20000 x g for 10 minutes at 4^{o}C. The pellet which consisted of membranous parasite materials was then extracted in extraction buffer on ice for 30 minutes with shearing using fine needle syringes. The lysates were centrifuged at 20000 X g for 10 minutes at 4^{o}C. The protein concentration of the supernatant was determined using the Bradford assay prior to phosphatase treatment.

About 100 µg of protein was used in the phosphatase reaction. The phosphatase reaction mixtures contained phosphatase reaction buffer and 50 Unit of bovine intestinal alkaline phosphatase enzyme (Sigma). The reaction was also done in the presence of phosphatase inhibitor cocktail (Sigma). The reaction was performed at 37^{o}C for 4 hours to ensure a large amount of protein dephosphorylation. The reaction was stopped by the addition of 1:1 Laemmli sample buffer and heated at 95^{o}C for 10 minutes prior to SDS-PAGE protein separation and western blotting analysis as mentioned (Section 2.9).

2.13 ^{32}P-phosphate metabolic labelling of *P. falciparum* schizont

2.13.1 Buffers and reagents

The solutions used were phosphate free RPMI 1640 medium and human serum. The reagent used was phosphorus-32 radionuclide, 2 mCi (74 MBq), specific activity: 900-1100 mCi (33.3-40.7 GBq)/mMole, disodium phosphate in 1 ml water (Perkin Elmer). All steps involving the ^{32}P-phosphate was conducted in a radioactivity restricted area using shielding with Perspex glass.

2.13.1 Methods

The parasites were synchronized as mentioned (Section 2.6). The schizonts (~39 hours post invasion) were enriched by 70% Percoll as above and washed twice with phosphate free RPMI medium. The schizonts (100 µl) were resuspended in 10 ml phosphate free RPMI containing 10% human serum and incubated at 37^{o}C for 30 minutes. Then, 25 MBq of ^{32}P-phosphate was added to the culture and the incubation was continued for 2 hours. After 2 hours incubation, the ~42 hours post invasion schizonts were pelleted at 200 x g for 5 minutes. The pelleted schizonts were washed twice with serum free RPMI and centrifuged at 200 x g for 5 minutes. Then, the ^{32}P-phosphate labelled schizont pellets were used for immunoprecipitation using the GFP-Trap® system as mentioned in section 2.11.2. The immunoprecipitated GFP-GAP45 proteins were separated by SDS-PAGE and the gel fixed and dried as mentioned in section 2.4.2.1. The corresponding phosphorylated protein bands were detected by film exposure for 2 weeks at -80^{o}C.

2.14 Parasite protein identification by liquid chromatography- mass spectrometry (LC-MS/MS)

2.14.1 Buffers and reagents

The solutions used were destaining solution (200 mM ammonium bicarbonate, 50% acetonitrile), reducing solution (20 mM DTT, 200 mM ammonium bicarbonate, 50%

acetonitrile), alkylation solution (5 mM iodoacetamide, 200 mM ammonium bicarbonate, 50% acetonitrile), washing solution (20 mM ammonium bicarbonate, 50% acetonitrile), gel fixing solution (50% methanol, 10% acetic acid) and gel destaining solution (10% methanol, 7% acetic acid). The reagents used were SYPRO Ruby gel stain (Invitrogen) and sequencing grade modified trypsin (Promega).

2.14.2 Methods

The parasite proteins or immunoprecipitation products were resolved by SDS-PAGE. The protein was either stained with coomassie blue or SYPRO Ruby (Invitrogen). For SYPRO Ruby staining, the gel was fixed with gel fixing solution for 15 minutes with shaking prior to staining overnight. The stained gel was destained with gel destaining solution for 30 minutes with shaking. The destaining solution was removed and this step was repeated once prior to washing with ultrapure water twice at 5 minutes interval. The protein bands were visualized using Pharos FX™ Plus Molecular Imager (Biorad). The protein bands were excised by EXQuest™ Spot Cutter (Biorad).

The gel pieces were placed in a non-coloured 0.5ml Eppendorf tube. The SDS and stains were extracted by incubating in 500 µl of destaining solution for 30 minutes at room temperature and this step was repeated twice. The protein band was reduced by incubating in 200 µl reducing solution for 1 hour at room temperature. The DTT was removed by washing with 500 µl destaining solution. The cysteine of the protein was then alkylated by incubating in 100 µl of freshly made alkylation solution for 20 minutes in dark at room temperature. The alkylation solution was removed and the gel washed twice with 500 µl washing solution. The washed gel piece was incubated in 500 µl of neat acetonitrile for 15 minutes till it turned white. The acetonitrile was removed and the gel piece was left to dry in a laminar hood for about an hour. The dried gel containing protein band can be stored at room temperature prior to the trypsinization step. The dried gel was incubated in 12 µl of trypsin solution (1 µg/ml of trypsin in 5 mM ammonium bicarbonate) at 37^{o}C overnight. The trypsin solution was added so that it covered the gel piece. The trypsinized protein band was subjected to protein identification by LC-MS/MS using

LTQ Orbitrap Velos mass spectrometer (Thermo Scientific) which was run and analysed by Dr. Steven Howell, National Institute for Medical Research.

Table 2.1: The primers used for substitution of GAP45 serine or threonine to alanine in site-directed mutagenesis. Two complementary oligonucleotides containing a S/T to alanine codon mutation were used in the sample reactions containing reaction buffer, plasmid DNA containing GAP45 gene, dNTP mix and PfuUltra HF DNA polymerase. The mutagenesis process was started using a thermal cycler with recommended cycling parameters. *Dpn* I was added directly to each amplification reaction to digest the parental DNA prior to DNA transformation into the XL1-Blue supercompetent cells and grown overnight on agar plate containing 100 μg/ml of ampicillin at 37^{o}C. The positive colonies were picked and grown overnight in LB media prior to plasmid DNA extraction using a miniprep kit (Qiagen). The purified plasmid DNA was then transferred into the expression host, BL21 (DE3) RIL competent cells (Stratagene) prior to expression induction and protein purification. (specific changes are in bold and the codon underlined: T84A, 5'- -3').

GAP45 protein	Primer used in mutagenesis
S6A	ATGGGAAATAAATGT**G**CAAGAAGCAAAGTAAAGG
S8A	ATGGGAAATAAATGTTCAAGA**GCA**AAAGTAAAGGAACCCAAACG
S31A	GAAAATTTAAAAAAACAA**G**CTGAAGAAATAATTGAAG
S89A	CAAGAAAATAAA**G**CATTTGAAGAAAAACAT
S101A	GATTTAGAAAGA**G**CTAATGCAGATATTTAT
S103A	GAAAGATCTAAT**G**CAGATATTTATTCAGAA
S107A	TCAGATATTTAT**G**CAGAATCTCAAAAATTT
S109A	ATTTATTCAGAA**G**CTCAAAAATTTGATAAT
S116A	GATATTTATTCAGAATCTCAAAAATTTGATAATGCT**GC**TGATAAATTAGAAACAGGAACTCAATT
S128A	AAACAGGAACTCAATTAACCTTA**G**CTACTGAAGCCACTGG
S142A	AAATAACTAAATTA**GC**TGAACCCGCCCATG
S149A	CCGCCCATGAAGAA**GC**TATATATTTTACTTA
S156A	CCCATGAAGAAAGTATATATTTTACTTATAGA**G**CTGTAACACCTTGTGATATGAATAAA
S173A	GAAACCGCTAAAGTTTTT**G**CAAGAAGATGTGGATG
S198A	TGAAAATGCATGTAAAATTTGTAGAAAAATTGATTTA**G**CCGATACACCTTTATTGAG
S204A	GATTTATCCGATACACCTTTATTG**GCA**TAACCGGGCTTCTCCTCAAATCTCGAG
T84A	GAAATAGATTATGCA**G**CTCAAGAAAATAAA
S89A/S103A	GAAAGATCTAAT**G**CAGATATTTATTCAGAA on sample S89A
S89A/S103A/S142A	AAATAACTAAATTA**GC**TGAACCCGCCCATG on sample S89A/S103A
S89A/S103A/S149A	CCGCCCATGAAGAA**GC**TATATATTTTACTTA on sample S89A/S103A
S89D	GAAGAAATAGATTATGCAACTCAAGAAAATAAA**GAT**TTTGAAGAAAAACATTTAGAAGATTTAGAA
S103D	ACATTTAGAAGATTTAGAAAGATCTAAT**GAT**GATATTTATTCAGAATCTCAAAAATTTGATAATGC
S89D/S103D	ACATTTAGAAGATTTAGAAAGATCTAAT**GAT**GATATTTATTCAGAATCTCAAAAATTTGATAATGC on sample 89D

Name	Species	Type	Dilutions/Quantity			Source
			WB	IFA	IP	
Primary:						
α-GAP45	Rabbit	Polyclonal AP[a]	1:5000	1:1000	N/A[d]	Raised by Harlan
α-MTIP	Rabbit	Polyclonal AP[a]	1:5000	1:1000	N/A[d]	Dr JL Green
α-MyoA	Rabbit	Polyclonal AP[a]	1:10000	N/A[d]	N/A[d]	Dr JC Fordham
α-GAP50	Rabbit	Polyclonal AP[a]	N/A[d]	1:200	N/A[d]	Raised in house
α-RON10	Rabbit	Polyclonal AP[a]	1:5000	1:2000	N/A[d]	Dr E Knuepfer
α-MSP1	Mouse	Monoclonal	1:5000	1:1000	N/A[d]	Dr E Knuepfer
α-MSP7	Rabbit	Polyclonal AP[a]	1:10000	N/A[d]	N/A[d]	Dr M Kadekoppala
α-SERA5	Rabbit	Polyclonal AP[a]	1:20000	N/A[d]	N/A[d]	Dr R Stallmach
α-CDPK1	Rabbit	Polyclonal AP[a]	1:5000	N/A[d]	N/A[d]	Dr JL Green
α-GFP	Mouse	Monoclonal	1:1000	N/A[d]	N/A[d]	Roche
α-His	Rabbit	Polyclonal AP[a]	1:2000	N/A[d]	N/A[d]	Santa Cruz
GFP-Trap® Beads	Camel	Monoclonal (heavy chain only-agarose)[b]	N/A[d]	N/A[d]	30 µl[e]	Chromotek
GFP-Booster	Camel	Monoclonal (heavy chain only-fluor 488)[c]	N/A[d]	1:200	N/A[d]	Chromotek
Secondary:						
α-Mouse IgG HRP	Goat	Polyclonal AP[a]	1:5000	1:1000	N/A[d]	Biorad
α-Rabbit IgG HRP	Goat	Polyclonal AP[a]	1:5000	1:1000	N/A[d]	Biorad
α-Rabbit Alexa fluor® 488	Goat	Polyclonal AP[a]	N/A[d]	1:5000	N/A[d]	Invitrogen
α-Mouse Alexa fluor® 594	Goat	Polyclonal AP[a]	N/A[d]	1:5000	N/A[d]	Invitrogen
α-Rabbit Alexa fluor® 594	Goat	Polyclonal AP[a]	N/A[d]	1:5000	N/A[d]	Invitrogen

Table 2.2: The list of antibodies used in this experiment. a: Antibody affinity-purified; b: A VHH domain binding protein derived from camelid heavy chain-only antibodies is coupled to agarose beads for immunoprecipitation; c: A VHH domain binding protein derived from camelid heavy chain-only antibodies is coupled to a strong fluorescent dye-488) to both stabilize GFP and enhance its fluorescence signals; d: Antibody not used in or was un-suitable for the marked procedure; e: 1 µl resin can efficiently bind 1-3 µg proteins.

Chapter 3

In vitro phosphorylation of GAP45 protein by CDPK1

3.1 Introduction

Both the glideosome associated protein 45 (GAP45) and myosin tail domain-interacting protein (MTIP) have been shown to be phosphorylated by CDPK1 *in vitro*. Doublet protein bands of GAP45 as observed by SDS-PAGE analysis have been characterized as phosphorylated and unphosphorylated forms (Green et al., 2008). Based on several studies, GAP45 is a substrate protein for several post-translation modification processes. In addition to the myristoylation and palmitoylation that take place at its N-terminus (Rees-Channer et al., 2006), it was shown to be a substrate for two calcium activated kinases: PKB (Vaid et al., 2008) and CDPK1 (Green et al., 2008). A previous study has shown that GAP45 phosphopeptides from free merozoites could be detected by MALDI-TOF analysis (Green et al., 2008). Furthermore, several GAP45 phosphopeptides have been identified by phosphoproteomic studies on schizont stage parasites (Solyakov et al., 2011; Treeck et al., 2011). One of the phosphopeptides (DYATQENKSFEEKHLE) detected following phosphorylation by CDPK1 *in vitro*, was also found in the *in vivo*–derived parasite protein, hence strengthening the argument that GAP45 protein is a substrate for CDPK1 (Green et al., 2008). However, information from the previous analysis was limited as it was unable to show precisely the phosphorylated residues. In this study, the specific sites for CDPK1 phosphorylation of GAP45 were determined using an exhaustive site directed mutagenesis approach where all of the serine residues and selected threonine residues were converted to alanine. This

approach has successfully identified the major CDPK1 phosphorylation sites of GAP45 *in vitro*.

3.2 Extraction and purification of recombinant GAP45 protein

The GAP45 gene was cloned into the pET-46 Ek/LIC expression vector, which created a 6X His tag on the N-terminus of GAP45. The resultant pET-46-GAP45 plasmid was transformed into BL21 (DE3) RIL competent cells for expression. The expression of recombinant GAP45 protein was induced by IPTG which resulted in ~35-37 kDa protein as judged by SDS-PAGE. The expression of GAP45 was optimized using different culture conditions and induction temperatures until the protein was highly expressed and soluble (i.e. present in the lysate supernatant). The best conditions for expression were performing induction at 27ºC for 3 hours with 1 mM IPTG (Figure 3.1).

Since recombinant GAP45 was tagged with 6X His on its N-terminus, the isolation of this protein was achieved using affinity purification through the binding of His-tagged GAP45 protein between histidine and the metal ion nickel of Ni-NTA agarose. The washing and elution were done through a column with phosphate buffer pH 8.0 containing 20 mM and 250 mM imidazole respectively. Elution of the His-tagged GAP45 gave a high yield of a ~37 kDa protein with small amounts of impurities or protein breakdown products which it was not possible to eliminate (Figure 3.2). All recombinant GAP45 protein variants (substitution of serine (S) to alanine (A)) were also expressed and purified at similar amounts as wild type (WT) recombinant GAP45 protein.

The predicted molecular mass of recombinant GAP45 is 25.2 kDa; considerably smaller than the ~37 kDa band detected by SDS-PAGE. Similar to GAP45, merozoite surface protein 2 (MSP-2) has been characterized as a highly hydrophilic protein showing a relative molecular mass of 45 to 55 kDa, which is twice the molecular mass calculated from the sequence (Ishino et al., 2005). The possible anomalous migration behaviour may be due to an elongated structure or the

high content of charged residues in the protein that are likely to affect SDS binding (Baum et al., 2006b; Gaskins et al., 2004; Matagne et al., 1991).

3.3 *In vitro* CDPK1 kinase assay

As a previous study had found evidence of phosphorylated GAP45 *in vitro* and *in vivo* (Green et al. 2008), the present study has made an effort to further determine the specific amino acid residue(s) phosphorylated by CDPK1. This attempt was made by using GAP45 variants, substituting serine or threonine with alanine, in a CDPK1 kinase assay. The CDPK1 kinase assay was performed using several methods: with or without ^{32}P-ATP radiolabel, and was analysed by autoradiography, scintillation counting and the electrospray-mass spectrometry (ESi-MS) technique (without radiolabel).

Following phosphorylation catalysed by CDPK1 *in vitro*, ^{32}P-ATP autoradiography has showed that the level of ^{32}P incorporation into GAP45 variant protein bands except S103A is similar to that of WT GAP45 (Figure 3.3), indicating comparable levels of phosphorylation by CDPK1. The S103A protein band showed less incorporation of label as compared to the others. After densitometry analysis from three different experiments, the S103A variant showed a significant decrease ($p<0.05$) in its phosphorylation level of about 60% as compared to WT GAP45 (Figure 3.3). In addition, GAP45 that contained the S89A substitution showed a slight decrease in its phosphorylation of about 12% as compared to WT GAP45 (Figure 3.3). Following the above findings, a double mutation of GAP45 containing both S89A and S103A was produced. As expected, the phosphorylation of the S89A/S103A GAP45 decreased when compared to WT GAP45. However, the S89A/S103A GAP45 variant showed only 5% less ^{32}P incorporation compared to S103A (Figure 3.3). These results suggest that there are more CDPK1 phosphorylation sites on GAP45 that remain undiscovered. S103 is the major CDPK1 phosphorylation site on GAP45, as substitution of serine with alanine at this site contributes to more than 50% reduction of GAP45 phosphorylation.

The T84A GAP45 variant was included in the assay as it might have been the remaining CDPK1 phosphorylation site contributes to the low level of phosphorylation of S89A/S103A GAP45 (Figure 3.3). However, the T84A GAP45 variant was phosphorylated at the same level as WT GAP45 confirming that T84 is not a phosphorylation site for CDPK1 *in vitro*.

A CDPK1 kinase assay was also performed as a time course and analysed by scintillation counting (Figure 3.4). The results from this assay showed clearly that S89 of GAP45 is phosphorylated by CDPK1 as the S89A variant has decreased ^{32}P incorporation. However, this is not evident at t=10 min, when incorporation of ^{32}P into S89A GAP45 is indistinguishable from that of WT GAP45. The reduced incorporation of ^{32}P is only apparent in the later time points of the assay (from 15 min onwards) (Figure 3.4A). During the early period of the reaction, both WT and S89A proteins were phosphorylated at similar levels, presumably at S103, which is the major phosphorylation site for CDPK1 (Figure 3.4A). After 10 minutes of reaction, the level of phosphorylated WT GAP45 was still increasing, in contrast to S89A, where incorporation starts to slow down and remains unchanged after 40 minutes of reaction (Figure 3.4A). As shown by the S103A GAP45 variant, the incorporation of ^{32}P starts to slow down and remains unchanged after 5 minutes of reaction (Figure 3.4A). This result is similar with the double mutant protein, S89A/S103A (Figure 3.4A). This latter result also explains the insignificant decrease of GAP45 phosphorylation between S103A and S89A/S103A variants using the autoradiography technique (Figure 3.3). For further kinetic analysis, the CDPK1 kinase assay was also performed on a different concentration of GAP45 starting from 0.06 to 32 μM and analysed by scintillation counting. As we thought, the Vmax values for each GAP45 variants were decreasing starting from WT (9495 cpm), S89A (7278 cpm), S103A (3770 cpm) and S89A/S103A (2730 cpm) (Figure 3.4B).

3.4 Other possible CDPK1 phosphorylation sites on GAP45

In addition to the 'DYATQENKSFEEKHLE' GAP45 phosphopeptide, previous studies have also shown the existence of a second *in vivo* phosphorylated GAP45

peptide detected by MS-MALDI TOF analysis and this peptide, 'LSEPAHEESIYFTYR', contains two phosphorylatable serine amino acids, S142 and S149 (Green et al., 2008). Both S142A and S149A GAP45 variants were subjected to a CDPK1 kinase assay, as previously described in section 2.4 and analysed by autoradiography, scintillation counting and ES-MS. By autoradiography, neither S142A nor S149A variants show any decrease in GAP45 phosphorylation as compared to WT GAP45 (Figure 3.5). In contrast, S142A and S149A variants showed an increased in phosphorylation level of GAP45 to about 1.5 to 2.5 fold that of WT GAP45 (Figure 3.5). Triple substitutions, S89A/S103A/S142A and S89A/S103A/S142A, showed decreased phosphorylation of GAP45 to about 26 and 30 percent of wild type levels, respectively (Figure 3.5). Scintillation analysis shows higher levels of phosphorylation of the S142A and S149A GAP45 variants compared to WT over time (Figure 3.6). As found in the autoradiography analysis, triple GAP45 variants, S89A/S103A/S142A and S89A/S103A/S142A, show decreased GAP45 phosphorylation (Figure 3.6). These findings suggest that substitution of S142 or S149 with alanine increases the amount of either S89 or S103 phosphorylation by CDPK1.

Neither the S103A nor the S89A/S103A substitutions were able to ablate phosphorylation of GAP45 completely (Figure 3.3). Similar results were also shown by triple GAP45 variants, S89A/S103A/S142A and S89A/S103A/S142A where there was still approximately 20% to 30% phosphorylation compared to the wild type protein (Figure 3.5). Since additional CDPK1 phosphorylation sites on GAP45 were suspected, all the serine residues were substituted to alanine. By autoradiography, all of the GAP45 variants except S103A, S89A/S103A, S142A and S149A had no significant effect compared to the WT GAP45 protein (Table 3.1; Appendix A). The other phosphorylated residues are likely to be S31 and S156, identified as possible CDPK1 targets in the analysis of individual serine substitution of GAP45, which showed a similar phosphorylation level as S89 (Table 3.1; Appendix A).

3.5 Electrospray mass spectrometry analysis of unphosphorylated and phosphorylated recombinant GAP45 protein

To further confirm the presence of other CDPK1 phosphorylation sites on GAP45, WT-GAP45 and all the GAP45 mutants were subjected to ES-MS analysis. ES-MS can measure the mass of a recombinant protein using either intact molecules or proteolytically digested molecules (Mann and Wilm, 1995). The proteins are protonated, fragmented and detected by the mass spectrometer according to their mass/charge ratio (m/z). The resulting mass spectrum is characterized by a series of peaks caused by multiple charges on the protein molecules which then can be deconvoluted into a single peak of protein mass with an accuracy typically within 1 Da in every 10 kDa (Mann & Wilm 1995). So, it is possible to detect the different forms of GAP45, unphosphorylated and phosphorylated. The electrospray mass spectrometry will detect any addition of a ~80 Dalton phosphate moiety on intact GAP45 hence showing the number of phosphate molecules being added by CDPK1.

For the purpose of this analysis, a large amount of highly phosphorylated GAP45 was required and some modification to assay conditions was needed. The CDPK1 kinase assay was done without radiolabelling and using a high concentration of CDPK1 (0.04 µg/µl or 658 nM) and 1 mM ATP (10X higher than the previous assay). The reaction time was also prolonged to 90 minutes. As a negative control, the assay was performed in the absence of Ca^{2+}. From the deconvoluted MS spectrum, the unphosphorylated GAP45 shows a primary peak sized 25212.357 Da (Figure 3.7, i). The peak size corresponded to the recombinant GAP45 size that was estimated by ExPASy ProtParam tool as 25213.4 Da. As expected, a reduction of molecular mass is detected in the spectrum of GAP45 mutants, 16 Da for a serine to alanine single mutation and 32 Da for the double mutation, due to the molecular weight differences between serine and alanine (Figure 3.7).

Phosphorylated WT GAP45 shows 4 forms, with additional 80, 160, 240 and 320 Da increases in size corresponding to one, two, three and four phosphate incorporations respectively (Figure 3.7, ii). No unphosphorylated peak was detected showing that all of the WT GAP45 was phosphorylated on at least one site under

these conditions. The S89A GAP45 variant spectrum showed the disappearance of the four-phosphate GAP45 peak and similar results were also shown by the S103A GAP45 variant but with an additional peak corresponding to unphosphorylated GAP45 (Figure 3.7, iii & iv). As shown by previous autoradiography results, the S103A GAP45 variant has largely reduced the level of phosphorylation when compared to the S89A GAP45 variant (Figure 3.3). However, the amount of phosphorylated GAP45 detected for S103A GAP45 variant in this experiment was similar to that of the S89A GAP45 variant (Figure 3.7, iii & iv). This is because of the different conditions used in the two experiments, such as the high concentration of CDPK1 and prolonged reaction time adopted for the ES-MS analysis.

For the double substitutions, the S89A/S103A GAP45 spectrum only showed the first and second phosphate incorporated GAP45 with an additional unphosphorylated peak (Figure 3.7, v). Again, mass spectrometry shows the importance of S89 and S103 amino acid residues for CDPK1 phosphorylation of GAP45 with the latter residue most important as it reduced GAP45 phosphorylation, as demonstrated by the appearance of an unphosphorylated peak (Figure 3.7, v). However, even the double substitutions of GAP45 still show 2 forms of phosphorylated GAP45 which correspond to one and two phosphate additions by CDPK1.

A maximum of four phosphate groups can also be seen to be incorporated into both S142A and S149A GAP45, similar to WT GAP45 (Figure 3.7, vi & vii). In contrast, in the assay with S142A or S149A GAP45 a minimum of two phosphates were added (Figure 3.7, vi & vii). Thus, substitution of S142 or S149 with alanine increases the phosphorylation of GAP45, with the majority of the protein containing three phosphorylated residues (Figure 3.7, vi & vii). The reason for this phenomenon could be that substitution of serine 142 or serine 149 of GAP45 with alanine contributes to changes in protein structure or folding hence increasing the accessibility of a major CDPK1 phosphorylation site such as S103 or S89. To test this hypothesis, S142A and S149A GAP45 together with other GAP45 variants were subjected to far UV circular dichroism analysis (CD), to detect any secondary structural changes to these proteins upon phosphorylation.

3.6 Secondary structure of phosphorylated GAP45

Circular dichrosim (CD) is a method for determining the conformation of a macromolecule in solution (Martin and Schilstra, 2008). With only a small amount of sample needed, it can monitor any secondary, tertiary and quarternary structural changes that might result from changes in environmental conditions, such as, pH, temperature, and ionic strength (Martin and Schilstra, 2008). In addition it is also used in structural analysis of recombinant protein and their variants (Martin and Schilstra, 2008). However it is not as powerful as nuclear magnetic resonance (NMR) and X-ray crystallography, which provide information about specific residues (Martin and Schilstra, 2008). The near UV spectral bands of proteins (310-255 nm) reflect the tertiary and quarternary structure of protein while far-UV spectral bands of proteins (below 250 nm) reflect the secondary structure of protein (Martin and Schilstra, 2008). After generating variant proteins, it is good practice to test for any significant effect of the substitution on the general conformation of a protein as compared to native or wild type protein. A difference between the far-UV CD spectra of the wild type and variant proteins can be an indication that the mutation has produced some change in secondary structure (Martin and Schilstra, 2008).

The GAP45 protein had previously being analysed by far UV CD (unpublished data) and it was recognised as a disordered or unstructured protein as also shown by this study (Figure 3.8). However, the protein is not fully disordered. After further analysis from the average of 60 readings, the spectrum was consistent with a protein containing 4% alpha helix, 22% beta sheet, 10% turn and 64% unstructured region (Sreerama and Woody, 2000). None of the GAP45 variants including S142A and S149A, which showed the high phosphorylation levels had any secondary structure changes as compared to the WT GAP45 revealed by the CD spectrum (Figure 3.8). To further analyse the potential of protein structure changes after phosphorylation, S142A and WT GAP45 mutants were phosphorylated and subjected to CD analysis. The CDPK1 kinase phosphorylation conditions were based on the condition used for ES-MS where the GAP45 was maximally phosphorylated, with at least one phosphate incorporation on all WT GAP45 molecules (Figure 3.7).

From these data, neither unphosphorylated nor phosphorylated GAP45 showed any changes in the secondary structure (Figure 3.8 & Figure 3.9).

The phosphorylation of GAP45 by CDPK1 might not result in any major structural changes; i.e. the phosphorylation of GAP45 might only result in electrostatic modification, addition of charge that might be important for its function. A further possible explanation for the increased phosphorylation in S142A and S149A GAP45 could be small changes in protein folding that could not be detected by CD analysis.

3.7 Discussion

Serine 103 of GAP45 is the major phosphorylation site in GAP45 for CDPK1 *in vitro*. There is a secondary phosphorylation site, serine 89, which is not so obvious in the autoradiography analysis but this site was shown to be phosphorylated at later time points of the assay by scintillation counting. However, there are still other unknown phosphorylation sites on GAP45 which we have been unable to determine by this study.

Since this work was performed, GAP45 was reported to be phosphorylated *in vitro* by CDPK1 at 9 residues (Ser31, Ser89, Ser103, Ser109, Ser121, Ser149, Ser156, Thr158, and Ser173) as detected by nano-ultra performance liquid chromatography-electrospray ionization-tandem mass spectrometry (UPLC–ESI–MS/MS) (Winter et al., 2009). This study also showed that protease digestion sites (such as trypsin) were interfered with by phosphorylation, leading to protease-resistant GAP45, particularly when the phosphorylation site is located in close proximity (-/+ 2) to the protease digestion site. This might also explain why MALDI-TOF analysis in a previous study (Green et al., 2008) was unable to detect all GAP45 phosphopeptides. Another study of the *P. falciparum* phosphoproteome revealed multiple phosphorylated residues of GAP45, including S89, S103 (Solyakov et al., 2011; Treeck et al., 2011) and also S156, identified here as a minor CDPK1 site (Treeck et al., 2011).

Phosphorylation of S89 and S103 has different kinetics, with S103 being faster than S89. This suggests the possibility of hierarchical phosphorylation of GAP45, where phosphorylation on S103 is needed for further phosphorylation on other sites. This phenomenon may also be explained by the preferred linear motif for CDPK1. Studies on plant CDPK1 have shown that most CDPK1 substrates have a consensus K/R_{-3}-x-x-S/T_0 (x, any residue) *in vitro* (Harper and Harmon, 2005; Hernandez Sebastia et al., 2004; Loog et al., 2000). This motif has been designated a "simple 1 motif" according to the nomenclature established by Harper and Harmon (2005) with the basic residue located at position -3 upstream of the phosphorylated residue (Table 3.2). As detected in this study, the sequence upstream of S103 is LE$\underline{R}^{100}$SN$\underline{S}^{103}$, which fits with the more preferable simple 1 motif (Table 3.2). Another motif called "simple 2" has been identified, with a basic residue at position +2. This motif fits with S109 in GAP45 (Table 3.2). In the case of S89, the sequence surrounding it does not fit to the simple 1 or simple 2 consensus motifs. Noting that CDPKs have more than one consensus motif (Harper and Harmon, 2005; Hernandez Sebastia et al., 2004), the S89 is a novel CDPK1 specific site on GAP45 of *P. falciparum*, where the basic residue is located at position -1 in the so called motif simple 3 (Table 3.2) (Winter et al., 2009).

Other possible sites for CDPK1 phosphorylation are serine 142 and serine 149 modifications which were previously detected in GAP45 purified from the merozoite (Green et al., 2008). Suprisingly, substitution of these sites with alanine increased the phosphorylation level of GAP45 by CDPK1 *in vitro*. It is possible that phosphorylation or dephosphorylation on these sites might play a role in regulating the ability of CDPK1 to access other sites such as S89 and S103 which could be hidden when S142 and/or S149 are phosphorylated. This possibility is supported by this study where substitution of either of these sites, S142 and S149, increased the phosphate incorporation on GAP45. However, substitution of S142 or S149 together with S89 and S103 to alanine decreased the enhancement effect on GAP45 phosphorylation (Figure 3.5 and Figure 3.6). The findings have suggested that the GAP45 phosphorylation may be allosterically regulated. A similar phenomenon has also been reported by other investigators specifically on S149 phosphorylation (Thomas et al., 2012). In addition, the position of S149 meets the sequence

requirements of an unusual CDPK1 motif, motif simple 3 (Winter et al., 2009). This motif is similar to the conventional motif simple 1 except the basic residue, histidine ($\underline{H}_{-3}$-x-x-S/T_0) carries a partial positive charge at neutral pH (Table 3.2) (Winter et al., 2009). In order to investigate more the enhancement effect on GAP45 phosphorylation, a different combination of S142 or S149 GAP45 variants with other serine (S/A) variants will give more information on the specific residues affected. For example, generating the serine to alanine double substitution of S142A/S89A or S142A/S103A might elucidate the specific residues (either S89 or S103) affected by the S142A and S149A variants.

Proteins that contain large segments of disordered structure under physiological conditions or in which the entire protein is disordered are known as instrinsically unstructured proteins. Intrinsically unstructured proteins are often involved in key biological processes, such as transcriptional or translational regulation, membrane fusion and transport, cell signal transduction and protein phosphorylation. The unstructured region will create larger intermolecular interfaces that enhance the interaction with potential binding partners without relying on tight binding, and provide a flexibility for the protein to bind diverse ligands (Feng et al., 2006). Functionally, GAP45 protein probably needs these characteristics in order to be flexible in interacting with other proteins.

Protein phosphorylation can cause structured or unstructured transition of the target protein (Johnson and Lewis, 2001). However, by CD analysis, phosphorylation did not cause any changes to the overall disordered structure of GAP45. It may be that some changes to specific regions could not be detected by CD analysis. For example, the inactivation gate of a K^+ channel is regulated by phosphorylation on its inactivation domain (ID), which comprises 1-30 residues that block the pore on the cytoplasmic side. As analysed by nuclear magnetic resonance (NMR), phosphorylation of serine 8, or 15 and 21 of the ID causes the residues around the phosphorylation area to form an ordered structure while the rest of the region (N and C terminus) remains disordered hence increasing the rate of dissociation from the receptor (Johnson and Lewis, 2001). Of course, it is possible that phosphorylation by CDPK1 per se might not be enough to trigger any major structural changes.

After analysing the GAP45 protein sequence using the ExPasy ProtParam tool (www.expasy.org/cgi-bin/protparam), the amino acid composition showed the characteristics of intrinsic unstructured proteins that are prone to phosphorylation. The GAP45 protein is depleted in rigid, buried and neutral amino acids (0% W, 2.8% C, 1.8% F, 4.6% I, 1.8% Y, 4.1% V and 6.9% L) and enriched in flexible surface exposed serine, proline, glutamic acid and lysine (7.4% S, 3.7% P, 19.4% E, 9.2% K) (Dunker et al., 2001; Iakoucheva et al., 2004). Thus, with the composition and characteristics of an unstructured protein, it is well suited for the GAP45 protein to be a flexible linker that mediates the interaction with other motor complex proteins in the IMC.

There are other *P. falciparum* proteins containing unstructured regions. For example, the *P. falciparum* protein, apical membrane antigen 1 (AMA1) has one or two unstructured and flexible regions that may protect a hydrophobic ligand-binding cleft from antibody binding. Erythrocyte membrane protein 1 (PfEMP1), the *var* gene product, has been reported to have this kind of flexible region that facilitates protein-protein interactions between Duffy binding-like (DBL) domains and host protein that lead to cytoadherence. Merozoite surface protein 3 (MSP-3) also has an unstructured region that extends from a highly ordered region. The unstructured region of MSP-3 is highly acidic and may be important for providing a negative charge to a cell surface that lacks sialoglycoproteins (all described in (Feng et al., 2006)). This group also includes the MSP-2 protein, which is largely disordered and one of the most abundant *P. falciparum* merozoite surface proteins. MSP-2 is likely to have a role in merozoite attachment to host red blood cells, and this binding may initiate the transition to a more ordered structure (Feng et al., 2006). In detail, the MSP-2 monomer has been characterized by the low complexity of its sequences and biased amino acid composition with highly hydrophilic residues, and it is also deficient in hydrophobic residues. These characteristics are consistent with it being instrinsically unstructured. This protein then polymerizes to form oligomers by intermolecular β-strand interactions that may contribute to the fibrillar surface coat on *P. falciparum* merozoites (Ishino et al., 2005).

In addition, most of the instrinsically unstructured proteins of the *P. falciparum* proteome are antigens. These include MSP2, Ag332, MESA, CS, and glutamate-rich protein which are highly immunogenic regarding their reactivity with antibodies. However, instrinsically unstructured regions of proteins have the ability to adopt more ordered structures when interacting with different target ligands. So, the antibodies induced by this region may recognize a variety of antigen conformers which may cause a poor reactivity to the actual functional protein (Feng et al., 2006).

These interesting findings have led this study on GAP45 protein to investigate further its functional role during *P. falciparum* growth. As an unstructured protein, it is interesting to find the possible phenotype or any upset of its function upon the removal of the phosphorylation sites, since this may influence GAP45 interactions with the motor complex or the subcellular localisation of GAP45 itself. From what has been discovered from the *in vitro* CDPK1 kinase assay, the next chapter will address the importance of CDPK1 phosphorylation of GAP45 on sites S89 and S103 *in vivo* and the effects of substitutions at these sites on parasite growth.

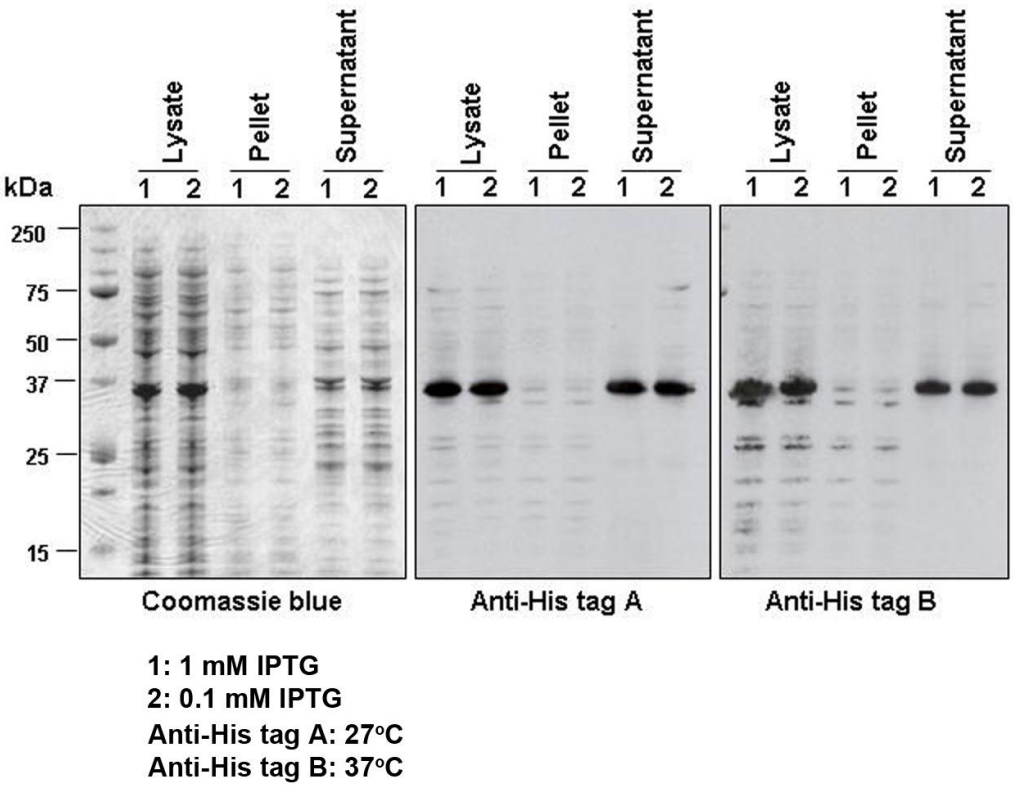

Figure 3.1: Recombinant PfGAP45 protein extraction. Protein expression was induced using (1) 1 mM or (2) 0.1 mM IPTG at 27^{o}C (A) or 37^{o}C (B). The lysate, pellet and supernatant fraction for each condition were separated by SDS-PAGE and analysed by western blotting using anti-His antibody and visualized by film exposure using the ECL system. The total protein profile (coomassie blue) was from the culture induce using 1mM IPTG at 27^{o}C. This was the optimized expression condition for the recombinant His-tagged GAP45 protein where it was totally produced in soluble form (Anti-His tag A) without any breakdown products (Anti-His tag B) as shown in western blots.

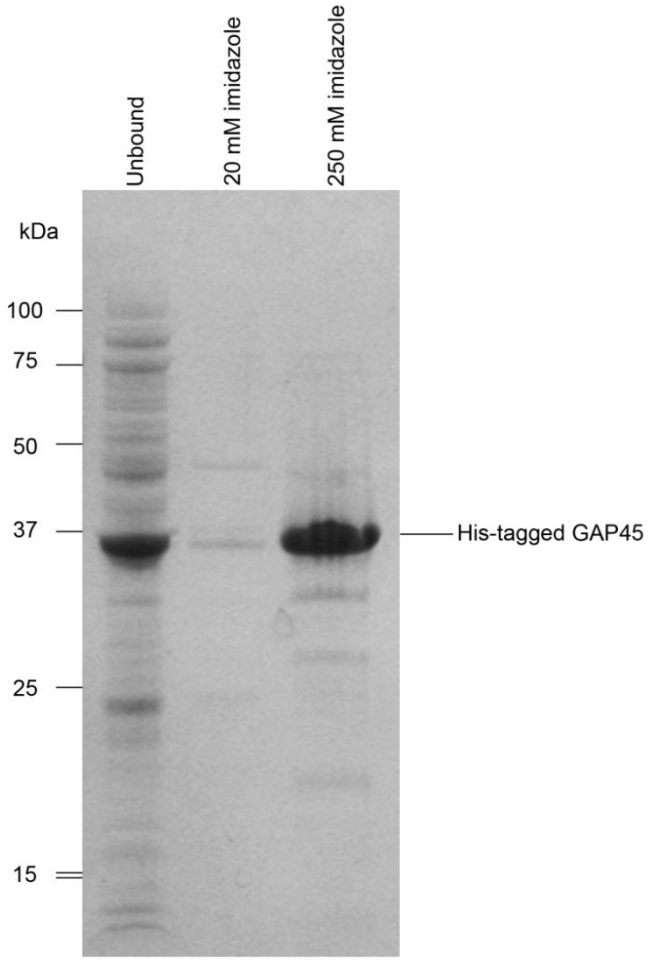

Figure 3.2: Purification of recombinant *Plasmodium falciparum* GAP45. The bacterial cell lysate supernatant was mixed with Ni-NTA agarose (batch method). The mixture was packed into a column and the unbound material (lane 1) was removed. The column was washed with phosphate buffer pH 6.5 containing 20 mM imidazole (lane 2) and eluted with the same buffer containing 250 mM imidazole (lane 3). Proteins were analysed by SDS-PAGE and coomassie blue staining; the migration of standard marker proteins (kDa) is shown on the left side of the figure and the location of His-tagged GAP45 is shown on the right side.

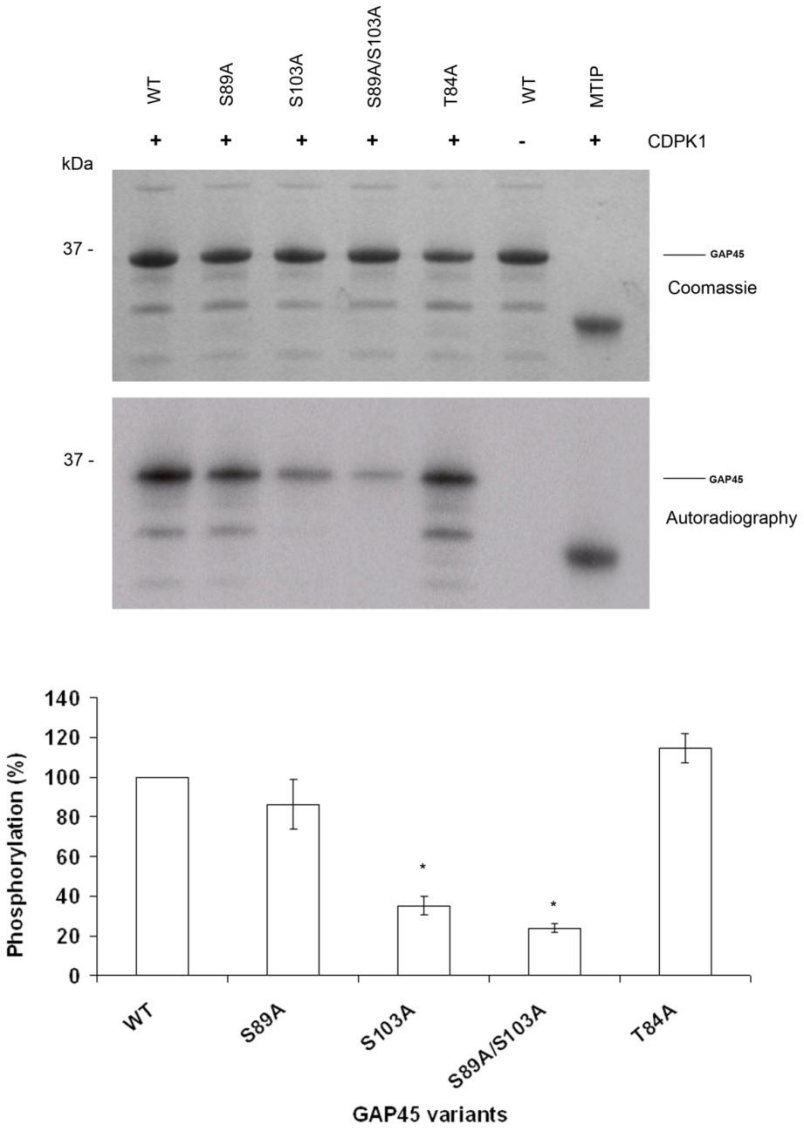

Figure 3.3: *In vitro* CDPK1 phosphorylation of recombinant PfGAP45 and variants at 30^{o}C, 10 minutes using 100 nM CDPK1. The intensity of the bands (autoradiography) were standardized against the protein concentration profile (coomassie) and analysed by ImageJ software. MTIP is a positive control for phosphorylation by CDPK1. The data are presented as a mean ± standard error of mean (S.E.M) from 5 different experiments. * denotes a significant difference ($p<0.05$).

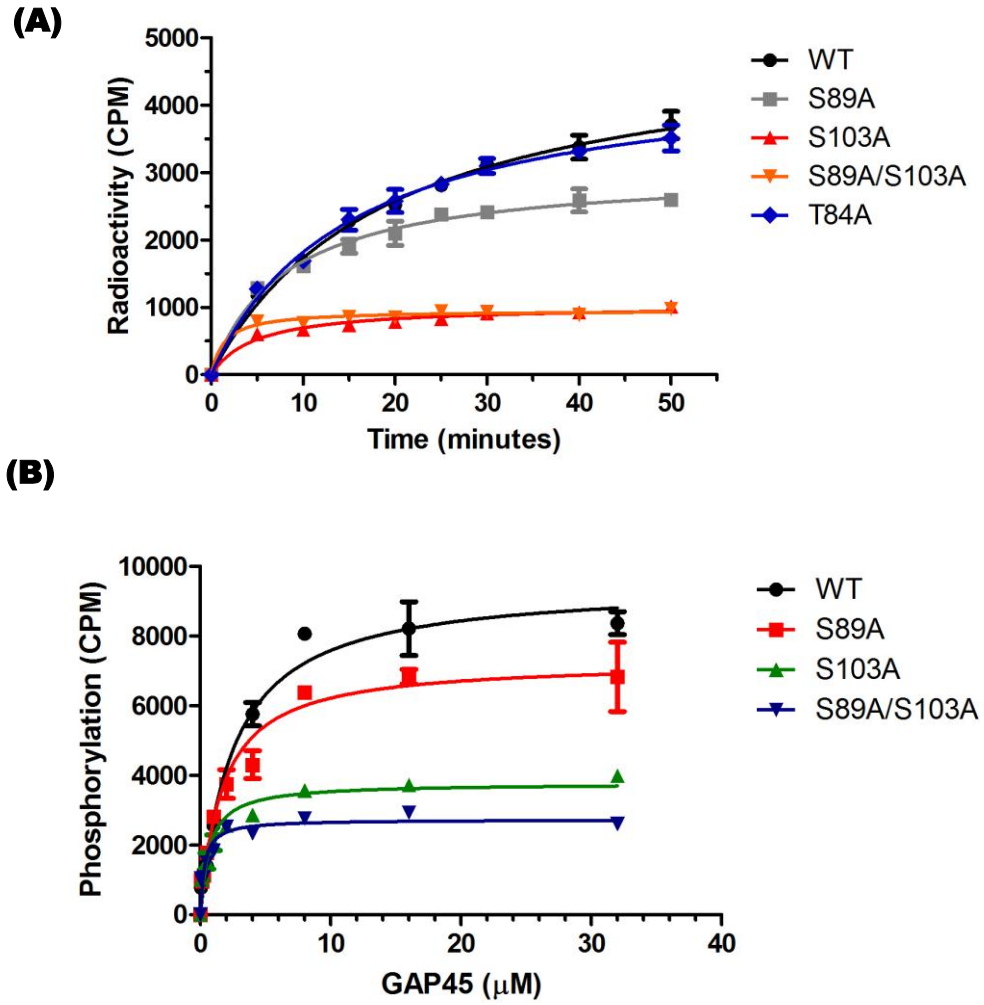

Vmax value (cpm)

WT: 9495; S89A: 7278; S103A: 3770 and S89A/S103A: 2730

Figure 3.4: **CDPK1-dependent phosphorylation of recombinant GAP45 proteins *in vitro* by incorporation of ^{32}P at 30^{o}C, using 100 nM CDPK1 and 0.1 mM [^{32}P]ATP and detection by scintillation counting.** The CDPK1 kinase assay was performed as a time dependent phosphorylation of GAP45 (8 μM) (A) and at different concentrations of GAP45 (10 minutes reaction time) (B). The data are presented as a mean from duplicate reactions for the unmodified protein (WT) or variants where a serine or a threonine have been replaced by alanine at either a single or up to two locations in the protein. The Vmax values were determined by GraphPad Prism analytical software. The data are presented as a mean ± S.E.M from duplicate experiments.

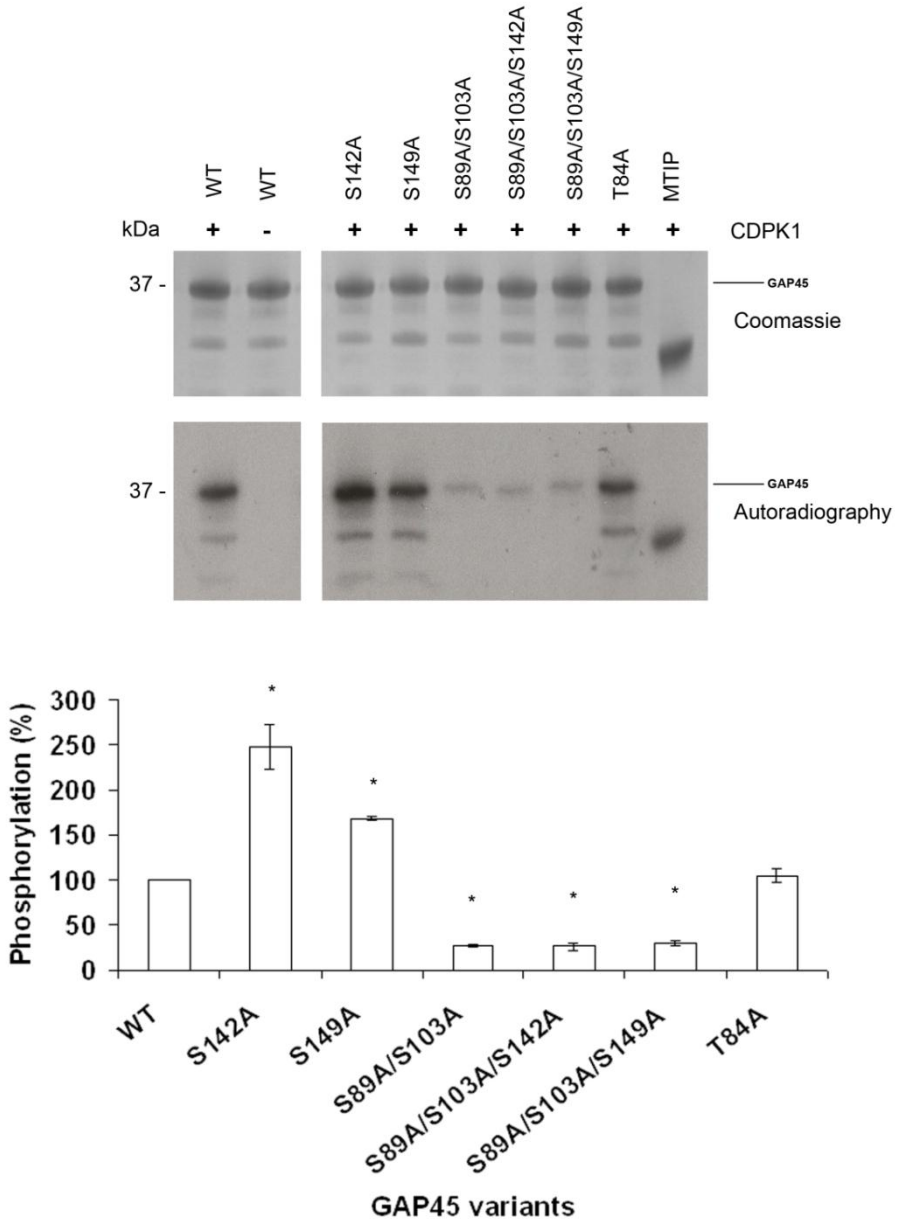

Figure 3.5: *In vitro* CDPK1 phosphorylation of recombinant PfGAP45 and variants at 30^{o}C, 10 minutes using 100 nM CDPK1. The intensity of the bands (autoradiography) was standardized with the protein concentration profile (coomassie) and analysed by ImageJ software. MTIP is a positive control for phosphorylation by CDPK1. The data are presented as a mean ± S.E.M from 3 different experiments. * denotes a significant difference ($p<0.05$).

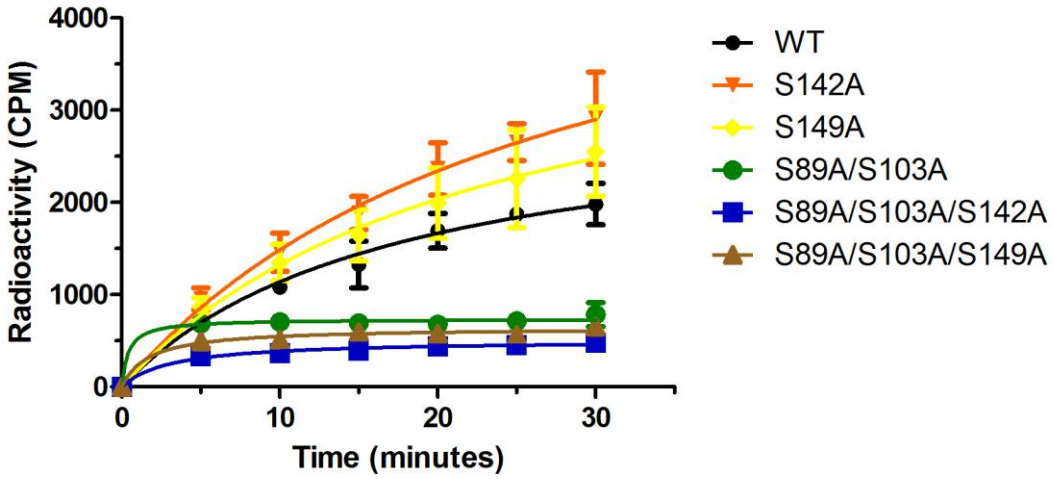

Figure 3.6: CDPK1-dependent phosphorylation of recombinant GAP45 proteins *in vitro* by incorporation of ^{32}P at 30^{o}C, using 100 nM CDPK1 and 0.1 mM [^{32}P]ATP and detection by scintillation counting. The data are presented as a mean ± S.E.M from duplicate reactions for the unmodified protein (WT) or variants where a serine has been replaced by alanine at either a single or up to three locations in the protein.

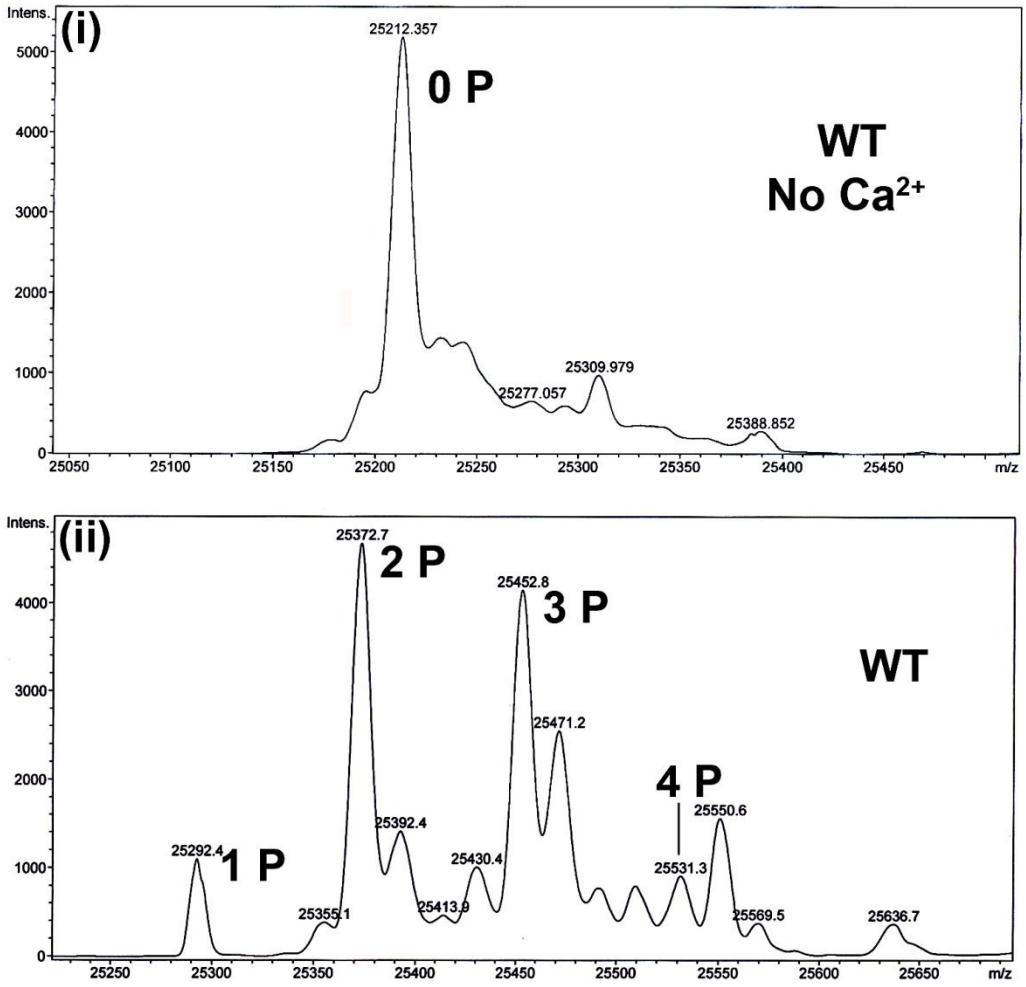

Figure 3.7: Electrospray-mass spectrometry analysis of (i) unphosphorylated and (ii) phosphorylated recombinant WT GAP45, (iii) phosphorylated S89A, (iv) S103A, (v) S89A/S103A, (vi) S142A and (vii) S149A mutant GAP45. Recombinant protein was phosphorylated with 650 nM CDPK1 at 30^{o}C for 90 mins. The phosphorylated WT GAP45 showed incorporation of up to 4 phosphate groups per molecule. Due to the molecular weight differences between serine and alanine, a reduction of molecular mass is detected in the spectrum of GAP45 mutants, 16 Da for a serine to alanine single mutation and 32 Da for the double mutation. Both S89A and S103A variants had decreased phosphorylation with up to 3 phosphate groups. The two-site variant, S89A/S103A had decreased phosphorylation, with up to 2 phosphates incorporated. The variants S142A and S149A had no detectable mono-phosphorylated form and a shift to increased relative amounts of the multiply phosphorylated forms, but with no more than four phosphate groups per molecule.

Figure 3.7 continued: Electrospray-mass spectrometry analysis of (i) unphosphorylated and (ii) phosphorylated recombinant WT GAP45, (iii) phosphorylated S89A, (iv) S103A, (v) S89A/S103A, (vi) S142A and (vii) S149A mutant GAP45.

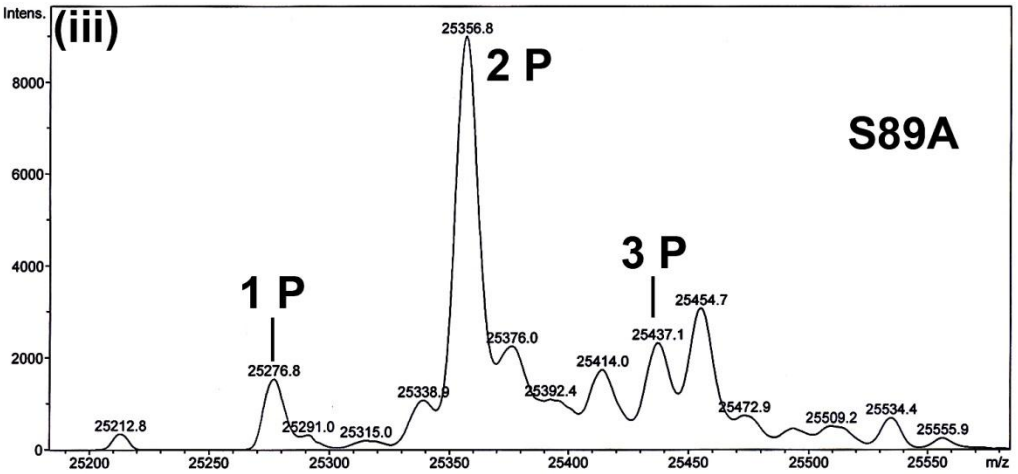

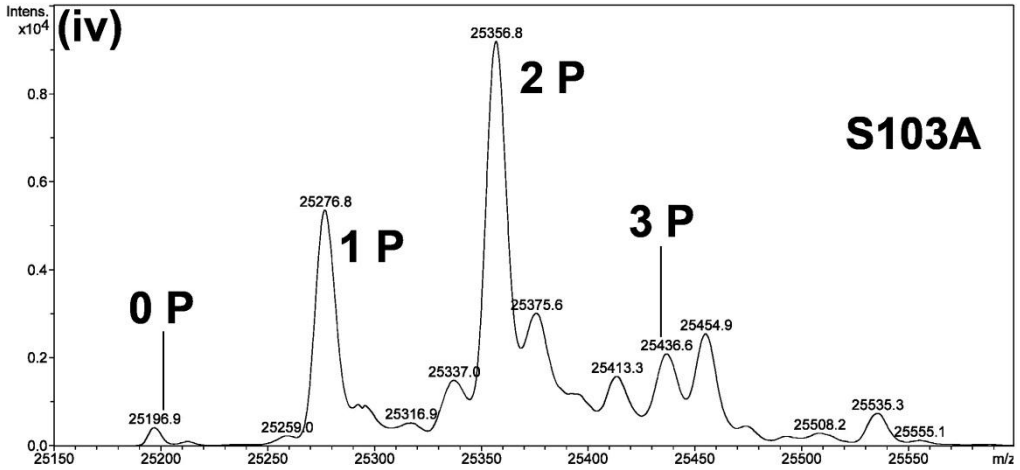

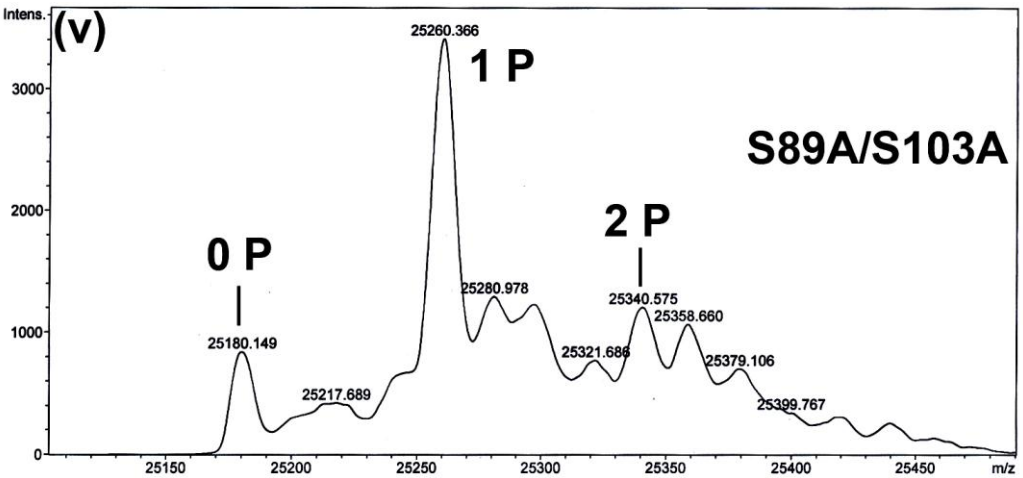

Figure 3.7 continued: Electrospray-mass spectrometry analysis of (i) unphosphorylated and (ii) phosphorylated recombinant WT GAP45, (iii) phosphorylated S89A, (iv) S103A, (v) S89A/S103A, (vi) S142A and (vii) S149A mutant GAP45.

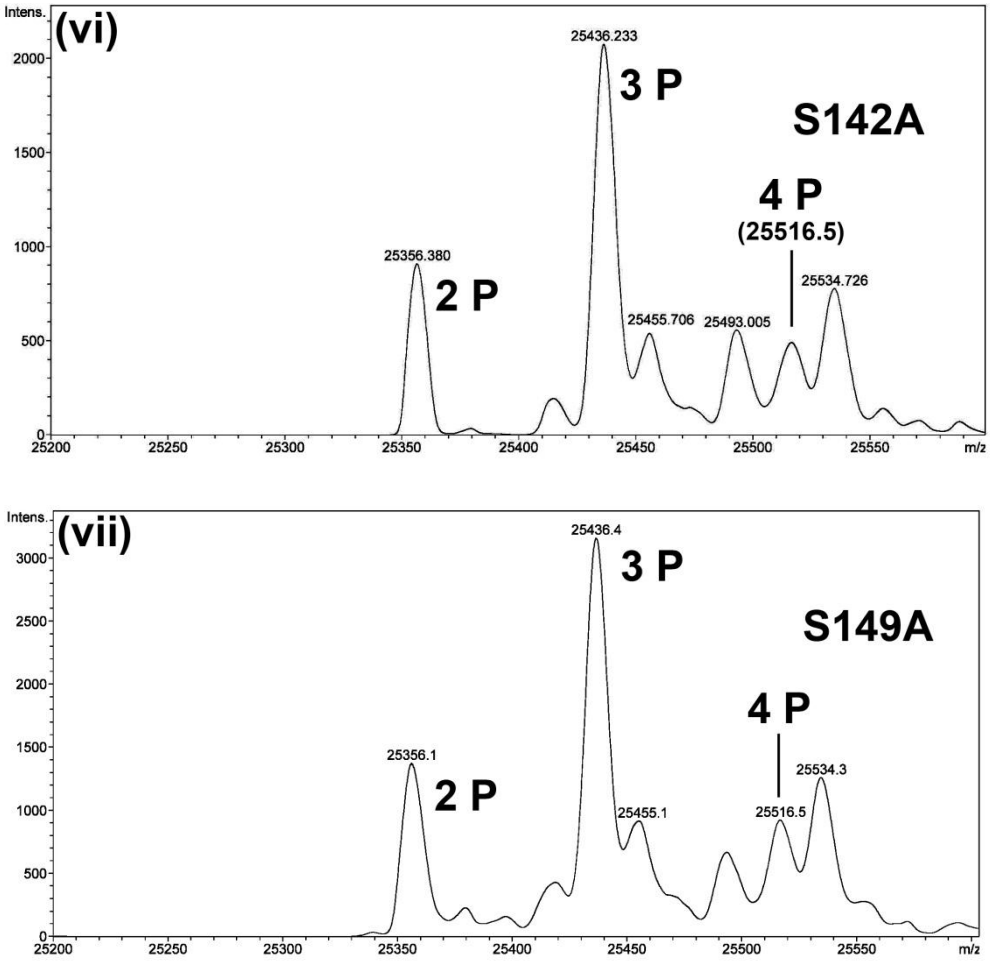

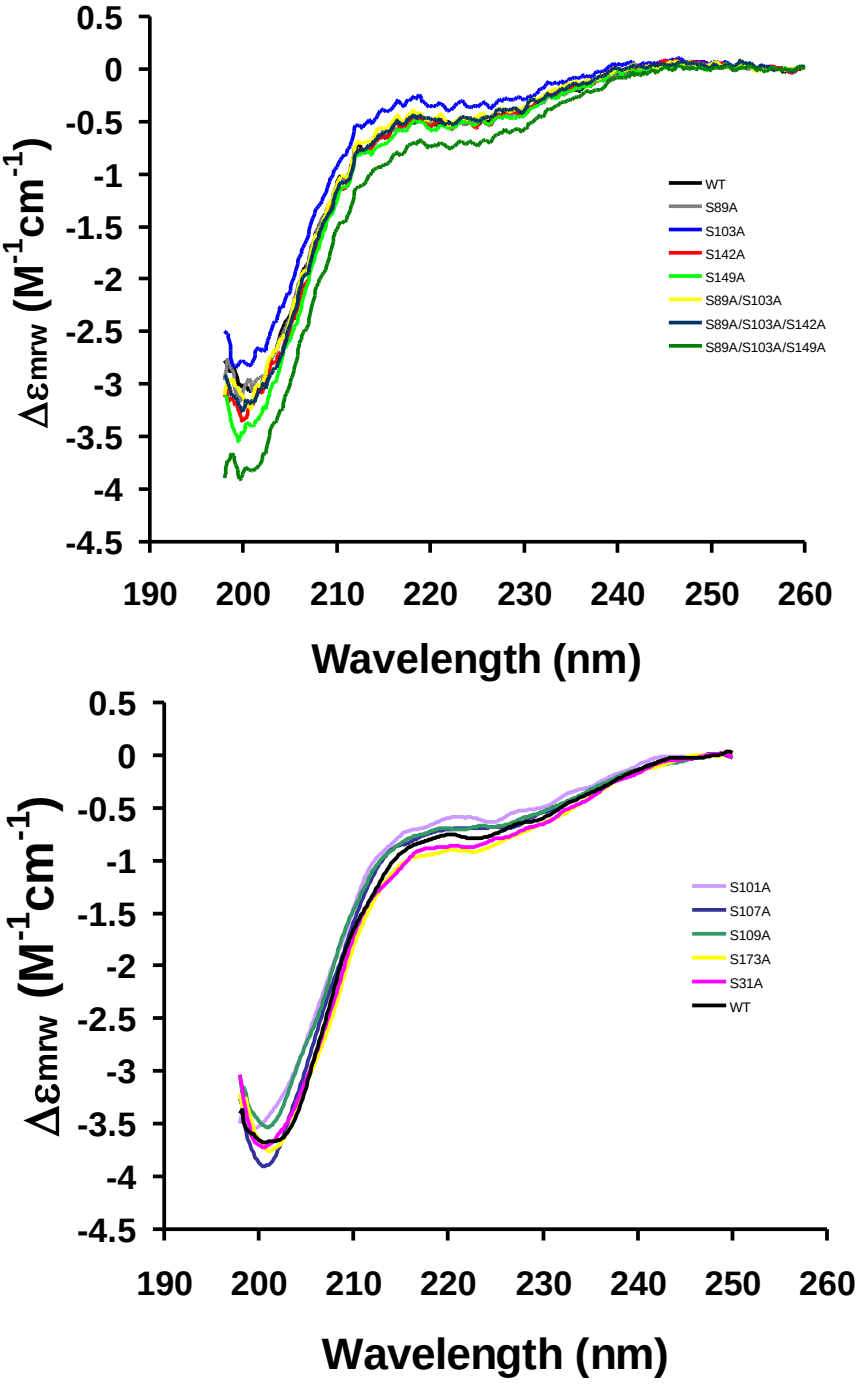

Figure 3.8: Far UV circular dichroism (CD) spectra of WT GAP45 and its variants. The purified GAP45 recombinant proteins were suspended in PBS prior to CD determination. The secondary structure of recombinant proteins was determined by monitoring CD in the far-UV region (190-260 nm). The values were averaged from multiple scans and presented on a mean residue weight ($\Delta\varepsilon_{MRW}$) basis.

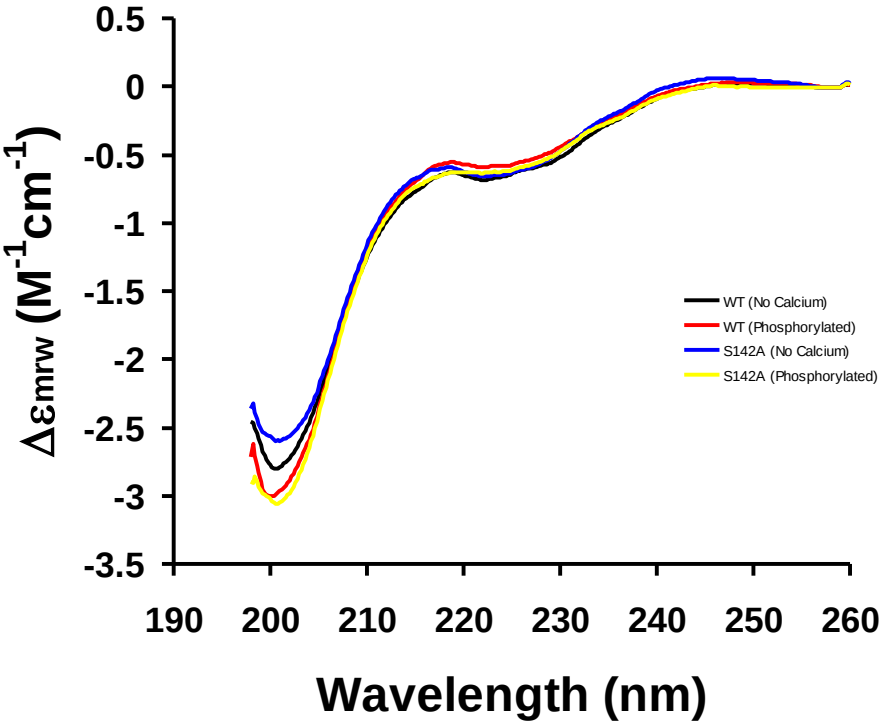

Figure 3.9: Far UV circular dichroism (CD) spectra of unphosphorylated and phosphorylated WT and S142A GAP45. The purified GAP45 recombinant proteins were subjected to CDPK1 phosphorylation with or without Ca^{2+} using 650 nM CDPK1 at 30^{o}C for 90 mins. The sample solution was buffer exchanged with PBS prior to CD determination. The secondary structure of recombinant proteins was determined by monitoring CD in the far-UV region (190-260 nm). The values were averaged from multiple scans and presented on a mean residue weight ($\Delta\varepsilon_{MRW}$) basis.

GAP45 protein	Phosphorylation ± SD (%)
WT	100.00 ± 0.00
S6A	104.63 ± 12.25[b]
S8A	116.72 ± 9.51 [b]
S31A	90.09 ± 7.92[b]
S89A	86.29 ± 27.79[c]
S101A	97.21 ± 0.94[a]
S103A	35.26 ± 10.54[c]
S107A	93.90 ± 5.34
S109A	131.78 ± 0.67
S116A	128.20 ± 23.50 [b]
S128A	127.29 ± 26.88 [b]
S142A	248.04 ± 41.74[b]
S149A	167.62 ± 4.62[b]
S156A	87.79 ± 6.89 [b]
S173A	106.06 ± 13.60[b]
S198A	116.12 ± 10.33 [b]
S204A	123.09 ± 15.98 [b]
T84A	114.28 ± 16.33[c]
S89A/S103A	23.83 ± 5.00[c]
S89A/S103A/S142A	25.96 ± 6.22[b]
S89A/S103A/S149A	29.77 ± 6.36[b]

Table 3.1: *In vitro* CDPK1 phosphorylation of recombinant PfGAP45 and its variants at 30^{o}C, 10 minutes using 100 nM CDPK1. The intensity of the bands (autoradiography) were standardized against the protein concentration profile (coomassie) and analysed by ImageJ software. The data are presented as a mean percentage ± S.D. a= 2 independent experiments, duplicate each; b= 3 independent experiments, duplicate each; c= 5 independent experiments, duplicate each and Unlabelled= duplicate. (The graph view is available in Appendix A).

(Winter et al., 2009)

Table 3.2: **Sequence motifs (± residues) flanking the phosphorylation sites identified in PfGAP45**. Six out of nine phosphorylated residues were found to meet the CDPK1 simple 1 motif. The major phosphorylation site, S103 of GAP45, meets the simple 1 motif. The S109 residue meets the CDPK1 simple 2 motif. The S89 and S156 meet the simple 3 motif (Winter et al., 2009).

Chapter 4

Characterization of *P. falciparum* GFP-tagged GAP45

4.1 Introduction

The GAP45 protein was first identified as a component of the motor complex machinery in *T. gondii*. It was located around the periphery of the parasite, specifically binding to the IMC (Johnson et al., 2007). Further investigation in *T. gondii* has embraced the dual role played by the GAP45 protein during parasite development and invasion. First, the GAP45 protein is a protein that is responsible for recruiting other motor complex proteins such as MTIP and MyoA to the IMC. This process is governed by vesicle transportation (Agop-Nersesian et al., 2009) and post translational modification such as phosphorylation (Gilk et al., 2009) and C-terminal palmitoylation (Frenal et al., 2010). The second function of this protein is to maintain the structure of the parasite pellicle during invasion which is played by the N-terminal myristoylation that binds the protein to the plasma membrane, and the length of the coiled-coil domain in GAP45 (Frenal et al., 2010). However, apart from an *in vitro* study, there is no clear evidence of GAP45 roles in *Plasmodium* parasites. It is hoped that further study of the GAP45 protein in *Plasmodium* parasites will elaborate new ideas about its function during parasite growth and invasion. Whether its function will or will not be similar to TgGAP45 is another exciting area that is worth investigating. With that in mind, this study has made an effort to create an episomal plasmid transfection construct programmed to express the GFP-tagged GAP45 protein in *P. falciparum* during blood stage schizogony.

Given that GAP45 is an important component of the motor complex, the level of essentiality of this protein in parasite growth has to be considered before

performing any transfection process. Any modification to the native GAP45 protein might be detrimental to parasite development hence destroying the effort of determining the function of this protein due to a dead phenotype. The most suitable method to study this protein *in vivo* is by performing episomal transfection. Episomal transfected parasites can withstand any modification of an essential protein, as any harmful or lethal phenotype can be compensated for by the endogenous GAP45 that is still expressed.

The N-terminus and C-terminus of GAP45 have been shown to be important in specific localisation to the plasma membrane and protein-protein interaction respectively. The N terminus contains the sites for myristoylation and palmitoylation which direct the protein to the plasma membrane (Rees-Channer et al., 2006). The C-terminus of TgGAP45 is important for motor complex interaction, especially with TgMLC1 (MTIP) (Frenal et al., 2010). Previous work also in *T. gondii* revealed that the addition of a YFP tag on the C terminus of TgGAP45 abrogated its binding to the rest of the motor complex, but did not prevent it from being targeted to the IMC (Johnson et al., 2007). So, with these considerations, it would not be suitable for this protein to be tagged at either the N or C-terminus. An alternative approach is to introduce a tag at an internal position, in the unconserved region of the protein that may not serve any important function. For the purpose of this study, green fluorescent protein (GFP) was used to tag the GAP45 protein. The GFP protein has been used in many studies, mostly without any interruption to the original protein function. The benefit of using GFP as a tagging protein has been highlighted by many live imaging studies (Talman et al., 2010; Tavare et al., 2001; Tilley et al., 2007; Treeck et al., 2009; Tsien, 1998).

The present study has generated 3 different GFP-tagged GAP45 episomal constructs (FL-GAP45, N-GAP45 and C-GAP45). In detail, the GFP protein was inserted in the middle of the GAP45 unconserved region between amino acids and 29 and 30. The expression of GFP-tagged GAP45 protein was controlled by the *P. falciparum* merozoite surface protein 3 (MSP3) promoter. This promoter is active at a similar time frame as GAP45 protein is expressed; between 36 to 45 hours post red blood cell invasion. The C-terminal part of GAP45 protein that contains the

important phosphorylation sites for CDPK1, S89 and S103, was fused to the C-terminus of GFP. Insertion of the C-terminal part of GAP45 produced a full length (FL-GAP45) GFP-tagged GAP45 (Figure 4.1A).

Once the construct is episomally expressed in *P. falciparum*, it is important that the GFP-GAP45 protein maintains the characteristics of endogenous GAP45 with regard to timing of expression and subcellular localisation. Besides examining the localisation of the GFP-tagged GAP45 protein, the important roles of this protein such as participation in actin-myosin motor complex formation also need to be confirmed. To further study the role of both the N- and C-termini of GAP45 in parasites, the C- (N-GAP45) and N-terminally truncated (C-GAP45) GFP tagged GAP45 protein were constructed. The N-GAP45 construct consists of only 29 amino acids from the N-terminus of GAP45 fused to GFP (Figure 4.1B). The C-GAP45 construct lacks the 1-29 N-terminal region and only consists of amino acids 30-204 of GAP45, fused to the C-terminus of GFP (Figure 4.1C).

4.2 Expression and localisation of GFP tagged GAP45 protein in *P. falciparum* schizonts

Transfection was performed using 100 μg of plasmid DNA construct containing GFP tagged GAP45 insert and the blasticidin resistant gene. As the expression of GFP tagged GAP45 is controlled by the MSP-3 promoter, expression started at the schizont stage of the parasite. However, the expression of GFP-tagged GAP45 protein in each parasite was not homogenous. In order to get a homogenous GFP-tagged GAP45 expression, the GFP-tagged GAP45 expressing parasites stage were sorted by fluorescence-activated cell sorting (FACS). The FACSCalibur flowcytometer was programmed so that only the schizont parasites with high intensity GFP signal were selected. The selected parasites were grown in culture medium prior to being used.

The full length GFP-tagged GAP45 (FL-GAP45) and the N-terminal truncated (C-GAP45) GFP-tagged GAP45 proteins were expressed successfully in parasites producing a protein of apparent molecular weight of ~64 kDa (Figure 4.2).

Although the predicted molecular weight of GFP-tagged GAP45 is ~50.3 kDa (~23.6 kDa GAP45 + ~26.7 kDa GFP), the anomalous behaviour of GAP45 in SDS-PAGE causes a decrease in the migration of this protein resulting in an increase in apparent molecular weight of the fusion protein. The transfected parasites also expressed the native GAP45 protein (~37 kDa), confirming that the GFP-GAP45 fusion proteins are expressed from an episomal plasmid. The third GAP45 variant, GFP-tagged GAP45 lacking the C-terminal region (N-GAP45) expressed a smaller truncated GAP45 protein band with an approximate molecular weight of 30 kDa. The 3D7 control parasite lysate showed only endogenous GAP45. By using an anti-GFP monoclonal antibody, the full length GFP-tagged GAP45 protein bands were detected as a major protein band at ~64 kDa, with some degraded products. The degraded products migrated at lower molecular weight, with two protein bands different in size at around 37 kDa. These results show that GAP45 can be episomally expressed in *P. falciparum* parasites.

GAP45 has been reported to be membrane associated because of myristoylation and palmitoylation on its N-terminus. In order to confirm that the FL-GAP45 protein is also a membrane bound protein, a subcellular fractionation experiment was performed in which parasite proteins were extracted in a series of buffers designed to solubilise protein based on their degree of membrane association (Papakrivos et al., 2005). Only integral proteins or those extremely tightly associated with membranes would fail to be solubilised by a high pH carbonate buffer. In this experiment, FL-GAP45 together with N-GAP45 and C-GAP45 proteins were detected only in the carbonate insoluble fraction (Figure 4.2). These findings confirmed the tight association of these proteins to the membrane compartment. Another motor complex protein component, MTIP, was also insoluble in carbonate buffer (Figure 4.2). The parasite surface and peripheral membrane protein, MSP7 was slightly detected in the carbonate soluble fraction, with most of the protein remaining insoluble (Figure 4.2). SERA5, a protein of the parasitophorous vacuole that is not membrane associated is largely released upon parasite treatment with a hypotonic solution (Figure 4.2, lane 1).

As a conclusion, the GFP-tagged GAP45 proteins (FL-GAP45, N-GAP45 and C-GAP45) show similar properties to native GAP45 protein, a membrane bound protein. Although MTIP is not directly associated with membranes, it is located between the parasite plasma membrane and the outer IMC membrane. It could be that the tight association between the motor complex proteins may hold the parasite plasma membrane and IMC together, which could hinder the motor complex protein component from being exposed to chemical dissociation under high pH carbonate solution.

4.3 IMC localisation pattern of GFP-tagged GAP45 protein

The GFP-tagged GAP45 proteins have been shown to be successfully expressed in *P. falciparum* parasites. However, the FL-GAP45 protein must localise at the correct site, which is at the parasite periphery specifically to the inner membrane complex (IMC), in order to function. In the *T. gondii* parasite (tachyzoite), the only way to distinguish the IMC and the parasite plasma membrane is by treating the parasite with *Clostridium septicum* α-toxin (Gaskins et al., 2004) or *Aeromonas hydrophila* aerolysin (Frenal et al., 2010). This treatment will cause the parasites plasma membrane to swell away from the IMC. However, in *P. falciparum*, the IMC and parasite plasma membrane can be distinguished in a different way: both IMC and plasma membrane can be easily be differentiated by monitoring young schizont development. At early schizogony, prior to segmentation, the IMC associated protein was found to be localised to ring-like structures of developing IMC for nascent merozoites while the plasma membrane was still surrounding the periphery of parental parasites (Bullen et al., 2009; Hu et al., 2010; Kono et al., 2012; Yeoman et al., 2011).

We present evidence that shows the localisation of the GFP-tagged GAP45 proteins in early schizont stages, between 36 to 39 hours post invasion, the FL-GAP45 protein shows a distinct localisation pattern as compared to the N-GAP45 protein which lacks the C terminus (Figure 4.3). A live time course microscopy study was done (Section 2.10) to directly monitor the development or localisation pattern

of GFP-tagged GAP45 proteins (FL-GAP45, N-GAP45 and C-GAP45). Tightly synchronized transfected *P. falciparum* parasites were harvested at 3 different times post invasion starting from 30 hours till 45 hours post invasion. At young schizont stages, ~36 hours post invasion, the FL- GAP45 and N-GAP45 show different localisations; a distinct parasite IMC and parasite plasma membrane localisation pattern respectively. FL-GAP45 was found to be localised to ring-like structures that are situated in close proximity with single nuclei (~33 hours post invasion) (Figure 4.3A). The GFP signal became more obvious as the number of nuclei increased at around 36 hours post invasion, where it formed a ring-like structure (Figure 4.3A). In contrast, without the 30-204 amino acid sequences, N-GAP45 exhibited an even distribution of fluorescence around the entire parasite periphery (Figure 4.3B).

Interestingly, the localisation of C-GAP45, lacking the N-terminal acylation motifs, resembled very closely that seen for FL-GAP45. In early schizonts (~33 hours post invasion), C-GAP45 was present in discrete foci (Figure 4.3C) that progress to small ring-like structures as development continues (~36 hours post invasion) and finally in the segmented schizont the protein was evenly distributed around the periphery of each merozoite (~42 hours post invasion) (Figure 4.3C). At this time point, both the IMC and parasite plasma membrane have invaginated, surrounding individual merozoites, which makes the IMC and parasite membrane indistinguishable (Figure 4.3 A, B and C).

The differences between IMC and parasite membrane localisation at early schizogony (36 hours post invasion) was further analysed by IFA (Figure 4.4). Several protein markers were used for co-localisation in this experiment. The antibodies used were anti-GAP45 as an IMC marker, anti-MSP1 as a parasite plasma membrane marker, and anti-rhoptry neck protein 10 (RON10) as a marker for the apex of the merozoite. GFP-Booster, a specific GFP-binding protein coupled to the fluorescent dye ATTO 488 (Chromotek), was used to detect the GFP-tagged GAP45 protein signal. The signal of GFP tagged GAP45 protein was merged with that of the other protein markers in order to determine with which (if any) of the proteins localise to the same structures. As expected, at the 36 hour schizont stage, the ring-like structure GFP signal of FL-GAP45 protein was co-localised nicely with the

native GAP45 (Figure 4.4A, i) but not with MSP1 (Figure 4.4B, i). This phenomenon was also observed with C-GAP45 (Figure 4.4A & B, iii). In contrast, N-GAP45 was not co-localised with the native GAP45 protein (Figure 4.4A, ii). Instead, N-GAP45 co-localised well with MSP1 (Figure 4.4B, ii). However, both FL- GAP45 and N-GAP45 were found to be co-localised with both IMC (GAP45) and parasite surface or membrane (MSP1) proteins at late schizont stage (~39-42 hours post invasion) (Figure 4.4A & B).

The IMC components have been shown to form starting from the apical end of each developing merozoite and extend towards the posterior of the parasites (Bannister et al., 2000b). To further confirm the IMC ring-like structure of the GFP-GAP45 signal, the apical protein marker, rhoptry-neck protein 10 (RON10), was included in this experiment. The RON10 protein was found to be expressed at early schizont stages (E. Knuepfer and O. Suleyman, unpublished) and localised in close proximity with the FL-GAP45 protein ring-like structure pattern (Figure 4.4C, i). Interestingly, in early schizonts, most of the punctate signal of RON10 coincides with the IMC of each developing IMC, and is situated on the edge or sometimes at the centre of the ring-like staining of FL-GAP45 in the early schizont (Figure 4.4C, i & Chapter 5, Figure 5.9C). In contrast, the localisation of N-GAP45 protein seems not to be in close proximity with RON10 as the N-GAP45 was evenly distributed on the surface of the parental cell (Figure 4.4C, ii).

The ring-like IMC localisation shown by FL-and C-GAP45 at early schizont stages was clearly observed using high resolution microscopy (Figure 4.5A). In combination with Z-stack imaging and deconvolution, the ring like-IMC localisation structure was very clearly seen in early schizont stages as the background signal could be computationally eliminated (Figure 4.5A; Appendix B, i). A similar analysis was also done on late schizont stages which resulted in an imperceptible improvement as compared to the normal fluorescent microscopy analysis (Appendix B, ii). In addition, similar microscopy analysis was performed on live samples of each of the GFP-GAP45 variant expressing parasites at 36 hours and 42 hours schizont stages (Appendix C) to further confirm the appearance of ring-like structures of FL- and C-GAP45.

The early schizont stage of native GAP45 (~36 hours post invasion) from untransfected parasites (3D7) also showed the ring-like localisation pattern which is similar to FL-GAP45 and C-GAP45, suggesting that the GFP signal does indeed represent the true GAP45 protein localisation pattern, rather than any artefacts owing to GFP-tagging (Figure 4.5B). The development of punctate to a ring-like structure of GAP45 protein per nucleus was observed at an earlier time point (30 to 36 hours post invasion) of schizogony (Figure 4.5B). A similar pattern of localisation was also demonstrated by FL-GAP45 GFP live signal at this time point (Figure 4.6A). However, this is not the case for N-GAP45, as it was evenly distributed around the parasite's periphery as early as 30 hours post invasion (Figure 4.6B). Starting at 39 hours of schizont development, the native GAP45 and the GFP-tagged GAP45 signal was partially surrounding the developing merozoites. As shown earlier (Figure 4.3), this process is complete at 42 hours post invasion producing the individual merozoites ready to egress (Figure 4.5B and 4.6A and B).

In addition, parasite plasma membrane proteins such as CDPK1 (Green et al., 2008) and MSP1 (Dluzewski et al., 2008) have been shown to accumulate around residual bodies, which contains the food vacuole, of the late schizont stage. The food vacuole is an organelle formed by the combination of endocytosed red blood cell cytosol and the parasite's parasitophorous vacuole and plasma membrane (Aikawa et al., 1966; Langreth et al., 1978; Lazarus et al., 2008; Slomianny, 1990; Slomianny et al., 1985; Yayon et al., 1984) . The engulfed red blood cell cytosol containing haemoglobin is digested and forms hemozoin (Egan, 2008; Egan et al., 2002; Pagola et al., 2000). As the schizont matures, individual merozoites are pinched off from the syncytium and the residual body is encapsulated by plasma membrane, but not the IMC. Residual bodies therefore stain for plasma membrane proteins (e.g. MSP1), but not IMC proteins (e.g. GAP50 and GAP45) (Green et al., 2008). To further investigate the plasma membrane localisation of N-GAP45, IFA was done on blood smears prepared 42-45 hours post invasion using the GAP50 and MSP1 antibodies as IMC and parasite membrane protein marker, respectively. The results showed that the N-GAP45 protein seems to be colocalised with MSP1 around the residual bodies (Figure 4.7B), rather than with GAP50 at the IMC (Figure 4.7A). As expected, the FL- and C-GAP45 did not localise with MSP1 around the residual bodies (Figure

4.7B). Both of these proteins showed a similar localisation profile as GAP50, the IMC protein marker (Figure 4.7A). These results strongly suggest that both FL-GAP45 and C-GAP45 proteins localise to the IMC while N-GAP45 protein is targeted to the plasma membrane of *P.falciparum*.

4.4 Tetrameric motor complex of GFP-tagged GAP45 in *P. falciparum*

GAP45 forms part of the parasite's motor complex. Although GFP-tagged GAP45 was localised at the IMC, the functionality of this protein which is modified by GFP insertion within the protein is still questionable. One of the characteristics that can confirm the functionality of this protein is whether it retains the ability to interact and be part of the tetrameric motor complex. In order to investigate this, immunoprecipitation of GFP-tagged GAP45 was performed by pull-down assays using anti-GFP antibodies coupled to agarose beads. The GFP antibodies will only bind the GFP-tagged GAP45 protein, hence isolating this protein from the native GAP45. The pull-down assay used was a GFP-Trap® system which utilises camel monoclonal GFP antibodies. These antibodies are suitable for the purpose of this experiment because of their short heavy chain and they have no light chain. The characteristic of this antibody eliminates the cross reaction of antibodies to heavy and light chain from conventional antibodies, a common problem in such experiments.

Schizont parasite proteins were solubilised using extraction buffer containing 1% NP40 prior to an immunoprecipitation experiment with the GFP-Trap® system. As shown in Figure 4.8A and Figure 4.8B, FL-GAP45 and C-GAP45 proteins are efficiently immunoprecipitated by the camelid GFP antibodies (GFP-Trap®). The immunoprecipitated GFP-GAP45 was confirmed by both GAP45 and GFP antibodies in western blotting. In order to detect the co-immunoprecipitated motor complex proteins, western blotting was performed on a similar sample probed with MTIP, GAP50 and MyoA antibodies. Both FL-GAP45 and C-GAP45 were pulled down together with the other motor complex component proteins; MTIP, GAP50 and

MyoA (Figure 4.8A). N-GAP45 does not co-precipitate these other proteins (Figure 4.8B; Appendix D). These results suggest that the C terminus of GAP45 is responsible for binding to other protein components of the motor complex. The absence of native GAP45 in the precipitates also suggests that the GAP45 proteins do not form homo-oligomers. As a control, the 3D7 untransfected parasite lysate did not show any appearance of the motor complex proteins (Figure 4.8 A and B).

4.5 Discussion

The GFP-tagged GAP45 proteins (FL-GAP45, N-GAP45 and C-GAP45) were insoluble in carbonate buffer, indicating a strong association with membrane. As expected, the dual acylation on the N-terminus of GAP45, specifically on glycine (G2) and cysteine (C5), have probably helped this protein to interact with the membrane (Rees-Channer et al., 2006). Additional acylation or palymitoylation processes may also take place on its C-terminal region. Substitution of the conserved double cysteine (C230 and C233) to alanine on the C-terminal region of N-terminal truncated TgGAP45 causes mislocalisation of this protein to cytoplasm (Frenal et al., 2010). Thus, a combination of multiple acylation processes makes GAP45 a strong membrane binding protein.

The N-and C-terminal parts of GAP45 appear to be important in mediating the interaction with the parasite membrane and other motor complex proteins respectively (Frenal et al., 2010; Johnson et al., 2007). As mentioned earlier, the only way to fluorescently label this protein is by inserting the tag in the middle of the unconserved region of GAP45 protein; this strategy has proven to be successful in TgGAP45 protein (Frenal et al., 2010; Gilk et al., 2009). We have shown that in *P. falciparum*, inserting GFP at an internal position in the GAP45 protein allows this protein to localise correctly at the IMC. The localisation pattern of GAP45 to the IMC and parasite membrane has been distinguished at young schizont stages (33-36 hours post invasion). During schizogony, cell replication is initiated where nuclear division occurs and other organelles develop within a cytoplasm encapsulated by a single plasma membrane from the mother cell (Bullen et al., 2009). This process

produces daughter merozoites at late schizogony when cytokinesis takes place, followed by release of the free merozoites (Bullen et al., 2009). By monitoring the localisation of GFP-tagged GAP45 and truncated variants throughout schizogony, it has been possible to visualise and distinguish between the multiple forming IMCs and the single bounding plasma membrane.

In detail, the development of punctate to ring-like structures of GFP-tagged GAP45 which can be seen at early schizogony (30-36 hours post invasion) is a characteristic of IMC development in *P. falciparum*. A similar localisation pattern of IMC specific proteins has been shown by other motor complex proteins such as GAPM1 and GAPM2 (Bullen et al., 2009; Hu et al., 2010) and GAP50 (Yeoman et al., 2011). The study by Yeoman et al (2011) observed similar structures in parasites expressing GFP-tagged GAP50. Using 3D SIM microscopy, the authors were able to show that the IMC precursor is present as a flattened ellipsoid that is punctured by two holes (showing a ring-like pattern in IFA) which then separated into two opposing claw-shaped structures as the nucleus starts to divide (Yeoman et al., 2011). The IMC cisterna extends outwards from the apical rings or caps, leaving a central region that is free of cisternal membrane (Bannister et al., 2000b), which may represent the holes observed in the GFP-tagged GAP50 parasite (Yeoman et al., 2011) and the GFP-tagged GAP45 signal in this study.

The present study clearly shows that GAP45 is synthesized and localised to the IMC at earlier schizont stages (~30-33 hrs post invasion) concomitantly with the DNA replication process which normally occurs at early schizogony. Not only GAP45, but also the rhoptry organelle, parasite pellicle components and apical protein have also been shown to be generated while the DNA is replicating at early schizogony (Bannister et al., 2000b; Striepen et al., 2007). This is further demonstrated in this study, which found that the rhoptry neck protein RON10 is located in close proximity to the ring-like structures of GFP-tagged GAP45 (FL-GAP45), presumably the region occupied by apical organelles such as rhoptry and polar ring (Figure 4.4C). These IMC-like patterns not only occur in *Plasmodium* parasites. The *T. gondii* IMC protein called IMC-sub-compartment protein 1 (ISP1) which localises at a cone-shaped structure at the periphery of the apical end of the

parasite has been shown to be visible as a pair of a small rings in each mother cell at early endodyogeny. This pattern of localisation represents the IMC development for each of the daughter cells, starting from the apical cap of the nascent parasites (Beck et al., 2010).

As schizogony proceeds the localisation of GFP-tagged GAP45 proteins (FL-GAP45 and C-GAP45) extends towards the rear of the parasite and further encapsulates the merozoite at the end of schizogony (39-42 hours post invasion) as seen in this study (Figure 4.4 A & B; Figure 4.6). In contrast, the localisation signal of the parasite membrane specific protein was shown by the C-terminal truncated GFP-tagged GAP45 protein (N-GAP45). At early schizogony (~30-33 hrs post invasion), the N-GAP45 protein was evenly distributed to the single plasma membrane of the mother cells. Other plasma membrane specific proteins such as MSP1 and CDPK1 have been detected at the surface of the residual bodies of the parasites, which can only be seen at late schizont stage (Dluzewski et al., 2008; Green et al., 2008). The mechanism by which merozoites pinch off from the synctium within the red blood cell means that plasma membrane from the mother cell surrounds the residual body (Green et al., 2008). Of the three GFP-tagged GAP45 variants, only N-GAP45 was detected around residual bodies. Therefore, this study demonstrates the plasma membrane localisation of N-GAP45 as shown by the co-localisation of N-GAP45 with the parasite membrane marker, MSP1, indicating that the N-terminal region of GAP45 protein is associated with parasite plasma membrane.

The importance of the C-terminal region of GAP45 in targeting the protein to the IMC (C-GAP45) has been elucidated. The N-terminus of GAP45 (N-GAP45) was found to be associated with the parasite membrane and not in a complex with other motor proteins. In contrast, C-GAP45, which is without the first 30 amino acids of the protein, was able to form a complex with the other motor proteins MTIP, GAP50, and MyoA. These observations fit with a recent model of the motor complex in *T. gondii* tachyzoites where GAP45 is anchored in the plasma membrane by dual acylation of its N-terminus and interacts with GAP50 in the IMC membrane via its C-terminus (Frenal et al., 2010). Association with the IMC is strengthened by a

double palmitoylation within the C-terminus. An N-terminally truncated TgGAP45 protein (MycGFPCtGAP45) was able to form a complex with other motor protein such as MLC1 or MTIP and MyoA and localised to the IMC. A double mutation of C230 and C233 to alanine (MycGFPCtGAP45CC-AA) (C217 and C220 in the case of PfGAP45) of this protein leads to a cytosolic localisation, whereas a CC/AA mutation in the full-length protein causes TgGAP45 to localise to the parasite membrane instead of the IMC (Frenal et al., 2010). These findings clearly suggest the dual role of the GAP45 C-terminus, which binds to other motor complex proteins and also anchors it to the IMC by virtue of palmitoylation of cysteine residues.

This study also suggests that even at very early stages of merozoite formation, before plasma membrane formation around individual merozoites, GAP45 interacts with other proteins in the developing IMC membranes. If the motor complex is only required for merozoite invasion of red blood cells why is it assembled so much earlier in the developing schizont? It appears that IMC formation occurs concurrently with plasma membrane encapsulation of daughter merozoites. It is possible that a molecular motor is involved in this process. In other systems, myosins are crucial for cell division, for example myosin II is the primary motor protein responsible for cytokinesis in eukaryotes (Burgess, 2005; Field et al., 1999; Matsumura, 2005). Notably, in another apicomplexan parasite, *T. gondii* myosin B has been implicated in the process of cell division (Delbac et al., 2001). Because of the unusual arrangement of membranes in the development of merozoites, it may be that *Plasmodium* achieves cytokinesis and segmentation using a myosin XIV in a motor complex that effectively brings the plasma membrane and IMC together by virtue of a member of the complex, GAP45, bridging the gap between the two membranes. In fact, protein phosphorylation of motor complex proteins (MTIP and GAP45) has been highlighted in a previous study (Green et al., 2008). The *Plasmodium* growth inhibitory effect of a CDPK1 inhibitor (Green et al., 2008) could be the result of defective motor complex protein that leads to impairment of cytokinesis. However, the inhibitor used, K252a, is fairly non-specific and will almost certainly inhibit kinases other than CDPK1 such as PKB which might show a similar effect.

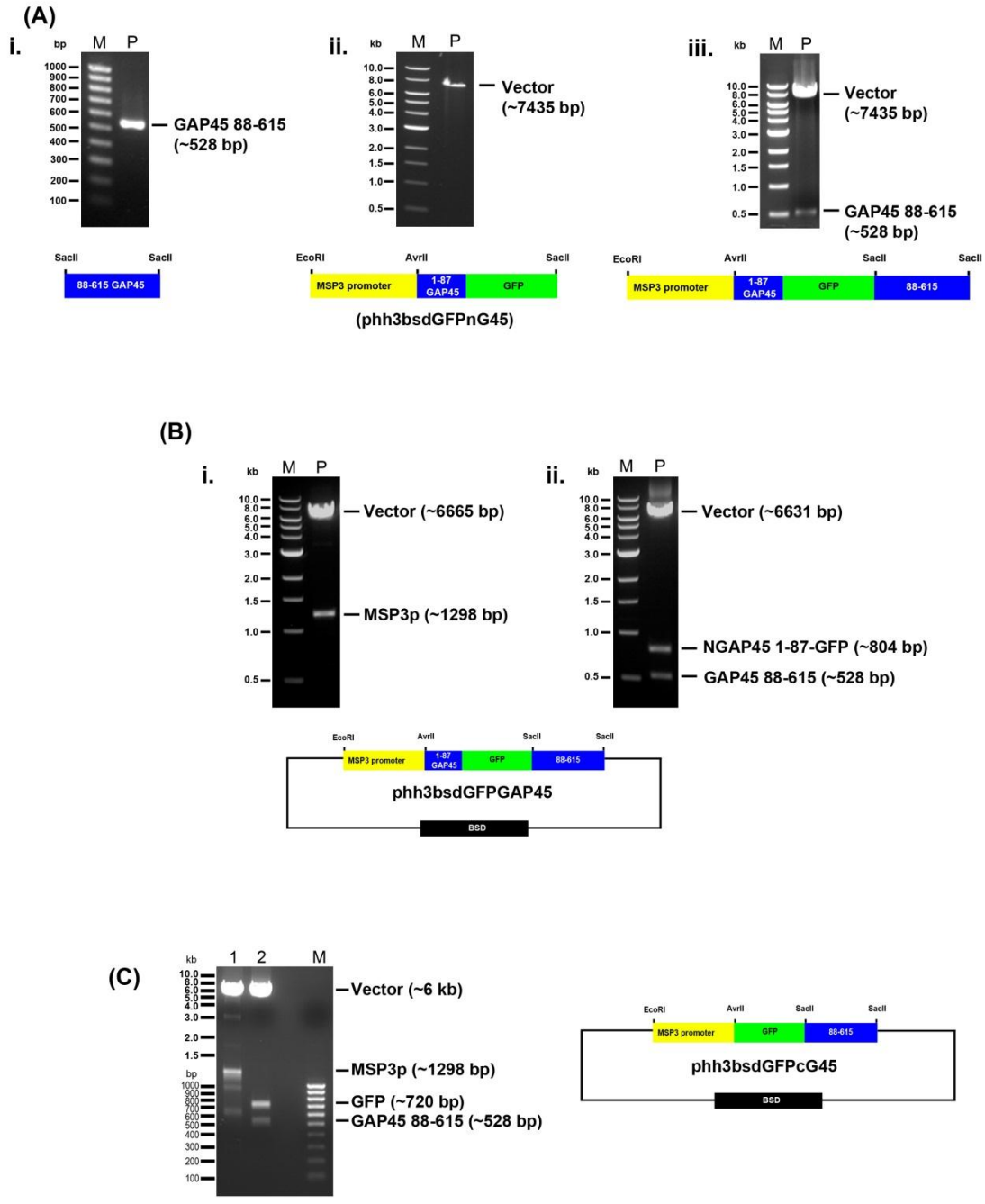

Figure 4.1: The design of GFP-tagged GAP45 episomal transfection constructs. The plasmid phh3bsdGFPnG45 was previously designed to episomally express the N-terminal 29 residues of GAP45 fused to GFP (N-GAP45) (7435 bp) (A, ii). DNA sequence coding for the N-terminal 29 amino acids of GAP45 (~87 bp) were fused in front of sequence coding for GFP as mentioned in section 2.7.2.1 (Knuepfer and

Holder, unpublished). A second plasmid (phh3bsdGFPGAP45) was constructed to add an internal GFP tag to the GAP45 sequence, located between residues 29 and 30. The sequence encoding the N-terminal part of GAP45 fused with GFP was amplified by PCR eliminating the terminal stop codon (Section 2.7.2.1). The PCR product was reinserted into the pHH3 vector via *Avr*II/*Sac*II restriction enzyme cleavage after the MSP3 promoter. The sequence encoding the C-terminal portion of GAP45 from residue 30 to the stop codon was amplified by PCR (~528 bp) (A, i) and ligated into the transfection vector via *Sac*II restriction enzyme cleavage after the GFP tag sequence (A, iii) (Section 2.7.2.1). The ligation product was confirmed by plasmid digestion using *Sac*II restriction enzyme (A, iii). The expression component of this plasmid, the MSP3 promoter and the GFP-tagged GAP45 gene were reconfirmed by plasmid digestion using double digestion enzymes, *EcoR*I/*Avr*II (B, i) and *Avr*II/*Sac*II (B, ii) respectively. This plasmid, phh3bsdGFPGAP45, will episomally express the full length internally GFP tagged GAP45 (FL-GAP45). A third plasmid (phh3bsdGFPcG45) which will expressed the N-terminal truncated GFP-tagged GAP45 (C-GAP45) was also constructed by a similar approach by reconstructing the second plasmid phh3bsdGFPGAP45. The N-terminal 29 amino acids of GAP45 fused to GFP sequence in plasmid phh3bsdGFPGAP45 was cut out and replaced with the GFP sequence only (without stop codon) via *Avr*II/*Sac*II restriction enzyme cleavage after the MSP3 promoter. The sequence encoding the C-terminal portion of GAP45 from residue 30 to the stop codon was inserted via *Sac*II restriction enzyme cleavage after the GFP tag sequence. This plasmid will express the GFP-tagged GAP45 that only contains 30-204 amino acid residues (lacking the first 29 amino acid N-terminus residues) (C-GAP45). The expression component of this plasmid, the MSP3 promoter and the GFP-tagged GAP45 gene were reconfirmed by plasmid digestion using double digestion enzymes, *EcoR*I/*Avr*II (C, lane 1) and *Avr*II/*Sac*II (C, lane 2) respectively. Label M is a DNA marker and P is a PCR or digestion product.

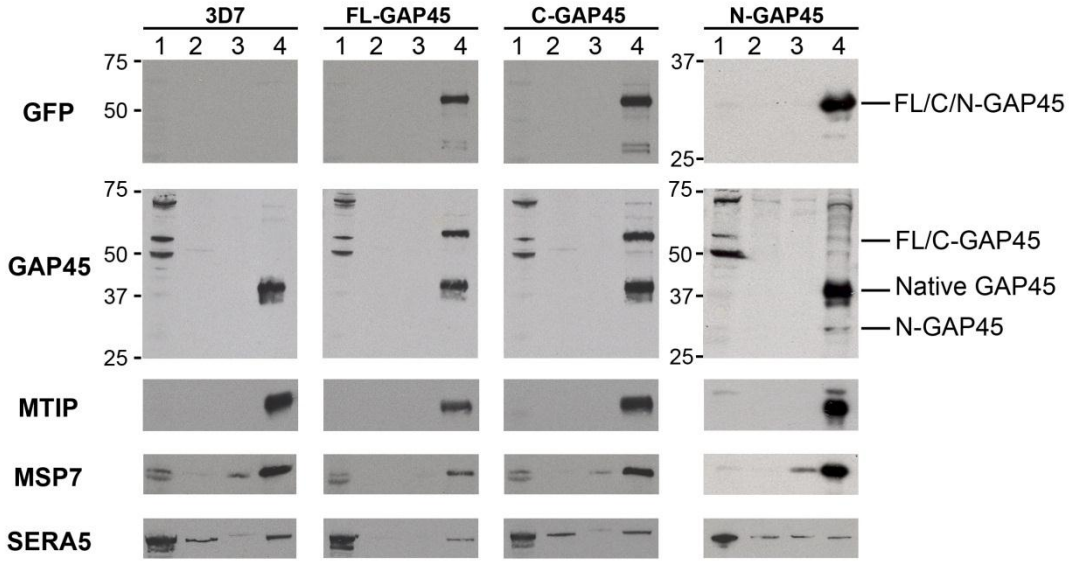

Figure 4.2: The subcellular fractionation of WT or full length (FL-GAP45), N-terminal truncated (C-GAP45) and C-terminal truncated (N-GAP45) GFP-tagged GAP45 proteins. The subcellular fractionation was performed subsequently starting with the hypotonic lysis buffer, high salt buffer, and sodium carbonate buffer. All parasite solubilized fractions, hypotonic lysis (1), high salt (2), carbonate supernatant (3) and carbonate pellet (4) were separated by SDS-PAGE and analysed by western blotting, using antibodies to GFP, GAP45, MTIP, MSP7 and SERA5. The 3D7 parasite was used as a control for untransfected parasites. Nonspecific protein bands were detected in the hypotonic lysis fraction by the GAP45 polyclonal antibody but not by the GFP monoclonal antibody.

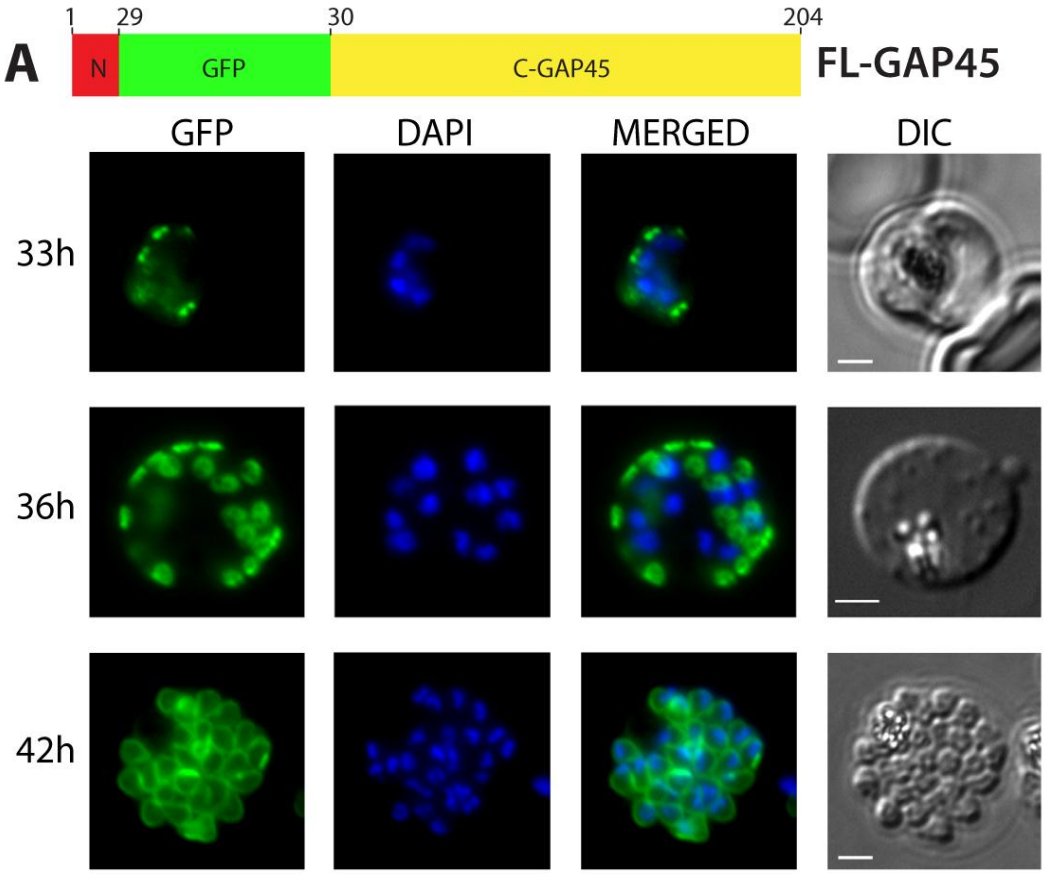

Figure 4.3: The live microscopy time course analysis of full length GFP-tagged GAP45 (FL-GAP45) (A), C-terminal truncated GFP-tagged GAP45 (N-GAP45) (B) and N-terminal truncated GFP-tagged GAP45 (C-GAP45) expressing *P. falciparum*. Synchronized transfected parasites were separated into several cultures. Each culture was harvested at 33 hours, 36 hours and 42 hours post invasion. The harvested parasites were visualized and analysed by fluorescence microscopy. The nucleus was labelled with Hoechst stain prior to microscopic analysis at 1000 X magnification. In the early schizont stages, small localised structures of GFP signal of FL- and C-GAP45 were observed around the parasite's periphery, typical of an IMC location. The N-GAP45 protein produced a different pattern of GFP signal, probably corresponding to the parasite plasma membrane. At the late schizont stage (42 hrs post invasion) the GFP signal was detected at the periphery of merozoites developing within the schizont and at this time point the putative IMC and parasite plasma membrane patterns were indistinguishable. Scale bar is 2 µm.

Figure 4.3 continued: The live microscopy time course analysis of full length GFP-tagged GAP45 (FL-GAP45) (A), C-terminal truncated GFP-tagged GAP45 (N-GAP45) (B) and N-terminal truncated GFP-tagged GAP45 (C-GAP45) expressing *P. falciparum*.

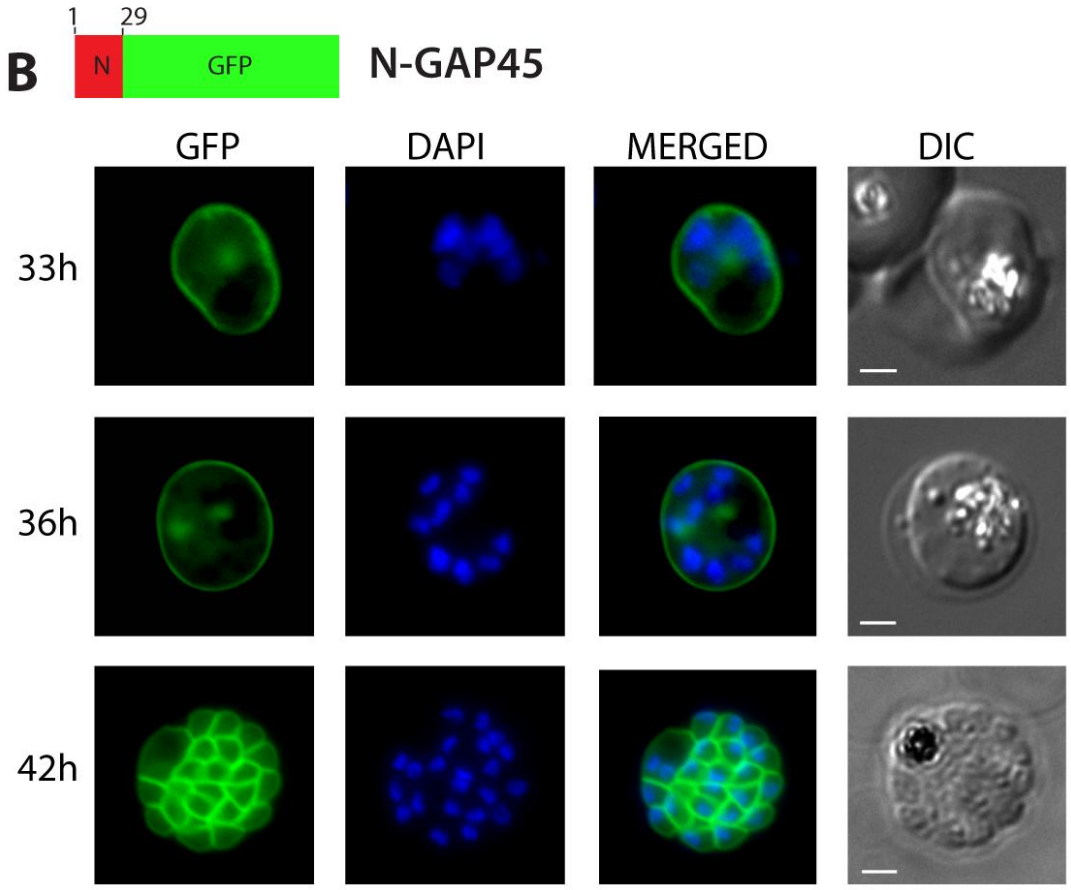

Figure 4.3 continued: The live microscopy time course analysis of full length GFP-tagged GAP45 (FL-GAP45) (A), C-terminal truncated GFP-tagged GAP45 (N-GAP45) (B) and N-terminal truncated GFP-tagged GAP45 (C-GAP45) expressing *P. falciparum*.

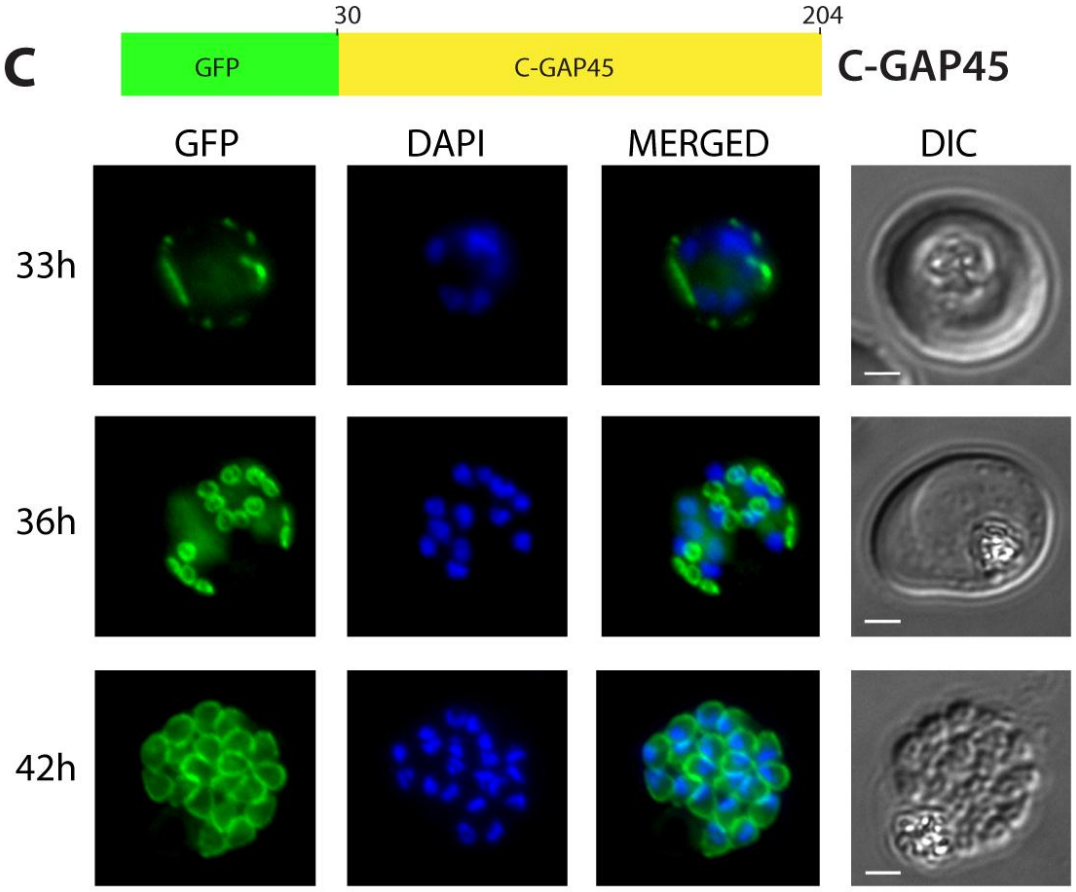

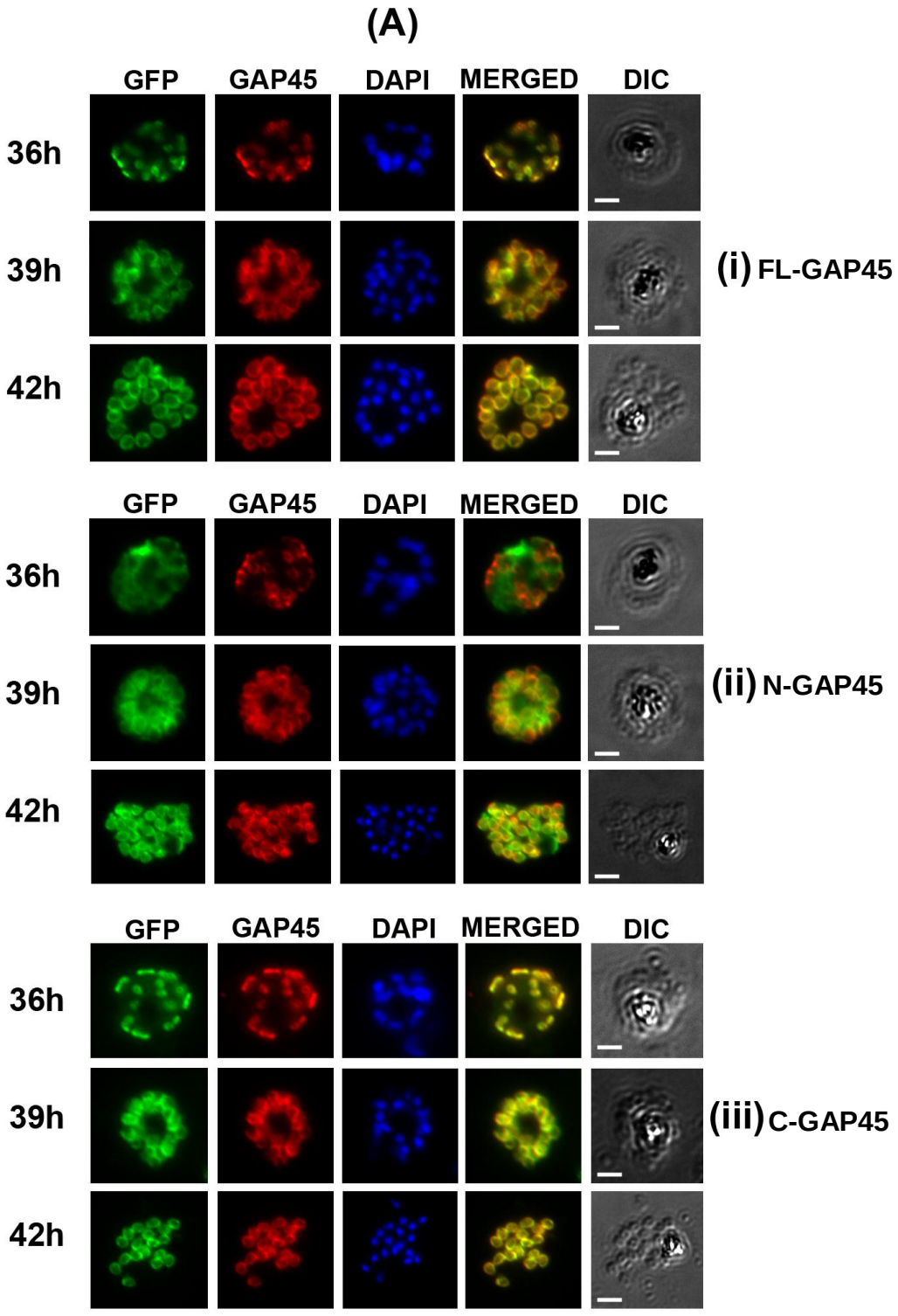

Figure 4.4: Indirect immunofluorescence assay (IFA) microscopy analysis of (i) FL-GAP45, (ii) C-terminally truncated (N-GAP45) and (iii) N-terminally truncated (C-GAP45) GFP-tagged GAP45 expressing parasites. The monoclonal anti-GFP and polyclonal anti-GAP45 antibodies (A) were used to detect the GFP-

tagged GAP45 and native GAP45 proteins respectively. The slides were mounted by using DAPI containing antifade reagent prior to microscopy analysis at 1000 X magnification. FL-GAP45 is co-located with GAP45, whereas N-GAP45 is co-located with the parasite plasma membrane marker MSP1 at all stages of schizont development. In (A) the binding of a monoclonal anti-GFP antibody (green) was compared to that of polyclonal anti-GAP45 antibodies (red). In (B) the binding of the GFP antibody (green) was compared with the binding of an MSP1-specific antibody (red) as a marker for the parasite plasma membrane. In (C) the binding of GFP antibody (green) was compared with the binding of RON10-specific antibody as a marker for apical protein. Merged images together with the corresponding differential interference contrast (DIC) picture are also shown. On the left of each panel the time post invasion is indicated in hours. Scale bar is 2 µm.

Figure 4.4 continued: Indirect immunofluorescence assay (IFA) microscopy analysis of (i) FL-GAP45, (ii) C-terminally truncated (N-GAP45) and (iii) N-terminally truncated (C-GAP45) GFP-tagged GAP45 expressing parasites.

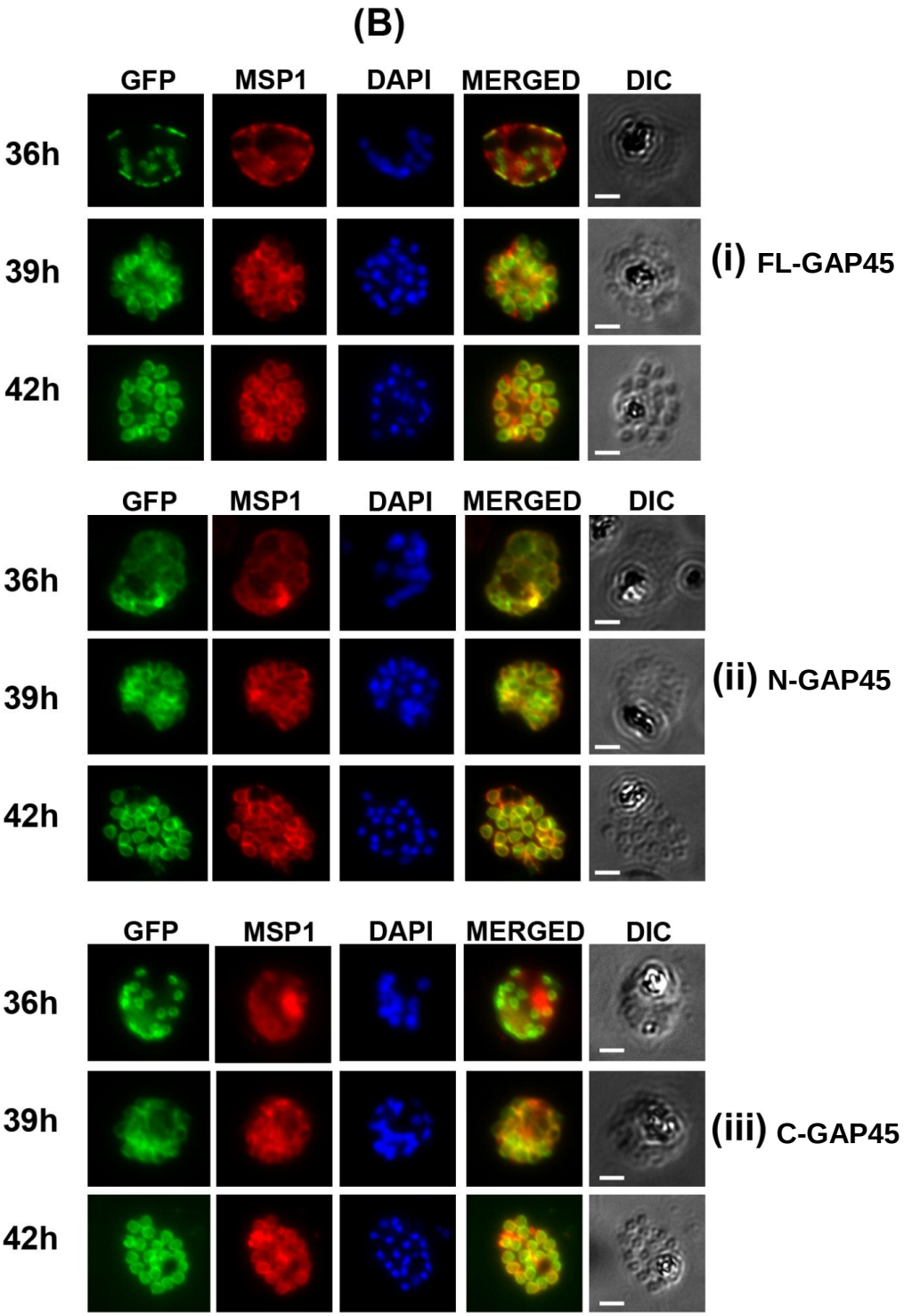

Figure 4.4 continued: Indirect immunofluorescence assay (IFA) microscopy analysis of (i) FL-GAP45 and (ii) N-terminally truncated (C-GAP45) GFP-tagged GAP45 expressing parasites.

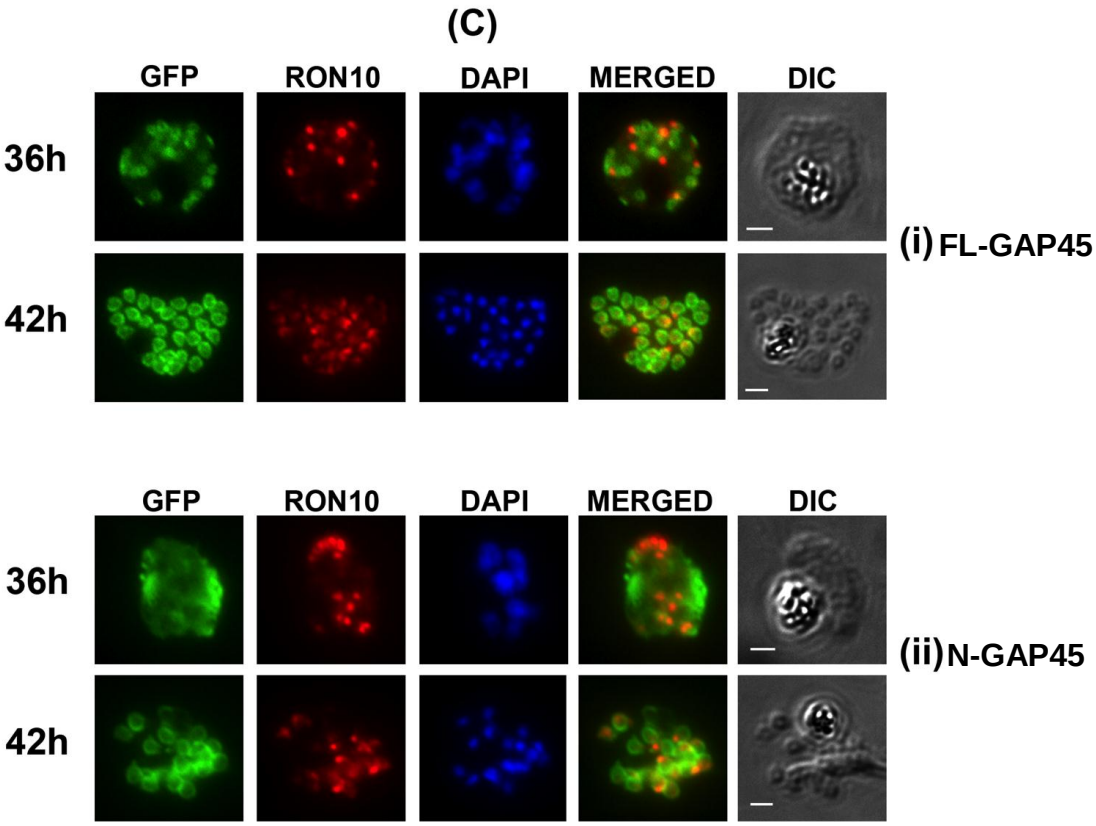

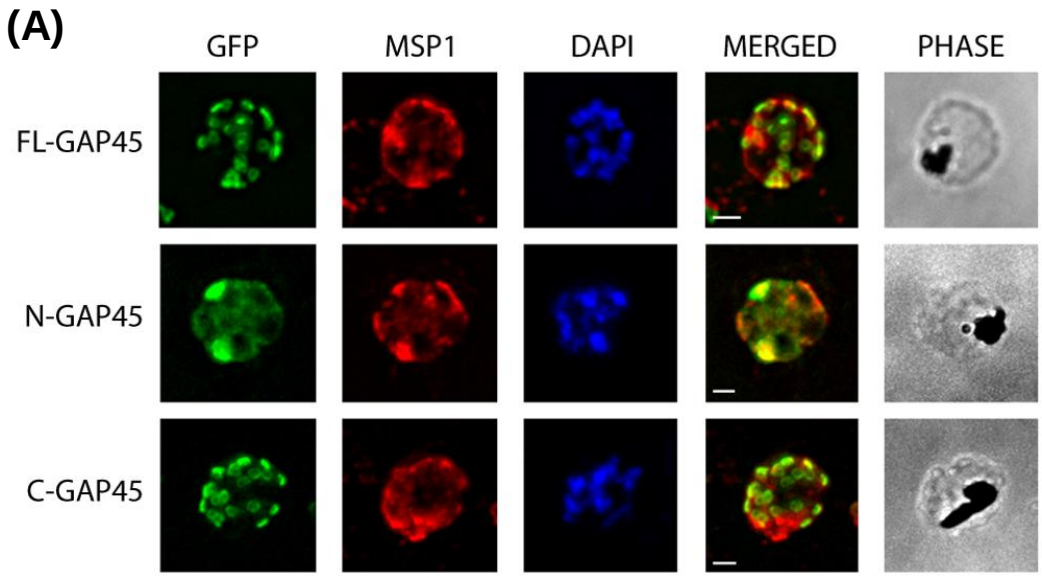

Figure 4.5: The localisation of GFP-tagged GAP45 variants at early schizont stage after high resolution immunofluorescent imaging analysis with Z-stack and deconvolution processing. (A) The ring-like IMC localisation pattern of both FL-GAP45 and C-GAP45 was obviously seen and distinguishable from the N-GAP45 parasite plasma membrane-like localisation pattern. (B) The native GAP45 in 3D7 untransfected *P. falciparum* parasites was localised in a similar manner as FL-GAP45 and C-GAP45 at early schizont stage. The slides were mounted by using DAPI containing antifade reagent prior to microscopy analysis at 1000 X plus 1.6X magnification. Scale bar is 2 µm.

Figure 4.5 continued: The localisation of GFP-tagged GAP45 variants at early schizont stage after high resolution immunofluorescent imaging analysis with Z-stack and deconvolution processing.

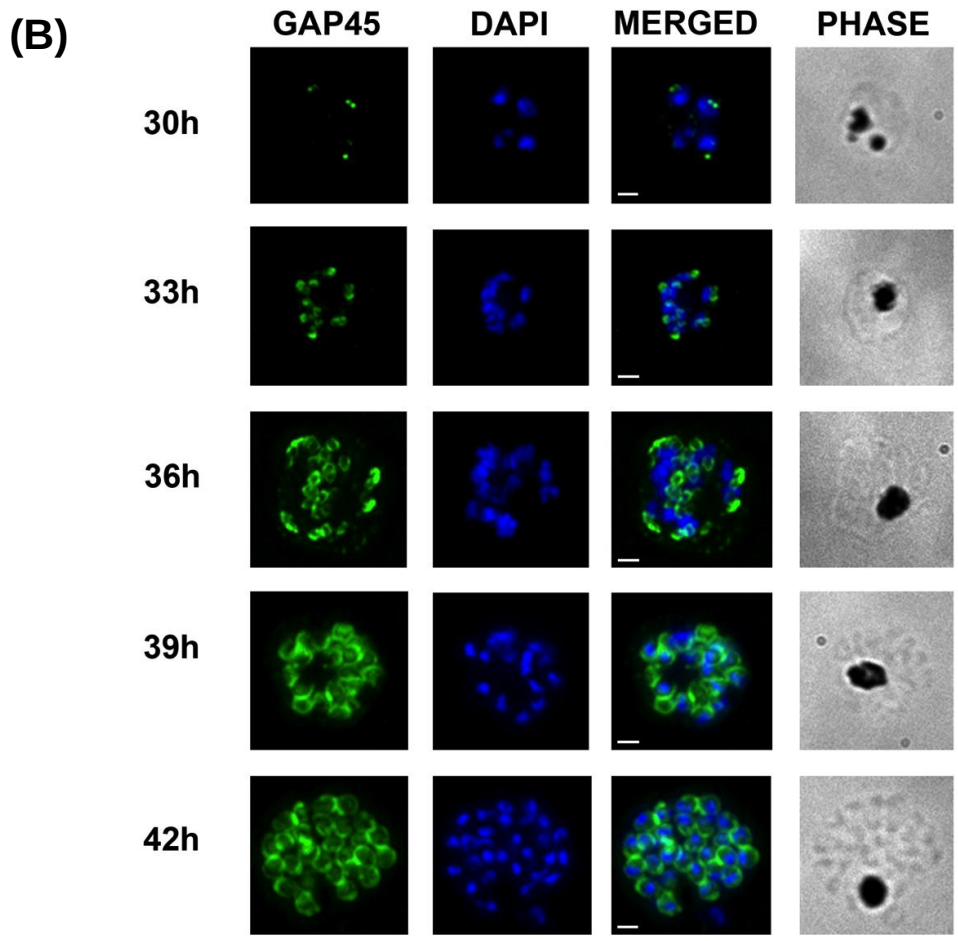

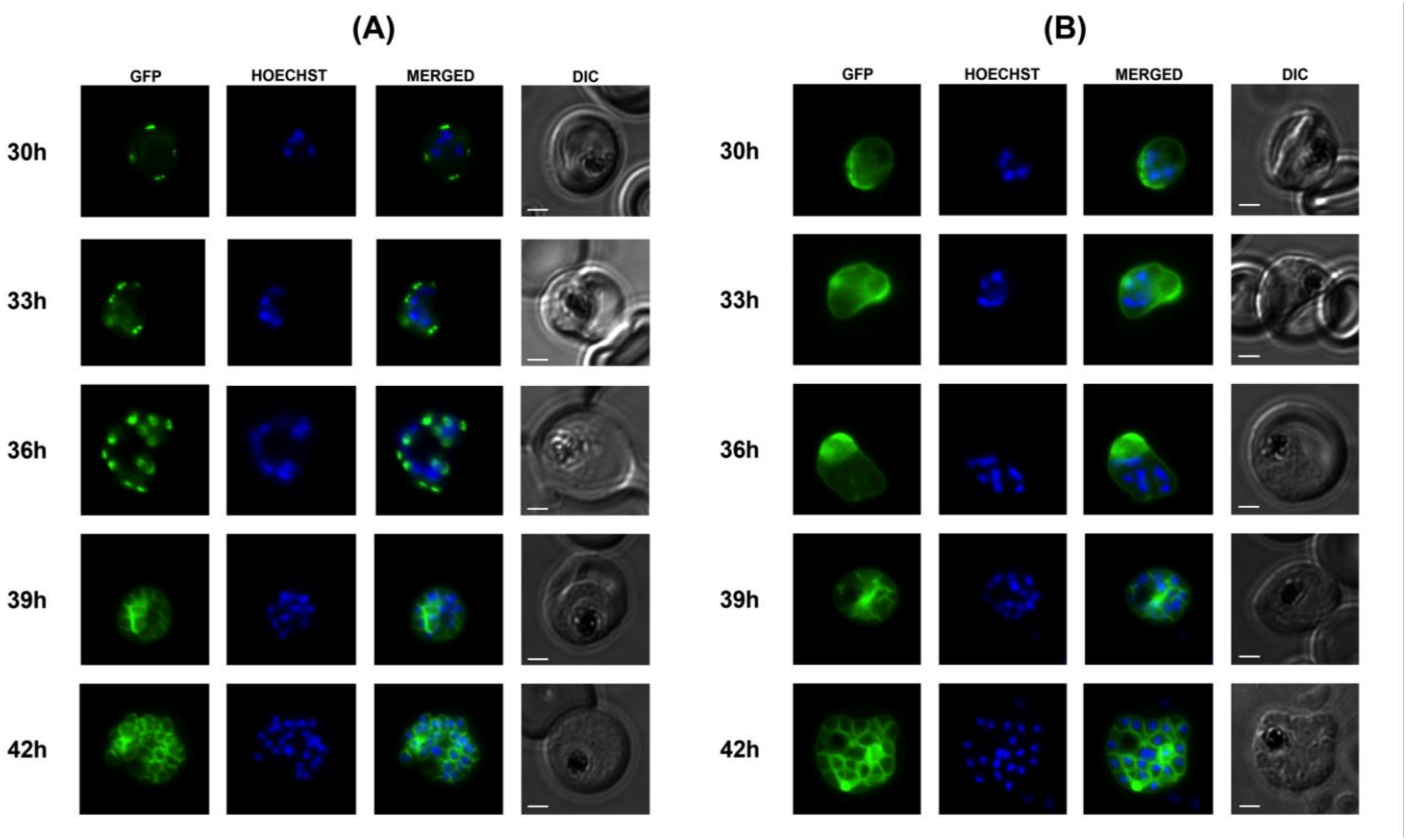

Figure 4.6: The location of (A) GFP-tagged wild type GAP45 (FL-GAP45) and (B) GFP-tagged C-terminal truncated GAP45 (N-GAP45) during schizont development (30-42 hours post invasion). Transfected parasite populations were synchronized and examined at 3-hr intervals from 30 to 42 hrs post invasion by fluorescence microscopy to detect GFP (green). The nucleus was labelled

with Hoechst stain (blue) prior to microscope analysis at 1000 X magnification. The merged image of the two is also shown together with the corresponding differential interference contrast (DIC) picture. In the early schizont stages (30-36 hrs), small punctate to ring like localised structures of GAP45 GFP signal were observed around the parasite's periphery, typical of an IMC location (A). The N-GAP45 protein produced a different pattern corresponding to the parasite plasma membrane (B). At the late schizont stage (42 hrs post invasion) the GFP signal was detected at the periphery of merozoites developing within the schizont and at this time point the putative IMC and parasite plasma membrane patterns were indistinguishable. Scale bar is 2 μm.

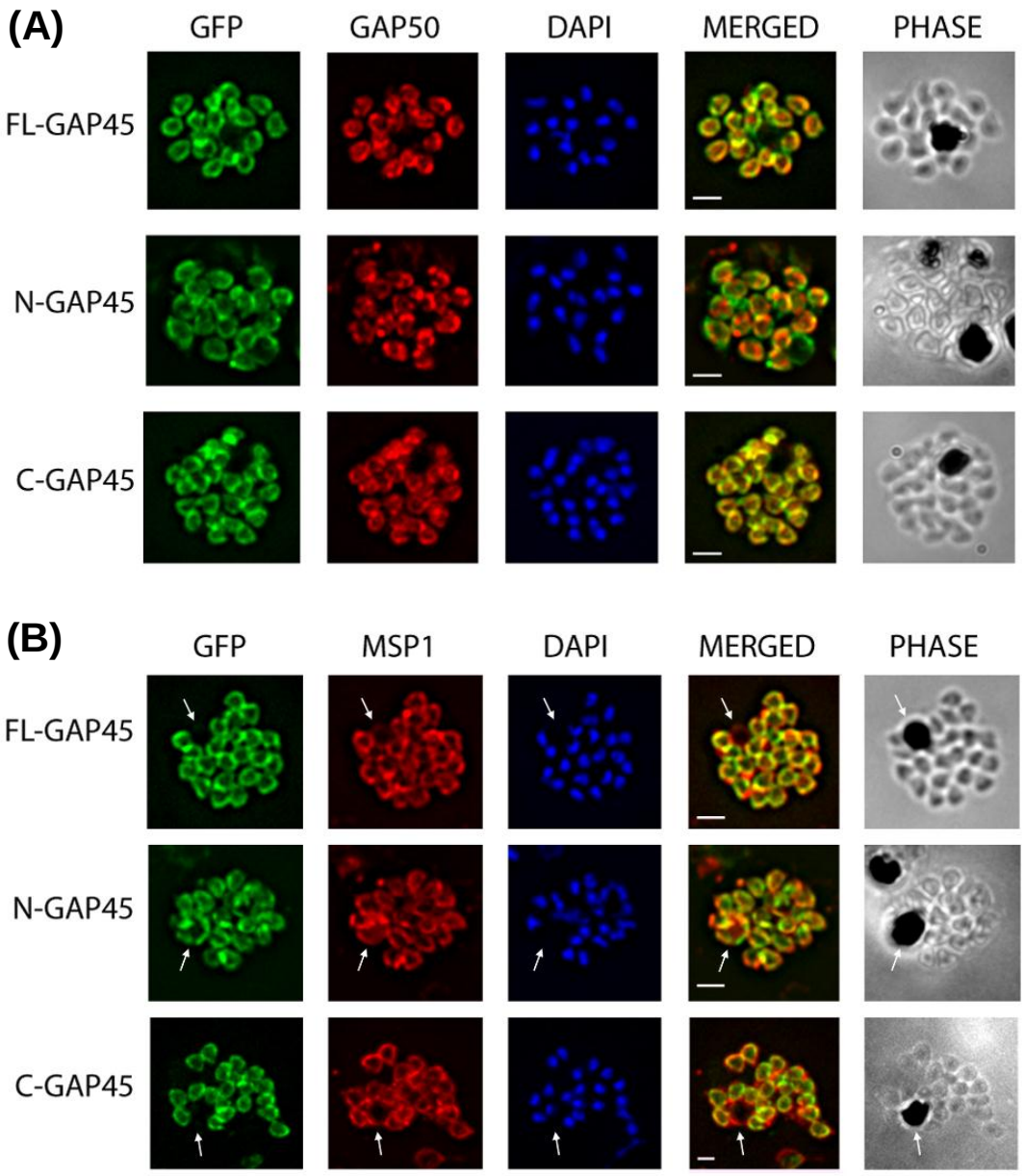

Figure 4.7: N-GAP45 is associated with the residual body whereas FL-GAP45 is not. The mature schizonts (~42 h) from the three transfected parasite lines were fixed and probed with a GFP binding protein and antibodies specific for either GAP50 (A) or MSP1 (B). The residual body containing the large semi-crystalline hemozoin granule is visible in the differential interference contrast pictures. Merged images allow the location of the different antibody reactivities to be compared with each other and with the residual body, which is marked with the white arrowheads for

clarity. The residual body was reactive with the anti-MSP1 antibody but not with the anti-GAP50 antibodies or the GFP-binding protein in both FL-GAP45 and C-GAP45 lines. In the N-GAP45 line the residual bodies stained positive for GFP. The slides were mounted by using DAPI containing antifade reagent prior to microscopy analysis at 1000X magnification. Scale bar is 2 µm.

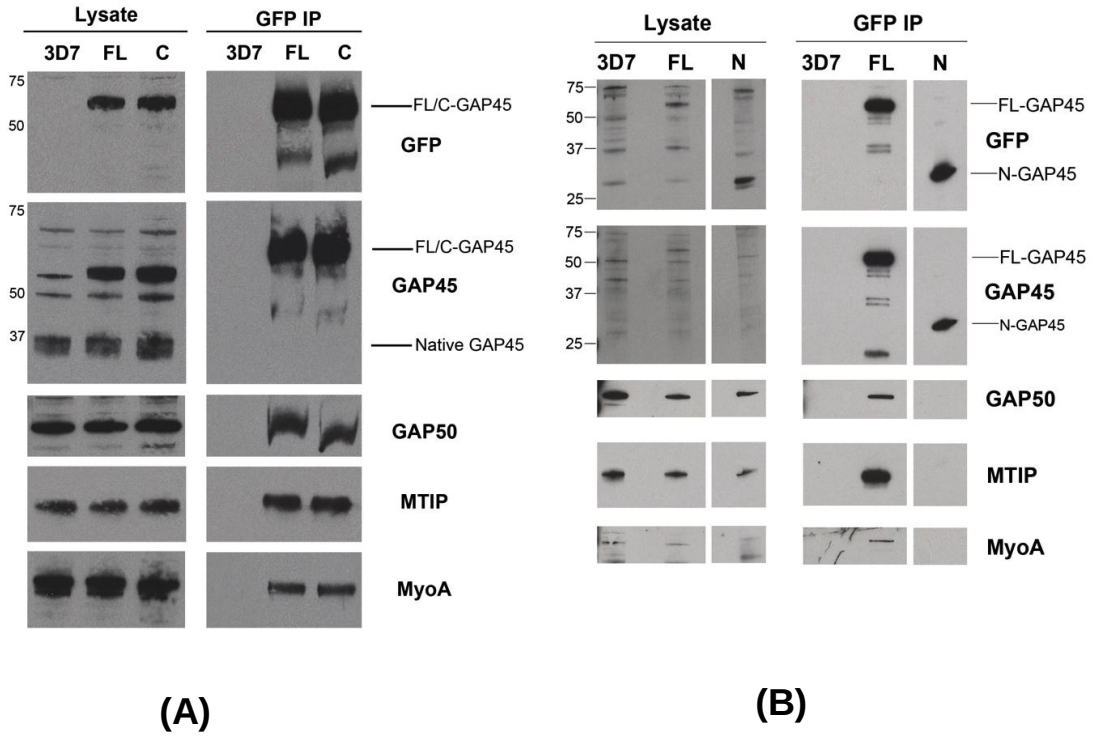

Figure 4.8: The FL-GAP45 and C-GAP45 proteins assemble into the motor protein complex, whereas N-GAP45 does not. The schizont stage parasite proteins were solubilised by extraction buffer containing 1% NP40 prior to immunoprecipitation by using monoclonal GFP antibody (GFP-Trap®). Precipitated proteins and a sample of each corresponding lysate were resolved by SDS-PAGE and then analysed by western blotting using antibodies to GFP, GAP45, GAP50, MTIP and MyoA. A: The FL-GAP45 (FL) and C-GAP45 (C) co-precipitated other motor complex proteins such as MTIP, GAP50 and MyoA. B: The N-GAP45 (N) was unable to co-precipitate other motor complex protein such as MyoA, MTIP and GAP50. 3D7 is a control for untransfected *P. falciparum* parasites.

Chapter 5

Phosphorylation of GFP-tagged GAP45 in the parasite

5.1 Introduction

The sites of GAP45 phosphorylation by CDPK1, serine 89 and serine 103, have been identified in this study. One of the residues, S89, has been identified in a GAP45 phosphopeptide detected in parasites (Green et al., 2008). These findings led us to further investigate the effect of these phosphorylation events on *P. falciparum in vivo*. As episomal transfection to express GFP-tagged GAP45 has been shown to be successful in the previous chapter (Chapter 4), a similar approach was used. Mutations at residues S89, S103, S89/S103 in GFP-tagged GAP45 were made where the serine residue(s) were substituted with alanine which is a non-polar and non-reactive amino acid residue. In order to mimic a phosphorylated residue, replacement of serine (S) residues with an acidic residue such as glutamic acid (E) or aspartic acid (D) can be performed. In this experiment, aspartic acid was chosen as a phosphomimetic residue for serine as it only involves a slight change in the size of the residue. The replacement of serine (S) by aspartate (D) did not cause any changes to the overall structure of GAP45, as shown in far UV CD spectroscopy analysis (Figure 5.1).

Using the same technique as mentioned in chapter 4, the GFP-GAP45 mutant constructs were introduced into the parasites by episomal transfection. The actual function of GAP45 phosphorylation is still unclear in *P. falciparum*. Phosphorylation of GAP45 starts to occur at the early schizont stage and peaks at late schizont stage (Green et al., 2008), suggesting a possible role of GAP45 phosphorylation in the regulation of motor complex assembly prior to invasion. Phosphorylation might

affect the localisation of GAP45 to the IMC. As shown in the previous chapter (Chapter 4), GFP-tagged GAP45 was assembled in the IMC during early schizogony, with 36-hour schizont stages showing a specific ring-like IMC localisation pattern. Any mislocalisation of this protein due to the effect of phosphorylation or dephosphorylation on S89 and/or S103 would be clearly evident, and we would be able to distinguish between protein localised to the parasite plasma membrane or cytoplasm instead of the IMC of the parasite. Even if phosphorylation has no effect on GAP45 localisation, in order to be functional it must still form a tetrameric motor complex (GAP45-GAP50-MTIP-MyoA). In *T. gondii*, phosphorylation of GAP45 has been shown to be important in motor complex assembly. In detail, substitution of S163 and S167 to both alanine and glutamate had no effect on TgGAP45 distribution on the parasite IMC. However, replacement of these residues (S163 and S167) by glutamate (phosphomimetic form) prevented the trimeric complex, MyoA-MLC-GAP45 interacting with GAP50 (Gilk et al., 2009). This study has highlighted the possibility that phosphorylation of GAP45 might also have a role in *Plasmodium* motor complex assembly.

5.2 The effect of phosphatase treatment on GFP-tagged GAP45 protein.

The *P. falciparum* GAP45 protein has been previously shown to be highly phosphorylated in the schizont stage. The appearance of a double protein band in SDS-PAGE is a feature of schizont GAP45 protein, where the upper band is phosphorylated (Green et al., 2008). Upon treatment with alkaline phosphatase, the migration of this protein band is affected such that it shifts to the lower molecular weight band by the removal of phosphate molecules from the protein. This experiment will show whether or not the GFP-tagged GAP45 protein, which was tagged internally, is phosphorylated in parasites (Figure 5.2).

By treatment with alkaline phosphatase, both FL-GAP45 and C-GAP45, together with the native GAP45 protein bands shifted to lower molecular weight (Figure 5.2A). This effect was stopped (or significantly reduced) in the presence of a

phosphatase inhibitor cocktail containing sodium orthovanadate, sodium molybdate, sodium tartrate and imidazole (Figure 5.2A, lane 3). Without the C-terminal region that contains most of the phosphorylation sites, the N-GAP45 protein does not seem to be affected by phosphatase activity (Figure 5.2B). Therefore, the GFP-tagged GAP45 appears to be phosphorylated mainly on its C-terminal sequence. Although the native GAP45 band is shifted to a lower molecular weight upon phosphatase treatment, there is still a remaining phosphorylated band which could be due to incomplete dephosphorylation by the phosphatase treatment in this study. This could also be due to other post-translational modifications of the GAP45 protein such as N-myristoylation and palmitoylation which have been reported by Rees-Channer et al. (2006).

The S89A/S103A GFP-GAP45 protein was also affected by phosphatase treatment whereby its protein band also shifted to a lower molecular weight (Figure 5.3). This suggests that additional unknown residues are phosphorylated on GFP-tagged GAP45.

5.3 ^{32}P-phosphate incorporation into GFP-tagged GAP45 protein in parasites

As shown by phosphatase treatment in the previous section, the WT and S89A/S103A GFP-GAP45 proteins are phosphorylated in the parasite. However, we wish to know more about the level of WT GFP-GAP45 phosphorylation as compared with the S89A/S103A GFP-GAP45 protein. By performing ^{32}P-phosphate parasite metabolic labelling, the quantity of phosphate incorporation into the GFP-GAP45 protein can be measured. The radiolabelled GFP-GAP45 was immunoprecipitated by pull down assay using the GFP-Trap® system. The level of GFP-GAP45 protein phosphorylation was visualized by autoradiography.

As expected, the WT and S89A/S103A GFP-GAP45 protein bands showed incorporation of ^{32}P-phosphate (Figure 5.4). After considering the total amount of GFP-GAP45 protein being pulled down for both WT and S89A/S103A variant, where there was less S89A/S103A than WT protein, there was no obvious difference

in the level of ^{32}P-phosphate incorporation between them. The results suggest that S89 and/or S103 residues of GAP45 may not be the dominantly phosphorylated residues in parasites, and their phosphorylation is sub-stoichiometric. In order to check the integrity of the motor complex protein components that had been pulled down together with GFP-GAP45 protein, the same ^{32}P-phosphate radiolabelled samples were subjected to western blotting and probed with antibodies against each member of the motor complex. All of the tetrameric motor complex proteins (MyoA, MTIP, GAP50 and of course the GFP-GAP45) were detected in the precipitated protein samples (Figure 5.4).

Surprisingly, besides the appearance of other ^{32}P-phosphate radiolabelled protein bands such as MTIP and MyoA, which have been reported to be phosphorylated in parasites (Green et al., 2008; Treeck et al., 2011), this experiment also detected other unknown phosphorylated protein bands. The phosphorylated protein bands were referred as unknown phosphoprotein 1 and unknown phosphoprotein 2 (Figure 5.4). The unknown phosphoprotein 1 migrated at approximately 180 kDa while unknown phosphoprotein 2 migrated just below the 50 kDa marker. Unknown phosphoprotein 2 has the strongest signal of ^{32}P-phosphate incorporation, similar in intensity to that of GFP-GAP45 (Figure 5.4). To ensure that unknown phosphoprotein 2 was not a breakdown product of GFP-GAP45, western blotting using anti-GFP and GAP45 antibodies was performed. Neither antibody reacted with a protein of this size (Appendix E). The unknown phosphorylated proteins are either heavily phosphorylated in parasites, or are abundant phosphoproteins. However, judging by SYPRO Ruby staining of immunoprecipitation products, the relevant band for each unknown phosphoprotein did not appear to be abundant. Even the unknown phosphoprotein 2 did not show a clear protein band at the appropriate molecular weight (~50 kDa or slightly lower) (Appendix F). This indicates that the unknown phosphoproteins, especially phosphoprotein 2, are heavily phosphorylated.

5.4 GAP40 is part of the motor complex protein

The identification of unknown phosphoprotein 2 was performed by liquid chromatography mass spectrometry (LC-MS/MS), implementing the electrospray ionization methodology. The immunoprecipitation of GFP-tagged GAP45 was performed as described in section 2.11. The immunoprecipitated proteins were separated by SDS-PAGE. As the protein concentration was likely to be too low for visualisation using coomassie blue staining, the protein bands were stained using SYPRO Ruby. A distinct ~50 kDa protein band (slightly lower than 50 kDa marker) was seen in the immunoprecipitate from the GFP-GAP45 schizont lysate (Figure 5.5A). There were also other distinct protein bands detected which were absent from the control 3D7 parasite lysate. These were likely to correspond to GFP-GAP45 and GAP50 protein (Figure 5.5A). The distinct protein bands related to unknown phosphoprotein band 2, GFP-GAP45 and GAP50 were excised and prepared for trypsin digestion prior to protein identification by LC-MS/MS analysis. Other motor complex protein bands such as MyoA and MTIP were not visible in the staining hence it was not possible to identify these proteins. However, the presence of MyoA and MTIP in the same immunoprecipitate was confirmed by western blots (Figure 5.5B).

LC-MS/MS analysis identified unknown phosphoprotein 2 as the *P. falciparum* protein, PFE0785c (Figure 5.5A). By referring to the *Plasmodium* genome database (PlasmoDB) (http://plasmodb.org/plasmo/), this protein is annotated as glideosome associated protein 40 (GAP40). Based on its amino acid sequence, the predicted molecular weight of this protein is 51.8 kDa, and transcriptional profiling showed that it is highly expressed in asexual blood stage schizonts (Bozdech et al., 2003). In phosphoproteomic analysis, this protein was found to be highly phosphorylated at the schizont stage, with 15 phosphorylated residues detected (Treeck et al., 2011). Moreover, its orthologue, TgGAP40, has been identified in *Toxoplasma* tachyzoites as a member of the actin-myosin motor complex (Frenal et al., 2010). The GFP-GAP45 and GAP50 protein bands were also confirmed by LC-MS/MS (Figure 5.5A). Other than that, there were background proteins detected in both 3D7 and GFP-GAP45 immunoprecipitated products such as

adenosylhomocysteinase (P50250) and elongation factor-1 gamma (PF13_0214). These proteins may bind non-specifically and be resistant to the washing conditions used in the immunoprecipitation assay. Due to the low amount of immunoprecipitated protein, it was not possible to identify unknown phosphoprotein 1 (Figure 5.4).

5.5 The effect of S89 and S103 phosphorylation on the localisation of GFP-tagged GAP45.

Similar to FL-GAP45 protein, the single (S89A, S103A, S89D and S103D) and double variant (S89A/S103A or S89D/S103D) GFP-tagged GAP45 proteins were resistant to solubilisation in high pH carbonate buffer (Figure 5.6). These results demonstrate that substitution of S89 and S103, to either alanine or aspartate, does not affect the membrane binding properties of GFP-tagged GAP45 proteins. As a control, MTIP was also insoluble in carbonate buffer, as expected (Figure 5.6). The parasite surface and peripheral membrane protein, MSP7 was partially detected in the carbonate soluble fraction with most of the protein remaining insoluble (Figure 5.6). SERA5, a protein of the parasitophorous vacuole that is not membrane associated is largely released upon parasite treatment with a hypotonic solution (lane 1, Figure 5.6).

By live microscopy, GFP-GAP45 proteins with S89 and S103 variants (S89A, S89D, S103A, S103D, S89A/S103A and S89D/S103D) were localised in a similar manner as WT/FL-GAP45 in both young and late schizont stages (Figure 5.7A & B). These findings show that substitution of S89 and S103 residues by either alanine (A) or aspartate (D) does not contribute to any differences in the GFP-tagged GAP45 localisation pattern: the appearance of ring-like GFP signal in 36-hour schizonts (early schizont) and peripheral GFP signal in 42-hour schizonts (late stage schizont). The double GFP-GAP45 variants, S89A/S103A and S89D/S103D, also showed an identical localisation pattern as that of WT or FL-GAP45 (Figure 5.7A & B). These findings were further confirmed by IFA, where at late schizont stage the WT or FL-GAP45 protein, together with its variants (S89A, S89D, S103A, S103D,

S89A/S103A and S89D/S103D), were co-localised well with GAP45, MTIP, MSP1, and GAP50 proteins (Figure 5.8A-D). As expected, the RON10 protein was located at the anterior of each developing merozoite (Figure 5.8E).

Similar to the WT or FL-GAP45 (Figure 5.9A), the ring-like localisation pattern of GFP-tagged GAP45 variants (S89A, S89D, S103A, S103D, S89A/S103A and S89D/S103D) did not co-localise with parasite plasma membrane markers such as MSP1 in the young schizont stage where the parasites are not completely segmented (Figure 5.9B). RON10 is located in close proximity to each ring-like localisation pattern of GFP-tagged GAP45 variants (Figure 5.9C), as seen previously with WT and FL-GAP45. In conclusion, it seems that phosphorylation of S89 and S103 in GFP-tagged GAP45 has no influence on GAP45 localisation during parasite schizogony.

5.6 The effect of S89 and S103 mutation on the GAP45 tetrameric actin-myosin motor complex

As shown previously in this study, WT and FL-GAP45 protein were able to interact with other motor complex protein partners (Figure 4.8; Appendix D). The substitution of either or both S89 and S103 of GFP-tagged GAP45 with alanine (S89A and S103A) or aspartate (S89D and S103D) does not seem to interrupt the binding ability of this protein to the motor complex protein partners.

In Figure 5.10A and B, it is clearly shown that none of the substitutions interrupt the interaction of GFP-tagged GAP45 with MTIP, GAP50 and MyoA. The same findings were made in identical experiments performed with GFP-GAP45 containing both S89A and S103A substitutions (S89A/S103A) (Appendix D). These data suggest that phosphorylation and dephosphorylation of GFP-GAP45 on S89 and S103 has no effect at all on the ability of GAP45 to interact with other components of the motor complex. A truly accurate analysis by densitometry was not possible, as the intensity of the protein band had reached its saturated level, so small effects could have been overlooked by this analysis.

N-GAP45 acted as a control in this experiment. This protein is a truncated GFP tagged GAP45 protein which encodes the first 29 amino acids of GAP45 fused at the N-terminus of GFP. This region of GAP45 is thought to be important in targeting to the plasma membrane. Another negative control protein, CDPK1 is a non-motor complex protein and localises at the parasite plasma membrane. As expected, CDPK1 does not co-immunoprecipitate with GFP-tagged GAP45 protein, as shown in Figure 5.10A and B.

5.7 Discussion

Both CDPK1 expression and GAP45 phosphorylation peak at the late schizont stage, suggesting a possible role of CDPK1-mediated phosphorylation in the regulation of motor complex assembly (Green et al., 2006). Although GFP-tagged GAP45 was localised at the IMC, the functionality of this protein, with the GFP insertion at the middle of the GAP45 protein sequences, needed to be confirmed. One of the characteristics that can confirm the functionality of this protein is the ability of the protein to be phosphorylated.

The results clearly show that GFP-GAP45 (FL- and C-GAP45) is phosphorylated in parasite lysates (Figure 5.2). GAP45 is a hyperphosphorylated protein, as GFP-GAP45 containing S89A/S103A substitutions is still affected by phosphatase treatment (Figure 5.3), suggesting phosphorylation of additional residues. This was further supported by massive incorporation of ^{32}P-phosphate into FL-GAP45 and S89A/S103A GFP-GAP45 at similar levels (Figure 5.4). C-GAP45 (N-terminal truncated GFP-GAP45) was also found to be phosphorylated (Figure 5.2), indicating that phosphorylation of the C-terminal region is independent of the N-terminus of GAP45. This also suggests that phosphorylation of GAP45 is not dependent on the protein being associated with the parasite plasma membrane through N-terminal dual acylation.

The immunoprecipitation of GFP-GAP45 ^{32}P-phosphate radiolabelled protein revealed five phosphorylated protein bands (Figure 5.4). One of these is GFP-GAP45, whilst a further two were demonstrated to correspond to MyoA and MTIP

proteins. Both MyoA and MTIP have been shown to be phosphorylated in schizonts (Green et al., 2008; Treeck et al., 2011). The other two phosphorylated protein bands, unknown phosphoprotein 1 and 2 were detected at around ~150kDa and ~50 kDa respectively (Figure 5.4). Unknown phosphoprotein 2, was identified as GAP40 (~50 kDa) and has an extremely high level of radiolabel incorporated (Figure 5.4). A phosphoproteomic study demonstrated that GAP40 is phosphorylated on at least 15 amino acid residues (Treeck et al., 2011). The GAP40 orthologue, TgGAP40 has been demonstrated to form a complex with TgGAP45 and other motor complex proteins (Frenal et al., 2010). TgGAP40 has nine membrane spanning domains and may play a role in anchoring the motor complex proteins to the IMC (Frenal et al., 2010). One possible protein candidate with a size near to the ~180 kDa of unknown phosphoprotein 1 is ALV6. However, there is no clear evidence of ALV6 forming a complex with GAP45 or other motor complex proteins. According to a phosphoproteome study, ALV6 is highly expressed in schizonts and is phosphorylated at 23 amino acid residues (Treeck et al., 2011). Although ALV6 (MAL13P1.260) involvement in motor complex formation is unknown, two of its family members, ALV4 and ALV5, together with GAP45 and GAP50 proteins were detected in the proteins immunoprecipitated with antibodies against GAPMs proteins (Bullen et al., 2009). The alveolin family members (some of them are also known as inner membrane complex proteins) have been shown to be associated with the IMC of both *P. berghei* (IMC1a, IMC1b and IMC1h/PfALV3) and *T. gondii* (IMC1-14 except IMC2 due to lack of an alveolin motif) parasites (Anderson-White et al., 2011; Gould et al., 2008; Khater et al., 2004; Mann and Beckers, 2001; Tremp and Dessens, 2011; Tremp et al., 2008). Other uncharacterized *Plasmodium* alveolin-related proteins are IMC1c, IMC1d, IMC1e, IMC1f and IMC1g (Khater et al., 2004).

Phosphorylation at S89 and/or S103 does not affecting the localisation of GAP45 to the IMC. The substitution of S89 and S103 to either alanine (A) or aspartate (D) does not seem to cause any difference in localisation pattern throughout schizogony, at the young (~36 hours post invasion) and late (~42 hours post invasion) schizont stages. This suggests that phosphorylation or dephosphorylation of S89 and S103 does not have an important role in GAP45 targeting to the IMC. All of the GFP-tagged GAP45 variants (S89A, S89D, S103A, S103D, S89A/S103A

and S89D/S103D) showed similar localisation patterns as WT GFP-tagged GAP45 by live microscopy and co-localised well with IMC markers MTIP and GAP50 in late stage schizonts. The localisation of GAP45 to the IMC has also been shown to be unaffected by phosphorylation in another apicomplexan parasite *T. gondii* (Gilk et al., 2009).

Phosphorylation on S89 and S103 also does not seem to affect association of GFP-GAP45 into the motor complex of *P. falciparum*. In contrast, in *T. gondii*, the importance of GAP45 phosphorylation has been highlighted in the final step of assembly of the motor complex with GAP50, where it causes the dissociation of the trimeric MyoA-MTIP-GAP45 complex from GAP50 (Gilk et al., 2009). The best explanation for this is that the phosphorylated residues in TgGAP45 (S163 and S167) are in the least conserved region of the protein and are not identical in *P. falciparum* GAP45 where the equivalent positions are D117 and T121. The TgGAP45 mutation S163E causes dissociation of the motor complex (Gilk et al., 2009), whereas the equivalent position in PfGAP45 is an acidic aspartate, suggesting that the mechanism of regulation of motor complex formation may not be conserved between the two species, or that negative charge alone was not the cause of complex dissociation in the TgGAP45 mutant protein.

Phosphorylation of S89 and S103 is clearly not responsible for regulating motor complex assembly in *P. falciparum*, but there are other phosphorylated residues that may perform that function. For example, S142A and S149A GAP45 variants were shown to increase GAP45 phosphorylation in this study. It will be important to study the function of S142 and S149 phosphorylation, as this might have a role in regulating the overall phosphorylation of GAP45. Another possibility is that eliminating phosphorylation of S89 and S103 of GAP45 may not be sufficient to cause any effect on motor complex formation, as more CDPK1 phosphorylation sites have been detected in GAP45 *in vitro* (Winter et al., 2009). By phosphoproteome analysis on parasite schizonts using liquid chromatography-tandem mass spectrometry (LC-MS/MS), GAP45 was shown to be phosphorylated on 8 residues: S89, S103, S107, S142, S149, S156, T158 and S198 (Treeck et al., 2011). A recent study on calcium-induced *T. gondii* tachyzoites also showed that

TgGAP45 is phosphorylated at multiple sites (Nebl et al., 2011). Briefly, by a combination of different methods such as ^{32}[P]/2-dimensional electrophoresis autoradiograph spot analysis and Multi-dimensional liquid chromatography Protein Identification Technology (MudPIT), 5 phosphorylated residues (S153, Y158, S163, S167 and S184) were detected in TgGAP45. An exhaustive investigation into the *T. gondii* motor complex components was done using Stable Isotope Labelling of Amino Acids in Culture (SILAC)-based quantitative LC-MS/MS with Orbitrap analysis. This method detected additional phosphorylation sites on TgGAP45: S169, S184/185 and T189. This technique also showed that only phosphorylation on S184/185 and T189 is enhanced by calcium, suggesting that GAP45 is a substrate for other kinases which are calcium-independent (Nebl et al., 2011).

Another interesting finding by Nebl et al. (2011) is that the calcium-sensitive phosphorylated residue, S185, is conserved throughout apicomplexan GAP45 sequences and the comparable residue in *P. falciparum* GAP45 is S149. The formation of the motor complex is enhanced or increased in calcium-treated *T. gondii* parasites as compared to non-induced parasites (Nebl et al., 2011). In contrast, a study by Gilk et al. (2009) focusing on calcium-independent phosphorylation sites (S163 and S167) of TgGAP45 demonstrated dissociation of GAP45 from GAP50 when it is phosphorylated at these sites. Taken together, these data suggest that the formation of the motor complex can be regulated through phosphorylation, specifically on GAP45, by two different pathways, one of which is calcium-dependent and increases motor complex association, whilst the other is calcium-independent and promotes motor complex dissociation. Although such speculation is possible, it has to borne in mind that the study by Nebl et al. (2011) did not show any direct evidence about the effect of S185 in TgGAP45 (S149 in PfGAP45) phosphorylation on the increased motor complex assembly. They only show that the two phenomena, phosphorylation and increase in motor complex assembly, occur in response to calcium induction.

There is direct evidence about the kinases responsible for phosphorylating GAP45 in parasites. Other than CDPK1, PKB has been reported to phosphorylate GAP45 in parasites (Vaid et al., 2008). Briefly, the PKB inhibitor peptide called

calmodulin binding domain 1-15 (CBD_{1-15}) was able to reduce GAP45 phosphorylation through inhibiting PKB activity in parasite (Vaid et al., 2008). Further studies by the same group also showed that GAP45 phosphorylation on S103 and S149 was regulated by calcium signal through the activation of the phospholipase C (PLC) pathway. In addition, PKB was shown to phosphorylate S103 of GAP45 in the parasite (Thomas et al., 2012). Another potential calcium-dependent kinase is the *P. falciparum* protein kinase 2 (PfPK2), homologous to human calcium/calmodulin-dependent protein kinase, which is expressed in merozoites (Kato et al., 2008a). The calmodulin antagonist W-7 has been shown to inhibit PfPK2 activity and also decreased the parasitemia of ring forms in invasion assays (Kato et al., 2008a). However, the calmodulin antagonist used in the Kato et al. (2008) study will have effects on other calmodulin dependent kinases or pathways. For example, the calmodulin antagonist might also inhibit PKB, which is a Ca^{2+}/calmodulin dependent kinases as mentioned above.

Other studies have suggested that the phosphorylation of GAP45 is governed by calcium-independent and staurosporine resistant kinases, as treating the parasite with both intracellular calcium chelators (A23187, BAPTA AM and dantrolene) and kinase inhibitor (staurosporine) failed to inhibit GAP45 phosphorylation and motor complex association completely (Jones et al., 2009). However treatment with staurosporine does show some depletion in motor complex protein components (Jones et al., 2009). This further supports the notion that GAP45 is being phosphorylated sequentially by different kinases. As suggested by Jones et al. (2009), other than the calcium-dependent protein kinases CDPK1 and PKB, there are other potential kinases that may phosphorylate GAP45 such as casein kinase II, which is known to be active during *T. gondii* tachyzoite invasion (Delorme et al., 2003). Casein kinase II is not sensitive to staurosporine and does not rely on a second messenger for activation (Jones et al., 2009; Meggio et al., 1995). Additionally, protein kinase A (PKA) has been reported to phosphorylate apical membrane antigen 1 (AMA1) at S610, an important protein in merozoite tight junction formation prior to red blood cell invasion (Leykauf et al., 2010). Last but not least, PKG is another kinase that may phosphorylate GAP45. Inhibition of this kinase by compound 1, a

specific PKG inhibitor, prevents schizont maturation in asexual blood stages of *P. falciparum* (Taylor et al., 2010).

Phosphorylation events on GAP45 protein may be crucial in the motile /invasive stages of *P. falciparum*: merozoites, ookinetes and sporozoites. Again this is another obvious difference between *P. falciparum* and *T. gondii* studies; the studies on *T. gondii* were on the motile stage, the tachyzoite, whereas *P. falciparum* studies (including this one) were generally performed on schizonts. During red blood cell invasion the assembly or disassembly of motor complex proteins, which is regulated by phosphorylation, may be occurring, and by restricting our studies to schizonts we may miss important events, particularly relating to disassembly. Alternatively, phosphorylation of the residues we have studied, S89 and S103, may have a completely different consequence that was not evident in this study. Thus, studying GAP45 phosphorylation in the merozoite stage is imperative.

As the parasite was episomally transfected, the GFP-tagged GAP45 was expressed together with an endogenous GAP45. It is possible that the presence of endogenous GAP45 has prevented a dominant phenotypic effect of these GAP45 variants. An attempt to replace the native GAP45 with WT GFP-tagged GAP45 by single cross-over was unsuccessful, possibly due to the presence of only a short low complexity region at the 5' UTR to allow recombination. For future experiments, a different mechanism for allelic replacement is needed to study the effect of GAP45 phosphorylation (particularly by CDPK1) on *Plasmodium* growth and invasion.

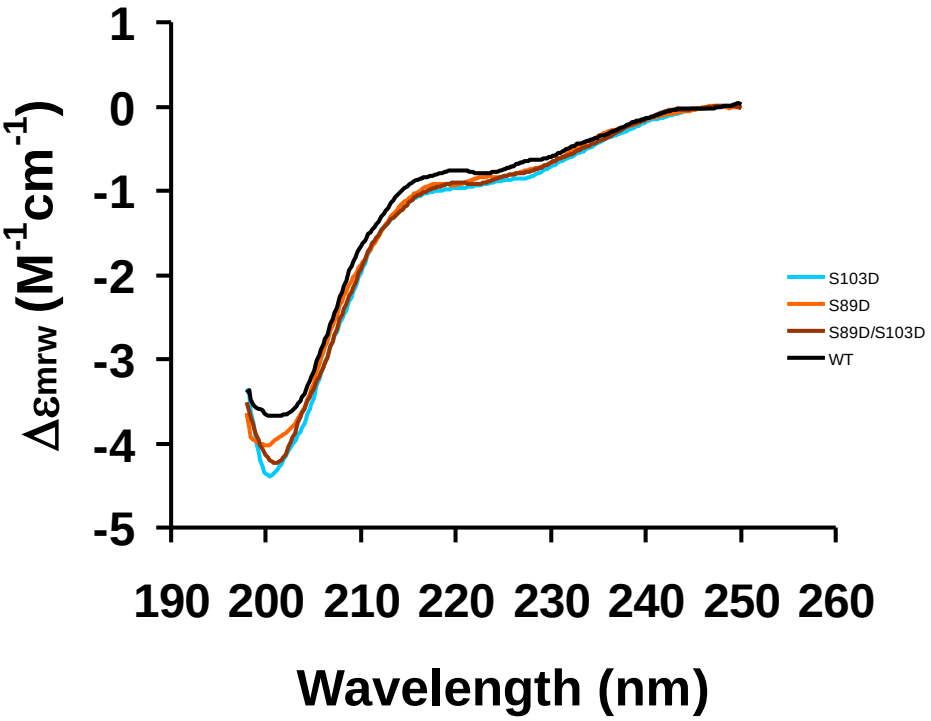

Figure 5.1: Far UV circular dichroism (CD) spectra for WT, S89D, S103D and S89D/S103D GAP45 recombinant proteins. The purified GAP45 recombinant proteins were suspended in PBS prior to CD determination. The secondary structure of recombinant proteins was determined by monitoring CD in the far-UV region (190-260 nm). The values were averaged from multiple scans and presented on a mean residue weight ($\Delta\varepsilon_{MRW}$) basis.

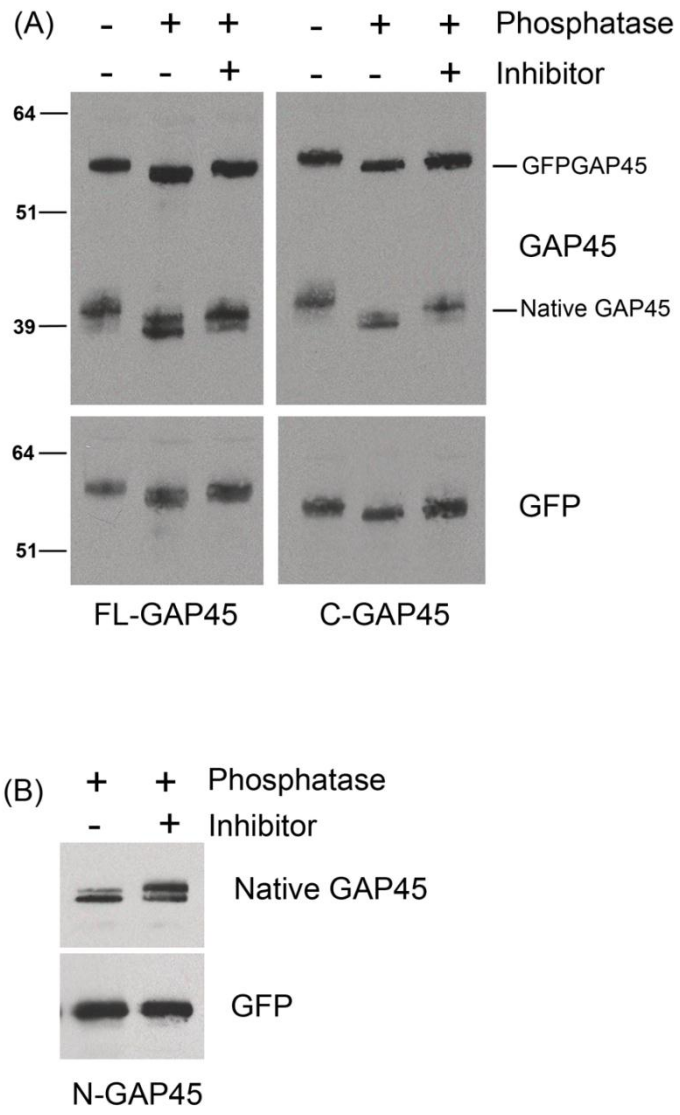

Figure 5.2: The GFP-GAP45 protein is phosphorylated in the parasite. The parasite lysate was treated with bovine intestinal alkaline phosphatase enzyme and analysed by western blotting using anti-GAP45 and anti-GFP antibodies. The GFPGAP45 protein band from FL-GAP45 and C-GAP45 (A) was shifted to a lower molecular weight upon treatment with alkaline phosphatase (lane 2) as compared to control without phosphatase (lane 1) or with phosphatase inhibitor cocktail (lane 3). The N-GAP45 protein band does not show any changes in its migration upon treatment or without phosphatase treatment (B). The native GAP45 band shifted to a lower molecular weight upon treatment with phosphatase.

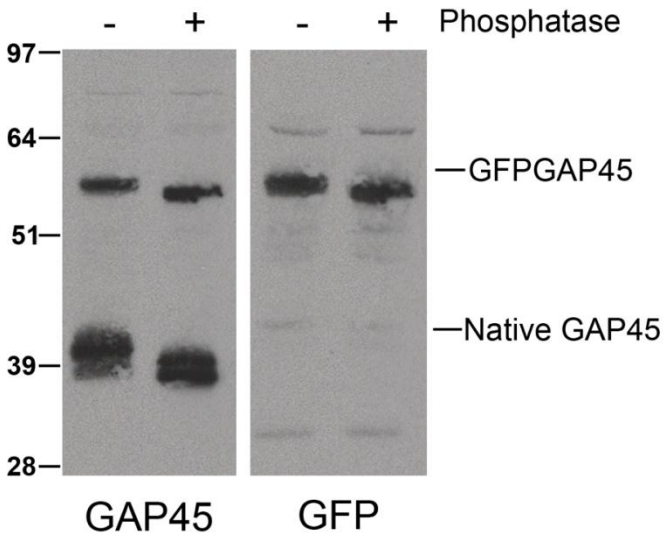

Figure 5.3: The S89A/S103A GFP-GAP45 protein is also phosphorylated in the parasite. The parasite lysate was treated with bovine intestinal alkaline phosphatase and analysed by western blotting using anti-GAP45 and anti-GFP antibodies. The S89A/S103A GFPGAP45 protein band was shifted to a lower molecular weight upon treated with the alkaline phosphatase (lane 2) as compared to control without phosphatase (lane 1).

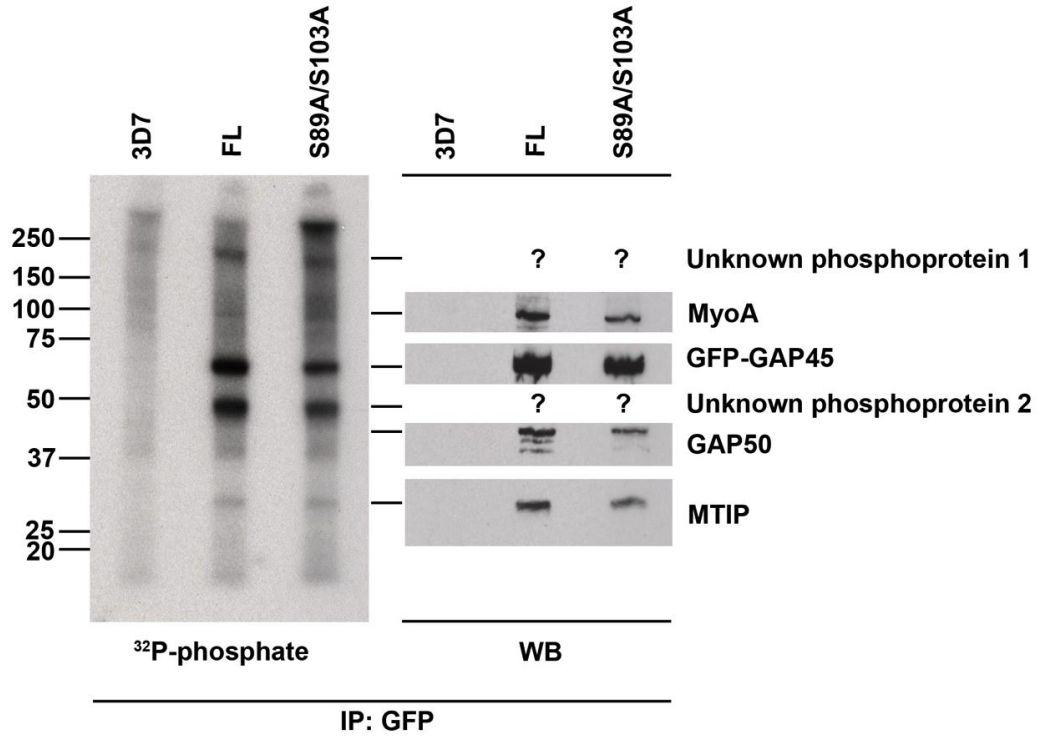

Figure 5.4: The S89A/S103A GFP-GAP45 is phosphorylated and at similar level as WT GFP-GAP45 (FL). Synchronized parasites were metabolically radiolabelled with ^{32}P-phosphate at the schizont stage prior to immunoprecipitation with the GFP-Trap® system. The precipitated samples were separated by SDS-PAGE and dried for autoradiography analysis. Western blotting was performed on a similar sample to identify the protein or phosphoprotein that has been pulled down. The identified motor complex proteins (GAP45, MyoA, MTIP and GAP50) were labelled as above. The new co-precipitated phosphoproteins were labelled as unknown phosphoprotein 1 and 2 (?).

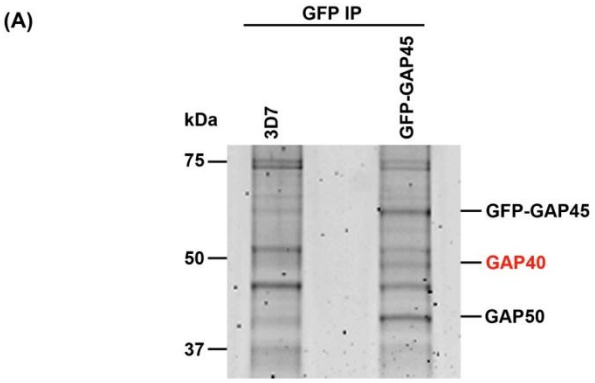

Protein identification	Number of unique peptides	List of peptides
PFE0785c (GAP40)	2 (coverage 3.29 %)	VEINENMLK, FAYFPK
PFL1090w (GAP45) P42212 (GFP)	13 (coverage 38.2%) 6 (coverage 23.5%)	DIDELAERENLK, LDETAKVFSR, etc. SAMPEGYVQER, AEVKFEGDTLVNR, etc.
PFI0880c (GAP50)	3 (coverage 8.3%)	DADATNYPK, VTFIVSPGSNFIDGVK, etc.

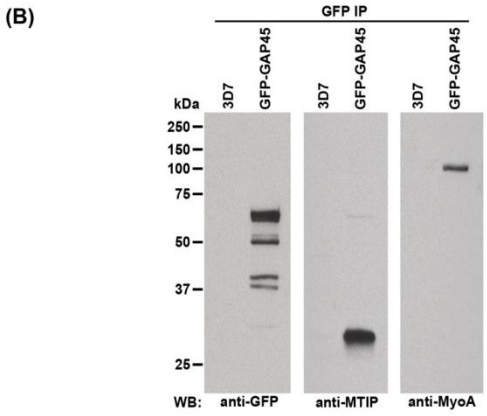

Figure 5.5: The identification of GAP40 as a phosphorylated motor complex protein. (A) GFP-GAP45 protein was immunoprecipitated using the GFP-Trap® system. The immunoprecipitate was separated on a 10% NuPAGE gel and stained with SYPRO Ruby. The related protein band was excised by 2D gel spot picker. The excised gel was processed and digested with trypsin prior to LC-MS/MS analysis. GAP40 protein (PFE0785c) was identified as a motor complex protein in GFP-GAP45 immunoprecipitation. GAP40 was not detected in the control 3D7 *P. falciparum* immunoprecipitate. GFP-GAP45 and GAP50 protein bands were also confirmed by LC-MS/MS. **(B)** The presence of MyoA and MTIP proteins was confirmed by western blotting as their corresponded protein bands could not be visualized by SYPRO Ruby staining.

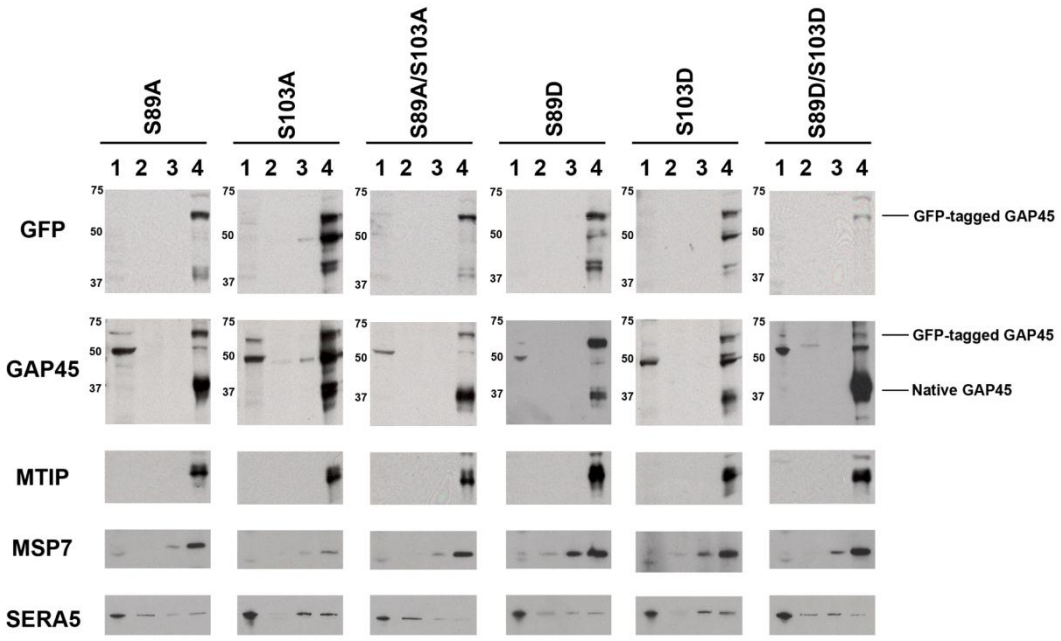

Figure 5.6: Subcellular fractionation of S89 and S103 variants of GFP-tagged GAP45 proteins. Subcellular fractionation was performed starting with extraction using hypotonic lysis buffer, followed by high salt buffer, and sodium carbonate buffer. All parasite solubilized fractions, hypotonic lysis (1), high salt (2), carbonate supernatant (3) and carbonate pellet (4), were separated by SDS-PAGE and analysed by western blotting, using antibodies to GFP, GAP45, MTIP, MSP7 and SERA5.

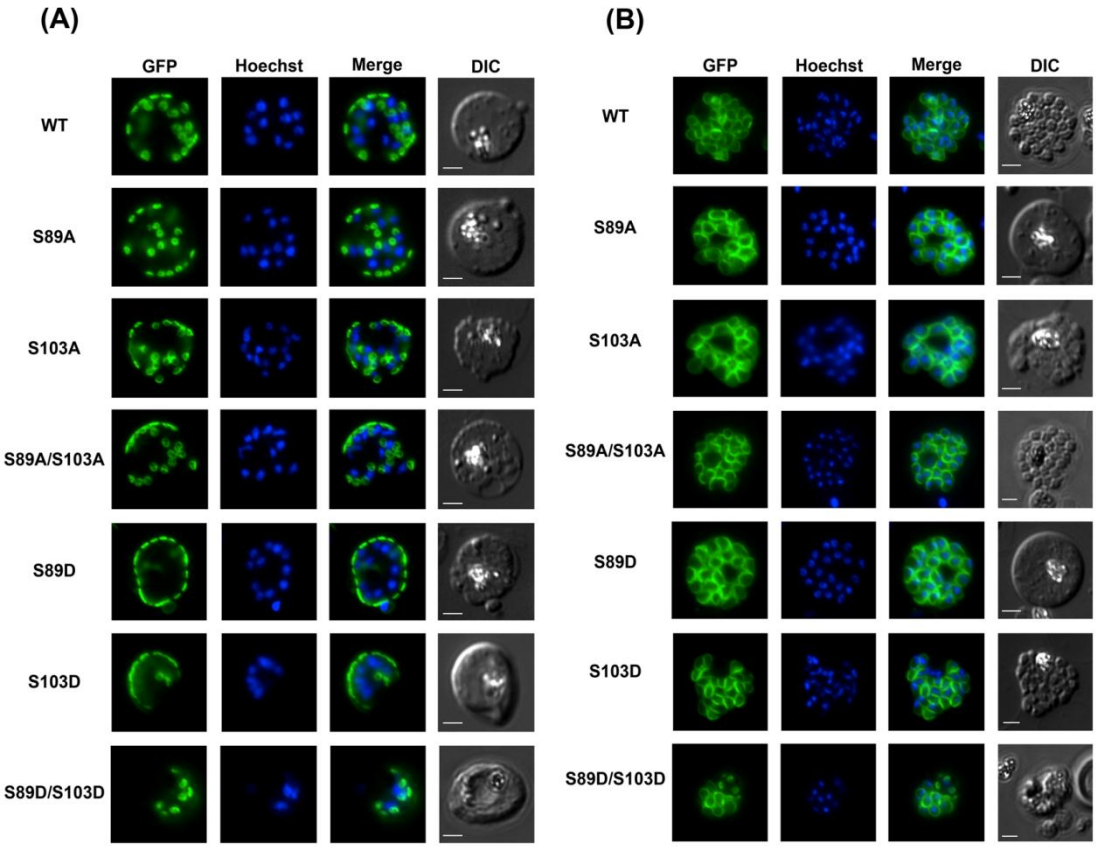

Figure 5.7: The location of GFP-tagged GAP45 and a number of variants in (A) early and (B) late schizonts, by live fluorescence microscopy (green). Parasite DNA was stained with Hoechst dye (blue); merged images and the differential interference contrast pictures are also shown. In early schizont stages, small localised regions of GAP45-GFP signal were observed around the parasite's periphery, typical of an IMC location. At the late schizont stage the GFP signal was detected at the periphery of merozoites developing within the schizont. There was no difference in the pattern of location between the wild type (WT) or FL-GAP45 and its variants. As these pictures were not analysed by Z-stack imaging, some of the images of early schizont stages lack the ring-like IMC structures (S89D, S103D and S89D/S103D), which should mostly be visible at the center of the cell. At a certain focusing plane, only the punctate GFP-signal was seen at the periphery of the parasite. Scale bar is 2 µm.

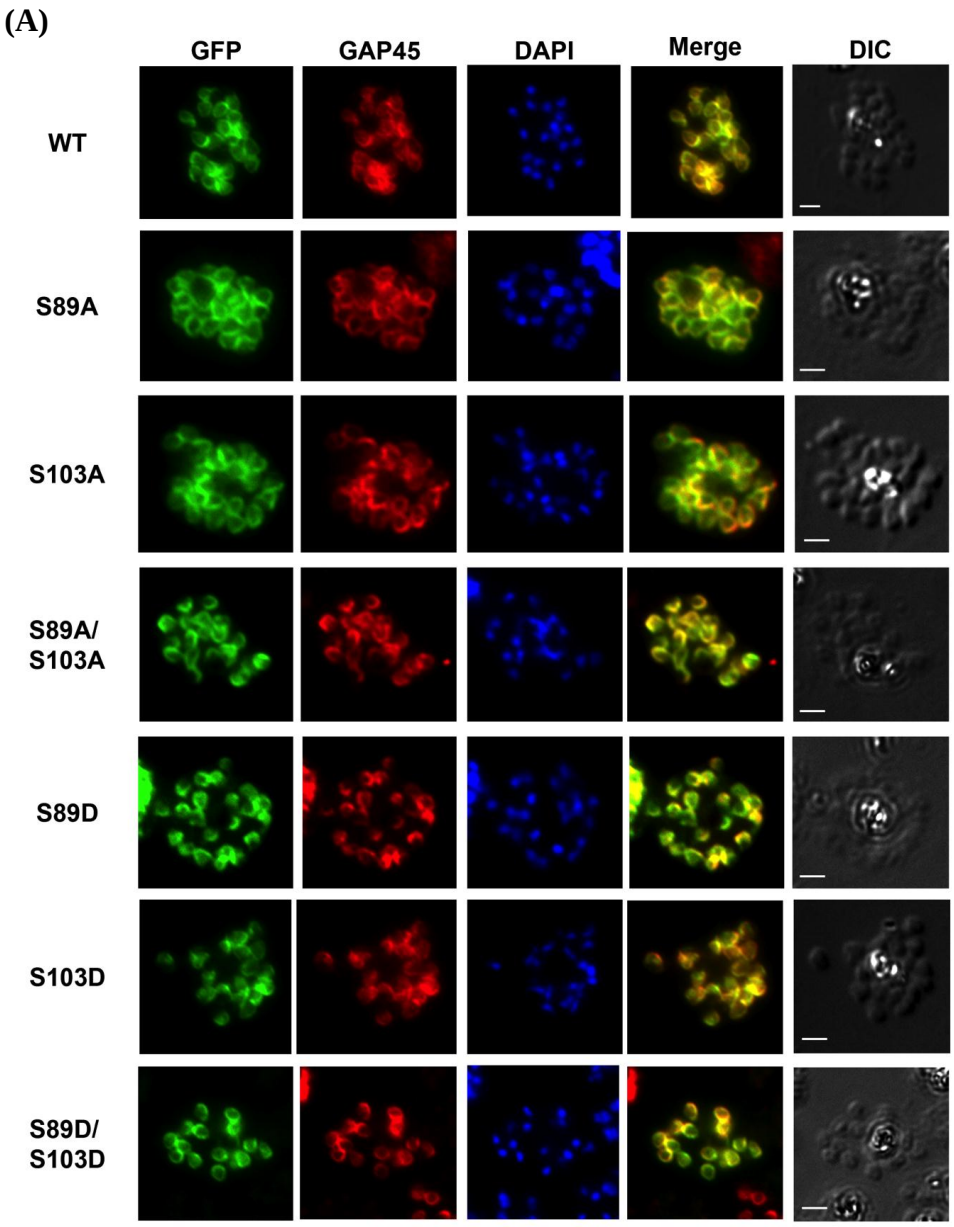

Figure 5.8: Localisation of GFP-tagged GAP45 variants in mature schizonts. Indirect immunofluorescence assays were performed by costaining the GFP-tagged GAP45 with antibodies specific for GAP45 (A), MTIP (B), GAP50 (C), MSP1 (D) and RON10 (E) protein signals. The GAP45, MTIP and GAP50 antibodies are markers for inner membrane complex proteins. The MSP1 and RON10 antibodies were used as parasite plasma membrane and apical markers respectively. The parasite variants are WT or FL-GAP45, S89A, S103A, S89A/S103A, S89D, S103D and S89D/S103D GFP-tagged GAP45. Scale bar is 2 µm.

Figure 5.8 continued: Localisation of GFP-tagged GAP45 variants in mature schizonts.

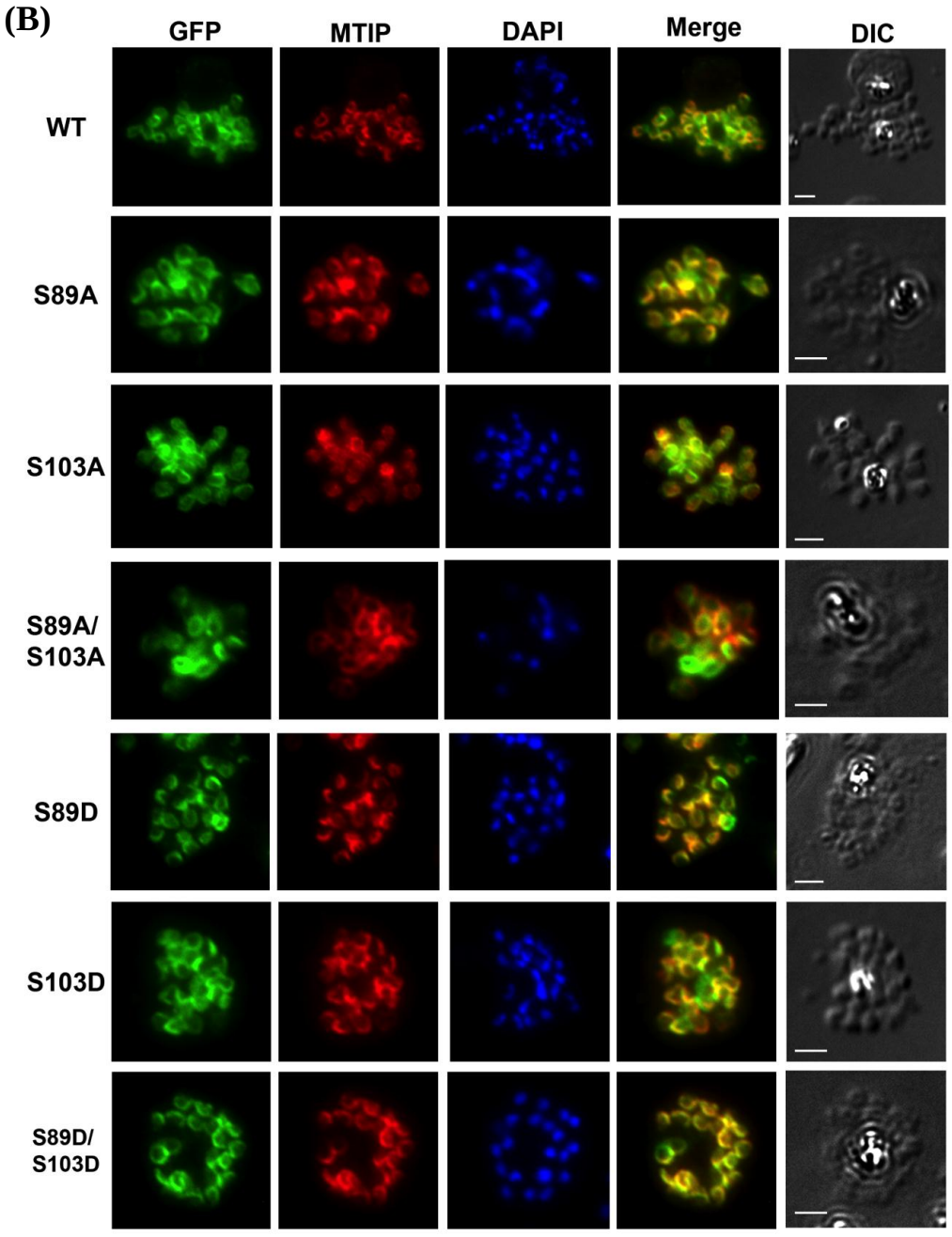

Figure 5.8 continued: Localisation of GFP-tagged GAP45 variants in mature schizonts.

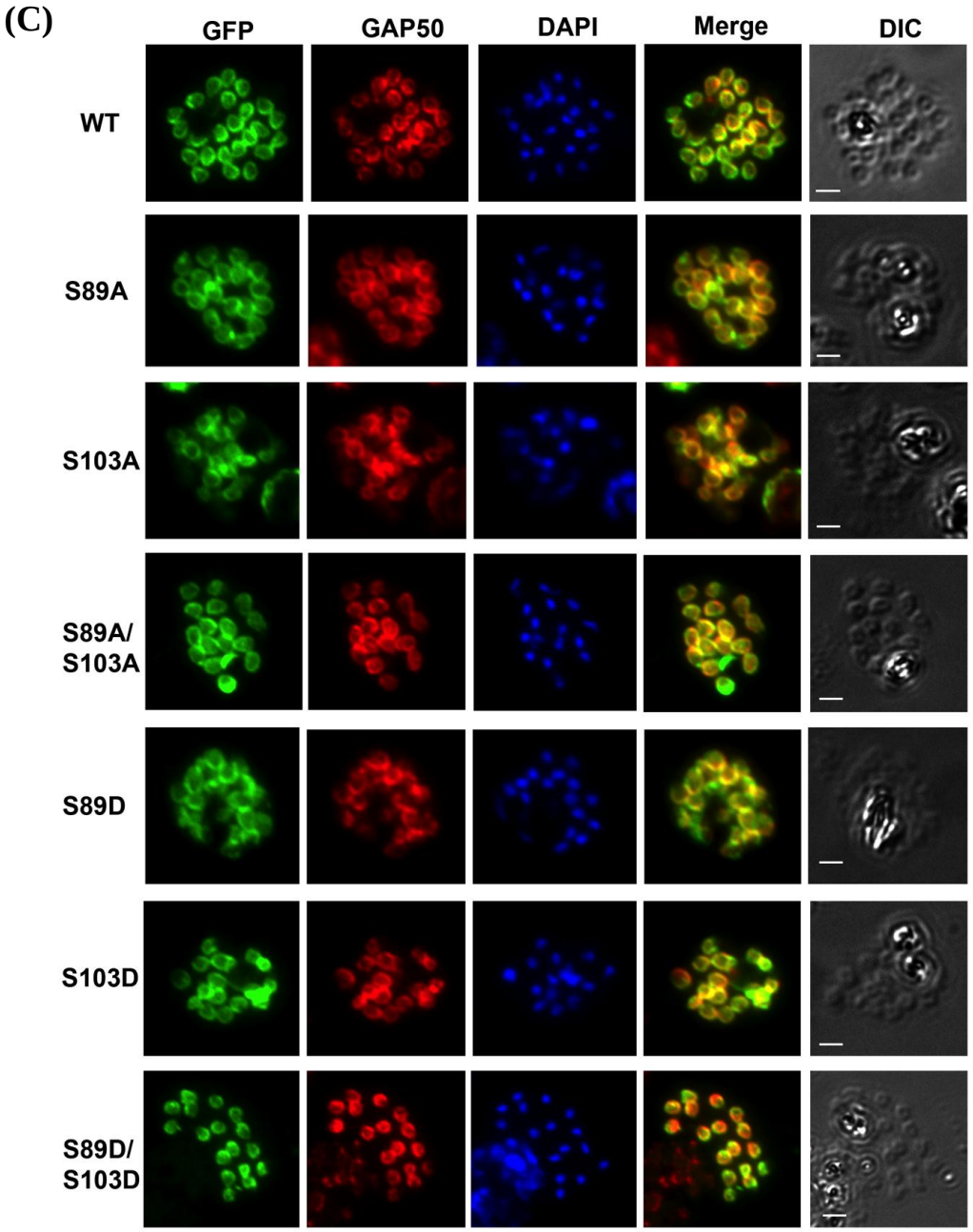

Figure 5.8 continued: Localisation of GFP-tagged GAP45 variants in mature schizonts.

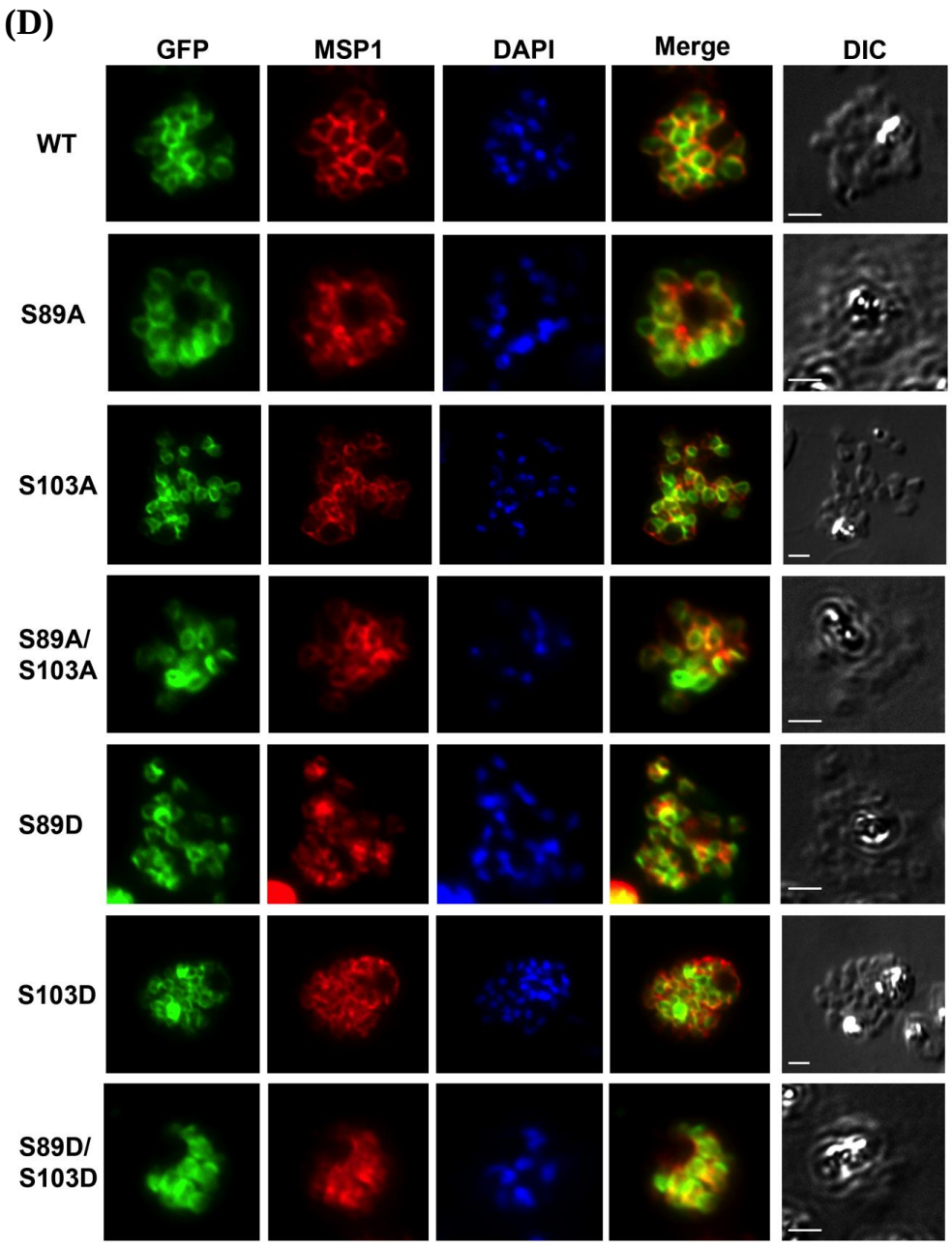

Figure 5.8 continued: Localisation of GFP-tagged GAP45 variants in mature schizonts.

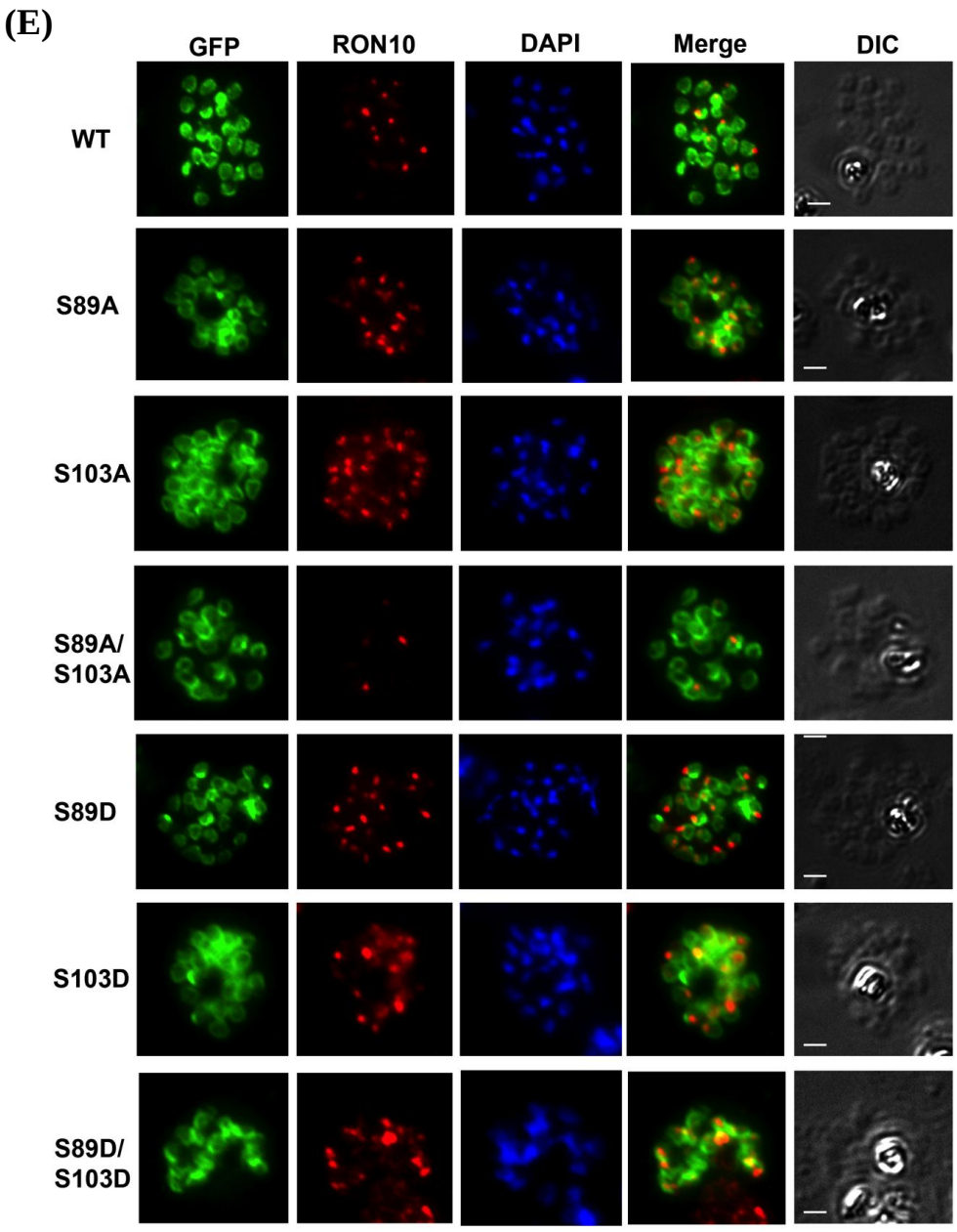

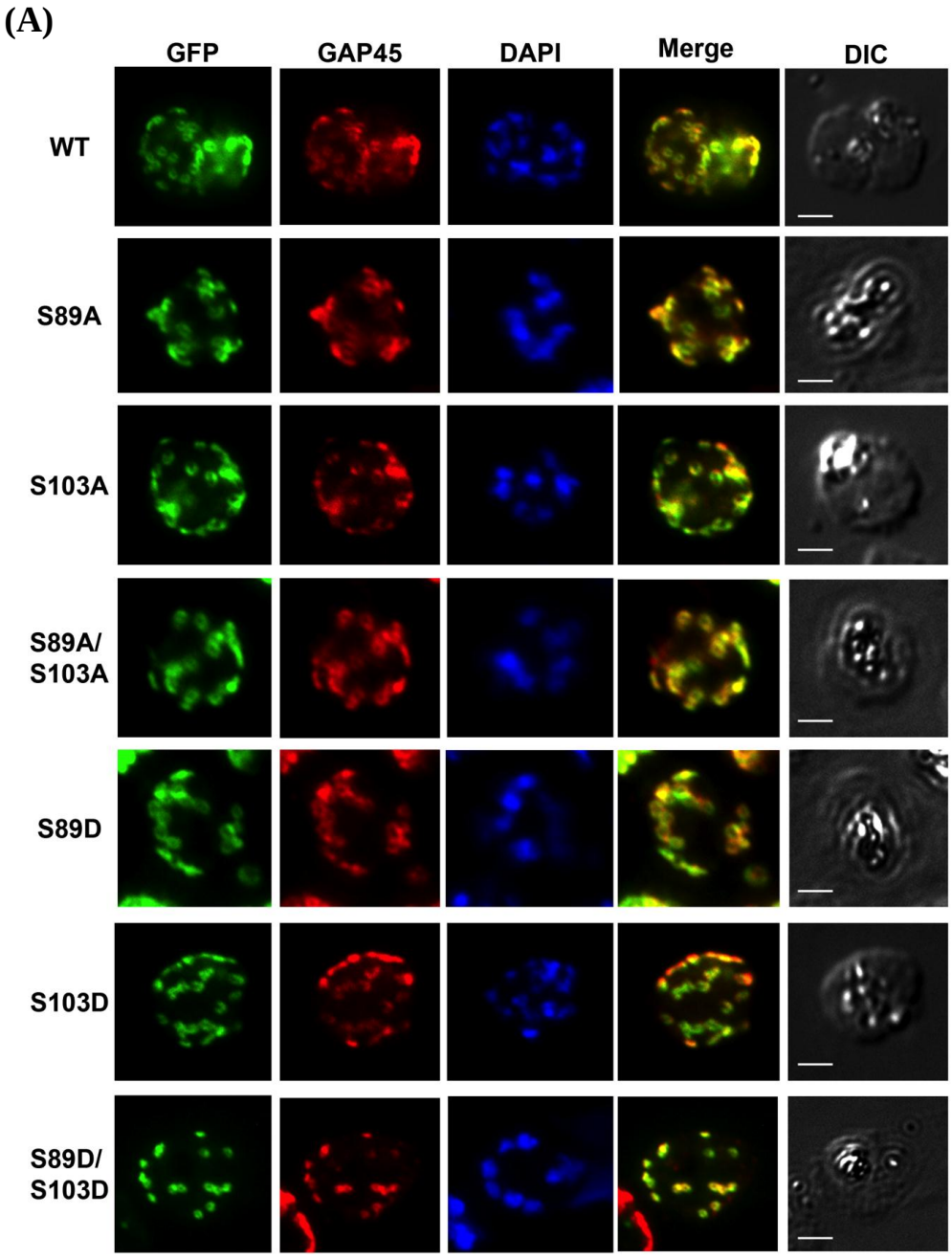

Figure 5.9: Localisation of GFP-tagged GAP45 variants in young schizonts. Indirect immunofluorescence assays were performed by co-staining the GFP-tagged GAP45 with antibodies specific for GAP45 (A), MSP1 (B) and RON10 (C). The GAP45, MTIP and GAP50 antibodies are markers for inner membrane complex proteins. The MSP1 and RON10 antibodies were used as parasite plasma membrane and apical markers respectively. The parasite variants are WT or FL-GAP45, S89A, S103A, S89A/S103A, S89D, S103D and S89D/S103D GFP-tagged GAP45. Scale bar is 2 µm.

Figure 5.9 continued: Localisation of GFP-tagged GAP45 variants in young schizonts.

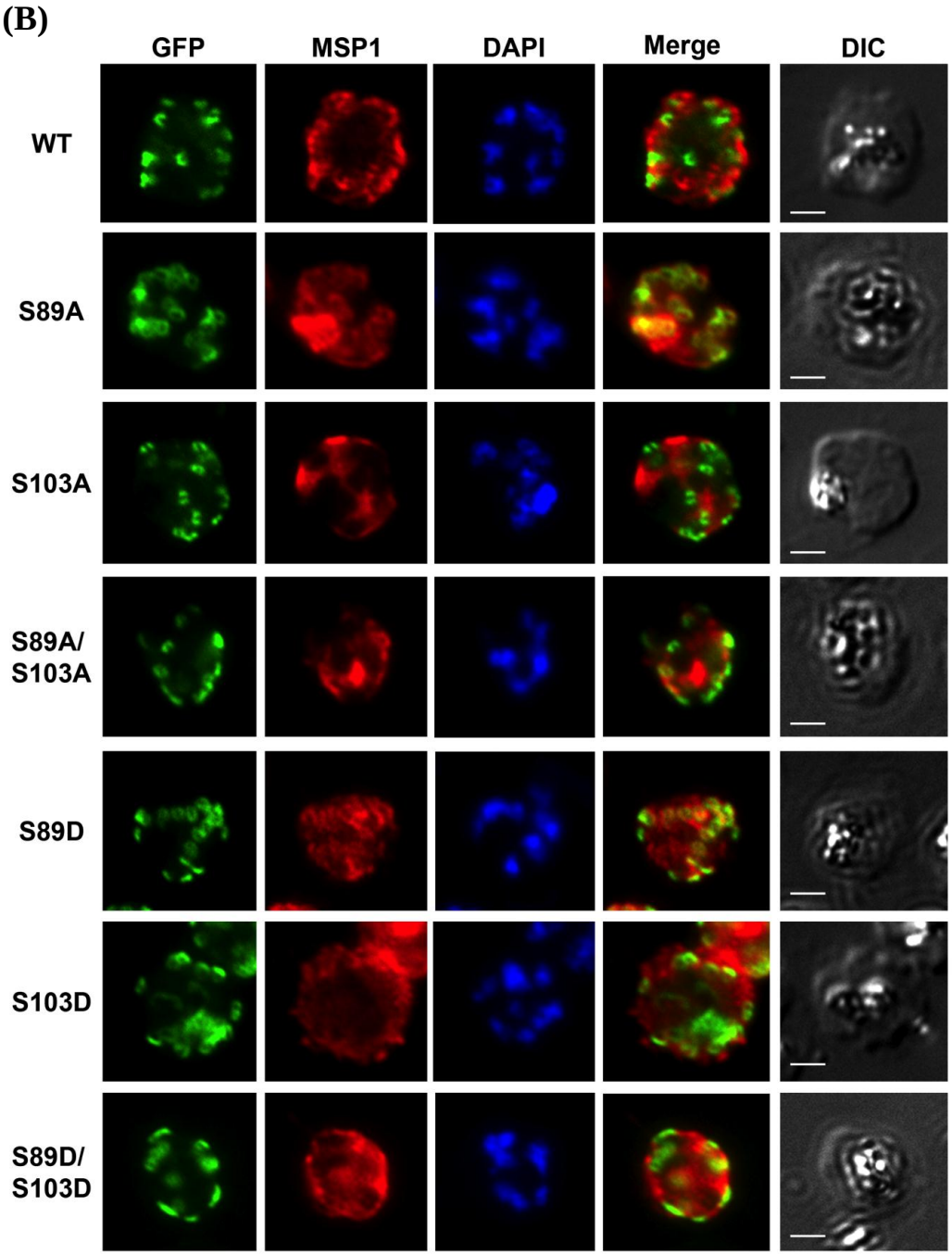

Figure 5.9 continued: Localisation of GFP-tagged GAP45 variants in young schizonts.

(C)

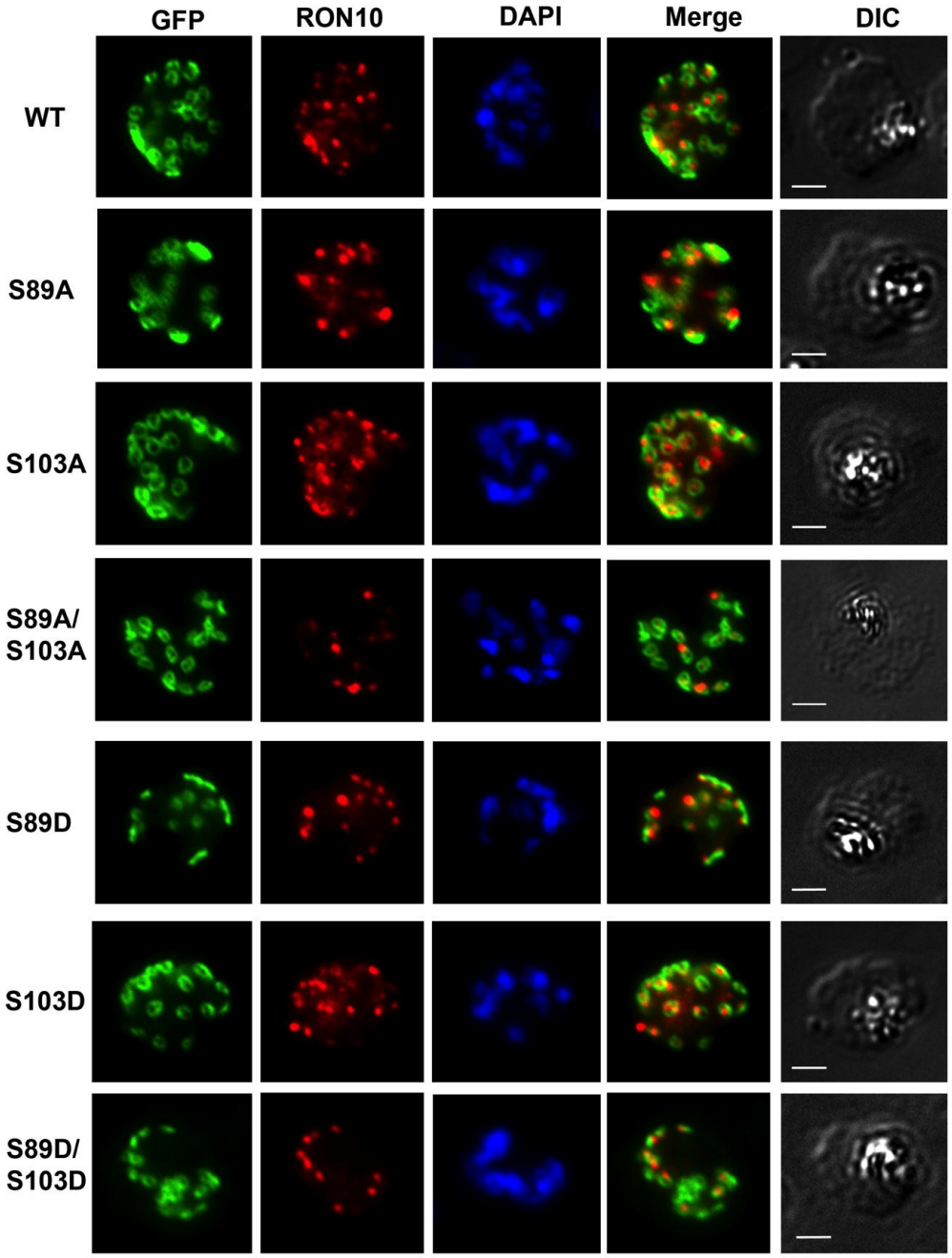

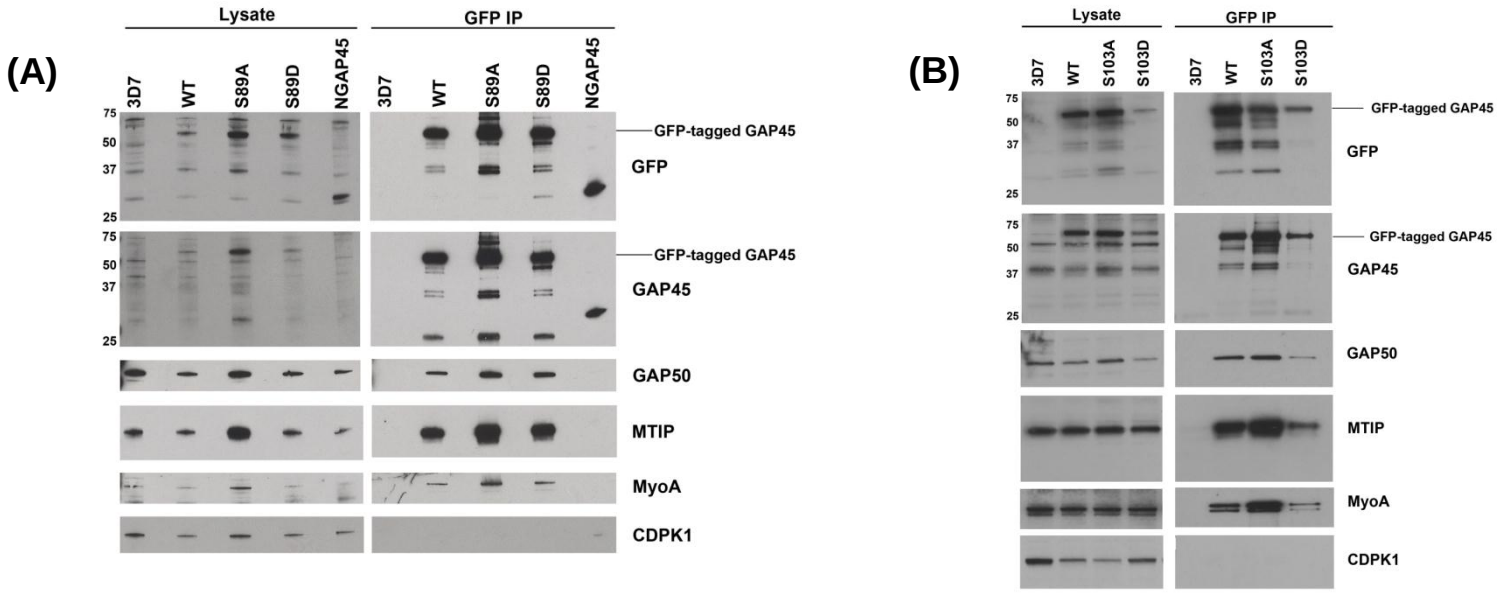

Figure 5.10: WT/FL-GAP45 proteins and its variants assemble into the motor protein complex, whereas N-GAP45 does not. Detergent lysates (1% NP40) of schizont stage-parasites were prepared from untransfected 3D7 or parasites transfected with plasmid to express the WT, S89A, S89D GFP-tagged GAP45 variants and N-GAP45 (A) and S103A, S103D GFP-tagged GAP45 variants (B). WT/FL-GAP45 and variants were immunoprecipitated using the GFP-Trap® system. Precipitated proteins and a sample of each corresponding lysate were resolved by SDS-PAGE and then analysed by western blotting using antibodies to GFP, GAP45, GAP50, MTIP, MyoA and CDPK1. The GFP antibody immunoprecipitated the GFP-tagged GAP45 protein together with its interacting proteins such as GAP50, MTIP and MyoA. CDPK1 is known to not be part of the motor complex and therefore was used as a control.

As untransfected 3D7 parasites were not expressing GFP-tagged GAP45 proteins, no immunoprecipitation product was detected in this lysate. The results show that all of the GFP-tagged GAP45 proteins formed a tetrameric motor complex with other motor proteins except for N-GAP45. The GFP-tagged GAP45 proteins tend to degrade after immunoprecipitation, hence 2 or 3 breakdown products between ~50kDa to ~30 kDa were detected by both GFP and GAP45 antibodies.

Chapter 6
Research summary

6.1 CDPK1 phosphorylates multiple residues on the GAP45 protein

GAP45 is an unstructured protein. By CD analysis, it consists of 4% alpha helix, 22% beta sheet, 10% turn and is 64% unstructured. As suggested in *Toxoplasma* studies (Frenal et al., 2010), most of the structured region of GAP45 is situated at the C-terminus of the protein. GAP45 protein has two likely functions. While recruiting the motor complex to the IMC via its C-terminus, this protein may also have a role in maintaining the gap between IMC and plasma membrane of the parasite. Interactions with each of these membranes are mediated by acylation; the dual acylation of the N-terminus and one or more acylation in the C-terminal region. Therefore it is not surprising that tagging this protein at either the N- or C-terminus causes mislocalisation of the protein and prevents it from interacting with other motor complex proteins such as GAP50, MTIP and MyoA (Frenal et al., 2010; Johnson et al., 2007). As shown in this study and others (Frenal et al., 2010; Gilk et al., 2009), tagging the GAP45 protein internally preserves the function of the protein, at least with regard to its localisation and interaction with other motor complex members at the IMC.

GAP45 is a highly phosphorylated protein (Green et al., 2008; Treeck et al., 2011). Previously, it has been shown to be a substrate for CDPK1 *in vitro* (Green et al., 2008; Winter et al., 2009). By mutagenesis, in this study we have found several CDPK1 phosphorylation sites *in vitro*, particularly S89 and S103 (Chapter 3, Figure 3.3), the residues that were found on GAP45 phosphopeptides enriched from merozoite lysates and detected by MALDI-TOF analysis (Green et al., 2008). As analysed by ES-MS, substitution of both serines to alanines resulted in a decrease in the level of phosphorylated GAP45 protein (Chapter 3, Figure 3.7). The other

possible CDPK1 phosphorylation sites identified in this study were S31, S156, S142 and S149. Modification of S142 and S149 residues to alanine resulted in a very significant increase in the overall level of GAP45 phosphorylation *in vitro* (Chapter 3, Figure 3.5-3.6) suggesting the presence of a switching mechanism, where the phosphorylation/dephosphorylation of some residues may change the exposure of other residues (perhaps S89 or S103) on GAP45 and cause them to be more readily phosphorylated. As shown by ES-MS analysis, the maximum number of phosphates incorporated (4 phosphates) into S142A and S149A GAP45 variants was still the same as for WT GAP45 but the proportion of GAP45 with 3 or 4 phosphates was increased. For example, the population of S142A and S149A GAP45 proteins with 3 phosphate groups incorporated upon CDPK1 phosphorylation was increased as compared to WT GAP45 protein and there was no population of S142A or S149A GAP45 with only one phosphate incorporation detected (Chapter 3, Figure 3.7).

6.2 GFP-tagged GAP45 forms part of the motor complex at the inner membrane complex: a possible interaction with the IMC and parasite plasma membrane via its C-terminal and N-terminal regions respectively.

With current technology, excluding *T. gondii* tachyzoite GAP45, there is no other way of observing the localisation of GFP tagged GAP45 to IMC other than monitoring the development of GAP45 in the early schizont stage. During *P. falciparum* IMC development, parasites show discrete foci of GAP45 at their periphery which has also been shown by other IMC interacting proteins such as GAP50 (Yeoman et al., 2011), MTIP (R. Moon, NIMR, unpublished) and GAPM (Bullen et al., 2009; Hu et al., 2010). GFP-tagged GAP45 also showed a similar localisation pattern in early schizogony. This study has also demonstrated that truncated GFP-tagged GAP45, consisting of the first 29 amino acids from the N-terminus (N-GAP45), was localised to a different membrane compartment at the early schizont stage, resulting in an even GFP distribution pattern surrounding the

developing schizont which is clearly distinct from that of the full length GFP-tagged (FL-GAP45) and endogenous GAP45.

The IMC is a system of flattened membrane cisternae stabilized by a membrane-associated protein from the inner and outer side of its structure (Striepen et al., 2007). The IMC starts to develop at early schizogony forming the foci and ring like structures. As shown by the IMC interacting protein localisation pattern in this study, GFP-tagged GAP45 (FL-GAP45), the ring-like or punctate structure is situated in close proximity with each nucleus (33 hrs post invasion) (Figure 6.1A, i). The ring-like structures become more distinctive as the nuclei replicate (Figure 6.1A, ii) (36 hrs post invasion). The ring-like structure of GFP-tagged GAP45 may represent the starting point of where the IMC starts to develop, which is the apical ring. Previous ultrastructural studies of early schizont stage parasites have suggested that the developing IMC with its associated protein, GAP50, is localised at the apical ring, forming a membrane collar surrounding the apical pore (Yeoman et al., 2011). The GFP-tagged GAP45 signal then starts to surround the nuclei which represent the formation of a pellicular structure around developing merozoites (39 hrs post invasion) (Figure 6.1A, iii). At the end of schizogony, GFP-tagged GAP45 fully surrounds the developed merozoites (42 hrs post invasion) (Figure 6.1A, iv). At this point of schizogony, the plasma membrane and the IMC of the parasites are indistinguishable by fluorescence microscopy as they are situated close to each other (~25 nm as estimated from the electron microscopy figure of Pinder and colleagues (Pinder et al., 2000)). In *Toxoplasma* endodyogeny, the localisation of GAP45 is somewhat different than that of *Plasmodium* as it cannot be seen in the newly developing IMC of daughter cells. This also accounts for a major difference in the cytokinesis process between these *Apicomplexa*. Furthermore, in newly developed tachyzoites, only the integral membrane proteins GAP40 and GAP50 are found to be located at the developing IMC, whereas GAP45, MLC1 and MyoA proteins are absent. These proteins will only localise at the IMC once cytokinesis is complete (Frenal et al., 2010; Gaskins et al., 2004).

As shown by IFA and live imaging of early schizont development, it is clear that inserting GFP within the GAP45 protein does not affect the localisation of the

protein to the IMC (Chapter 4, Figure 4.3-4.7). This may be explained by the fact that the site of GFP tag insertion on GAP45 falls between amino acid residues 29 and 30 which are not conserved throughout the *Plasmodium* species and other apicomplexan parasites (Chapter 1, Figure 1.7 and Figure 1.10). In other words, the sequence might not be so important for GAP45 localisation and/or function. It has also been proven by this study that the GFP-tagged GAP45 was able to interact with other motor complex proteins (Chapter 4, Figure 4.8; Appendix D; Chapter 5, Figure 5.5). Apart from that, this study has highlighted a probable orientation of PfGAP45 that is similar to that in the previously mentioned TgGAP45 model. The ability of C-GAP45 to localise at the IMC and interact with other motor complex proteins while N-GAP45 is only able to localise at the parasite membrane, strengthens the application of this model to *Plasmodium*. As suggested by Frenal et al. (2010), GAP45 is localised between the IMC and parasite membrane by spanning the gap between the membranes through association of the N-terminus and C-terminus of the protein with the parasite membrane and IMC respectively (Figure 6.1B).

The internal tagging of PfGAP45 still preserves the integrity of the coiled-coil domain and the structured C-terminal region that is important for GAP45 function. As this study is based on episomal tranfection of GFP-tagged GAP45, restricted to just three constructs (FL-GAP45, C-GAP45 and N-GAP45), it is not possible to speculate on the role of this protein other than through its localisation and motor complex protein interaction. However, other transfection studies in *Toxoplasma* have elucidated the possible function of this protein in the parasite. By using an inducible knockout system, TgGAP45 was found to be an essential protein specifically in motility, invasion and egress (Frenal et al., 2010). Moreover, the internal GFP-tagged TgGAP45 protein (MycGFPGAP45) was able to complement the functional phenotype in GAP45 depleted parasites as observed by its localisation and ability to form plaques on human foreskin fibroblasts (HFFs) (Frenal et al., 2010). Other TgGAP45 variants such N-terminal GC-AA mutants and one without the coiled-coil domain were unable to complement the depletion of TgGAP45, in that the parasites were unable to invade or form plaques (Frenal et al., 2010). In addition, an electron microscopy analysis has observed that the parasites expressing both defective TgGAP45 variants (N-terminal GC-AA mutants and coiled-coil mutants)

exhibited a deformation and irregular spacing between IMC and plasma membrane. This also includes the extra IMC membranes formed at the posterior pole of the parasite after the invasion (Frenal et al., 2010). As shown by the phenotypic effect of this protein in the *T. gondii* study, this suggests the second function of GAP45 protein is in maintaining the cohesion of the pellicle during invasion. The N-terminal acylation together with the coiled-coil domain could have a role in maintaining a fixed distance and tight connection between the two membranes in the context of tensions upon invasion and gliding motility (Frenal et al., 2010).

6.3 Localisation and motor complex assembly of GAP45 is not affected by phosphorylation on S89 and S103 in parasites.

CDPK1 can phosphorylate GAP45 *in vitro* on residues including S89 and S103. Both of these residues were previously found to be phosphorylated in *P. falciparum* (Green et al., 2008; Treeck et al., 2011). As shown by additional analysis such as electrospray mass spectrometry, replacement of S89 and S103 residues by alanine decreased GAP45 phosphorylation. In order to study the effect of this phosphorylation on the parasite, constructs to express GAP45 modified at S89 and S103 were transfected into *P. falciparum* parasites. However, parasites expressing S89A, S103A or S89A/S103A GAP45 variants showed no difference in GAP45 localisation compared with WT GAP45 (Chapter 5, Figure 5.7). Substitution of each residue left intact the interaction of GAP45 protein with other motor complex proteins such as MTIP, GAP50 and MyoA (Chapter 5, Figure 5.10 and Appendix D).

The phosphorylation of GAP45 by CDPK1 might not be enough to induce any changes in GAP45 localisation or interaction with motor complex proteins. As reported earlier, GAP45 is a multisubstrate protein for another kinase called protein kinase B (PKB) (Thomas et al., 2012; Vaid et al., 2008). Phosphorylation of this protein by both CDPK1 and PKB may complete the post-translational modification process and activate GAP45 function. As well as S89 and S103, parasite-derived GAP45 was found to be phosphorylated at multiple sites: S107, S142, S149, S156, S158 and S198 (Treeck et al., 2011). It may be that these sites are phosphorylated by

kinases other than CDPK1. Substituting a combination of, or all of, these phosphorylated residues may contribute to a more obvious phenotypic effect in GAP45 function than studying two sites in isolation. There might be other CDPK1 sites left unidentified. In section 3.4 we showed that S31, S142, S149 and S156 might also be substrates for CDPK1 (Chapter 3, Figure 3.5-3.7, Table 3.1). Interestingly, S156 is located in the structured C-terminal region of GAP45 which might serve an important role in recruiting the motor complex to the IMC. It is possible that modification of residues here could perturb motor complex formation.

As phosphorylation of GAP45 increases from early schizont and peaks in the late schizont, it does not seem likely that the fully phosphorylated GAP45 protein has importance in invasion and post-invasion by the merozoite, where the assembly and disassembly of the motor complex components occur. This study has also found that the GFP-tagged GAP45 can form a tetrameric motor complex in free merozoite stages (Figure 6.2A). However, this study did not have any data from the GFP-tagged GAP45 variants (i. e. S89A and S103A) in the free merozoite stage. It has been shown in *T. gondii* that phosphorylation of TgGAP45 in the invasive tachyzoite caused dissociation of GAP50 from the trimeric motor complex GAP45-MTIP-MyoA (Gilk et al., 2009). We have also found some evidence that the native GAP45 protein is hyperphosphorylated in the merozoite, the *Plasmodium* invasive blood stage form where the GAP45 protein appears as a single band in SDS-PAGE with higher molecular weight as compared to late schizont GAP45 protein (Figure 6.2A and B). These data suggest that further phosphorylation of GAP45 occurs in the *Plasmodium* merozoite.

6.4 Future studies

The present study has addressed two aspects of GAP45 function in *P. falciparum*. The first aspect was to determine the localisation of GFP-tagged GAP45 throughout schizogony. The second aspect of this study was to assess the effect of GAP45 phosphorylation by CDPK1 in *P. falciparum*, specifically on IMC localisation and motor complex assembly. The study has shown that GFP-tagged GAP45 (FL-

GAP45) is able to localise at the IMC and interact with other motor complex components, suggesting it is functional. However, further phenotype identification is limited in this study which depends on episomally expressed GFP-GAP45. Even if there is a phenotypic effect, it may be masked by the function of native GAP45 that is still expressed from its endogenous locus. Any effects of GFP-tagged GAP45 on the parasite such as on growth and invasion rate could be determined by integrating the GFP-tagged GAP45 gene into the *P. falciparum* genome. In other words, the integration of GFP-tagged GAP45 must replace the endogenous GAP45 by performing a total gene replacement. An alternative approach would be to generate an inducible knockout of the endogenous GAP45 gene coupled with expression of GFP-GAP45 from a plasmid. Whilst successful in *T. gondii*, technology for the latter approach is currently unavailable for *Plasmodium*. Such experiments will further elucidate the functional phenotype effect of GFP-tagged GAP45 and its variants in *P. falciparum* schizogony.

It is important to study more the other CDPK1 phosphorylation sites such as S142, S149, S156 and S31. A series of replacements (S to A) at these residues might show an obvious effect and elucidate more information about GAP45 phosphorylation in the parasite. It might also be interesting if the effect of S89 and S103 substitution or others can be monitored throughout schizogony. For example, a time course pull down assay might be worth doing so that the effect of phosphorylation on motor complex assembly could be seen at specific stages or time points of schizogony. The effect of GAP45 phosphorylation might be stage specific. As phosphorylation on S89 and S103 in late schizonts (42-45 hours post invasion) does not seem to be important, a similar study on free merozoites might lead to interesting findings.

The localisation of GFP-tagged GAP45 to the IMC has been shown to occur in parallel with cytokinesis and segmentation in schizogony. A close examination of this process might shed light on and provide new knowledge of GAP45 localisation to the IMC. It is important to know which segment or region of GAP45 is responsible for the localisation to the IMC specifically and also for motor complex protein recruitment. Whilst this study has roughly proposed the possible orientation

and function of the N and C termini of GAP45, the function of specific GAP45 regions such as the coiled-coil domain and structured C-terminal domain are still unclear and worth investigating. By implementing an experiment using a series of truncated GAP45 proteins, with or without a certain region of C terminal or N terminal sequence may uncover the role of GAP45 in the *P. falciparum* life cycle in greater detail. For example, besides N-terminal dual acylation (myristoylation and palmitoylation), C terminal cysteine residue(s) of GAP45 may also be palmitoylated. Replacement of cysteine residues by alanine will give a clear picture of how this post-translational modification process can contribute to the localisation and motor complex recruitment to the IMC.

Although CDPK1 phosphorylates GAP45 *in vitro*, an *in vivo* role of this process remains unclear. However, with the discovery of specific CDPK1 inhibitors in the future, it may be possible to study the effect of GAP45 phosphorylation specifically by CDPK1 in the parasite. With CDPK1 fully or partially inhibited, any specific phenotype and biochemical effects of GFP-tagged GAP45 phosphorylation can be determined. However, it has been reported that CDPK1 can phosphorylate more than one substrate such as MTIP (Green et al., 2008). So, any effect of a CDPK1 inhibitor may not represent the inability of CDPK1 to phosphorylate only GAP45. A system or experiment that allows monitoring of the specific effect of CDPK1 inhibitor on GAP45 phosphorylation is needed although it might be impossible at this time.

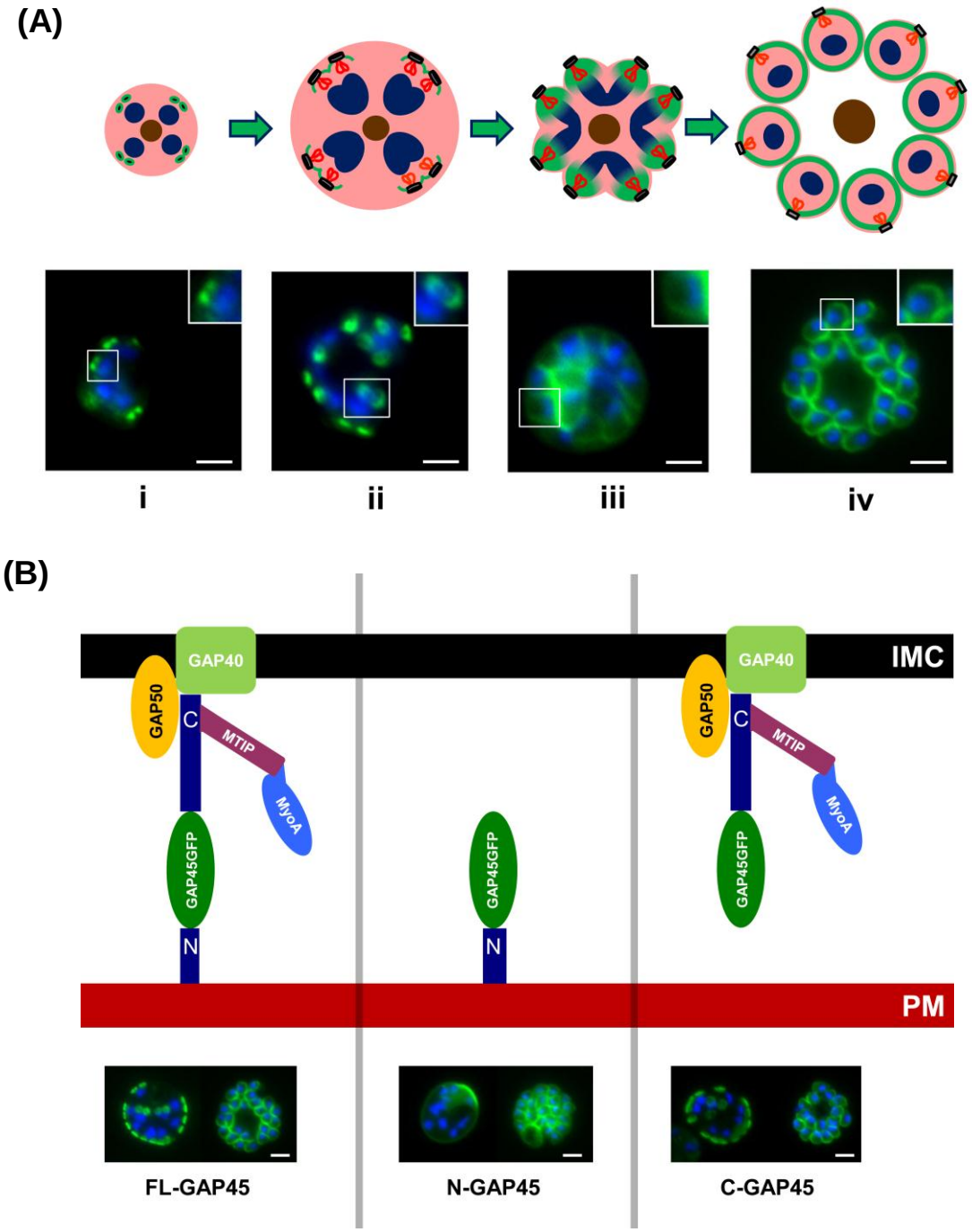

Figure 6.1: The development and location of the IMC interacting protein GFP-GAP45 during schizogony. (A) The punctate structure of GFP-GAP45 starts to develop as early as 33 hrs post invasion (i). The development from punctate to ring-like structure was seen as the nuclei replicate (around 4 to 8 nucleus) at ~36 hours post invasion (ii). GFP-GAP45 protein partially surrounds the replicated nucleus which is also representing the formation of the new merozoites pellicles (~39 hours

post invasion) (iii). At the end of schizogony, ~42 hours post invasion, GFP-GAP45 has completely encapsulated individual merozoites (iv). Enlargement of distinct structures is marked (white square) and shown in inset (~2X magnification). Labels, green: GFP tagged GAP45; red: rhoptries; blue: nucleus; pink: plasma membrane; brown: residual body/food vacuole. (B) The model for the *Plasmodium* GAP45 protein orientation as discussed in this study. The full length GFP-tagged GAP45 (FL-GAP45) is associated with the IMC and parasite plasma membrane (PM) via the C-terminus and N-terminus respectively. Without the large proportion of its C-terminus (20-204 amino acids) (N-GAP45), the protein mislocalises to the parasite PM. Without the N-terminal region (1-29 amino acids) (C-GAP45), the protein was associated with the IMC and still able to recruit the other motor complex protein such as MyoA and MTIP. Scale bar is 2 μm.

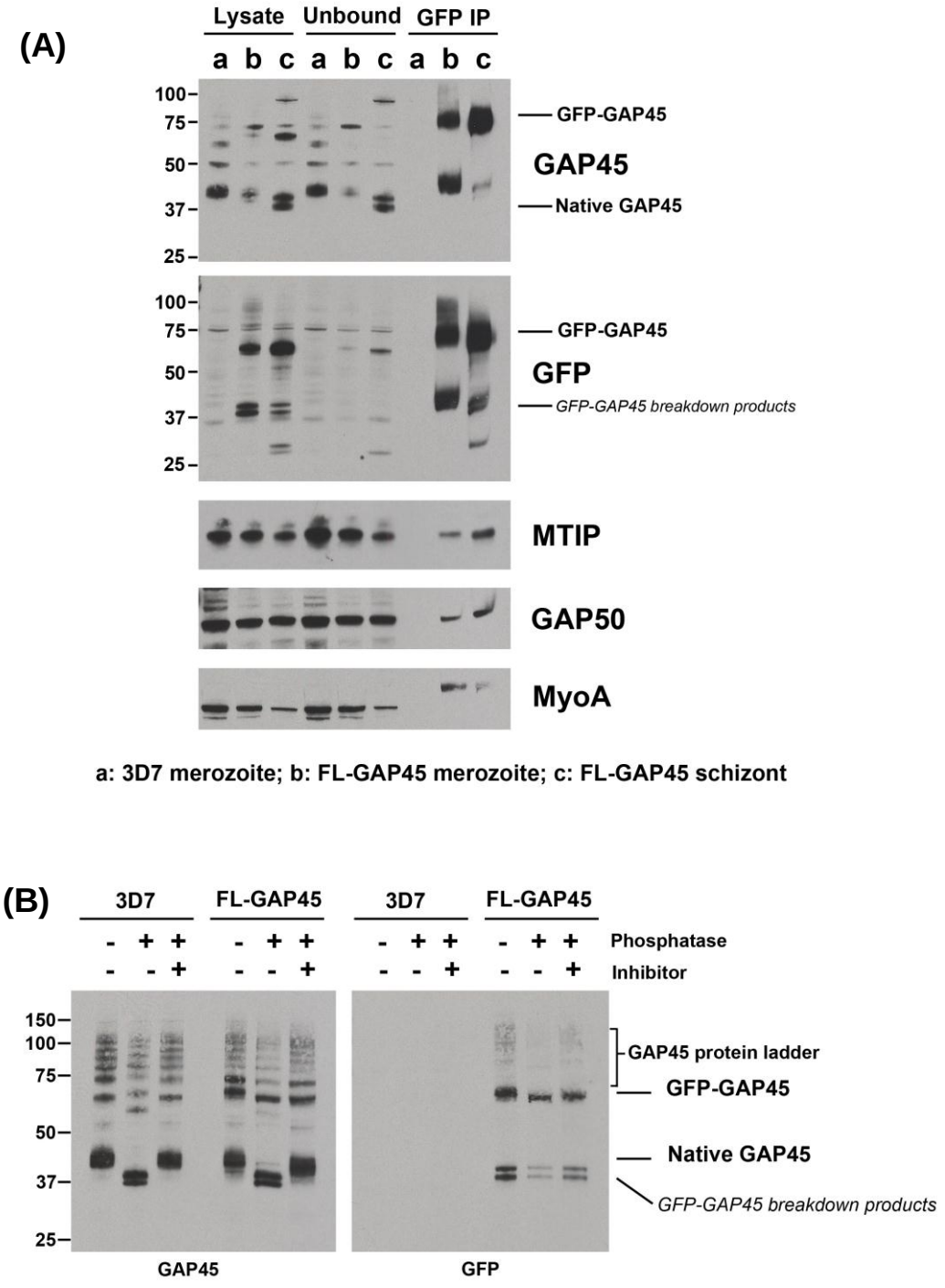

Figure 6.2: GAP45 was highly phosphorylated in merozoite blood stage. (A) *The immunoprecipation of GFP-tagged GAP45 in merozoites***.** The purified schizont was left to rupture prior to merozoite isolation. The merozoite fraction was extracted in 1% NP40 and subjected to co-immunoprecipitation by GFP-Trap®. The GFP-tagged GAP45 (FL-GAP45) (GFP IP) appears to interact with other motor complex protein such as MyoA, MTIP and GAP50 in both schizont (GFP IP, lane C) and free

merozoites stage (GFP IP, lane b). The native GAP45 protein band expressed in GFP-tagged GAP45 transfected parasite (lysate, lane b) appears as a single smudge and higher in molecular weight (similar to native GAP45 in 3D7 untransfected parasite, lysate lane a) as compared to its schizont stage which exists as a doublet that corresponded to unphosphorylated and phosphorylated protein bands (lysate, lane c). However, the GFP-tagged GAP45 (FL-GAP45) protein band doesn't show any difference in molecular weight between schizont and free merozoite parasites. **(B)** *The effect of phosphatase treatment on GAP45 protein in free merozoites*. The purified merozoites were extracted and treated with alkaline phosphatase. Both native GAP45 expressed in untransfected parasites and GFP-tagged GAP45 (FL-GAP45) transfected parasites have decreased molecular weight upon phosphatase treatment. This effect can be prevented by including a phosphatase inhibitor. The FL-GAP45 protein band was also decreased in its molecular weight after being treated with phosphatase. In contrast, the decrease in molecular weight of this protein did not happen upon phosphatase treatment with the addition of phosphatase inhibitor. These results suggest the GAP45 protein is highly phosphorylated in merozoite stage parasites. In the protein extract from free merozoites, the GAP45 proteins were also detected at higher molecular weight and appeared as a protein ladder between ~60 kDa to ~100 kDa. The GAP45 protein ladder was detergent resistant and could not be dissociated by urea, a powerful protein denaturant (unpublished data). It is possible that some of this GAP45 ladder is hyperphosphorylated as it was shown to be affected by phosphatase treatment (this figure). Another possibility is that the GAP45 protein may undergo ubiquitination allowing interaction with a ubiquitin complex prior to digestion by proteasomes. GAP45 protein ladders were detected by a ubiquitin-specific antibody (unpublished data) in western blotting analysis of the GAP45 immunoprecipitation product. This process possibly occurs in free merozoites where disassembly of the motor complex proteins might become active. However, the GAP45 protein ladder was not obviously detected by the GFP antibody binding to GFP-tagged GAP45. It could be that the hyperphosphorylated or ubiquitinated GFP-tagged GAP45 might produce higher molecular mass protein ladder products that could not be resolved by 10% SDS-PAGE.

References

Agop-Nersesian, C., Egarter, S., Langsley, G., Foth, B.J., Ferguson, D.J., Meissner, M., 2010. Biogenesis of the inner membrane complex is dependent on vesicular transport by the alveolate specific GTPase Rab11B. PLoS Pathog 6, e1001029.

Agop-Nersesian, C., Naissant, B., Ben Rached, F., Rauch, M., Kretzschmar, A., Thiberge, S., Menard, R., Ferguson, D.J., Meissner, M., Langsley, G., 2009. Rab11A-controlled assembly of the inner membrane complex is required for completion of apicomplexan cytokinesis. PLoS Pathog 5, e1000270.

Aikawa, M., Huff, C.G., Spinz, H., 1966. Comparative feeding mechanisms of avian and primate malarial parasites. Mil Med 131, Suppl:969-983.

Aikawa, M., Miller, L.H., Johnson, J., Rabbege, J., 1978. Erythrocyte entry by malarial parasites. A moving junction between erythrocyte and parasite. J Cell Biol 77, 72-82.

Aikawa, M., Uni, Y., Andrutis, A.T., Howard, R.J., 1986. Membrane-associated electron-dense material of the asexual stages of Plasmodium falciparum: evidence for movement from the intracellular parasite to the erythrocyte membrane. Am J Trop Med Hyg 35, 30-36.

Amino, R., Giovannini, D., Thiberge, S., Gueirard, P., Boisson, B., Dubremetz, J.F., Prevost, M.C., Ishino, T., Yuda, M., Menard, R., 2008. Host cell traversal is important for progression of the malaria parasite through the dermis to the liver. Cell host & microbe 3, 88-96.

Anderson-White, B.R., Ivey, F.D., Cheng, K., Szatanek, T., Lorestani, A., Beckers, C.J., Ferguson, D.J., Sahoo, N., Gubbels, M.J., 2011. A family of

intermediate filament-like proteins is sequentially assembled into the cytoskeleton of Toxoplasma gondii. Cellular microbiology 13, 18-31.

Angrisano, F., Riglar, D.T., Sturm, A., Volz, J.C., Delves, M.J., Zuccala, E.S., Turnbull, L., Dekiwadia, C., Olshina, M.A., Marapana, D.S., Wong, W., Mollard, V., Bradin, C.H., Tonkin, C.J., Gunning, P.W., Ralph, S.A., Whitchurch, C.B., Sinden, R.E., Cowman, A.F., McFadden, G.I., Baum, J., 2012. Spatial localisation of actin filaments across developmental stages of the malaria parasite. PloS one 7, e32188.

Antinori, S., Galimberti, L., Milazzo, L., Corbellino, M., 2012. Biology of human malaria plasmodia including Plasmodium knowlesi. Mediterr J Hematol Infect Dis 4, e2012013.

Atkinson, C.T., Aikawa, M., 1990. Ultrastructure of malaria-infected erythrocytes. Blood Cells 16, 351-368.

Avruch, J., Khokhlatchev, A., Kyriakis, J.M., Luo, Z., Tzivion, G., Vavvas, D., Zhang, X.F., 2001. Ras activation of the Raf kinase: tyrosine kinase recruitment of the MAP kinase cascade. Recent Prog Horm Res 56, 127-155.

Baer, K., Klotz, C., Kappe, S.H., Schnieder, T., Frevert, U., 2007. Release of hepatic Plasmodium yoelii merozoites into the pulmonary microvasculature. PLoS pathogens 3, e171.

Baker, R.P., Wijetilaka, R., Urban, S., 2006. Two Plasmodium rhomboid proteases preferentially cleave different adhesins implicated in all invasive stages of malaria. PLoS pathogens 2, e113.

Bannister, L., Mitchell, G., 2003. The ins, outs and roundabouts of malaria. Trends in parasitology 19, 209-213.

Bannister, L.H., Hopkins, J.M., Dluzewski, A.R., Margos, G., Williams, I.T., Blackman, M.J., Kocken, C.H., Thomas, A.W., Mitchell, G.H., 2003. Plasmodium falciparum apical membrane antigen 1 (PfAMA-1) is translocated within micronemes along subpellicular microtubules during merozoite development. J Cell Sci 116, 3825-3834.

Bannister, L.H., Hopkins, J.M., Fowler, R.E., Krishna, S., Mitchell, G.H., 2000a. A brief illustrated guide to the ultrastructure of Plasmodium falciparum asexual blood stages. Parasitol Today 16, 427-433.

Bannister, L.H., Hopkins, J.M., Fowler, R.E., Krishna, S., Mitchell, G.H., 2000b. Ultrastructure of rhoptry development in Plasmodium falciparum erythrocytic schizonts. Parasitology 121 (Pt 3), 273-287.

Baum, J., Chen, L., Healer, J., Lopaticki, S., Boyle, M., Triglia, T., Ehlgen, F., Ralph, S.A., Beeson, J.G., Cowman, A.F., 2009. Reticulocyte-binding protein homologue 5 - an essential adhesin involved in invasion of human erythrocytes by Plasmodium falciparum. Int J Parasitol 39, 371-380.

Baum, J., Gilberger, T.W., Frischknecht, F., Meissner, M., 2008a. Host-cell invasion by malaria parasites: insights from Plasmodium and Toxoplasma. Trends Parasitol 24, 557-563.

Baum, J., Maier, A.G., Good, R.T., Simpson, K.M., Cowman, A.F., 2005. Invasion by P. falciparum merozoites suggests a hierarchy of molecular interactions. PLoS Pathog 1, e37.

Baum, J., Papenfuss, A.T., Baum, B., Speed, T.P., Cowman, A.F., 2006a. Regulation of apicomplexan actin-based motility. Nat Rev Microbiol 4, 621-628.

Baum, J., Richard, D., Healer, J., Rug, M., Krnajski, Z., Gilberger, T.W., Green, J.L., Holder, A.A., Cowman, A.F., 2006b. A conserved molecular motor drives

cell invasion and gliding motility across malaria life cycle stages and other apicomplexan parasites. J Biol Chem 281, 5197-5208.

Baum, J., Tonkin, C.J., Paul, A.S., Rug, M., Smith, B.J., Gould, S.B., Richard, D., Pollard, T.D., Cowman, A.F., 2008b. A malaria parasite formin regulates actin polymerization and localizes to the parasite-erythrocyte moving junction during invasion. Cell Host Microbe 3, 188-198.

Beck, J.R., Rodriguez-Fernandez, I.A., Cruz de Leon, J., Huynh, M.H., Carruthers, V.B., Morrissette, N.S., Bradley, P.J., 2010. A novel family of Toxoplasma IMC proteins displays a hierarchical organization and functions in coordinating parasite division. PLoS Pathog 6, e1001094.

Bergman, L.W., Kaiser, K., Fujioka, H., Coppens, I., Daly, T.M., Fox, S., Matuschewski, K., Nussenzweig, V., Kappe, S.H., 2003. Myosin A tail domain interacting protein (MTIP) localizes to the inner membrane complex of Plasmodium sporozoites. J Cell Sci 116, 39-49.

Billker, O., Dechamps, S., Tewari, R., Wenig, G., Franke-Fayard, B., Brinkmann, V., 2004. Calcium and a calcium-dependent protein kinase regulate gamete formation and mosquito transmission in a malaria parasite. Cell 117, 503-514.

Billker, O., Lindo, V., Panico, M., Etienne, A.E., Paxton, T., Dell, A., Rogers, M., Sinden, R.E., Morris, H.R., 1998. Identification of xanthurenic acid as the putative inducer of malaria development in the mosquito. Nature 392, 289-292.

Billker, O., Lourido, S., Sibley, L.D., 2009. Calcium-dependent signaling and kinases in apicomplexan parasites. Cell Host Microbe 5, 612-622.

Billker, O., Shaw, M.K., Margos, G., Sinden, R.E., 1997. The roles of temperature, pH and mosquito factors as triggers of male and female gametogenesis of Plasmodium berghei in vitro. Parasitology 115 (Pt 1), 1-7.

Black, C.G., Wang, L., Wu, T., Coppel, R.L., 2003. Apical location of a novel EGF-like domain-containing protein of Plasmodium falciparum. Molecular and biochemical parasitology 127, 59-68.

Black, C.G., Wu, T., Wang, L., Hibbs, A.R., Coppel, R.L., 2001. Merozoite surface protein 8 of Plasmodium falciparum contains two epidermal growth factor-like domains. Molecular and biochemical parasitology 114, 217-226.

Blackman, M.J., Dennis, E.D., Hirst, E.M., Kocken, C.H., Scott-Finnigan, T.J., Thomas, A.W., 1996. Plasmodium knowlesi: secondary processing of the malaria merozoite surface protein-1. Exp Parasitol 83, 229-239.

Blackman, M.J., Ling, I.T., Nicholls, S.C., Holder, A.A., 1991. Proteolytic processing of the Plasmodium falciparum merozoite surface protein-1 produces a membrane-bound fragment containing two epidermal growth factor-like domains. Mol Biochem Parasitol 49, 29-33.

Bosch, J., Buscaglia, C.A., Krumm, B., Ingason, B.P., Lucas, R., Roach, C., Cardozo, T., Nussenzweig, V., Hol, W.G., 2007a. Aldolase provides an unusual binding site for thrombospondin-related anonymous protein in the invasion machinery of the malaria parasite. Proc Natl Acad Sci U S A 104, 7015-7020.

Bosch, J., Turley, S., Daly, T.M., Bogh, S.M., Villasmil, M.L., Roach, C., Zhou, N., Morrisey, J.M., Vaidya, A.B., Bergman, L.W., Hol, W.G., 2006. Structure of the MTIP-MyoA complex, a key component of the malaria parasite invasion motor. Proc Natl Acad Sci U S A 103, 4852-4857.

Bosch, J., Turley, S., Roach, C.M., Daly, T.M., Bergman, L.W., Hol, W.G., 2007b. The closed MTIP-myosin A-tail complex from the malaria parasite invasion machinery. J Mol Biol 372, 77-88.

Bozdech, Z., Llinas, M., Pulliam, B.L., Wong, E.D., Zhu, J., DeRisi, J.L., 2003. The transcriptome of the intraerythrocytic developmental cycle of Plasmodium falciparum. PLoS Biol 1, E5.

Bradley, P.J., Ward, C., Cheng, S.J., Alexander, D.L., Coller, S., Coombs, G.H., Dunn, J.D., Ferguson, D.J., Sanderson, S.J., Wastling, J.M., Boothroyd, J.C., 2005. Proteomic analysis of rhoptry organelles reveals many novel constituents for host-parasite interactions in Toxoplasma gondii. The Journal of biological chemistry 280, 34245-34258.

Brossier, F., Jewett, T.J., Sibley, L.D., Urban, S., 2005. A spatially localized rhomboid protease cleaves cell surface adhesins essential for invasion by Toxoplasma. Proceedings of the National Academy of Sciences of the United States of America 102, 4146-4151.

Bullen, H.E., Tonkin, C.J., O'Donnell, R.A., Tham, W.H., Papenfuss, A.T., Gould, S., Cowman, A.F., Crabb, B.S., Gilson, P.R., 2009. A novel family of Apicomplexan glideosome-associated proteins with an inner membrane-anchoring role. J Biol Chem 284, 25353-25363.

Burgess, D.R., 2005. Cytokinesis: new roles for myosin. Curr Biol 15, R310-311.

Buscaglia, C.A., Coppens, I., Hol, W.G., Nussenzweig, V., 2003. Sites of interaction between aldolase and thrombospondin-related anonymous protein in plasmodium. Molecular biology of the cell 14, 4947-4957.

Capdeville, R., Buchdunger, E., Zimmermann, J., Matter, A., 2002. Glivec (STI571, imatinib), a rationally developed, targeted anticancer drug. Nat Rev Drug Discov 1, 493-502.

Carmichael, W.W., 1994. The toxins of cyanobacteria. Scientific American 270, 78-86.

Carter, R., Mendis, K.N., 2002. Evolutionary and historical aspects of the burden of malaria. Clinical microbiology reviews 15, 564-594.

Casals-Pascual, C., Kai, O., Cheung, J.O., Williams, S., Lowe, B., Nyanoti, M., Williams, T.N., Maitland, K., Molyneux, M., Newton, C.R., Peshu, N., Watt, S.M., Roberts, D.J., 2006. Suppression of erythropoiesis in malarial anemia is associated with hemozoin in vitro and in vivo. Blood 108, 2569-2577.

Chang, L., Chiang, S.H., Saltiel, A.R., 2004. Insulin signaling and the regulation of glucose transport. Mol Med 10, 65-71.

Chaparro-Olaya, J., Margos, G., Coles, D.J., Dluzewski, A.R., Mitchell, G.H., Wasserman, M.M., Pinder, J.C., 2005. Plasmodium falciparum myosins: transcription and translation during asexual parasite development. Cell Motil Cytoskeleton 60, 200-213.

Chow, C.M., Neto, H., Foucart, C., Moore, I., 2008. Rab-A2 and Rab-A3 GTPases define a trans-golgi endosomal membrane domain in Arabidopsis that contributes substantially to the cell plate. Plant Cell 20, 101-123.

Chung, D.W., Ponts, N., Cervantes, S., Le Roch, K.G., 2009. Post-translational modifications in Plasmodium: more than you think! Molecular and biochemical parasitology 168, 123-134.

Clark, I.A., Cowden, W.B., 2003. The pathophysiology of falciparum malaria. Pharmacol Ther 99, 221-260.

Cohen, P., 2001. The role of protein phosphorylation in human health and disease. The Sir Hans Krebs Medal Lecture. European journal of biochemistry / FEBS 268, 5001-5010.

Cohen, P., 2002. The origins of protein phosphorylation. Nat Cell Biol 4, E127-130.

Cohen, P., Holmes, C.F., Tsukitani, Y., 1990. Okadaic acid: a new probe for the study of cellular regulation. Trends in biochemical sciences 15, 98-102.

Cooke, B., Coppel, R., Wahlgren, M., 2000. Falciparum malaria: sticking up, standing out and out-standing. Parasitol Today 16, 416-420.

Coppi, A., Tewari, R., Bishop, J.R., Bennett, B.L., Lawrence, R., Esko, J.D., Billker, O., Sinnis, P., 2007. Heparan sulfate proteoglycans provide a signal to Plasmodium sporozoites to stop migrating and productively invade host cells. Cell Host Microbe 2, 316-327.

Cowman, A.F., Crabb, B.S., 2006. Invasion of red blood cells by malaria parasites. Cell 124, 755-766.

Cox-Singh, J., Davis, T.M., Lee, K.S., Shamsul, S.S., Matusop, A., Ratnam, S., Rahman, H.A., Conway, D.J., Singh, B., 2008. Plasmodium knowlesi malaria in humans is widely distributed and potentially life threatening. Clin Infect Dis 46, 165-171.

Cox, F.E., 2010. History of the discovery of the malaria parasites and their vectors. Parasit Vectors 3, 5.

Crabb, B.S., Cooke, B.M., Reeder, J.C., Waller, R.F., Caruana, S.R., Davern, K.M., Wickham, M.E., Brown, G.V., Coppel, R.L., Cowman, A.F., 1997. Targeted gene disruption shows that knobs enable malaria-infected red cells to cytoadhere under physiological shear stress. Cell 89, 287-296.

Crosnier, C., Bustamante, L.Y., Bartholdson, S.J., Bei, A.K., Theron, M., Uchikawa, M., Mboup, S., Ndir, O., Kwiatkowski, D.P., Duraisingh, M.T., Rayner, J.C., Wright, G.J., 2011. Basigin is a receptor essential for erythrocyte invasion by Plasmodium falciparum. Nature 480, 534-537.

D'Avino, P.P., Savoian, M.S., Capalbo, L., Glover, D.M., 2006. RacGAP50C is sufficient to signal cleavage furrow formation during cytokinesis. J Cell Sci 119, 4402-4408.

D'Avino, P.P., Savoian, M.S., Glover, D.M., 2005. Cleavage furrow formation and ingression during animal cytokinesis: a microtubule legacy. J Cell Sci 118, 1549-1558.

Daly, T.M., Long, C.A., 1993. A recombinant 15-kilodalton carboxyl-terminal fragment of Plasmodium yoelii yoelii 17XL merozoite surface protein 1 induces a protective immune response in mice. Infection and immunity 61, 2462-2467.

Dekker, E., Hellerstein, M.K., Romijn, J.A., Neese, R.A., Peshu, N., Endert, E., Marsh, K., Sauerwein, H.P., 1997. Glucose homeostasis in children with falciparum malaria: precursor supply limits gluconeogenesis and glucose production. The Journal of clinical endocrinology and metabolism 82, 2514-2521.

Delbac, F., Sanger, A., Neuhaus, E.M., Stratmann, R., Ajioka, J.W., Toursel, C., Herm-Gotz, A., Tomavo, S., Soldati, T., Soldati, D., 2001. Toxoplasma gondii myosins B/C: one gene, two tails, two localizations, and a role in parasite division. The Journal of cell biology 155, 613-623.

Delorme, V., Cayla, X., Faure, G., Garcia, A., Tardieux, I., 2003. Actin dynamics is controlled by a casein kinase II and phosphatase 2C interplay on Toxoplasma gondii Toxofilin. Molecular biology of the cell 14, 1900-1912.

Dixon, M.W., Thompson, J., Gardiner, D.L., Trenholme, K.R., 2008. Sex in Plasmodium: a sign of commitment. Trends in parasitology 24, 168-175.

Dluzewski, A.R., Ling, I.T., Hopkins, J.M., Grainger, M., Margos, G., Mitchell, G.H., Holder, A.A., Bannister, L.H., 2008. Formation of the food vacuole in

Plasmodium falciparum: a potential role for the 19 kDa fragment of merozoite surface protein 1 (MSP1(19)). PloS one 3, e3085.

Doerig, C., Billker, O., 2010. A parasite calcium switch and Achilles' heel revealed. Nat Struct Mol Biol 17, 541-543.

Doerig, C., Billker, O., Haystead, T., Sharma, P., Tobin, A.B., Waters, N.C., 2008. Protein kinases of malaria parasites: an update. Trends Parasitol 24, 570-577.

Dowse, T.J., Pascall, J.C., Brown, K.D., Soldati, D., 2005. Apicomplexan rhomboids have a potential role in microneme protein cleavage during host cell invasion. International journal for parasitology 35, 747-756.

Dunker, A.K., Lawson, J.D., Brown, C.J., Williams, R.M., Romero, P., Oh, J.S., Oldfield, C.J., Campen, A.M., Ratliff, C.M., Hipps, K.W., Ausio, J., Nissen, M.S., Reeves, R., Kang, C., Kissinger, C.R., Bailey, R.W., Griswold, M.D., Chiu, W., Garner, E.C., Obradovic, Z., 2001. Intrinsically disordered protein. J Mol Graph Model 19, 26-59.

Dutta, S., Haynes, J.D., Moch, J.K., Barbosa, A., Lanar, D.E., 2003. Invasion-inhibitory antibodies inhibit proteolytic processing of apical membrane antigen 1 of Plasmodium falciparum merozoites. Proc Natl Acad Sci U S A 100, 12295-12300.

Dvorak, J.A., Miller, L.H., Whitehouse, W.C., Shiroishi, T., 1975. Invasion of erythrocytes by malaria merozoites. Science 187, 748-750.

Dvorin, J.D., Martyn, D.C., Patel, S.D., Grimley, J.S., Collins, C.R., Hopp, C.S., Bright, A.T., Westenberger, S., Winzeler, E., Blackman, M.J., Baker, D.A., Wandless, T.J., Duraisingh, M.T., 2010. A plant-like kinase in Plasmodium falciparum regulates parasite egress from erythrocytes. Science 328, 910-912.

Egan, T.J., 2008. Haemozoin formation. Molecular and biochemical parasitology 157, 127-136.

Egan, T.J., Combrinck, J.M., Egan, J., Hearne, G.R., Marques, H.M., Ntenteni, S., Sewell, B.T., Smith, P.J., Taylor, D., van Schalkwyk, D.A., Walden, J.C., 2002. Fate of haem iron in the malaria parasite Plasmodium falciparum. The Biochemical journal 365, 343-347.

Faderl, S., Talpaz, M., Estrov, Z., O'Brien, S., Kurzrock, R., Kantarjian, H.M., 1999. The biology of chronic myeloid leukemia. N Engl J Med 341, 164-172.

Falae, A., Combe, A., Amaladoss, A., Carvalho, T., Menard, R., Bhanot, P., 2010. Role of Plasmodium berghei cGMP-dependent protein kinase in late liver stage development. The Journal of biological chemistry 285, 3282-3288.

Farrow, R.E., Green, J., Katsimitsoulia, Z., Taylor, W.R., Holder, A.A., Molloy, J.E., 2011. The mechanism of erythrocyte invasion by the malarial parasite, Plasmodium falciparum. Semin Cell Dev Biol 22, 953-960.

Feng, Z.P., Zhang, X., Han, P., Arora, N., Anders, R.F., Norton, R.S., 2006. Abundance of intrinsically unstructured proteins in P. falciparum and other apicomplexan parasite proteomes. Mol Biochem Parasitol 150, 256-267.

Fidock, D.A., Wellems, T.E., 1997. Transformation with human dihydrofolate reductase renders malaria parasites insensitive to WR99210 but does not affect the intrinsic activity of proguanil. Proc Natl Acad Sci U S A 94, 10931-10936.

Field, C., Li, R., Oegema, K., 1999. Cytokinesis in eukaryotes: a mechanistic comparison. Curr Opin Cell Biol 11, 68-80.

Fielding, A.B., Schonteich, E., Matheson, J., Wilson, G., Yu, X., Hickson, G.R., Srivastava, S., Baldwin, S.A., Prekeris, R., Gould, G.W., 2005. Rab11-FIP3

and FIP4 interact with Arf6 and the exocyst to control membrane traffic in cytokinesis. Embo J 24, 3389-3399.

Fischer, E.H., Krebs, E.G., 1955. Conversion of phosphorylase b to phosphorylase a in muscle extracts. The Journal of biological chemistry 216, 121-132.

Foth, B.J., Goedecke, M.C., Soldati, D., 2006. New insights into myosin evolution and classification. Proceedings of the National Academy of Sciences of the United States of America 103, 3681-3686.

Francis, S.E., Sullivan, D.J., Jr., Goldberg, D.E., 1997. Hemoglobin metabolism in the malaria parasite Plasmodium falciparum. Annu Rev Microbiol 51, 97-123.

Frenal, K., Polonais, V., Marq, J.B., Stratmann, R., Limenitakis, J., Soldati-Favre, D., 2010. Functional dissection of the apicomplexan glideosome molecular architecture. Cell Host Microbe 8, 343-357.

Frevert, U., 2004. Sneaking in through the back entrance: the biology of malaria liver stages. Trends in parasitology 20, 417-424.

Frevert, U., Engelmann, S., Zougbede, S., Stange, J., Ng, B., Matuschewski, K., Liebes, L., Yee, H., 2005. Intravital observation of Plasmodium berghei sporozoite infection of the liver. PLoS Biol 3, e192.

Frevert, U., Sinnis, P., Cerami, C., Shreffler, W., Takacs, B., Nussenzweig, V., 1993. Malaria circumsporozoite protein binds to heparan sulfate proteoglycans associated with the surface membrane of hepatocytes. J Exp Med 177, 1287-1298.

Garnham, P.C., Bird, R.G., Baker, J.R., 1962. Electron microscope studies of motile stages of malaria parasites. III. The ookinetes of Haemamoeba and Plasmodium. Trans R Soc Trop Med Hyg 56, 116-120.

Garnham, P.C., Bird, R.G., Baker, J.R., Desser, S.S., el-Nahal, H.M., 1969. Electron microscope studies on motile stages of malaria parasites. VI. The ookinete of Plasmodium berghei yoelii and its transformation into the early oocyst. Trans R Soc Trop Med Hyg 63, 187-194.

Garnham, P.C.C., 1966. Life Cycle and Morphology, in: Garnham, P.C.C. (Ed.), Malaria Parasites and Other Haemosporidia, 1 ed. Blackwell Scientific Publication, Oxford, pp. 17-59.

Gaskins, E., Gilk, S., DeVore, N., Mann, T., Ward, G., Beckers, C., 2004. Identification of the membrane receptor of a class XIV myosin in Toxoplasma gondii. J Cell Biol 165, 383-393.

Gaur, D., Chitnis, C.E., 2011. Molecular interactions and signaling mechanisms during erythrocyte invasion by malaria parasites. Curr Opin Microbiol 14, 422-428.

Gaur, D., Mayer, D.C., Miller, L.H., 2004. Parasite ligand-host receptor interactions during invasion of erythrocytes by Plasmodium merozoites. Int J Parasitol 34, 1413-1429.

Gerold, P., Schofield, L., Blackman, M.J., Holder, A.A., Schwarz, R.T., 1996. Structural analysis of the glycosyl-phosphatidylinositol membrane anchor of the merozoite surface proteins-1 and -2 of Plasmodium falciparum. Molecular and biochemical parasitology 75, 131-143.

Gilk, S.D., Gaskins, E., Ward, G.E., Beckers, C.J., 2009. GAP45 phosphorylation controls assembly of the Toxoplasma myosin XIV complex. Eukaryot Cell 8, 190-196.

Giribaldi, G., Ulliers, D., Schwarzer, E., Roberts, I., Piacibello, W., Arese, P., 2004. Hemozoin- and 4-hydroxynonenal-mediated inhibition of erythropoiesis.

Possible role in malarial dyserythropoiesis and anemia. Haematologica 89, 492-493.

Goel, V.K., Li, X., Chen, H., Liu, S.C., Chishti, A.H., Oh, S.S., 2003. Band 3 is a host receptor binding merozoite surface protein 1 during the Plasmodium falciparum invasion of erythrocytes. Proc Natl Acad Sci U S A 100, 5164-5169.

Goosney, D.L., DeVinney, R., Pfuetzner, R.A., Frey, E.A., Strynadka, N.C., Finlay, B.B., 2000. Enteropathogenic E. coli translocated intimin receptor, Tir, interacts directly with alpha-actinin. Curr Biol 10, 735-738.

Gordon, J.L., Sibley, L.D., 2005. Comparative genome analysis reveals a conserved family of actin-like proteins in apicomplexan parasites. BMC Genomics 6, 179.

Gould, S.B., Tham, W.H., Cowman, A.F., McFadden, G.I., Waller, R.F., 2008. Alveolins, a new family of cortical proteins that define the protist infrakingdom Alveolata. Mol Biol Evol 25, 1219-1230.

Green, J.L., Martin, S.R., Fielden, J., Ksagoni, A., Grainger, M., Yim Lim, B.Y., Molloy, J.E., Holder, A.A., 2006. The MTIP-myosin A complex in blood stage malaria parasites. J Mol Biol 355, 933-941.

Green, J.L., Rees-Channer, R.R., Howell, S.A., Martin, S.R., Knuepfer, E., Taylor, H.M., Grainger, M., Holder, A.A., 2008. The motor complex of Plasmodium falciparum: phosphorylation by a calcium-dependent protein kinase. J Biol Chem 283, 30980-30989.

Guan, K.L., Dixon, J.E., 1990. Protein tyrosine phosphatase activity of an essential virulence determinant in Yersinia. Science 249, 553-556.

Hanks, S.K., 2003. Genomic analysis of the eukaryotic protein kinase superfamily: a perspective. Genome Biol 4, 111.

Harper, J.F., Harmon, A., 2005. Plants, symbiosis and parasites: a calcium signalling connection. Nat Rev Mol Cell Biol 6, 555-566.

Harper, J.F., Sussman, M.R., Schaller, G.E., Putnam-Evans, C., Charbonneau, H., Harmon, A.C., 1991. A calcium-dependent protein kinase with a regulatory domain similar to calmodulin. Science 252, 951-954.

Harris, P.K., Yeoh, S., Dluzewski, A.R., O'Donnell, R.A., Withers-Martinez, C., Hackett, F., Bannister, L.H., Mitchell, G.H., Blackman, M.J., 2005. Molecular identification of a malaria merozoite surface sheddase. PLoS pathogens 1, 241-251.

Hastie, C.J., McLauchlan, H.J., Cohen, P., 2006. Assay of protein kinases using radiolabeled ATP: a protocol. Nat Protoc 1, 968-971.

Hayes, J.S., Mayer, S.E., 1981. Regulation of guinea pig heart phosphorylase kinase by cAMP, protein kinase, and calcium. Am J Physiol 240, E340-349.

Healer, J., Crawford, S., Ralph, S., McFadden, G., Cowman, A.F., 2002. Independent translocation of two micronemal proteins in developing Plasmodium falciparum merozoites. Infect Immun 70, 5751-5758.

Herm-Gotz, A., Agop-Nersesian, C., Munter, S., Grimley, J.S., Wandless, T.J., Frischknecht, F., Meissner, M., 2007. Rapid control of protein level in the apicomplexan Toxoplasma gondii. Nat Methods 4, 1003-1005.

Herm-Gotz, A., Weiss, S., Stratmann, R., Fujita-Becker, S., Ruff, C., Meyhofer, E., Soldati, T., Manstein, D.J., Geeves, M.A., Soldati, D., 2002. Toxoplasma gondii myosin A and its light chain: a fast, single-headed, plus-end-directed motor. Embo J 21, 2149-2158.

Hernandez Sebastia, C., Hardin, S.C., Clouse, S.D., Kieber, J.J., Huber, S.C., 2004. Identification of a new motif for CDPK phosphorylation in vitro that suggests ACC synthase may be a CDPK substrate. Arch Biochem Biophys 428, 81-91.

Hodder, A.N., Crewther, P.E., Matthew, M.L., Reid, G.E., Moritz, R.L., Simpson, R.J., Anders, R.F., 1996. The disulfide bond structure of Plasmodium apical membrane antigen-1. J Biol Chem 271, 29446-29452.

Holder, A.A., Lockyer, M.J., Odink, K.G., Sandhu, J.S., Riveros-Moreno, V., Nicholls, S.C., Hillman, Y., Davey, L.S., Tizard, M.L., Schwarz, R.T., et al., 1985. Primary structure of the precursor to the three major surface antigens of Plasmodium falciparum merozoites. Nature 317, 270-273.

Holder, A.A., Sandhu, J.S., Hillman, Y., Davey, L.S., Nicholls, S.C., Cooper, H., Lockyer, M.J., 1987. Processing of the precursor to the major merozoite surface antigens of Plasmodium falciparum. Parasitology 94 (Pt 2), 199-208.

Holder, A.A., Veigel, C., 2009. Formin' an invasion machine: actin polymerization in invading apicomplexans. Trends in parasitology 25, 1-3.

Howell, S.A., Withers-Martinez, C., Kocken, C.H., Thomas, A.W., Blackman, M.J., 2001. Proteolytic processing and primary structure of Plasmodium falciparum apical membrane antigen-1. J Biol Chem 276, 31311-31320.

Hu, G., Cabrera, A., Kono, M., Mok, S., Chaal, B.K., Haase, S., Engelberg, K., Cheemadan, S., Spielmann, T., Preiser, P.R., Gilberger, T.W., Bozdech, Z., 2010. Transcriptional profiling of growth perturbations of the human malaria parasite Plasmodium falciparum. Nat Biotechnol 28, 91-98.

Hu, K., 2008. Organizational changes of the daughter basal complex during the parasite replication of Toxoplasma gondii. PLoS pathogens 4, e10.

Iakoucheva, L.M., Radivojac, P., Brown, C.J., O'Connor, T.R., Sikes, J.G., Obradovic, Z., Dunker, A.K., 2004. The importance of intrinsic disorder for protein phosphorylation. Nucleic Acids Res 32, 1037-1049.

Ishino, T., Chinzei, Y., Yuda, M., 2005. A Plasmodium sporozoite protein with a membrane attack complex domain is required for breaching the liver sinusoidal cell layer prior to hepatocyte infection. Cellular microbiology 7, 199-208.

Ishino, T., Orito, Y., Chinzei, Y., Yuda, M., 2006. A calcium-dependent protein kinase regulates Plasmodium ookinete access to the midgut epithelial cell. Molecular microbiology 59, 1175-1184.

Ishino, T., Yano, K., Chinzei, Y., Yuda, M., 2004. Cell-passage activity is required for the malarial parasite to cross the liver sinusoidal cell layer. PLoS Biol 2, E4.

Jewett, T.J., Sibley, L.D., 2003. Aldolase forms a bridge between cell surface adhesins and the actin cytoskeleton in apicomplexan parasites. Mol Cell 11, 885-894.

Johnson, L.N., Lewis, R.J., 2001. Structural basis for control by phosphorylation. Chem Rev 101, 2209-2242.

Johnson, T.M., Rajfur, Z., Jacobson, K., Beckers, C.J., 2007. Immobilization of the type XIV myosin complex in Toxoplasma gondii. Mol Biol Cell 18, 3039-3046.

Jones, M.L., Cottingham, C., Rayner, J.C., 2009. Effects of calcium signaling on Plasmodium falciparum erythrocyte invasion and post-translational modification of gliding-associated protein 45 (PfGAP45). Mol Biochem Parasitol 168, 55-62.

Jones, M.L., Kitson, E.L., Rayner, J.C., 2006. Plasmodium falciparum erythrocyte invasion: a conserved myosin associated complex. Mol Biochem Parasitol 147, 74-84.

Jongwutiwes, S., Buppan, P., Kosuvin, R., Seethamchai, S., Pattanawong, U., Sirichaisinthop, J., Putaporntip, C., 2011. Plasmodium knowlesi Malaria in humans and macaques, Thailand. Emerg Infect Dis 17, 1799-1806.

Jongwutiwes, S., Putaporntip, C., Iwasaki, T., Sata, T., Kanbara, H., 2004. Naturally acquired Plasmodium knowlesi malaria in human, Thailand. Emerg Infect Dis 10, 2211-2213.

Kappe, S., Bruderer, T., Gantt, S., Fujioka, H., Nussenzweig, V., Menard, R., 1999. Conservation of a gliding motility and cell invasion machinery in Apicomplexan parasites. The Journal of cell biology 147, 937-944.

Kariuki, M.M., Li, X., Yamodo, I., Chishti, A.H., Oh, S.S., 2005. Two Plasmodium falciparum merozoite proteins binding to erythrocyte band 3 form a direct complex. Biochem Biophys Res Commun 338, 1690-1695.

Kato, K., Sudo, A., Kobayashi, K., Tohya, Y., Akashi, H., 2008a. Characterization of Plasmodium falciparum protein kinase 2. Mol Biochem Parasitol 162, 87-95.

Kato, N., Sakata, T., Breton, G., Le Roch, K.G., Nagle, A., Andersen, C., Bursulaya, B., Henson, K., Johnson, J., Kumar, K.A., Marr, F., Mason, D., McNamara, C., Plouffe, D., Ramachandran, V., Spooner, M., Tuntland, T., Zhou, Y., Peters, E.C., Chatterjee, A., Schultz, P.G., Ward, G.E., Gray, N., Harper, J., Winzeler, E.A., 2008b. Gene expression signatures and small-molecule compounds link a protein kinase to Plasmodium falciparum motility. Nat Chem Biol 4, 347-356.

Keeley, A., Soldati, D., 2004. The glideosome: a molecular machine powering motility and host-cell invasion by Apicomplexa. Trends Cell Biol 14, 528-532.

Khater, E.I., Sinden, R.E., Dessens, J.T., 2004. A malaria membrane skeletal protein is essential for normal morphogenesis, motility, and infectivity of sporozoites. The Journal of cell biology 167, 425-432.

Kieschnick, H., Wakefield, T., Narducci, C.A., Beckers, C., 2001. Toxoplasma gondii attachment to host cells is regulated by a calmodulin-like domain protein kinase. J Biol Chem 276, 12369-12377.

Kirk, K., 2001. Membrane transport in the malaria-infected erythrocyte. Physiol Rev 81, 495-537.

Knudsen, E.S., Knudsen, K.E., 2006. Retinoblastoma tumor suppressor: where cancer meets the cell cycle. Exp Biol Med (Maywood) 231, 1271-1281.

Kono, M., Herrmann, S., Loughran, N.B., Cabrera, A., Engelberg, K., Lehmann, C., Sinha, D., Prinz, B., Ruch, U., Heussler, V., Spielmann, T., Parkinson, J., Gilberger, T.W., 2012. Evolution and Architecture of the Inner Membrane Complex in Asexual and Sexual Stages of the Malaria Parasite. Mol Biol Evol, (in press).

Kooij, T.W., Matuschewski, K., 2007. Triggers and tricks of Plasmodium sexual development. Current opinion in microbiology 10, 547-553.

Kostich, M., English, J., Madison, V., Gheyas, F., Wang, L., Qiu, P., Greene, J., Laz, T.M., 2002. Human members of the eukaryotic protein kinase family. Genome Biol 3, RESEARCH0043.

Koussis, K., Withers-Martinez, C., Yeoh, S., Child, M., Hackett, F., Knuepfer, E., Juliano, L., Woehlbier, U., Bujard, H., Blackman, M.J., 2009. A

multifunctional serine protease primes the malaria parasite for red blood cell invasion. Embo J 28, 725-735.

Krebs, E.G., Fischer, E.H., 1955. Phosphorylase activity of skeletal muscle extracts. The Journal of biological chemistry 216, 113-120.

Kugelstadt, D., Winter, D., Pluckhahn, K., Lehmann, W.D., Kappes, B., 2007. Raf kinase inhibitor protein affects activity of Plasmodium falciparum calcium-dependent protein kinase 1. Mol Biochem Parasitol 151, 111-117.

Kumar, S., Yadava, A., Keister, D.B., Tian, J.H., Ohl, M., Perdue-Greenfield, K.A., Miller, L.H., Kaslow, D.C., 1995. Immunogenicity and in vivo efficacy of recombinant Plasmodium falciparum merozoite surface protein-1 in Aotus monkeys. Mol Med 1, 325-332.

Lambros, C., Vanderberg, J.P., 1979. Synchronization of Plasmodium falciparum erythrocytic stages in culture. J Parasitol 65, 418-420.

Lamikanra, A.A., Theron, M., Kooij, T.W., Roberts, D.J., 2009. Hemozoin (malarial pigment) directly promotes apoptosis of erythroid precursors. PloS one 4, e8446.

Langreth, S.G., Jensen, J.B., Reese, R.T., Trager, W., 1978. Fine structure of human malaria in vitro. J Protozool 25, 443-452.

Langsley, G., Chakrabarti, D., 1996. Plasmodium falciparum: the small GTPase rab11. Exp Parasitol 83, 250-251.

Lazarus, M.D., Schneider, T.G., Taraschi, T.F., 2008. A new model for hemoglobin ingestion and transport by the human malaria parasite Plasmodium falciparum. J Cell Sci 121, 1937-1949.

Leykauf, K., Treeck, M., Gilson, P.R., Nebl, T., Braulke, T., Cowman, A.F., Gilberger, T.W., Crabb, B.S., 2010. Protein kinase a dependent phosphorylation of apical membrane antigen 1 plays an important role in erythrocyte invasion by the malaria parasite. PLoS Pathog 6, e1000941.

Li, X., Chen, H., Oo, T.H., Daly, T.M., Bergman, L.W., Liu, S.C., Chishti, A.H., Oh, S.S., 2004. A co-ligand complex anchors Plasmodium falciparum merozoites to the erythrocyte invasion receptor band 3. J Biol Chem 279, 5765-5771.

Ling, I.T., Ogun, S.A., Holder, A.A., 1994. Immunization against malaria with a recombinant protein. Parasite Immunol 16, 63-67.

Lingelbach, K., Joiner, K.A., 1998. The parasitophorous vacuole membrane surrounding Plasmodium and Toxoplasma: an unusual compartment in infected cells. J Cell Sci 111 (Pt 11), 1467-1475.

Liu, J., Farmer, J.D., Jr., Lane, W.S., Friedman, J., Weissman, I., Schreiber, S.L., 1991. Calcineurin is a common target of cyclophilin-cyclosporin A and FKBP-FK506 complexes. Cell 66, 807-815.

Lobo, C.A., Rodriguez, M., Reid, M., Lustigman, S., 2003. Glycophorin C is the receptor for the Plasmodium falciparum erythrocyte binding ligand PfEBP-2 (baebl). Blood 101, 4628-4631.

Loog, M., Toomik, R., Sak, K., Muszynska, G., Jarv, J., Ek, P., 2000. Peptide phosphorylation by calcium-dependent protein kinase from maize seedlings. Eur J Biochem 267, 337-343.

Lourido, S., Shuman, J., Zhang, C., Shokat, K.M., Hui, R., Sibley, L.D., 2010. Calcium-dependent protein kinase 1 is an essential regulator of exocytosis in Toxoplasma. Nature 465, 359-362.

Luchavez, J., Espino, F., Curameng, P., Espina, R., Bell, D., Chiodini, P., Nolder, D., Sutherland, C., Lee, K.S., Singh, B., 2008. Human Infections with Plasmodium knowlesi, the Philippines. Emerg Infect Dis 14, 811-813.

MacKintosh, C., Beattie, K.A., Klumpp, S., Cohen, P., Codd, G.A., 1990. Cyanobacterial microcystin-LR is a potent and specific inhibitor of protein phosphatases 1 and 2A from both mammals and higher plants. FEBS Lett 264, 187-192.

Maier, A.G., Duraisingh, M.T., Reeder, J.C., Patel, S.S., Kazura, J.W., Zimmerman, P.A., Cowman, A.F., 2003. Plasmodium falciparum erythrocyte invasion through glycophorin C and selection for Gerbich negativity in human populations. Nat Med 9, 87-92.

Mann, M., Wilm, M., 1995. Electrospray mass spectrometry for protein characterization. Trends Biochem Sci 20, 219-224.

Mann, T., Beckers, C., 2001. Characterization of the subpellicular network, a filamentous membrane skeletal component in the parasite Toxoplasma gondii. Molecular and biochemical parasitology 115, 257-268.

Manning, G., Whyte, D.B., Martinez, R., Hunter, T., Sudarsanam, S., 2002. The protein kinase complement of the human genome. Science 298, 1912-1934.

Marshall, V.M., Silva, A., Foley, M., Cranmer, S., Wang, L., McColl, D.J., Kemp, D.J., Coppel, R.L., 1997. A second merozoite surface protein (MSP-4) of Plasmodium falciparum that contains an epidermal growth factor-like domain. Infection and immunity 65, 4460-4467.

Marshall, V.M., Tieqiao, W., Coppel, R.L., 1998. Close linkage of three merozoite surface protein genes on chromosome 2 of Plasmodium falciparum. Molecular and biochemical parasitology 94, 13-25.

Martin, S.R., Schilstra, M.J., 2008. Circular dichroism and its application to the study of biomolecules. Methods Cell Biol 84, 263-293.

Matagne, A., Joris, B., Frere, J.M., 1991. Anomalous behaviour of a protein during SDS/PAGE corrected by chemical modification of carboxylic groups. Biochem J 280 (Pt 2), 553-556.

Matsumura, F., 2005. Regulation of myosin II during cytokinesis in higher eukaryotes. Trends in cell biology 15, 371-377.

Matuschewski, K., Mota, M.M., Pinder, J.C., Nussenzweig, V., Kappe, S.H., 2001. Identification of the class XIV myosins Pb-MyoA and Py-MyoA and expression in Plasmodium sporozoites. Molecular and biochemical parasitology 112, 157-161.

Mayer, D.C., Cofie, J., Jiang, L., Hartl, D.L., Tracy, E., Kabat, J., Mendoza, L.H., Miller, L.H., 2009. Glycophorin B is the erythrocyte receptor of Plasmodium falciparum erythrocyte-binding ligand, EBL-1. Proceedings of the National Academy of Sciences of the United States of America 106, 5348-5352.

McCallum, L., Price, S., Planque, N., Perbal, B., Pierce, A., Whetton, A.D., Irvine, A.E., 2006. A novel mechanism for BCR-ABL action: stimulated secretion of CCN3 is involved in growth and differentiation regulation. Blood 108, 1716-1723.

McColl, D.J., Anders, R.F., 1997. Conservation of structural motifs and antigenic diversity in the Plasmodium falciparum merozoite surface protein-3 (MSP-3). Molecular and biochemical parasitology 90, 21-31.

McRobert, L., Taylor, C.J., Deng, W., Fivelman, Q.L., Cummings, R.M., Polley, S.D., Billker, O., Baker, D.A., 2008. Gametogenesis in malaria parasites is mediated by the cGMP-dependent protein kinase. PLoS Biol 6, e139.

Meggio, F., Donella Deana, A., Ruzzene, M., Brunati, A.M., Cesaro, L., Guerra, B., Meyer, T., Mett, H., Fabbro, D., Furet, P., et al., 1995. Different susceptibility of protein kinases to staurosporine inhibition. Kinetic studies and molecular bases for the resistance of protein kinase CK2. European journal of biochemistry / FEBS 234, 317-322.

Meissner, M., Schluter, D., Soldati, D., 2002. Role of Toxoplasma gondii myosin A in powering parasite gliding and host cell invasion. Science 298, 837-840.

Mitchell, G.H., Thomas, A.W., Margos, G., Dluzewski, A.R., Bannister, L.H., 2004. Apical membrane antigen 1, a major malaria vaccine candidate, mediates the close attachment of invasive merozoites to host red blood cells. Infect Immun 72, 154-158.

Moon, R.W., Taylor, C.J., Bex, C., Schepers, R., Goulding, D., Janse, C.J., Waters, A.P., Baker, D.A., Billker, O., 2009. A cyclic GMP signalling module that regulates gliding motility in a malaria parasite. PLoS Pathog 5, e1000599.

Morahan, B.J., Wang, L., Coppel, R.L., 2009. No TRAP, no invasion. Trends Parasitol 25, 77-84.

Moreno, S.N., Docampo, R., 2003. Calcium regulation in protozoan parasites. Current opinion in microbiology 6, 359-364.

Morrissette, N.S., Sibley, L.D., 2002. Cytoskeleton of apicomplexan parasites. Microbiol Mol Biol Rev 66, 21-38; table of contents.

Moskes, C., Burghaus, P.A., Wernli, B., Sauder, U., Durrenberger, M., Kappes, B., 2004. Export of Plasmodium falciparum calcium-dependent protein kinase 1 to the parasitophorous vacuole is dependent on three N-terminal membrane anchor motifs. Mol Microbiol 54, 676-691.

Murray, C.J., Rosenfeld, L.C., Lim, S.S., Andrews, K.G., Foreman, K.J., Haring, D., Fullman, N., Naghavi, M., Lozano, R., Lopez, A.D., 2012. Global malaria mortality between 1980 and 2010: a systematic analysis. Lancet 379, 413-431.

Narum, D.L., Thomas, A.W., 1994. Differential localization of full-length and processed forms of PF83/AMA-1 an apical membrane antigen of Plasmodium falciparum merozoites. Mol Biochem Parasitol 67, 59-68.

Nebl, T., Prieto, J.H., Kapp, E., Smith, B.J., Williams, M.J., Yates, J.R., 3rd, Cowman, A.F., Tonkin, C.J., 2011. Quantitative in vivo analyses reveal calcium-dependent phosphorylation sites and identifies a novel component of the Toxoplasma invasion motor complex. PLoS Pathog 7, e1002222.

Ng, O.T., Ooi, E.E., Lee, C.C., Lee, P.J., Ng, L.C., Pei, S.W., Tu, T.M., Loh, J.P., Leo, Y.S., 2008. Naturally acquired human Plasmodium knowlesi infection, Singapore. Emerg Infect Dis 14, 814-816.

Nishi, M., Hu, K., Murray, J.M., Roos, D.S., 2008. Organellar dynamics during the cell cycle of Toxoplasma gondii. J Cell Sci 121, 1559-1568.

Ono, T., Cabrita-Santos, L., Leitao, R., Bettiol, E., Purcell, L.A., Diaz-Pulido, O., Andrews, L.B., Tadakuma, T., Bhanot, P., Mota, M.M., Rodriguez, A., 2008. Adenylyl cyclase alpha and cAMP signaling mediate Plasmodium sporozoite apical regulated exocytosis and hepatocyte infection. PLoS pathogens 4, e1000008.

Opitz, C., Di Cristina, M., Reiss, M., Ruppert, T., Crisanti, A., Soldati, D., 2002. Intramembrane cleavage of microneme proteins at the surface of the apicomplexan parasite Toxoplasma gondii. Embo J 21, 1577-1585.

Pachebat, J.A., Ling, I.T., Grainger, M., Trucco, C., Howell, S., Fernandez-Reyes, D., Gunaratne, R., Holder, A.A., 2001. The 22 kDa component of the protein

complex on the surface of Plasmodium falciparum merozoites is derived from a larger precursor, merozoite surface protein 7. Mol Biochem Parasitol 117, 83-89.

Pagola, S., Stephens, P.W., Bohle, D.S., Kosar, A.D., Madsen, S.K., 2000. The structure of malaria pigment beta-haematin. Nature 404, 307-310.

Papakrivos, J., Newbold, C.I., Lingelbach, K., 2005. A potential novel mechanism for the insertion of a membrane protein revealed by a biochemical analysis of the Plasmodium falciparum cytoadherence molecule PfEMP-1. Molecular microbiology 55, 1272-1284.

Peifer, M., Polakis, P., 2000. Wnt signaling in oncogenesis and embryogenesis--a look outside the nucleus. Science 287, 1606-1609.

Phillips, R.S., 2001. Current status of malaria and potential for control. Clin Microbiol Rev 14, 208-226.

Phyo, A.P., Nkhoma, S., Stepniewska, K., Ashley, E.A., Nair, S., McGready, R., Ler Moo, C., Al-Saai, S., Dondorp, A.M., Lwin, K.M., Singhasivanon, P., Day, N.P., White, N.J., Anderson, T.J., Nosten, F., 2012. Emergence of artemisinin-resistant malaria on the western border of Thailand: a longitudinal study. Lancet, (in press).

Pinder, J., Fowler, R., Bannister, L., Dluzewski, A., Mitchell, G.H., 2000. Motile systems in malaria merozoites: how is the red blood cell invaded? Parasitol Today 16, 240-245.

Pinder, J.C., Fowler, R.E., Dluzewski, A.R., Bannister, L.H., Lavin, F.M., Mitchell, G.H., Wilson, R.J., Gratzer, W.B., 1998. Actomyosin motor in the merozoite of the malaria parasite, Plasmodium falciparum: implications for red cell invasion. J Cell Sci 111 (Pt 13), 1831-1839.

Preiser, P., Kaviratne, M., Khan, S., Bannister, L., Jarra, W., 2000. The apical organelles of malaria merozoites: host cell selection, invasion, host immunity and immune evasion. Microbes Infect 2, 1461-1477.

Quevillon, E., Spielmann, T., Brahimi, K., Chattopadhyay, D., Yeramian, E., Langsley, G., 2003. The Plasmodium falciparum family of Rab GTPases. Gene 306, 13-25.

Ranjan, R., Ahmed, A., Gourinath, S., Sharma, P., 2009. Dissection of mechanisms involved in the regulation of Plasmodium falciparum calcium-dependent protein kinase 4. J Biol Chem 284, 15267-15276.

Rees-Channer, R.R., Martin, S.R., Green, J.L., Bowyer, P.W., Grainger, M., Molloy, J.E., Holder, A.A., 2006. Dual acylation of the 45 kDa gliding-associated protein (GAP45) in Plasmodium falciparum merozoites. Mol Biochem Parasitol 149, 113-116.

Reis, R.S., Horn, F., 2010. Enteropathogenic Escherichia coli, Samonella, Shigella and Yersinia: cellular aspects of host-bacteria interactions in enteric diseases. Gut Pathog 2, 8.

Richard, D., MacRaild, C.A., Riglar, D.T., Chan, J.A., Foley, M., Baum, J., Ralph, S.A., Norton, R.S., Cowman, A.F., 2010. Interaction between Plasmodium falciparum apical membrane antigen 1 and the rhoptry neck protein complex defines a key step in the erythrocyte invasion process of malaria parasites. The Journal of biological chemistry 285, 14815-14822.

Riglar, D.T., Richard, D., Wilson, D.W., Boyle, M.J., Dekiwadia, C., Turnbull, L., Angrisano, F., Marapana, D.S., Rogers, K.L., Whitchurch, C.B., Beeson, J.G., Cowman, A.F., Ralph, S.A., Baum, J., 2011. Super-resolution dissection of coordinated events during malaria parasite invasion of the human erythrocyte. Cell Host Microbe 9, 9-20.

Sachs, J., Malaney, P., 2002. The economic and social burden of malaria. Nature 415, 680-685.

Sanders, P.R., Gilson, P.R., Cantin, G.T., Greenbaum, D.C., Nebl, T., Carucci, D.J., McConville, M.J., Schofield, L., Hodder, A.N., Yates, J.R., 3rd, Crabb, B.S., 2005. Distinct protein classes including novel merozoite surface antigens in Raft-like membranes of Plasmodium falciparum. J Biol Chem 280, 40169-40176.

Saraste, J., Goud, B., 2007. Functional symmetry of endomembranes. Molecular biology of the cell 18, 1430-1436.

Schmitz, S., Grainger, M., Howell, S., Calder, L.J., Gaeb, M., Pinder, J.C., Holder, A.A., Veigel, C., 2005. Malaria parasite actin filaments are very short. Journal of molecular biology 349, 113-125.

Seger, R., Krebs, E.G., 1995. The MAPK signaling cascade. Faseb J 9, 726-735.

Siden-Kiamos, I., Ecker, A., Nyback, S., Louis, C., Sinden, R.E., Billker, O., 2006a. Plasmodium berghei calcium-dependent protein kinase 3 is required for ookinete gliding motility and mosquito midgut invasion. Mol Microbiol 60, 1355-1363.

Siden-Kiamos, I., Ganter, M., Kunze, A., Hliscs, M., Steinbuchel, M., Mendoza, J., Sinden, R.E., Louis, C., Matuschewski, K., 2011. Stage-specific depletion of myosin A supports an essential role in motility of malarial ookinetes. Cellular microbiology 13, 1996-2006.

Siden-Kiamos, I., Pinder, J.C., Louis, C., 2006b. Involvement of actin and myosins in Plasmodium berghei ookinete motility. Mol Biochem Parasitol 150, 308-317.

Sim, B.K., Chitnis, C.E., Wasniowska, K., Hadley, T.J., Miller, L.H., 1994. Receptor and ligand domains for invasion of erythrocytes by Plasmodium falciparum. Science 264, 1941-1944.

Sinden, R.E., 1982. Gametocytogenesis of Plasmodium falciparum in vitro: an electron microscopic study. Parasitology 84, 1-11.

Sinden, R.E., Strong, K., 1978. An ultrastructural study of the sporogonic development of Plasmodium falciparum in Anopheles gambiae. Trans R Soc Trop Med Hyg 72, 477-491.

Singh, B., Daneshvar, C., 2010. Plasmodium knowlesi malaria in Malaysia. Med J Malaysia 65, 166-172.

Singh, S., Kennedy, M.C., Long, C.A., Saul, A.J., Miller, L.H., Stowers, A.W., 2003. Biochemical and immunological characterization of bacterially expressed and refolded Plasmodium falciparum 42-kilodalton C-terminal merozoite surface protein 1. Infection and immunity 71, 6766-6774.

Skorokhod, O.A., Caione, L., Marrocco, T., Migliardi, G., Barrera, V., Arese, P., Piacibello, W., Schwarzer, E., 2010. Inhibition of erythropoiesis in malaria anemia: role of hemozoin and hemozoin-generated 4-hydroxynonenal. Blood 116, 4328-4337.

Slomianny, C., 1990. Three-dimensional reconstruction of the feeding process of the malaria parasite. Blood Cells 16, 369-378.

Slomianny, C., Prensier, G., Charet, P., 1985. Ingestion of erythrocytic stroma by Plasmodium chabaudi trophozoites: ultrastructural study by serial sectioning and 3-dimensional reconstruction. Parasitology 90 (Pt 3), 579-588.

Solyakov, L., Halbert, J., Alam, M.M., Semblat, J.P., Dorin-Semblat, D., Reininger, L., Bottrill, A.R., Mistry, S., Abdi, A., Fennell, C., Holland, Z., Demarta, C.,

Bouza, Y., Sicard, A., Nivez, M.P., Eschenlauer, S., Lama, T., Thomas, D.C., Sharma, P., Agarwal, S., Kern, S., Pradel, G., Graciotti, M., Tobin, A.B., Doerig, C., 2011. Global kinomic and phospho-proteomic analyses of the human malaria parasite Plasmodium falciparum. Nat Commun 2, 565.

Sreerama, N., Woody, R.W., 2000. Estimation of protein secondary structure from circular dichroism spectra: comparison of CONTIN, SELCON, and CDSSTR methods with an expanded reference set. Anal Biochem 287, 252-260.

Srinivasan, P., Beatty, W.L., Diouf, A., Herrera, R., Ambroggio, X., Moch, J.K., Tyler, J.S., Narum, D.L., Pierce, S.K., Boothroyd, J.C., Haynes, J.D., Miller, L.H., 2011. Binding of Plasmodium merozoite proteins RON2 and AMA1 triggers commitment to invasion. Proc Natl Acad Sci U S A 108, 13275-13280.

Stahl, H.D., Bianco, A.E., Crewther, P.E., Anders, R.F., Kyne, A.P., Coppel, R.L., Mitchell, G.F., Kemp, D.J., Brown, G.V., 1986. Sorting large numbers of clones expressing Plasmodium falciparum antigens in Escherichia coli by differential antibody screening. Mol Biol Med 3, 351-368.

Straub, K.W., Cheng, S.J., Sohn, C.S., Bradley, P.J., 2009. Novel components of the Apicomplexan moving junction reveal conserved and coccidia-restricted elements. Cellular microbiology 11, 590-603.

Striepen, B., Jordan, C.N., Reiff, S., van Dooren, G.G., 2007. Building the perfect parasite: cell division in apicomplexa. PLoS pathogens 3, e78.

Stubbs, J., Simpson, K.M., Triglia, T., Plouffe, D., Tonkin, C.J., Duraisingh, M.T., Maier, A.G., Winzeler, E.A., Cowman, A.F., 2005. Molecular mechanism for switching of P. falciparum invasion pathways into human erythrocytes. Science 309, 1384-1387.

Sturm, A., Amino, R., van de Sand, C., Regen, T., Retzlaff, S., Rennenberg, A., Krueger, A., Pollok, J.M., Menard, R., Heussler, V.T., 2006. Manipulation of host hepatocytes by the malaria parasite for delivery into liver sinusoids. Science 313, 1287-1290.

Sugi, T., Kato, K., Kobayashi, K., Pandey, K., Takemae, H., Kurokawa, H., Tohya, Y., Akashi, H., 2009. Molecular analyses of Toxoplasma gondii calmodulin-like domain protein kinase isoform 3. Parasitol Int 58, 416-423.

Sultan, A.A., 1999. Molecular mechanisms of malaria sporozoite motility and invasion of host cells. Int Microbiol 2, 155-160.

Sultan, A.A., Thathy, V., Frevert, U., Robson, K.J., Crisanti, A., Nussenzweig, V., Nussenzweig, R.S., Menard, R., 1997. TRAP is necessary for gliding motility and infectivity of plasmodium sporozoites. Cell 90, 511-522.

Taira, M., Hashimoto, N., Shimada, F., Suzuki, Y., Kanatsuka, A., Nakamura, F., Ebina, Y., Tatibana, M., Makino, H., et al., 1989. Human diabetes associated with a deletion of the tyrosine kinase domain of the insulin receptor. Science 245, 63-66.

Talman, A.M., Blagborough, A.M., Sinden, R.E., 2010. A Plasmodium falciparum strain expressing GFP throughout the parasite's life-cycle. PloS one 5, e9156.

Tarrant, M.K., Cole, P.A., 2009. The chemical biology of protein phosphorylation. Annu Rev Biochem 78, 797-825.

Tavare, J.M., Fletcher, L.M., Welsh, G.I., 2001. Using green fluorescent protein to study intracellular signalling. J Endocrinol 170, 297-306.

Taylor, H.M., McRobert, L., Grainger, M., Sicard, A., Dluzewski, A.R., Hopp, C.S., Holder, A.A., Baker, D.A., 2010. The malaria parasite cyclic GMP-dependent

protein kinase plays a central role in blood-stage schizogony. Eukaryot Cell 9, 37-45.

Tewari, R., Dorin, D., Moon, R., Doerig, C., Billker, O., 2005. An atypical mitogen-activated protein kinase controls cytokinesis and flagellar motility during male gamete formation in a malaria parasite. Molecular microbiology 58, 1253-1263.

Tham, W.H., Wilson, D.W., Lopaticki, S., Schmidt, C.Q., Tetteh-Quarcoo, P.B., Barlow, P.N., Richard, D., Corbin, J.E., Beeson, J.G., Cowman, A.F., 2010. Complement receptor 1 is the host erythrocyte receptor for Plasmodium falciparum PfRh4 invasion ligand. Proceedings of the National Academy of Sciences of the United States of America 107, 17327-17332.

Thomas, D.C., Ahmed, A., Gilberger, T.W., Sharma, P., 2012. Regulation of Plasmodium falciparum Glideosome Associated Protein 45 (PfGAP45) Phosphorylation. PloS one 7, e35855.

Thomas, J.C., Green, J.L., Howson, R.I., Simpson, P., Moss, D.K., Martin, S.R., Holder, A.A., Cota, E., Tate, E.W., 2010. Interaction and dynamics of the Plasmodium falciparum MTIP-MyoA complex, a key component of the invasion motor in the malaria parasite. Mol Biosyst 6, 494-498.

Tilley, L., McFadden, G., Cowman, A., Klonis, N., 2007. Illuminating Plasmodium falciparum-infected red blood cells. Trends Parasitol 23, 268-277.

Trampuz, A., Jereb, M., Muzlovic, I., Prabhu, R.M., 2003. Clinical review: Severe malaria. Crit Care 7, 315-323.

Treeck, M., Sanders, J.L., Elias, J.E., Boothroyd, J.C., 2011. The phosphoproteomes of Plasmodium falciparum and Toxoplasma gondii reveal unusual adaptations within and beyond the parasites' boundaries. Cell host & microbe 10, 410-419.

Treeck, M., Zacherl, S., Herrmann, S., Cabrera, A., Kono, M., Struck, N.S., Engelberg, K., Haase, S., Frischknecht, F., Miura, K., Spielmann, T., Gilberger, T.W., 2009. Functional analysis of the leading malaria vaccine candidate AMA-1 reveals an essential role for the cytoplasmic domain in the invasion process. PLoS pathogens 5, e1000322.

Tremp, A.Z., Dessens, J.T., 2011. Malaria IMC1 membrane skeleton proteins operate autonomously and participate in motility independently of cell shape. The Journal of biological chemistry 286, 5383-5391.

Tremp, A.Z., Khater, E.I., Dessens, J.T., 2008. IMC1b is a putative membrane skeleton protein involved in cell shape, mechanical strength, motility, and infectivity of malaria ookinetes. The Journal of biological chemistry 283, 27604-27611.

Triglia, T., Chen, L., Lopaticki, S., Dekiwadia, C., Riglar, D.T., Hodder, A.N., Ralph, S.A., Baum, J., Cowman, A.F., 2011. Plasmodium falciparum merozoite invasion is inhibited by antibodies that target the PfRh2a and b binding domains. PLoS Pathog 7, e1002075.

Triglia, T., Healer, J., Caruana, S.R., Hodder, A.N., Anders, R.F., Crabb, B.S., Cowman, A.F., 2000. Apical membrane antigen 1 plays a central role in erythrocyte invasion by Plasmodium species. Mol Microbiol 38, 706-718.

Triglia, T., Tham, W.H., Hodder, A., Cowman, A.F., 2009. Reticulocyte binding protein homologues are key adhesins during erythrocyte invasion by Plasmodium falciparum. Cell Microbiol 11, 1671-1687.

Trucco, C., Fernandez-Reyes, D., Howell, S., Stafford, W.H., Scott-Finnigan, T.J., Grainger, M., Ogun, S.A., Taylor, W.R., Holder, A.A., 2001. The merozoite surface protein 6 gene codes for a 36 kDa protein associated with the Plasmodium falciparum merozoite surface protein-1 complex. Molecular and biochemical parasitology 112, 91-101.

Tsien, R.Y., 1998. The green fluorescent protein. Annu Rev Biochem 67, 509-544.

Uchime, O., Herrera, R., Reiter, K., Kotova, S., Shimp, R.L., Jr., Miura, K., Jones, D., Lebowitz, J., Ambroggio, X., Hurt, D.E., Jin, A.J., Long, C., Miller, L.H., Narum, D.L., 2012. Analysis of the conformation and function of the Plasmodium falciparum merozoite proteins MTRAP and PTRAMP. Eukaryotic cell 11, 615-625.

Vaid, A., Thomas, D.C., Sharma, P., 2008. Role of Ca2+/calmodulin-PfPKB signaling pathway in erythrocyte invasion by Plasmodium falciparum. J Biol Chem 283, 5589-5597.

Van den Eede, P., Van, H.N., Van Overmeir, C., Vythilingam, I., Duc, T.N., Hung le, X., Manh, H.N., Anne, J., D'Alessandro, U., Erhart, A., 2009. Human Plasmodium knowlesi infections in young children in central Vietnam. Malar J 8, 249.

Vaughan, A.M., Aly, A.S., Kappe, S.H., 2008. Malaria parasite pre-erythrocytic stage infection: gliding and hiding. Cell host & microbe 4, 209-218.

Weatherall, D.J., Miller, L.H., Baruch, D.I., Marsh, K., Doumbo, O.K., Casals-Pascual, C., Roberts, D.J., 2002. Malaria and the red cell. Hematology Am Soc Hematol Educ Program, 35-57.

Weber, J.L., Lyon, J.A., Wolff, R.H., Hall, T., Lowell, G.H., Chulay, J.D., 1988. Primary structure of a Plasmodium falciparum malaria antigen located at the merozoite surface and within the parasitophorous vacuole. The Journal of biological chemistry 263, 11421-11425.

Wernimont, A.K., Artz, J.D., Finerty, P., Jr., Lin, Y.H., Amani, M., Allali-Hassani, A., Senisterra, G., Vedadi, M., Tempel, W., Mackenzie, F., Chau, I., Lourido, S., Sibley, L.D., Hui, R., 2010. Structures of apicomplexan calcium-

dependent protein kinases reveal mechanism of activation by calcium. Nat Struct Mol Biol 17, 596-601.

WHO, 2011. World Malaria Report 2011. World Health Organization.

William, T., Menon, J., Rajahram, G., Chan, L., Ma, G., Donaldson, S., Khoo, S., Frederick, C., Jelip, J., Anstey, N.M., Yeo, T.W., 2011. Severe Plasmodium knowlesi malaria in a tertiary care hospital, Sabah, Malaysia. Emerg Infect Dis 17, 1248-1255.

Wilson, G.M., Fielding, A.B., Simon, G.C., Yu, X., Andrews, P.D., Hames, R.S., Frey, A.M., Peden, A.A., Gould, G.W., Prekeris, R., 2005. The FIP3-Rab11 protein complex regulates recycling endosome targeting to the cleavage furrow during late cytokinesis. Molecular biology of the cell 16, 849-860.

Winter, D., Kugelstadt, D., Seidler, J., Kappes, B., Lehmann, W.D., 2009. Protein phosphorylation influences proteolytic cleavage and kinase substrate properties exemplified by analysis of in vitro phosphorylated Plasmodium falciparum glideosome-associated protein 45 by nano-ultra performance liquid chromatography-tandem mass spectrometry. Anal Biochem 393, 41-47.

Wu, Y., Sifri, C.D., Lei, H.H., Su, X.Z., Wellems, T.E., 1995. Transfection of Plasmodium falciparum within human red blood cells. Proc Natl Acad Sci U S A 92, 973-977.

Yayon, A., Timberg, R., Friedman, S., Ginsburg, H., 1984. Effects of chloroquine on the feeding mechanism of the intraerythrocytic human malarial parasite Plasmodium falciparum. J Protozool 31, 367-372.

Yeoman, J.A., Hanssen, E., Maier, A.G., Klonis, N., Maco, B., Baum, J., Turnbull, L., Whitchurch, C.B., Dixon, M.W., Tilley, L., 2011. Tracking Glideosome-associated protein 50 reveals the development and organization of the inner membrane complex of Plasmodium falciparum. Eukaryot Cell 10, 556-564.

Appendix A: *In vitro* CDPK1 phosphorylation of recombinant PfGAP45 and its variants at 30^{o}C, 10 minutes using 100 nM CDPK1.

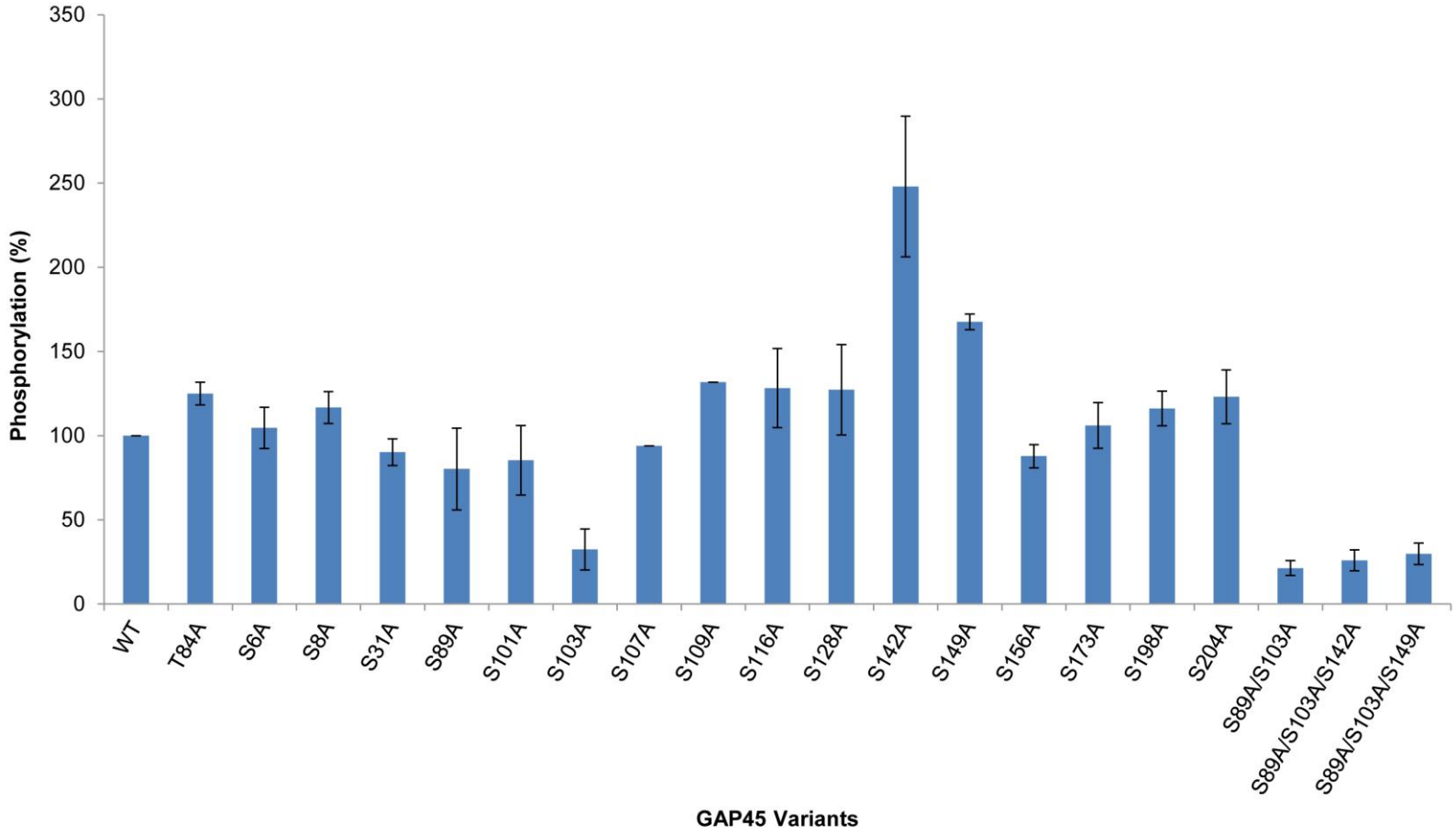

Appendix B: Dual antibody immunofluorescence of young (i) and mature (ii) schizonts using anti-GAP45 and anti-GFP antibodies. In young schizonts, the signal from GFP and GAP45 coincides perfectly for FL-GAP45 and C-GAP45 proteins, but not for N-GAP45. In mature schizonts, the staining of all of the GAP45 variants localises to the periphery of merozoites, but it is clear that for N-GAP45 there are many areas where this does not coincide with endogenous GAP45. For FL-GAP45 and C-GAP45 proteins, the colocalisation is exact. Scale bar is 2 µm.

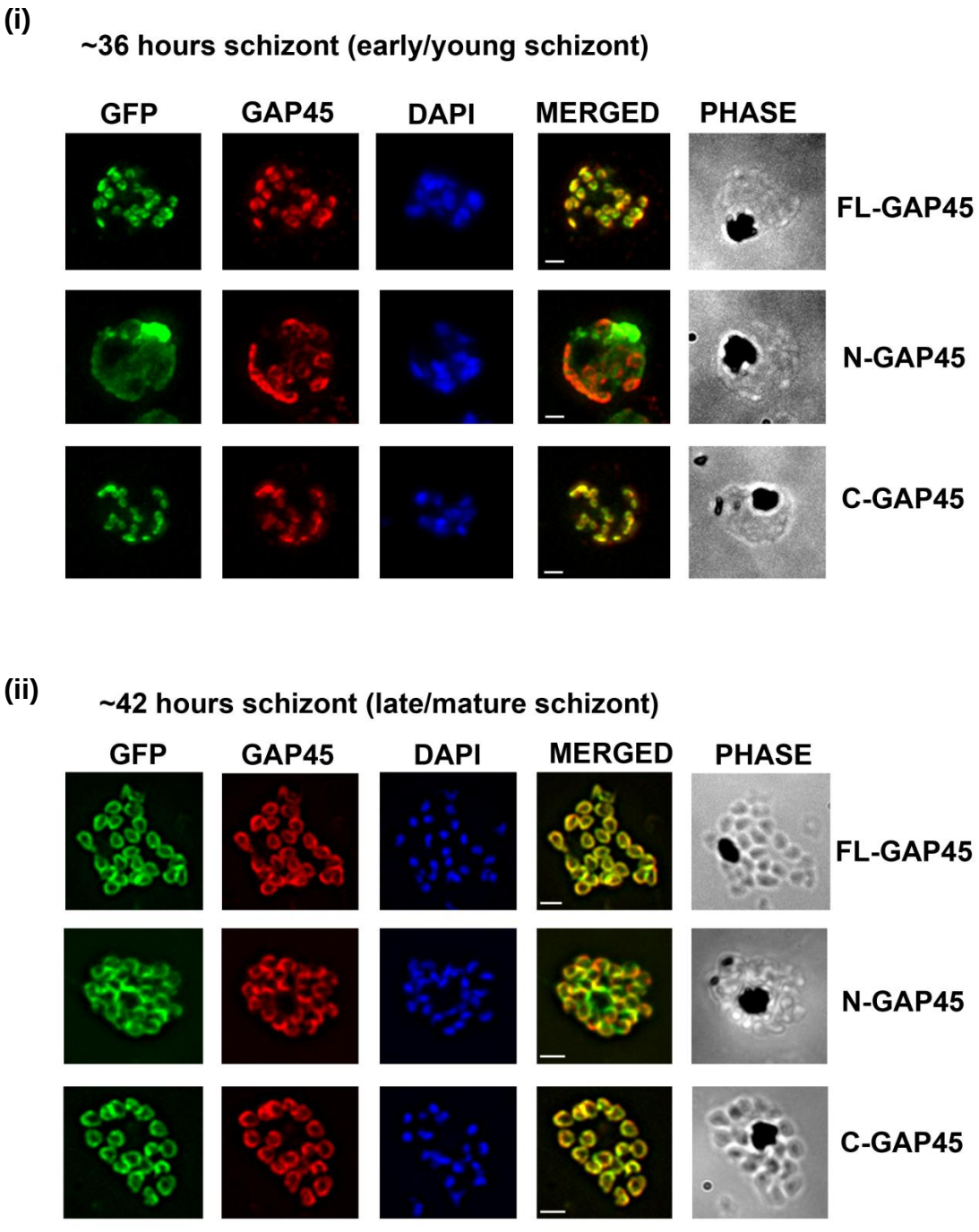

Appendix C: The localisation of GFP-tagged GAP45 variants at early schizont stage after high resolution live fluorescent imaging analysis with Z-stack and deconvolution processing.

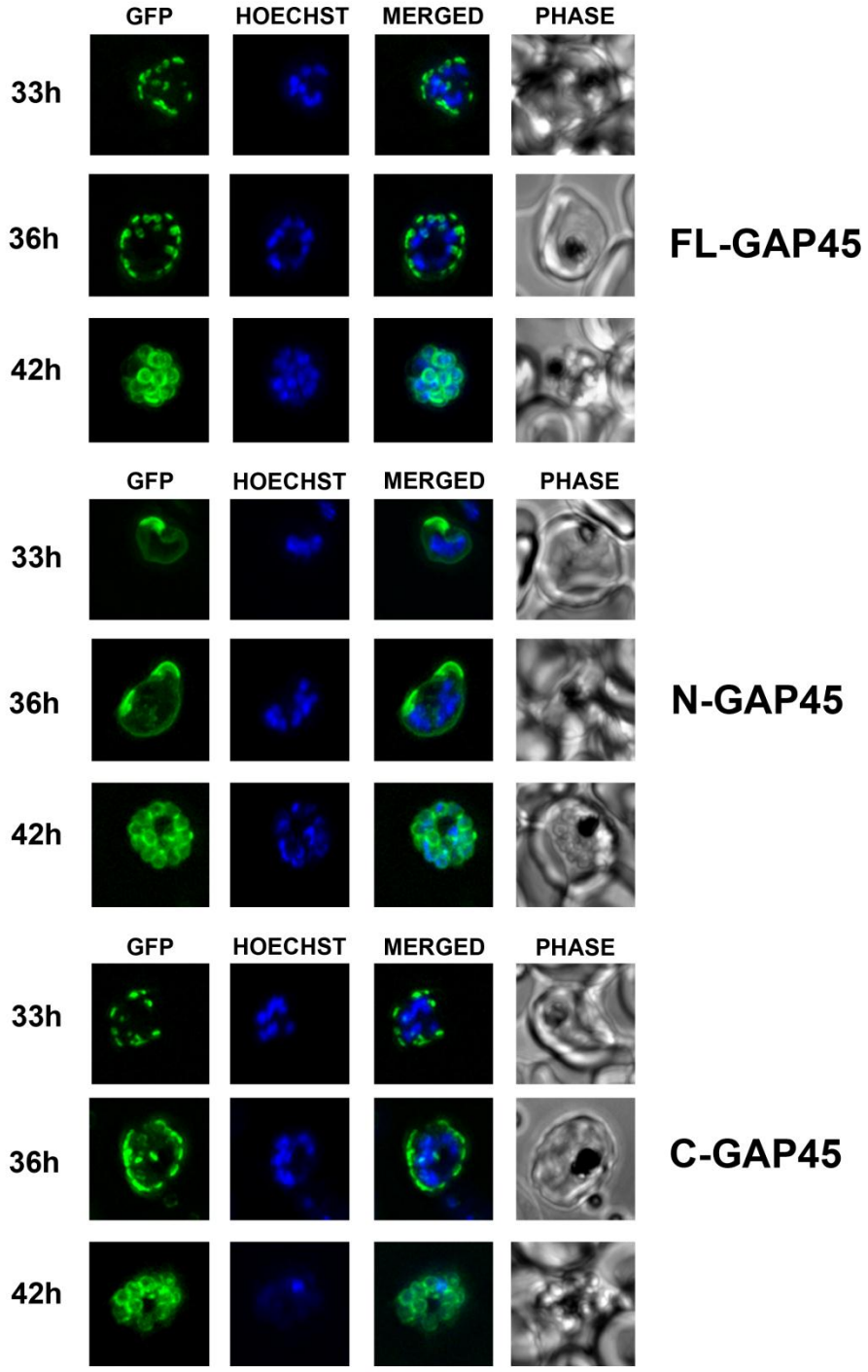

Appendix D: The FL-GAP45 (FL) and C-GAP45 (C) co-precipitated other motor complex proteins such as MTIP, GAP50 and MyoA. The N-GAP45 (N) was unable to co-precipitate other motor complex protein such as MyoA, MTIP and GAP50. The GFP-GAP45 variant containing both S89A and S103A (D4) substitutions was not affecting the integrity of motor complex proteins.

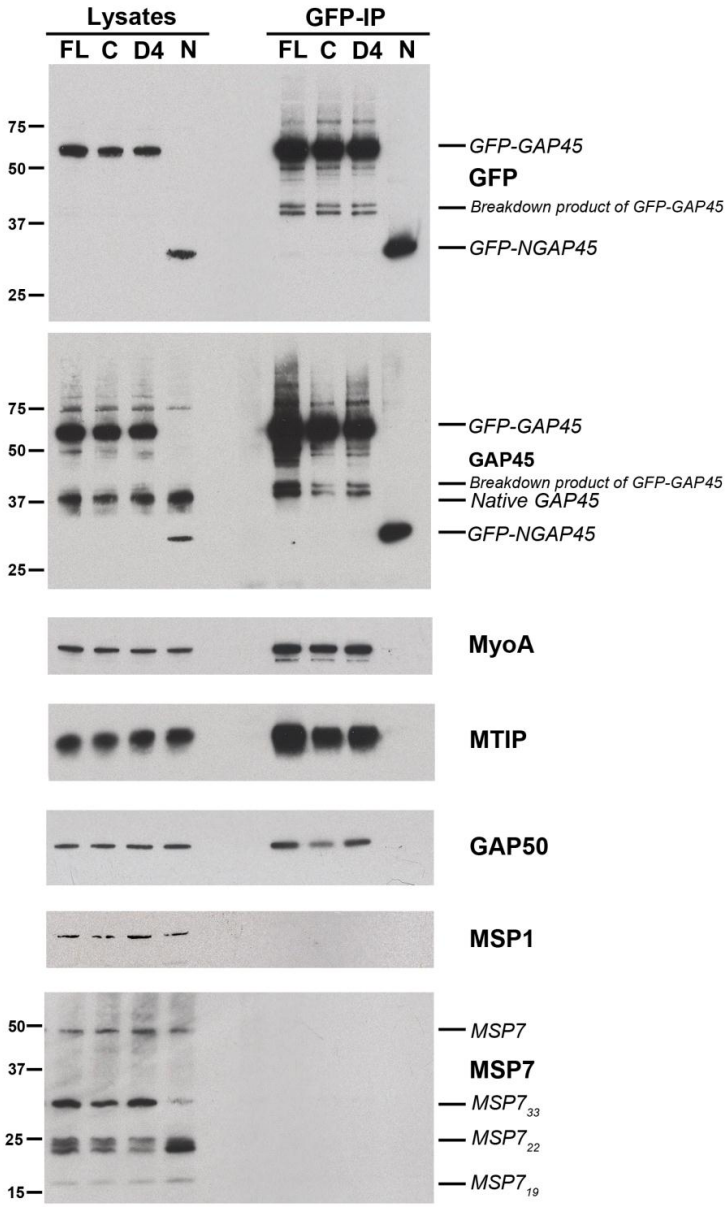

FL: FL-GAP45
C : C-GAP45
D4 : S89A/S103A GFP-GAP45
N : N-GAP45

Appendix E: Western blotting showing that the unknown phosphoprotein 2 was not a breakdown product of GFP-GAP45, as both anti-GFP and GAP45 antibodies were not reacted with a protein of this size.

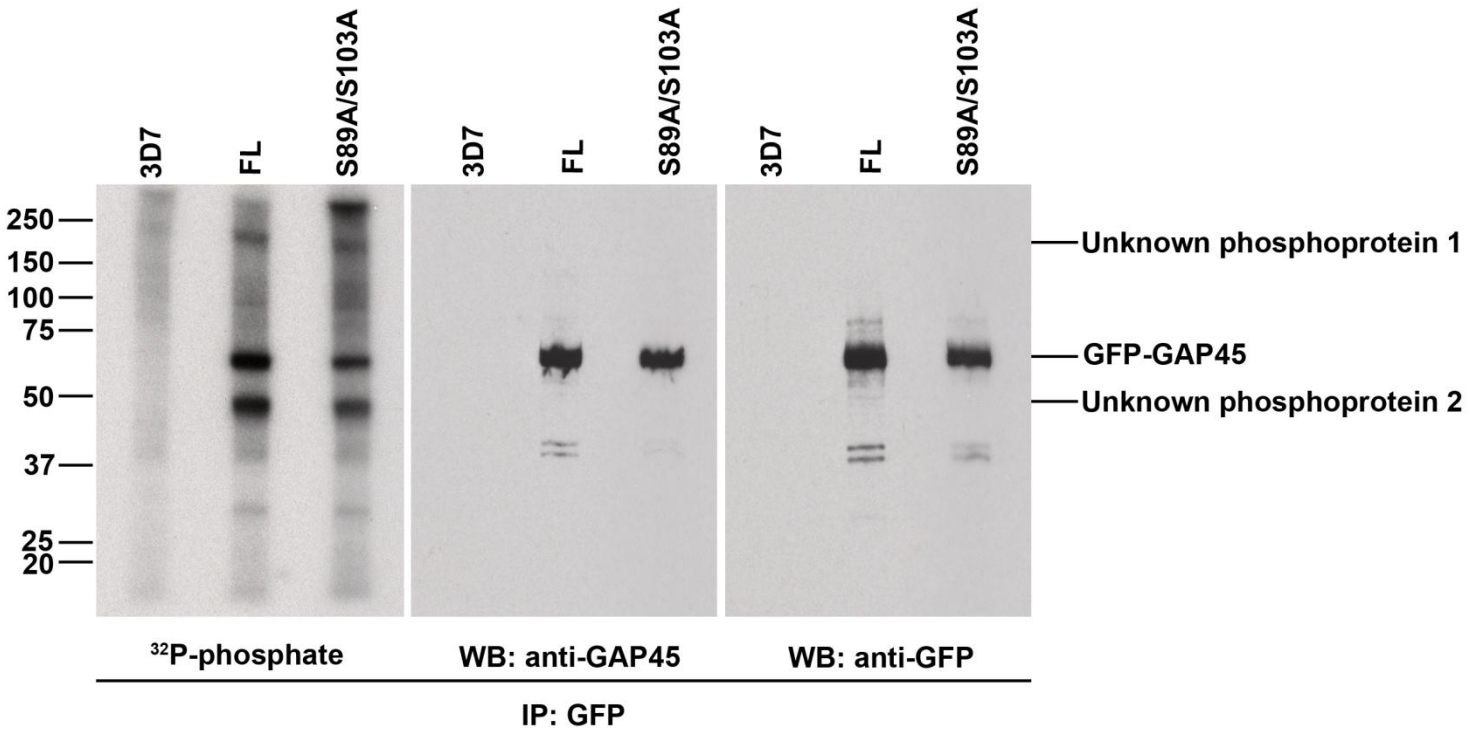

Appendix F: Protein profile of GFP IP products of GFP-GAP45 showing the location of unknown phosphoprotein 1 (probably ALV6 ?) and 2 (probably GAP40 ?) and other motor complex proteins such as MyoA, GFP-GAP45, GAP50 and MTIP.

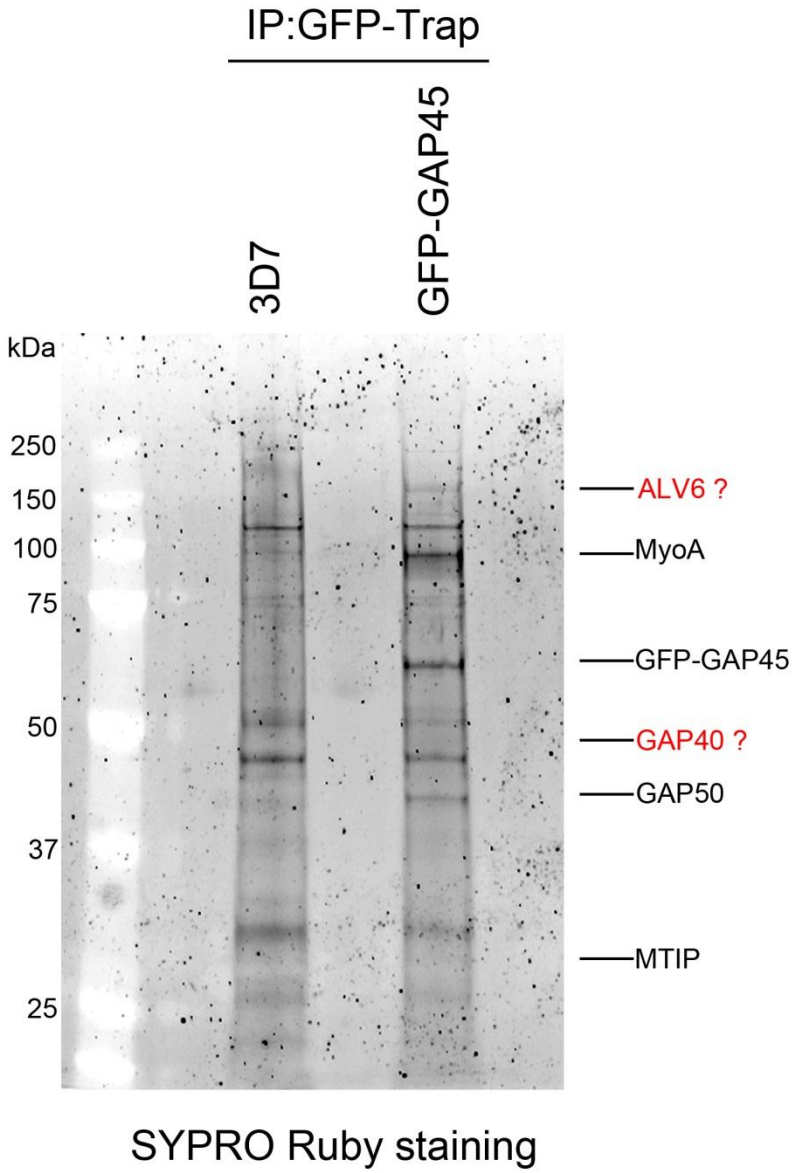

Appendix G: A scientific paper related to this thesis has been published by the author.

OPEN ACCESS Freely available online

PLoS one

Subcellular Location, Phosphorylation and Assembly into the Motor Complex of GAP45 during *Plasmodium falciparum* Schizont Development

Mohd A. Mohd Ridzuan[1,2], Robert W. Moon[1], Ellen Knuepfer[1], Sally Black[1], Anthony A. Holder[1], Judith L. Green[1]*

1 Division of Parasitology, MRC National Institute for Medical Research, London, United Kingdom, **2** Herbal Medicine Research Center, Institute for Medical Research, Jalan Pahang, Kuala Lumpur, Malaysia

Abstract

An actomyosin motor complex assembled below the parasite's plasma membrane drives erythrocyte invasion by *Plasmodium falciparum* merozoites. The complex is comprised of several proteins including myosin (MyoA), myosin tail domain interacting protein (MTIP) and glideosome associated proteins (GAP) 45 and 50, and is anchored on the inner membrane complex (IMC), which underlies the plasmalemma. A ternary complex of MyoA, MTIP and GAP45 is formed that then associates with GAP50. We show that full length GAP45 labelled internally with GFP is assembled into the motor complex and transported to the developing IMC in early schizogony, where it accumulates during intracellular development until merozoite release. We show that GAP45 is phosphorylated by calcium dependent protein kinase 1 (CDPK1), and identify the modified serine residues. Replacing these serine residues with alanine or aspartate has no apparent effect on GAP45 assembly into the motor protein complex or its subcellular location in the parasite. The early assembly of the motor complex suggests that it has functions in addition to its role in erythrocyte invasion.

Citation: Ridzuan MAM, Moon RW, Knuepfer E, Black S, Holder AA, et al. (2012) Subcellular Location, Phosphorylation and Assembly into the Motor Complex of GAP45 during *Plasmodium falciparum* Schizont Development. PLoS ONE 7(3): e33845. doi:10.1371/journal.pone.0033845

Editor: Gordon Langsley, Institut national de la santé et de la recherche médicale - Institut Cochin, France

Received December 22, 2011; **Accepted** February 19, 2012; **Published** March 30, 2012

Funding: MAMR was in receipt of a studentship and granted a full time study leave from the Ministry of Science, Technology and Innovation (MOSTI) and the Director of Institute for Medical Research, Ministry of Health, Malaysia, respectively. This work was funded by the Medical Research Council (U117532067) and the European Community's Seventh Framework Programme (FP7/2007–2013) under grant agreement no. 242095. No additional external funding was received for this study. The funders had no role in study design, data collection and analysis, decision to publish, or preparation of the manuscript.

Competing Interests: The authors have declared that no competing interests exist.

* E-mail: judith.green@nimr.mrc.ac.uk

Introduction

Malaria is a disease caused by protozoan parasites of the genus *Plasmodium* and results in almost a million deaths annually [1]. The life cycle is complex with alternate stages in a vertebrate host and a mosquito vector. In the asexual cycle in the host's blood stream the merozoite form of the parasite invades a red blood cell and develops into the so-called trophozoite. During subsequent schizogony, DNA replication and mitosis results in a multinucleate syncytium, this then undergoes cytokinesis or segmentation to produce new merozoites that are released to invade red blood cells. Segmentation is accompanied by the formation of the inner membrane complex (IMC), a series of flattened cisternae that are found immediately beneath the parasite plasma membrane (PM) [2]. The IMC may provide shape, rigidity and polarity to the developing merozoites, which bud off from the residual body prior to their release from the red cell. Polarity is also established by the synthesis and location of a set of apical organelles that participate in merozoite release and host cell reinvasion. Host cell invasion is an active process powered by an actin-myosin motor complex located between the parasite's PM and the IMC. Myosin is tethered to the IMC and during invasion moves filamentous (F) actin to the rear of the parasite. The actin filament is coupled to a junction involving the parasite PM and the host cell surface membrane via transmembrane adhesins, thus the action of the molecular motor results in forward motion of the parasite into the host cell (reviewed in [3,4]).

The motor complex consists of myosin A (MyoA, a type XIV myosin), a myosin light chain (called myosin tail domain-interacting protein (MTIP) in *Plasmodium*) and the glideosome associated proteins GAP50 and GAP45, which were first described in *Toxoplasma gondii* [5]. GAP50 has a signal peptide and is targeted to the IMC through the protein secretory pathway, whereas GAP45, MTIP and MyoA are translated on cytoplasmic ribosomes and form a complex cotranslationally [5,6]. The GAP45-MTIP-MyoA complex subsequently binds to GAP50, presumably at the IMC. Whilst GAP50 has been used as a marker for the development of the IMC [7], the assembly of the other elements of the myosin motor complex and the timing of their association with the IMC is unclear.

In *Plasmodium falciparum*, the most important human malaria parasite, GAP45 is expressed throughout schizogony and, in complex with MyoA, MTIP, and GAP50, accumulates and is abundant in late schizont stages [8]. Although PfGAP45 is only 204 amino acids, it migrates anomalously as multiple bands on SDS-PAGE, suggestive of post-translational modification. The protein is cotranslationally N-myristoylated and then palmitoylated [6]. In addition, GAP45 is phosphorylated *in vivo* and during the progression of schizogony the proportion of GAP45 that is phosphorylated increases [9]. It has been reported to be a substrate for calcium-dependent protein kinase 1 (CDPK1) and protein kinase B (PKB) *in vitro* thus highlighting the

potential importance of multiple kinases in regulating either the formation or the function of the parasite motor complex [9,10]. Both CDPK1 and PKB are regulated by calcium, consistent with an important role for calcium flux in regulating *Plasmodium* growth and invasion [11].

Two phosphopeptides have been isolated from GAP45 purified from *P. falciparum* merozoites (residues 81–96 and 141–155). These contain threonine and/or serine residues that may be phosphorylated by serine/threonine-specific protein kinase(s). In addition to peptide 81–96, CDPK1 also phosphorylated GAP45 *in vitro* on a single residue contained within the peptide 97–112 [9]. These regions of GAP45 are conserved across the *Plasmodium* genus, but this conservation does not extend to the GAP45 sequence in other Apicomplexan parasites such as *T. gondii*. The phosphorylation of GAP45 in *P. falciparum* starts from approximately 36 hours post invasion and increases throughout schizogony [9]. Furthermore, pulse chase studies suggest that GAP45 is phosphorylated before GAP50 joins the complex [6]. In *T. gondii* tachyzoites, phosphorylation of GAP45 at S163 and/or S167 has been shown to regulate association/dissociation of the motor complex [12], however these residues are in a poorly conserved region and are not present in PfGAP45. These issues need to be clarified, however current evidence suggests that post-translational modifications such as phosphorylation may be important for localisation of, and interaction between, proteins of the motor complex.

The mechanism and timing of motor complex formation and localisation is not clearly defined. During schizogony, nuclear division is accompanied by IMC development [13]. In early schizonts (with up to eight nuclei) integral membrane protein markers of the IMC such as GAP50, GAPM1 and GAPM2 are located at what are variously described as punctate, ring-like, doughnut-shaped, or clamp-like structures at the periphery of the parasite [7,14,15]. As the schizont develops further, these IMC-specific proteins are detected extending around the surface of the developing merozoites. In *T. gondii*, recruitment of motor complex proteins to the pellicle may also occur prior to segmentation to produce daughter cells [16,17]. However in *T. gondii*, cell division occurs via endodyogeny, a process distinct to schizogony [13], and during which distribution of motor complex proteins is not identical between mother and daughter tachyzoites. TgGAP50 and TgGAP40 (a recently identified IMC-associated protein) are found in the IMC of both mature parasites and immature daughter cells whereas TgMyoA, TgMLC1, and TgGAP45 are present at the IMC of mature parasites yet are entirely absent from developing daughter cells [5,17].

We wished to determine whether or not GAP45 is associated with the developing IMC throughout schizogony in *P. falciparum*, if sequences at the N-terminus are sufficient to target GAP45 to the IMC, and whether phosphorylation of the serine residues that are substrates for CDPK1 is important in the assembly and location of the motor complex. We have demonstrated that a GFP-tagged full length GAP45 can be expressed in the parasite and is targeted to the same location as the untagged form. We identified the GAP45 residues phosphorylated by CDPK1 *in vitro* and were able to examine the effect on both subcellular location and formation of the motor complex of substituting these residues with either alanine or aspartic acid in parasite-expressed GFP-tagged GAP45.

Results

The role of the N-terminus of PfGAP45 in protein localisation

The two acylation sites at the N-terminus of PfGAP45, G2, which is myristoylated, and C5, which is presumed to be palmitoylated, have been suggested to drive the localisation of GAP45 to the IMC [6]. However, calcium-dependent protein kinase-1 (CDPK1), another protein with a similar dual acylation motif, has been demonstrated to be targeted to the inner face of the plasma membrane of *P. falciparum* merozoites [9]. We wished to establish if the N-terminal 29 residues of GAP45 were sufficient to target a reporter protein, GFP, to the IMC. We compared the localisation of this extremely truncated GAP45 (N-GAP45) with that of full-length GAP45 in which GFP was inserted into the ORF just after the N-terminal 29 amino acids (FL-GAP45), and also with a construct that lacked the N-terminus of GAP45 and therefore the putative membrane targeting residues at the N-terminus (C-GAP45). We chose to introduce the GFP tag at an internal site of GAP45 as previous work in *T. gondii* revealed that the addition of a YFP tag to the C-terminus of TgGAP45 abrogated its binding to the rest of the motor complex [18] and only an internally located epitope tag was able to circumvent this problem [12].

Live fluorescent imaging of these parasites revealed striking differences between the localisation of N-GAP45 and the other proteins. FL-GAP45 localises to ring-like structures in the developing schizonts (Figure 1A, 33 and 36 h) that appear to be present towards the periphery of the parasite. In fully segmented schizonts, the protein fully surrounds each merozoite nucleus (Figure 1A, 42 h). By contrast, in early schizonts the fluorescence of N-GAP45 was more evenly distributed around the periphery of the entire parasite rather than in discrete foci and there were no ring-like structures evident (Figure 1B, 33 and 36 h). In mature, segmented schizonts N-GAP45 also was located around the periphery of each merozoite (Figure 1B, 42 h). Interestingly, the localisation of C-GAP45, lacking the N-terminal acylation motifs, resembled very closely that seen for the FL-GAP45: in early schizonts the protein was present in discrete foci (Figure 1C, 33 h) that progress to small ring-like structures as development continues (Figure 1C, 36 h) and finally in the segmented schizont the protein was evenly distributed around the periphery of each merozoite (Figure 1C, 42 h). We confirmed by immunofluorescence using antibodies raised against GAP45 that the endogenous protein is also located to ring-like structures during schizogony in the 3D7 parental parasite line (time course from 30 h to 42 h post-invasion shown in Figure S1A) and that FL-GAP45 and C-GAP45 fusion proteins colocalise exactly with endogenous GAP45 in immature and mature parasites, whereas N-GAP45 does not (Figure S1B).

To determine if all three GFP-fusion proteins were targeted to membranes of the parasite cellular proteins were extracted in a series of buffers designed to solubilise proteins based on their degree of membrane association [19]. Only integral membrane proteins or those extremely tightly associated with membranes would fail to be solubilised by a high pH carbonate buffer. All three GAP45-GFP proteins were insoluble in high pH carbonate buffer (Figure 2A), as was MTIP, another member of the motor complex. MSP7, a peripheral membrane protein was slightly solubilised by carbonate buffer with most of the protein remaining insoluble. SERA5, a protein of the parasitophorous vacuole that is not membrane associated is largely released upon parasite treatment with a hypotonic solution (lane 1). Thus our data suggest that the N-terminus of GAP45 is sufficient to target a protein to cell membranes, however a protein lacking this sequence (C-GAP45) is still tightly associated with the membrane fraction. We wished to determine whether or not this truncated GAP45 protein was able to form part of the motor complex with MyoA, MTIP and GAP50. Immunoprecipitations of GFP fusion proteins were performed followed by Western blotting with antibodies to components of the motor complex. Both FL-GAP45 and C-GAP45 coprecipitated MyoA, MTIP and GAP50

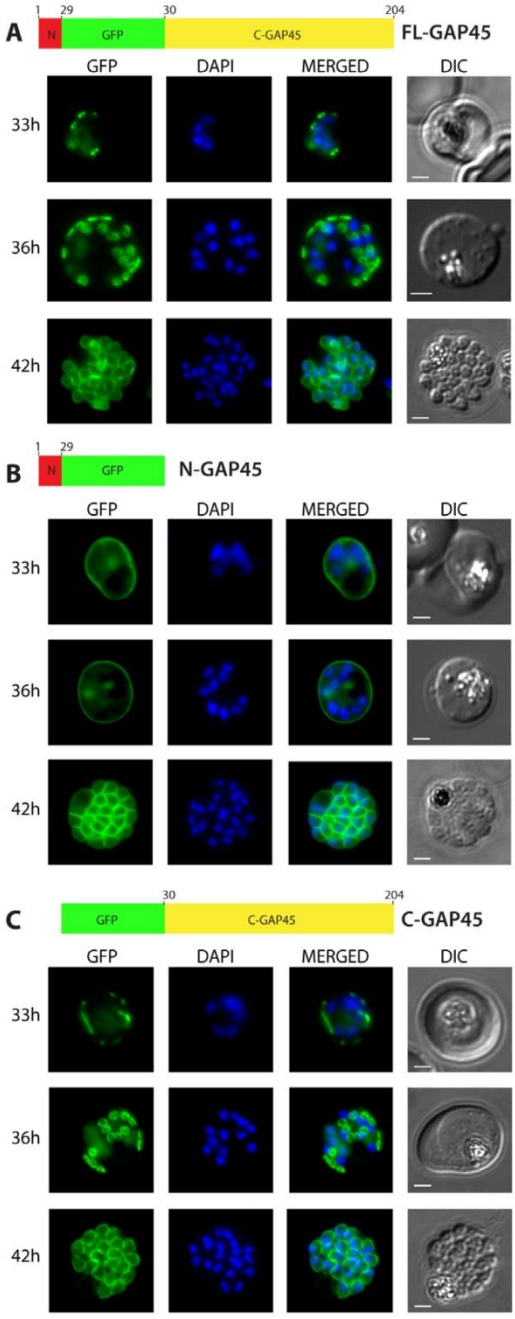

Figure 1. Subcellular localisation of GFP-tagged GAP45 protein and truncated derivatives. The location of (A) GFP-tagged wild type GAP45 (FL-GAP45), (B) GFP-tagged C- terminally truncated GAP45 (N-GAP45), and (C) GFP-tagged N-terminally truncated proteins (C-GAP45) during schizont development. Transfected parasite populations were synchronized and examined at 33, 36 and 42 h post invasion by fluorescence microscopy to detect GFP (green). Nuclei were labelled with Hoechst stain (blue) prior to analysis. The merged image of the two is also shown together with the corresponding differential interference contrast (DIC) picture. Scale bar is 2 μm. In the early schizont stages small, localised structures of GFP signal were observed around the parasite's periphery in both FL-GAP45 and C-GAP45, typical of an IMC location. N-GAP45 protein produced a different pattern of fluorescence probably corresponding to the parasite plasma membrane. At the late schizont stage (42 h post invasion) the GFP signal was detected at the periphery of merozoites developing within the schizont for all GAP45 variants, and at this time point the putative IMC and parasite plasma membrane patterns were indistinguishable.
doi:10.1371/journal.pone.0033845.g001

but not native GAP45 (Figure 2B). These results suggest that the C-terminus of GAP45 is responsible for binding to other protein components of the motor complex. The absence of native GAP45 in the precipitates also suggests that the GAP45 proteins do not form homo-oligomers and that there are not multiple copies of GAP45 within a single motor complex.

The N-terminus of GAP45 targets proteins to the plasma membrane but is not required for the association of GAP45 with the IMC

Whilst the N-GAP45 construct was shown to be membrane associated (Figure 2A), it is clear from cell imaging that it is targeted to a different membrane than FL-GAP45 and C-GAP45 proteins (Figure 1). We sought to clarify which peripheral membrane each protein is targeted to by immunofluorescence using antibodies to proteins of known membrane localisation. Merozoite surface protein 1 (MSP1) is a GPI-anchored protein of the parasite plasma membrane (PM); whereas glideosome associated protein 50 (GAP50) is an integral membrane protein of the IMC. All three of our GFP-fusion proteins localise to the periphery of mature, fully segmented schizonts and seem to colocalise with the IMC-specific marker GAP50 (Figure 3A), however such staining is indistinguishable from that of PM-specific proteins. In younger, unsegmented schizonts the picture is different; N-GAP45 colocalises with MSP1 at the PM, whereas the staining pattern of FL-GAP45 is distinct (Figure 3B).

In mature schizonts it is difficult to distinguish between the PM and IMC as they are so close together. Late in schizogony individual merozoites are pinched off from the syncytium and the residual body is encapsulated by plasma membrane, but not IMC. Residual bodies therefore stain for plasma membrane proteins (e.g. MSP1), but not IMC proteins (e.g. GAP50). Close examination of the residual bodies of mature schizonts expressing FL-GAP45, C-GAP45 or N-GAP45 revealed that only N-GAP45 was present around residual bodies (marked by arrows on Figure 3C), indicating a plasma membrane location for the truncated GAP45 and an IMC localisation for FL-GAP45 and C-GAP45.

CDPK1 phosphorylates S89 and S103 of PfGAP45

We sought to further investigate the targeting and complex formation of GAP45 by identifying residues of the protein that are phosphorylated, specifically by CDPK1. Phosphopeptides derived from GAP45 have been identified from late schizonts [20] and merozoites [9], and phosphorylation of residues 163 and/or 167 of *T. gondii* GAP45 has been shown to be crucial for binding of the trimeric complex of GAP45, MTIP and MyoA to the IMC protein GAP50 [12]. We undertook a rigorous site-directed mutagenesis approach to identify specific residues of GAP45 that were phosphorylated by CDPK1 *in vitro*. As there is no detectable threonine phosphorylation of GAP45 by CDPK1 (based on

phosphothreonine-specific antibody binding, data not shown), we restricted our analysis to the sixteen serine residues of GAP45. Each serine was mutated to an alanine, and the ability of CDPK1 to phosphorylate wild type and variant GAP45 proteins was examined using γ-^{32}P-labelled ATP incorporation. By autoradiography, all of the GAP45 variants except S103A had a similar intensity of labelling as the wild type GAP45 protein (Figure 4A and Table S1). Less incorporation of label was observed for the S103A protein, and by densitometry analysis of data from at least three different experiments the phosphorylation of the S103A variant was about 35% of that for the wild type protein, representing a significant decrease ($p<0.05$). In addition, the S31A, S89A and S156A variants also showed slight decreases in phosphorylation of 10, 14 and 13% respectively when compared to the wild type protein, although these values did not represent statistically significant differences (Fig. 4A and Table S1).

CDPK1 phosphorylation of wild-type GAP45 and the S89A, S103A and S89A/S103A variants was also examined as a time course with samples collected at sequential time points and analysed by scintillation counting (Figure 4B). The results from this assay confirmed that S89 and S103 are indeed targets of CDPK1 activity *in vitro*, with decreased ^{32}P incorporation, although at early time points the incorporation of ^{32}P into S89A GAP45 was indistinguishable from that into wild type GAP45. These findings complement the autoradiography results and are consistent with the *in vivo* data identifying phosphopeptides of GAP45 containing these residues [9,20]. Phosphorylation of the S89A/S103A variant was also decreased compared to that of wild type GAP45, but the double substitution showed only 5% less ^{32}P incorporation than the S103A variant (Figure 4B). In the case of this double mutant GAP45, there was still 24% phosphorylation compared to the wild-type protein. The phosphorylated residues are likely to be S31 and S156, identified as possible CDPK1 targets in the analysis of individual serine substitutions of GAP45 (Table S1). Since this work has been performed, an analysis of the *P. falciparum* phosphoproteome revealed multiple phosphorylated residues of GAP45, including S89, S103 and also S156, identified here as a minor CDPK1 site [20]. Our *in vitro* kinase assays verify that three of the GAP45 phosphosites identified by Treeck *et al* in their phosphoproteome analysis are substrates for CDPK1. Whilst this does not confirm that these phosphorylations are mediated by CDPK1 *in vivo*, the fact that the two proteins colocalise at the inner face of the plasma membrane strengthens the argument that this may also happen in the parasite. Our *in vitro* studies have also demonstrated that five of the eight sites identified by Treeck are not phosphorylated by CDPK1 *in vitro*, thereby implicating other kinases in the modification of this protein. We elected to focus further efforts on analysis of the role of S89 and S103 phosphorylation by CDPK1 *in vivo*, as S103 is the major CDPK1 site in GAP45 and S89 phosphopeptide had previously been isolated from merozoites [9].

Phosphorylation of S89 and/or S103 has no effect on trafficking or assembly of the motor complex

Having shown that GFP-tagged GAP45 behaves like native GAP45 in terms of its location in the cell throughout schizogony, we were next interested to examine the effect of modifying S89 and S103 in GFP-tagged GAP45 on its behaviour in the cell. Therefore we constructed plasmids for the episomal expression of GFP-tagged GAP45, in which either or both S89 and S103 were modified to Ala or to Asp. Ala was chosen to obviate a negative charge at the sequence position and Asp was chosen to introduce a phosphomimetic, permanently negatively charged residue at the position.

By live microscopy, the S89A and S103A modified GAP45 proteins were indistinguishable in their location from unmodified GAP45 in both early (Figure 5A) and late schizont (Figure 5B) stages. Neither the single Ala or Asp variants nor the double S89A/S103A and S89D/S103D substitutions had any effect on GAP45 localisation (Figure S2). As before, we immunoprecipitated GFP-tagged GAP45 from schizont lysates. By Western blotting each of the mutant proteins was found in complex with MyoA, MTIP and GAP50 and, as such, were indistinguishable from parasites expressing wild type GAP45 (S89A and S103A are shown in Figure 5C).

Discussion

The subcellular distribution that we see of a GFP-tagged GAP45 protein appears to be identical to the pattern of GAP50 expression observed in developing schizonts, where claw-shaped structures were seen [7], and that of other membrane localised IMC proteins GAPM1 [15] and GAPM2 [14]. These observations fit with a recent model of the motor complex in *T. gondii* tachyzoites where GAP45 is anchored in the plasma membrane by dual acylation of its N-terminus and interacts with GAP50 in the IMC membrane via its C-terminus. Whether this interaction is direct, or via other members of the motor complex (MTIP or MyoA, or the recently described GAP40) has not been determined. We have demonstrated that whilst the N-terminus of GAP45 containing the dual acylation motifs is able to target a reporter protein to the plasma membrane, it is not required for localisation and trafficking of the motor complex to the IMC; a protein lacking the N-terminus shares the same IMC localisation as FL-GAP45 and is able to form a tetrameric complex with MyoA, MTIP and GAP50. It is likely that we see no growth or structural phenotype as a result of this because the GAP45-GFP proteins in our studies are expressed from episomal plasmids and there is always native GAP45 expressed from the genomic locus in our parasites. However, we can say that there is no obvious detrimental effect on parasites in which a considerable proportion of the motor complex is not anchored to the plasma membrane via GAP45.

During schizogony, cell replication is initiated with nuclear division and replication of other organelles developing within the cytoplasm, encapsulated by a single plasma membrane from the mother cell [13,15]. After organelle replication merozoites are pinched off from the syncytium within the red blood cell by the plasma membrane surrounding individual merozoites. Our data suggest that even at very early stages of merozoite formation, before plasma membrane formation around individual merozoites, GAP45 interacts with proteins in the developing IMC membranes. If the motor complex is only required for merozoite invasion of red blood cells why is it assembled much earlier in the developing schizont? It appears that IMC formation occurs concurrently with plasma membrane encapsulation of daughter merozoites. It is likely that a molecular motor is involved in this process. In other systems, myosins are crucial for cell division, for example myosin II is the primary motor protein responsible for cytokinesis in eukaryotes [21–23]. Notably, in another Apicomplexan parasite, *T. gondii* myosin B has been implicated in the process of cell division [24]. Because of the unusual arrangement of membranes in the development of merozoites, it may be that *Plasmodium* achieves cytokinesis and segmentation using a myosin XIV in a motor complex that effectively brings the plasma membrane and IMC together by virtue of a member of the complex, GAP45, bridging the gap between the two membranes.

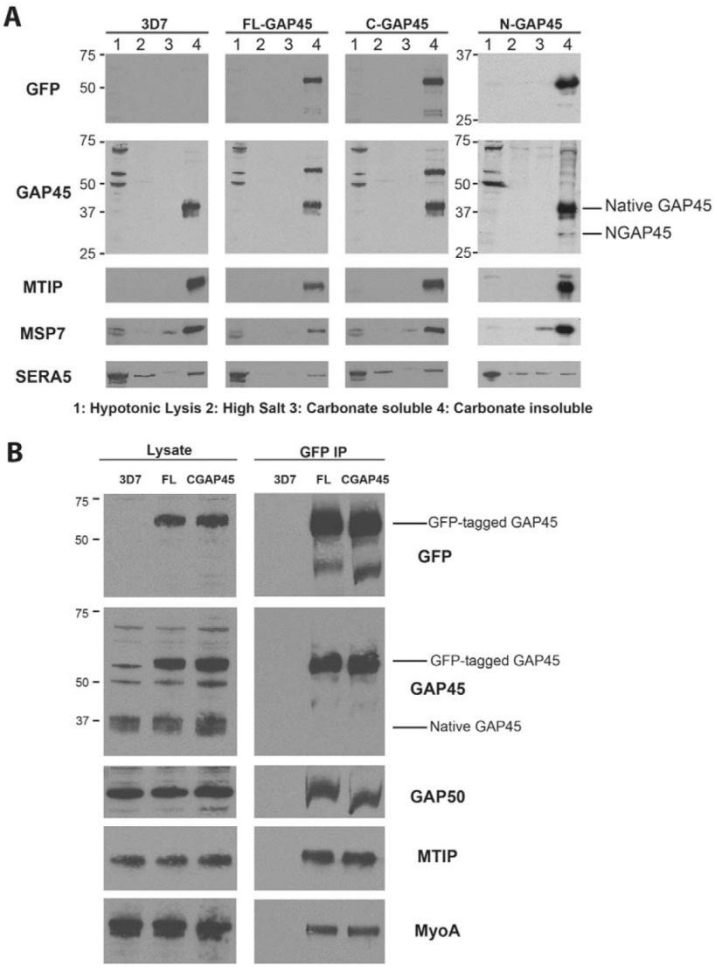

Figure 2. Endogenous GAP45 and GFP-tagged variants are membrane-associated proteins. (A) The subcellular fractionation of untransfected parasites (3D7) and parasites expressing FL-GAP45, C-GAP45 or N-GAP45 was performed sequentially, by (1) hypotonic buffer lysis, (2) high salt buffer, and (3) sodium carbonate buffer; the residual material (4) is the carbonate-insoluble pellet. All fractions were analysed by SDS-PAGE and Western blotting, using antibodies to GFP, GAP45, MTIP, MSP7, and SERA5. GAP45 proteins were all found in the carbonate-insoluble pellet. (B) Immunoprecipitation of GFP-fusion proteins followed by Western blotting demonstrates that both FL-GAP45 and C-GAP45 form a complex containing MyoA, MTIP and GAP50.
doi:10.1371/journal.pone.0033845.g002

As the expression of both CDPK1 and GAP45 peaks late in schizogony [9], it is possible that phosphorylation of GAP45 is important in the regulation of motor complex formation. We have shown that mutation of either or both S89 and S103 to alanine or aspartate does not affect the localisation of GAP45 to the IMC throughout all stages of schizogony. Nor do these mutations affect the ability of GAP45 to form the tetrameric complexes with MyoA, MTIP and GAP50. Phosphorylation of sites other than S89 and S103 may be important in actin-myosin motor complex assembly. The localisation of GAP45 to the IMC has also been shown to be unaffected by phosphorylation in another Apicomplexan parasite, *T. gondii*. However, phosphorylation of *T. gondii* GAP45 does causes dissociation of the trimeric MyoA-MTIP-GAP45 complex from GAP50 [12]. The phosphorylated residues in TgGAP45 (S163 and S167) are in the least conserved region of the protein and are not identical in *P. falciparum* GAP45; the equivalent positions are D117 and T121. The TgGAP45 mutation S163E causes dissociation of the motor complex [12], whereas the equivalent position in PfGAP45 is an acidic aspartate, suggesting that mechanisms of regulation of motor complex formation may not be conserved between the two species, or that negative charge alone was not the cause of complex dissociation in the TgGAP45 mutant protein. GAP45 has been shown to be multiply phosphorylated in vivo, with residues 107, 142, 149, 156, 158 and 198 being modified as well as serines 89 and 103 [20]. It may be that phosphorylation of one or more of these residues play an

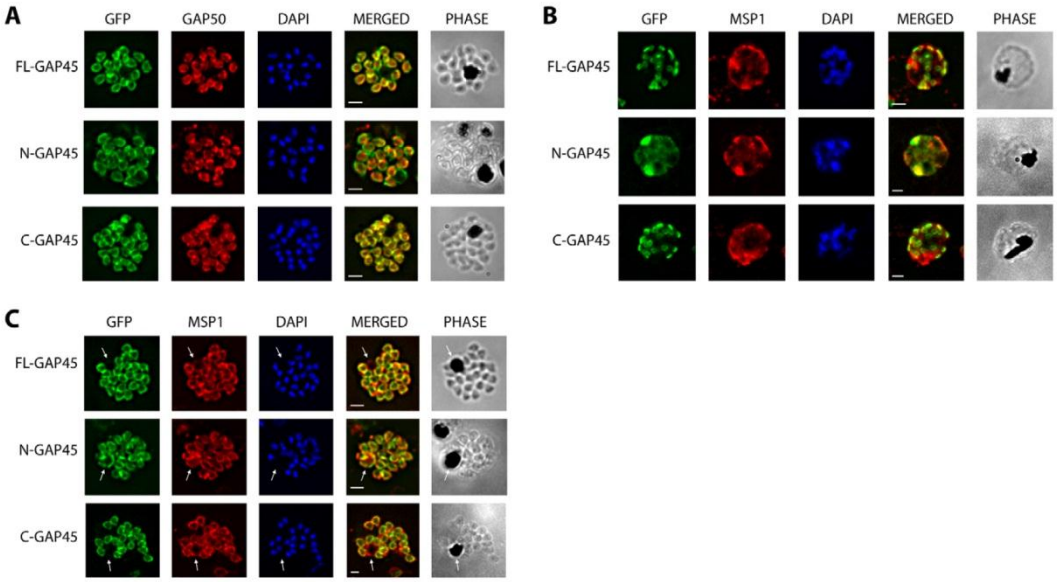

Figure 3. Immunofluorescent staining of GFP-tagged GAP45 variants with GAP50 in late stage schizonts. (A) Parasites were fixed and the location of GFP (green) and GAP50 (red), examined. FL-GAP45, C-GAP45 and N-GAP45 all appear to colocalise with GAP50 in segmented schizonts. (B) Staining with anti-MSP1 antibody (red) colocalises with only N-GFP in developing schizonts. FL-GAP45 AND C-GAP45 are present in distinctive ring-shaped structures at the periphery of the developing schizont. (C) In mature schizonts MSP1 (red) is present on membranes surrounding the residual body. N-GAP45 is also present on the residual body, but FL-GAP45 and C-GAP45 are absent. The white arrow in all images indicates the residual body. These data are consistent with a plasma membrane location for N-GAP45 and an inner membrane complex location for FL-GAP45. In all cases, parasite nuclei were stained with DAPI (blue); merged images are also shown. Scale bar is 2 μm.
doi:10.1371/journal.pone.0033845.g003

equivalent role to that of S163 *T. gondii*. Phosphorylation of PfGAP45 on S89 and S103 may be crucial during the invasive asexual stage of *P. falciparum*, the merozoite, or just after invasion in very early ring stages. At this stage, during or just after red blood cell invasion, the disassembly of the motor complex may be more critical, and phosphorylation/dephosphorylation of component proteins may play a role in this process. Alternatively, phosphorylation of these residues may have a completely different consequence that was not evident in our studies.

In conclusion, the present investigation has shown that phosphorylation of S89 and S103 residues on GAP45 does not affect the IMC localisation or the formation of the tetrameric motor complex during schizogony. Our studies have shed light on the processes of merozoite formation within the multinucleate syncytium and suggest that motor complex formation at the IMC occurs in parallel with cytokinesis and segmentation, a process that warrants closer scrutiny.

Materials and Methods

Ethics statement

The National Blood Transfusion Service provided human O+ erythrocytes from anonymous volunteers. Transfusion bags are bar coded and no records have been received linking individual donors to blood donations.

Parasite growth, synchronisation and transfection

P. falciparum parasites were maintained in human O+ erythrocytes provided by the National Blood Transfusion service. 3D7 is a cloned line derived from NF54 obtained from David Walliker at Edinburgh University [25]. Parasites were cultured in RPMI 1640 medium supplemented with 1% Albumax at 3% hematocrit in gassed (90% nitrogen, 5% oxygen, 5% carbon dioxide) flasks at 37°C. Parasites were synchronized using Percoll gradient centrifugation as previously described [26]. For transfection, *P. falciparum* 3D7 parasites were synchronized as described [26] and used at 10% ring stage parasitemia. Transfection vector DNA (100 μg in 100 mM Tris-HCl, 10 mM EDTA, pH 8.0 [TE] buffer) was transfected into parasites at ring stage as described [27,28]. Parasites were then grown in a medium containing 2.5 μg/ml blasticidin (Merck).

Live and indirect-immunofluorescence microscopy assay

Live synchronized parasite populations expressing GFP-tagged proteins were examined by epifluorescence microscopy on an Axio Imager M1 microscope (Zeiss). Parasites were labelled with Hoechst 33342 (Invitrogen) DNA stain, at 1 μg/ml, then a cell suspension was placed on a slide and overlaid with a Vaseline-rimmed coverslip. For immunofluorescence assays (IFA), thin smears of parasites were fixed with 4% paraformaldehyde for 10 min at RT. The fixed cells were washed 3 times with PBS, permeabilised with PBS containing 0.1% Triton X-100 for 5 min followed by blocking in 4% BSA (w/v) in PBS at 4°C overnight. After blocking, the slides were incubated for 1 h at RT with GFP-booster (a specific GFP-binding protein coupled to the fluorescent dye ATTO 488; Chromotek) followed by washing with PBS and addition of an antigen specific primary antibody. The slides were then incubated with IgG-specific secondary antibody coupled with

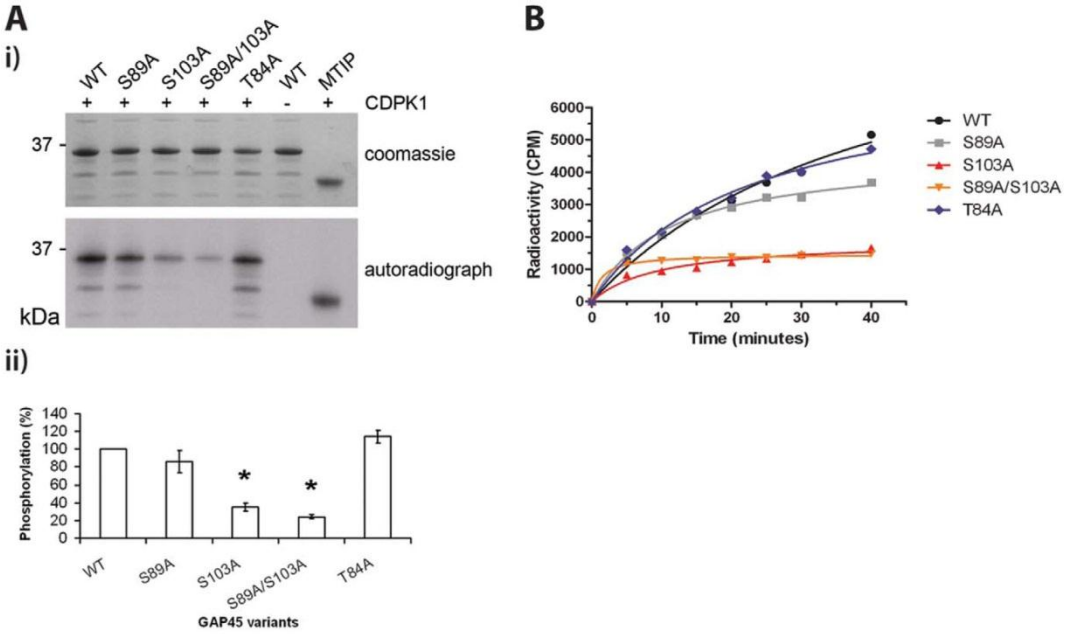

Figure 4. Identification of CDPK1 phosphorylation sites in GAP45. (A i) *In vitro* CDPK1-mediated phosphorylation of recombinant PfGAP45 (WT) and the S89A, S103A, and T84A variants using 100 nM CDPK1 and γ^{32}P-ATP at 30°C, for 10 min. MTIP was included as a substrate control for CDPK1. The upper panel shows the coomassie blue stained gel, and the lower panel shows the autoradiograph of the same gel. (A ii) The intensity of the phosphorylated GAP45 signal (autoradiography) was standardized against the amount of GAP45 protein (Coomassie blue stained) and analysed by ImageJ software. The data are presented as a mean ± S.E.M. from 3 to 5 different experiments. *denotes a significant difference ($p<0.05$) compared to wild type. (B) A time-course of CDPK1-dependent phosphorylation of recombinant GAP45 proteins by measuring incorporation of ^{32}P at 30°C, using 100 nM CDPK1 and 0.1 mM γ^{32}P-ATP and detection by scintillation counting. The data are presented as a mean from duplicate reactions for the unmodified protein (WT) or variants where S89 and/or S103 are replaced by alanine. T84A is included as a control as it is a substitution that had no effect on phosphorylation by CDPK1.
doi:10.1371/journal.pone.0033845.g004

Alexafluor 594 (Sigma) for 1 h at RT and washed 3 times with PBS. The smears were mounted for microscopic examination with Prolong® Gold antifade reagent with DAPI (Invitrogen). Images were acquired on a DeltaVision Core system (Applied Precision Inc., USA) based on an Olympus IX71 inverted microscope, using an Olympus 100× objective lens and images captured using a QuantEM 512SC EMCCD (Cascade 512×512) camera (Photometrics Ltd) using a Xenon light source. Images were deconvoluted using DeltaVision SoftWorx software suite 5.0 and prepared for publication with Adobe Photoshop.

Plasmid construction

The plasmid phh3-bsd-NGAP45GFP was designed to episomally express the N-terminal 29 residues of GAP45 fused to GFP. DNA sequence encoding the N-terminal 29 amino acids of GAP45 was fused in front of sequence encoding GFP as follows: Two overlapping primer pairs (Gap45for[TTCACCTAGGATGGGAAATAAGTGTAGTAGGTCAAAGGTAAAAGAACCAAAGAGAAAAGATATTGACGAGTTAGCAGAAAGGGAG]/Gap45ev[GACAACTCCAGTGAAAAGTTCTTCTCCTTTACTTTTCTTCAAGTTCTCCCTTTCTGCTAACTCGTCAATATC]) were fused to generate a long forward primer encoding the N-terminal 29 amino acids of GAP45. Following this, the long primer was used in combination with GFPrev primer (ATTTCT CCGCGGTTATTTGTATAGTTCATCCATGAAATGTGTAATCCC) to produce the GAP45-GFP fusion gene, which was subsequently inserted between the MSP3 promoter and the *hrp2* 3′UTR sequences in the pHH3 vector (Knuepfer and Holder, unpublished).

A second plasmid (phh3-bsd-GFPGAP45) was constructed to add an internal GFP tag between residues 29 and 30 of the GAP45 sequence. The sequence encoding the N-terminal part of GAP45 fused with GFP was amplified by PCR, eliminating the terminal stop codon using primers 5′ GCGCGCCCTAGGATGGGAAATAAATGTTCAAG 3′ and 5′ GCGCGCCCGCGGTTTGTATAGTTCATCCATGC 3′. The PCR product was reinserted into the pHH3 vector after the MSP3 promoter. The sequence encoding the C-terminal portion of GAP45 from residue 30 to the stop codon was amplified by PCR using primers 5′ GCGCGCCCGCGGCAATCTGAAGAAATAATTGAAG 3′ and 5′GCGCGCCCGCGGTTAGCTCAATAAAGGTGTATCG 3′ and inserted into the vector after the GFP tag sequence. A series of additional constructs were also made to express the full length GAP45 tagged with GFP and with amino acid substitutions (see below).

Production of GAP45 and variant proteins

The GAP45 open reading frame was cloned into the pET46 Ek/LIC expression vector (Novagen), containing an N-terminal hexa-His tag and transformed into BL21 (DE3) RIL competent

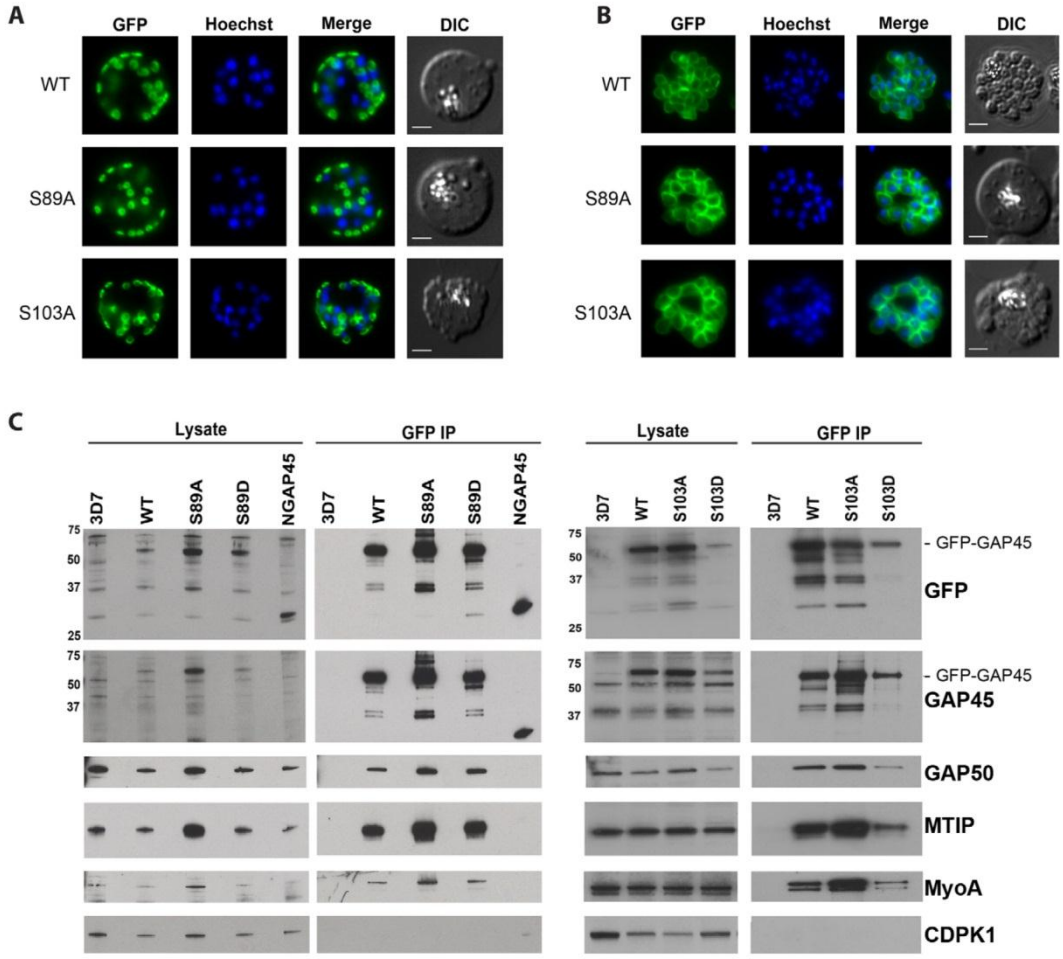

Figure 5. Mutation of S89 and/or S103 has no effect on subcellular localisation of GAP45 or its inclusion in the motor complex. The location of WT GFP-tagged GAP45, and mutants S89A and S103A determined in (A) early and (B) late schizonts, by live fluorescence microscopy (green). Parasite DNA was stained with Hoechst dye (blue); merged images and the differential interference contrast pictures are also shown. Scale bar is 2 μm. In the early schizont stages small, localised regions of GAP45GFP signal were observed around the parasite's periphery, typical of an IMC location. At the late schizont stage the GFP signal was detected at the periphery of merozoites developing within the schizont. There was no difference in the pattern of location between the wild type (WT) protein and any of the mutants (see also Figure S2). (C) Detergent lysates of schizont stage-parasites were prepared from untransfected 3D7 or parasites transfected with plasmid to express the WT, S89A, S89D, S103A and S103D mutant proteins. N-GAP45 (comprising the first 29 amino acids of GAP45 fused to GFP) was included as a negative control. Complexes were immunoprecipitated with an anti-GFP monoclonal antibody. Precipitated proteins and a sample of the corresponding whole-cell lysate were resolved by SDS-PAGE and analysed by western blotting using antibodies to GFP, GAP45, GAP50, MTIP, MyoA and CDPK1. CDPK1 is known to not be part of the motor complex and was therefore used as a negative control. The mobility of standard proteins is indicated on the left side of the gels. The results show that, with the exception of N-GAP45, all of the GFP-tagged GAP45 proteins are in complex with MTIP, MyoA and GAP50.
doi:10.1371/journal.pone.0033845.g005

cells (Stratagene). Protein expression was induced by the addition of 1 mM IPTG for 3 h at 27°C, then pelleted cells lysed and extracted in Bugbuster solution (Novagen) containing 1× protease inhibitor cocktail without EDTA (Roche) and benzonase (25 U/ml) (Novagen). The His-tagged GAP45 protein was then purified from lysates on Nickel-Nitrilotriacetic acid (Ni-NTA) agarose (Qiagen).

To produce variant proteins the gene sequence was first modified using a QuikChange II Site-Directed Mutagenesis kit (Stratagene) according to the manufacturer's instructions. All serine residues were replaced individually with Ala and additional variants with up to three replacements to Ala were also made. Variants S89A, S103A, S89A/S103A, S89D, S103D, and S89D/S103D were also prepared for expression in the parasites as GAP45GFP protein. HPLC-purified complementary oligonucleotides containing the required changes were purchased (Sigma) and are described in Table S1. Mutagenesis reactions were performed

with 10 ng plasmid DNA, according to the manufacturer's instructions. The presence of the desired mutation was confirmed by sequencing of the plasmid DNA.

Phosphorylation of GAP45 with CDPK1

Phosphorylation of recombinant GAP45 and its variants with CDPK1 and [γ^{32}P]ATP was performed in a solution containing 20 mM Tris HCl pH 8.0, 20 mM $MgCl_2$, 1 mM $CaCl_2$, 0.1 mM ATP (containing 0.1 MBq of [γ^{32}P]), 100 nM CDPK1 and 8 µM GAP45 at 30°C for 10 min unless otherwise stated. Radioactivity incorporation was determined either by autoradiography or scintillation counting. For autoradiography, the assay was stopped by adding equal volumes of SDS-PAGE sample buffer and incubation at 90°C for 5 min, before subjecting samples to SDS-PAGE. The gel was fixed, dried and exposed to Kodak Biomax MR film to visualize radiolabelled protein bands. Band intensities were measured and analysed by ImageJ software (www.rsbweb.nih.gov/ij/). For scintillation counting, reactions were started at 5 to 10 min intervals to ensure identical incubation times and then spotted onto P81 phosphocellulose discs (Whatman) and immersed in 75 mM phosphoric acid for 5 min. The discs were rinsed with acetone, dried, and then transferred to scintillation vials to measure the radioactivity by Cherenkov counting using a scintillation counter [29].

Subcellular fractionation, protein extraction from parasites and co-immunoprecipitation assay

Synchronized parasite populations were harvested and lysed with a hypotonic solution (10 mM Tris HCl, pH 8.0; 5 mM EDTA; and 1× protease inhibitor cocktail) for 1 h at 4°C. The mixture was centrifuged at 100,000 g for 10 min at 4°C and the supernatant ('hypotonic lysis soluble fraction') removed. The pellet was washed once with the hypotonic buffer and re- pelleted, prior to extraction with a high salt buffer (50 mM Tris HCl, pH 8.0; 5 mM EDTA; 500 mM NaCl; and 1× protease inhibitor cocktail) for 1 h at 4°C. The suspension was recentrifuged at 100,000 g and the supernatant ('high salt soluble') retained. The pellet was extracted again with 0.1 M sodium carbonate, pH 11.0 and refractionated to provide 'carbonate-soluble' and 'carbonate-insoluble' fractions.

For co-immunoprecipitation assays, purified parasites were lysed in 200 µl buffer (10 mM Tris-HCl, pH 7.5; 150 mM NaCl; 0.5 mM EDTA; 0.5% Nonidet P-40 [NP-40]; 1 mM PMSF and 1× protease inhibitor cocktail) on ice for 30 min. A soluble cell lysate was obtained by centrifugation at 20,000 g for 10 min at 4°C and diluted to 1000 µl with the same buffer lacking NP-40. GFP-Trap® beads (Chromotek) equilibrated with dilution buffer were added to the cell lysate for 1 h at RT, then recovered by centrifugation at 2000 g for 2 min at 4°C. The supernatant was retained and the beads were washed twice with the dilution buffer, then both fractions were mixed with SDS-PAGE sample buffer. After 10 min at 95°C soluble proteins were subjected to SDS-PAGE.

Protein samples were separated with 12% Nu-PAGE pre-cast Bis-Tris gels. Proteins were visualized by staining gels with Coomassie brilliant blue R-250, or subjected to western blotting. Following protein transfer to nitrocellulose membrane, the membrane was incubated in blocking solution (1% BSA in PBS containing 0.2% Tween 20 [PBST]) for 1 h and then incubated in primary antibody specific for GFP (Roche), GAP45, GAP50, MyoA, MTIP, SERA5, CDPK1 or MSP7. Following further washing, the membranes were incubated with secondary antibody (goat anti rabbit IgG or goat anti mouse IgG conjugated with horse radish peroxidase (HRP) (Biorad), as appropriate) and antibody binding detected by enhanced chemiluminescence reagent (ECL, GE Healthcare) and exposure to Biomax MR film (Kodak).

Supporting Information

Figure S1 The location of endogenous GAP45 and GAP45-GFP variants in developing schizonts. (A) Staining of endogenous GAP45 protein using specific antibodies in 3D7 parasites 30, 33, 36, 39 and 42 hours post-invasion. (B) Dual antibody immunofluorescence of young (i) and mature (ii) schizonts using anti-GAP45 and anti-GFP antibodies. In young schizonts, the signal from GFP and GAP45 coincides perfectly for FL-GAP45 and C-GAP45 proteins, but not for N-GAP45. In mature schizonts, the staining of all of the GAP45 variants localises to the periphery of merozoites, but it is clear that for N-GAP45 there are many areas where this does not coincide with endogenous GAP45. For FL-GAP45 and C-GAP45 proteins, the colocalisation is exact. Scale bar is 2 µm.
(TIF)

Figure S2 The location of GAP45-GFP and mutants (S89A, S103A, S89A/S103A, S89D, S103D, S89D/S103D) determined in (A) early and (B) late schizonts, by live fluorescence microscopy (green). Parasite DNA was stained with Hoechst dye (blue); merged images and the differential interference contrast pictures are also shown. Scale bar is 2 µm.
(TIF)

Table S1 In vitro CDPK1 phosphorylation of recombinant PfGAP45 and its variants. The intensity of the band (autoradiography) was standardised against the corresponding protein concentration profile (coomassie) and analysed using ImageJ software. The data are presented as a mean percentage ± S.D.
(TIF)

Acknowledgments

We thank Munira Grainger for help and advice in the cultivation of malaria parasites, Madhu Kadekoppala for antibodies to MSP7 and Robert Stallmach for antibodies to SERA5.

Author Contributions

Conceived and designed the experiments: MAMR EK AAH JLG. Performed the experiments: MAMR SB. Analyzed the data: MAMR RWM EK AAH JLG. Wrote the paper: MAMR AAH JLG.

References

1. World Health Organization (2011) World Malaria Report 2010. 204 p.
2. Bannister LH, Hopkins JM, Fowler RE, Krishna S, Mitchell GH (2000) A brief illustrated guide to the ultrastructure of Plasmodium falciparum asexual blood stages. Parasitol Today (Regul Ed) 16: 427–433.
3. Baum J, Gilberger T, Frischknecht F, Meissner M (2008) Host-cell invasion by malaria parasites: insights from Plasmodium and Toxoplasma. Trends Parasitol 24: 557–563. doi:10.1016/j.pt.2008.08.006.
4. Farrow RE, Green JL, Holder AA, Molloy JE (2011) The mechanism of erythrocyte invasion by the malarial parasite, Plasmodium falciparum. Seminars in cell & developmental biologydoi:10.1016/j.semcdb.2011.09.022.
5. Gaskins E, Gilk S, DeVore N, Mann T, Ward G, et al. (2004) Identification of the membrane receptor of a class XIV myosin in Toxoplasma gondii. J Cell Biol 165: 283–293.
6. Rees-Channer R, Martin SR, Green JL, Bowyer P, Grainger M, et al. (2006) Dual acylation of the 45 kDa gliding-associated protein (GAP45) in Plasmodium falciparum merozoites. Mol Biochem Parasitol 149: 113–116.
7. Yeoman JA, Hanssen E, Maier AG, Klonis N, Maco B, et al. (2011) Tracking glideosome-associated protein-50 reveals the development and organization of the inner membrane complex of P. falciparum. Eukaryotic Cell 10: 556–564. doi:10.1128/EC.00244-10.

8. Jones ML, Kitson EL, Rayner JC (2006) Plasmodium falciparum erythrocyte invasion: a conserved myosin associated complex. Mol Biochem Parasitol 147: 74–84. doi:10.1016/j.molbiopara.2006.01.009.
9. Green JL, Rees-Channer RR, Howell SA, Martin SR, Knuepfer E, et al. (2008) The Motor Complex of Plasmodium falciparum: phosphorylation by a calcium-dependent protein kinase. J Biol Chem 283: 30980–30989. doi:10.1074/jbc.M803129200.
10. Vaid A, Thomas DC, Sharma P (2008) Role of Ca2+/calmodulin-PfPKB signaling pathway in erythrocyte invasion by Plasmodium falciparum. J Biol Chem 283: 5589–5597. doi:10.1074/jbc.M708465200.
11. Billker O, Lourido S, Sibley LD (2009) Calcium-dependent signaling and kinases in apicomplexan parasites. Cell Host Microbe 5: 612–622. doi:10.1016/j.chom.2009.05.017.
12. Gilk SD, Gaskins E, Ward GE, Beckers CJM (2009) GAP45 phosphorylation controls assembly of the Toxoplasma myosin XIV complex. Eukaryotic Cell 8: 190–196. doi:10.1128/EC.00201-08.
13. Striepen B, Jordan CN, Reiff S, van Dooren GG (2007) Building the Perfect Parasite: Cell Division in Apicomplexa. PLoS Pathog 3: e78. doi:10.1371/journal.ppat.0030078.
14. Hu G, Cabrera A, Kono M, Mok S, Chaal BK, et al. (2010) Transcriptional profiling of growth perturbations of the human malaria parasite Plasmodium falciparum. Nature Biotechnology 28: 91–98. doi:10.1038/nbt.1597.
15. Bullen HE, Tonkin CJ, O'Donnell RA, Tham W-H, Papenfuss AT, et al. (2009) A Novel Family of Apicomplexan Glideosome-associated Proteins with an Inner Membrane-anchoring Role. J Biol Chem 284: 25353–25363. doi:10.1074/jbc.M109.036772.
16. Agop-Nersesian C, Naissant B, Ben Rached F, Rauch M, Kretzschmar A, et al. (2009) Rab11A-controlled assembly of the inner membrane complex is required for completion of apicomplexan cytokinesis. PLoS Pathog 5: e1000270. doi:10.1371/journal.ppat.1000270.
17. Frénal K, Polonais V, Marq J-B, Stratmann R, Limenitakis J, et al. (2010) Functional dissection of the apicomplexan glideosome molecular architecture. Cell Host Microbe 8: 343–357. doi:10.1016/j.chom.2010.09.002.
18. Johnson TM, Rajfur Z, Jacobson K, Beckers CJ (2007) Immobilization of the Type XIV Myosin Complex in Toxoplasma gondii. Mol Biol Celldoi:10.1091/mbc.E07-01-0040.
19. Papakrivos J, Newbold CI, Lingelbach K (2004) A potential novel mechanism for the insertion of a membrane protein revealed by a biochemical analysis of the Plasmodium falciparum cytoadherence molecule PfEMP-1. Mol Microbiol 55: 1272–1284. doi:10.1111/j.1365-2958.2004.04468.x.
20. Treeck M, Sanders JL, Elias JE, Boothroyd JC (2011) The Phosphoproteomes of Plasmodium falciparum and Toxoplasma gondii Reveal Unusual Adaptations Within and Beyond the Parasites' Boundaries. Cell Host Microbe 10: 410–419. doi:10.1016/j.chom.2011.09.004.
21. Matsumura F (2005) Regulation of myosin II during cytokinesis in higher eukaryotes. Trends Cell Biol 15: 371–377. doi:10.1016/j.tcb.2005.05.004.
22. Burgess DR (2005) Cytokinesis: new roles for myosin. Curr Biol 15: R310–1. doi:10.1016/j.cub.2005.04.008.
23. Field C, Li R, Oegema K (1999) Cytokinesis in eukaryotes: a mechanistic comparison. Curr Opin Cell Biol 11: 68–80.
24. Delbac F, Sanger A, Neuhaus E, Stratmann R, Ajioka J, et al. (2001) Toxoplasma gondii myosins B/C: one gene, two tails, two localizations, and a role in parasite division. J Cell Biol 155: 613–623.
25. Walliker D, Quakyi IA, Wellems TE, McCutchan TF, Szarfman A, et al. (1987) Genetic analysis of the human malaria parasite Plasmodium falciparum. Science 236: 1661–1666.
26. Lambros C, Vanderberg J (1979) Synchronization of Plasmodium falciparum erythrocytic stages in culture. J Parasitol 65: 418–420.
27. Wu Y, Sifri CD, Lei HH, Su XZ, Wellems TE (1995) Transfection of Plasmodium falciparum within human red blood cells. Proc Natl Acad Sci USA 92: 973–977.
28. Fidock DA, Wellems TE (1997) Transformation with human dihydrofolate reductase renders malaria parasites insensitive to WR99210 but does not affect the intrinsic activity of proguanil. Proc Natl Acad Sci USA 94: 10931–10936.
29. Hastie CJ, McLauchlan HJ, Cohen P (2006) Assay of protein kinases using radiolabeled ATP: a protocol. Nature protocols 1: 968–971. doi:10.1038/nprot.2006.149.